

All-In-One Photovoltaic Sensor

Senior Design II

University of Central Florida

Department of Electrical Engineering and Computer Science

Sponsored by the Orlando Utilities Commission

Group 6

Timothy Ajao, Electrical Engineering

Marco Herrera, Electrical Engineering

Andrew Hollands, Computer Engineering

Maguire Mulligan, Electrical Engineering

Advised by Mark Steiner and Rubin York

TABLE OF CONTENTS

1.	Executive Summary	1
2.	Project Narrative	2
2.1	Project Background.....	2
2.2	Project Objectives	2
2.3	Project Requirements	2
2.4	Initial Diagrams & Visualized Prototypes	2
3.	Constraints and Standards.....	6
3.1	Customer Constraints	6
3.2	Engineering Constraints.....	7
3.3	Other Related Standards	9
4.	Research.....	13
4.1	Relevant Technologies and Theories	13
4.1.1	Solar Arrays	13
4.1.2	DC Optimizers	14
4.1.3	Internet of Things.....	15
4.1.4	System on a Chip	17
4.1.5	PCB Design Software	18
4.1.6	Temperature Sensing	18
4.1.6.1	Signal Conditioning	21
4.1.6.2	Signal Conditioning Wire Noise	21
4.1.6.3	Signal Conditioning Amplification.....	23
4.1.6.4	Cold Junction Compensation	23
4.1.7	Data Loggers	24
4.1.7.1	CR310 & LoggerNet.....	25
4.2	Market Analysis & Existing Efforts	27
4.2.1	TIDA-00640.....	27
4.2.2	OpenGreenEnergy.....	29
4.3	Component Selection and Implementation	30
4.3.1	ADC Considerations	30
4.3.2	Microcontroller and Microprocessor	33
4.3.2.1	ESP32.....	33
4.3.2.2	Raspberry Pi.....	37
4.3.3	Current Sensor	38
4.3.4	Voltage Sensor	51
4.3.5	Temperature Sensor	58
4.3.5.1	Thermocouple Type	60
4.3.5.2	Thermocouple Conditioning Circuit	65
4.3.6	Irradiance Sensor	71
4.3.7	On-Board Component Power Supply	77
4.3.8	Communication Protocols.....	83
4.3.9	Other Communication Protocols.....	88
4.3.10	Programming Languages	91
4.3.11	Operating Systems	93
4.3.12	Data Storage Method	95
4.3.13	PCB Enclosure	95

5.	System Design	100
5.1	Hardware Design	100
5.2	Terminal Connections	100
5.3	On-Board Power Supply	101
5.4	Current and Voltage Sensing	102
5.5	Temperature Sensing	103
5.6	Initial Irradiance Sensing	104
5.6.1	Updated Irradiance Sensing	105
6.	Component Testing.....	107
6.1	Hardware Testing Protocol	107
6.1.1	On-Board Component Power Supply Testing	108
6.1.2	Voltage & Current Sensor Testing.....	108
6.1.2.1	Prototype Current Sensor Testing.....	109
6.1.2.2	Prototype Voltage Sensing.....	111
6.1.3	Temperature Sensor Testing	112
6.1.3.1	MAX6675 Accuracy	112
6.1.3.2	Type K Linearity	113
6.1.3.3	Compatibility Test	114
6.1.3.4	MAX6675 Single Day Temperature Readings	115
6.1.4	Irradiance Sensor Testing	116
6.1.4.1	Irradiance Circuitry Testing.....	119
6.1.4.2	Irradiance Circuitry Changes	122
6.2	Software Testing	123
6.2.1	Wireless Communication Tests	123
7.	Device Fabrication	123
7.1	PCB Fabrication.....	123
7.2	PCB Fabrication Revision.....	124
8.	Administrative Details	125
8.1	Initial Project Description & Goals.....	125
8.1.1	House of Quality Matrix	126
8.2	Project Milestones.....	127
8.3	Project Budget.....	129
9.	Project Summary & Conclusion	131
Appendix A – Image/Graphics Copyright Permissions		132
Appendix B - References		143

LIST OF FIGURES

Figure 2.1.	Hardware Block Diagram.....	4
Figure 2.2.	Software Block Diagram	4
Figure 2.3.	Prototype Design	5
Figure 3.1.	Male and Female MC4 Connectors	6
Figure 3.2.	10-AWG and 16-AWG Terminal Blocks	7
Figure 4.1.	Solar Cell Cross-Section.....	13
Figure 4.2.	Typical DC Optimizer Configuration.....	15
Figure 4.3.	OUC's DC Optimizer Configuration	15
Figure 4.4.	IoT Diagram	16

Figure 4.5. SoC Technology Diagram	18
Figure 4.6. Weld Beaded with Different Styles of Shielding Thermocouple	20
Figure 4.7. Basic Conditioning Signal Block Diagram	21
Figure 4.8. Parallel VS Braided Wire Configuration	22
Figure 4.9. OUC Datalogger for Solar Testing Array	25
Figure 4.10. CR310 Datalogger	25
Figure 4.11. Configuration for the CR310 with LoggerNet	26
Figure 4.12. Real-Time Monitoring of the CR310	27
Figure 4.13. TIDA-00640 Block Diagram.....	28
Figure 4.14. OpenGreenEnergy's Schematics.....	30
Figure 4.15. ESP32 Functional Block Diagram.....	34
Figure 4.16. ESP32-WROOM-32 Pin Layout	34
Figure 4.17. Integrated Crystal Oscillator.....	36
Figure 4.18. Capacitor Cross Section	37
Figure 4.19. Raspberry Pi 4 B+ Diagram	37
Figure 4.20. Shunt Resistor Configuration	39
Figure 4.21. High-Side Shunt Resistance Measurement	41
Figure 4.22. Low-Side Configuration.....	41
Figure 4.23. In-Line Configuration.....	42
Figure 4.24. INA219 Configuration.....	42
Figure 4.25. INA3221 Configuration.....	43
Figure 4.26. LM5056A Configuration.....	44
Figure 4.27. TLV342IDR Configuration	44
Figure 4.28. TLV342IDR Current Sensing Application.....	46
Figure 4.29. Hall Effect Sensing	48
Figure 4.30. Differences in Air Gap Size	49
Figure 4.31. Open Loop Topology for Current Sensing	50
Figure 4.32. Closed Loop Topology for Current Sensing	51
Figure 4.33. TLV342IDR Voltage Sensing Application	52
Figure 4.34. TIDA-00795 Block Diagram.....	53
Figure 4.35. TIDA-00528 Block Diagram.....	54
Figure 4.36. TIDA-01063 Block Diagram.....	56
Figure 4.37. Non-Inverting Configuration	57
Figure 4.38. Voltage Follower Configuration.....	58
Figure 4.39. Seebeck Effect	60
Figure 4.40. Voltage vs. Temperature Thermocouple Behavior	63
Figure 4.41. Thermocouple Basic Amplification	64
Figure 4.42. Typical Hot and Cold Junction Locations for a Type K Thermocouple	65
Figure 4.43. Amplifier using INA126 for Type T Thermocouple	66
Figure 4.44. Single Supply OPA335 Type K Thermocouple Amplifier	66
Figure 4.45. Two-Stage Amplification	67
Figure 4.46. Multistage Thermocouple Amplifier	67
Figure 4.47. MAX31886 Thermocouple Amplifier and Compensator.....	69
Figure 4.48. MAX6675 Thermocouple Amplifier and Compensator.....	69
Figure 4.49. MAX31856 IC Internals.....	70
Figure 4.50. MAX6675 IC Internals.....	70

Figure 4.51. Initial Proposed Pyranometer Implementation Circuit	73
Figure 4.52. Sirichote's Implementation of the INA101 DIP Package	74
Figure 4.53. Pyranometer Implementation using INA126PA	76
Figure 4.54. Linear Voltage Regulator Configuration	79
Figure 4.55. Switching Voltage Regulator Buck Configuration.....	80
Figure 4.56. WEBENCH Schematic of LMR36015ARNXR.....	83
Figure 4.57. Efficiency Curve of LMR36015.....	83
Figure 4.58. Ad-Hoc Mode vs Infrastructure Mode	86
Figure 4.59. VNC Diagram.....	89
Figure 4.60. SSH Diagram.....	91
Figure 4.61. LAMP Software Bundle	94
Figure 4.62. Layout of several prospective enclosures.....	97
Figure 4.63. INA290 Current Sense Error Analysis	47
Figure 4.64. INA293 Current Sense Error Analysis	47
Figure 5.1. Panel IN and OUT	100
Figure 5.2. Pyranometer and Thermocouple Inputs.....	101
Figure 5.3. LM5017 Step-Down Regulator	101
Figure 5.4. Type 2 LM5017 Ripple Configuration	102
Figure 5.5. TLV342 Current and Voltage Sensing Circuitry.....	102
Figure 5.6. MAX6675ISA Thermocouple Amplifier	103
Figure 5.7. MAX4194 Pyranometer Amplifier.....	104
Figure 5.8. MCP3008 Standalone Pseudo-Differential ADC	105
Figure 6.1. SMD Adapters with Header Pins	107
Figure 6.2. ESP-32 SMD Adapter & Dev Board.....	107
Figure 6.3. Current Sensing Breadboard Configuration	108
Figure 6.4. Voltage Sensing Breadboard Configuration.....	109
Figure 6.5. MAX6675 vs M400 Temperature Readings	113
Figure 6.6. Type K Thermocouple Linearity	113
Figure 6.7. SMD Adapter to Through Hole	114
Figure 6.8. Thermocouple Type T Prototype using ESP32	115
Figure 6.9. Access Point Temperature Output.....	115
Figure 6.10. Single Day Solar Cell Temperature.....	116
Figure 6.11. SP-110-SS Output vs. CR310 Value, Unshaded	118
Figure 6.12. SP-110-SS Output vs. CR310 Value, Shaded	119
Figure 6.13. MAX4194 Simulation Circuit	120
Figure 6.14. MAX4194 Testing with 1.5 Gain	120
Figure 6.15. MAX4194 Breadboard Testing	121
Figure 6.16. Difference between True and Theoretical MAX4194 Output	122
Figure 6.17. Difference between True and Solved Pyranometer Input	122
Figure 6.18. Input Current Vs. Sensed Current	110
Figure 6.19. Input Voltage Vs. Sensed Voltage.....	111
Figure 7.1. PCB Draft Design	124
Figure 7.2. V2.0 PCB Layout in Easy EDA	125
Figure 7.3. V3.0 PCB Layout in Easy EDA	125
Figure 8.1. House of Quality.....	127

LIST OF TABLES

Table 2.1. Specifications	3
Table 2.2. Constraints	3
Table 3.1. Summary of ISO 9060:2018 Pyranometer Classes.....	9
Table 4.1. Types of Thermocouples	20
Table 4.2. Summary of considered ADCs	33
Table 4.3. Shunt Resistor Considerations	39
Table 4.4. Comparison of Current Sense Amplifier Integrated Chips.....	45
Table 4.5. TIDA-00796 Voltage Sensing Specifications.....	54
Table 4.6. TIDA-00528 Voltage Sensing Specifications.....	55
Table 4.7. TIDA-00640 Voltage Sensing Specifications.....	57
Table 4.8. Temperature Sensor Comparison.....	59
Table 4.9. Overall Temperature Range for Typical Thermocouples	61
Table 4.10. Thermocouples Market Analysis	61
Table 4.11. Thermocouple Sensitivity	62
Table 4.12. Selected Thermocouples for Sensing Node	64
Table 4.13. MAX31856 and MAX6675 Specifications	68
Table 4.14. Summary of Considered Pyranometers	72
Table 4.15. Summary of Considered Pyranometer Amplifiers.....	75
Table 4.16. Further Instrumentation Amplifier Considerations.....	77
Table 4.17. Comparison of Switching and Linear Regulators	81
Table 4.18. Comparison of Considered Switching Regulators.....	82
Table 4.19. Wi-Fi Generations.....	84
Table 4.20. Ranges of Bluetooth Devices by Class	88
Table 4.21. Comparison of ZH101006 and ZH121006 Enclosures.....	97
Table 4.22. Aluminum vs. Copper Heat Sink	98
Table 4.23. Component Temperature Limits	98
Table 5.1. Current and Voltage Sensing BOM	103
Table 5.2. MAX6675 BOM	104
Table 5.3. Pyranometer BOM	105
Table 5.4. Updated Pyranometer BOM	106
Table 6.1. MAX6675 vs M400 Temperature Test.....	112
Table 6.2. Single Day Temperature reading for Type T and K Thermocouples	116
Table 6.3. SP-110-SS Testing Specifications	117
Table 6.4. SP-110-SS Output Vs. CR310 Recorded Value	118
Table 8.1. Initial Project Description & Goals	126
Table 8.2. Senior Design I Milestones.....	128
Table 8.3. Senior Design II Milestones	127
Table 8.4. Initial Project Budget for Redesigning Phase I.....	129
Table 8.5. Phase II Budget.....	130

1. EXECUTIVE SUMMARY

There exists a great push toward renewable energy on almost every front of the world's improvement. As time goes on, and the world continues with their journey to become completely carbon-neutral and embrace the wonders of renewable energy, people begin to question just how reliable this renewable energy is. One common doubt is the reliability of the renewable sources that depend on the weather, such as solar panels. As solar panels become more and more commonplace, it becomes that much more important to describe and highlight how it performs throughout the day. Without reliable measurement and an easy way to access these measurements, solar panels become a black box of energy generation that an average consumer cannot predict or depend on blindly. Moreover, how can the engineers and workers understand how a solar panel is performing without having a method to measure that performance? If a solar panel could come with a pre-installed sensor that can measure its outputs and surrounding environment, then maintenance and installation become a much clearer experience.

This project, bestowed upon us by the Orlando Utilities Commission via Rubin York, aims to combat that exact issue. Oftentimes, solar panels fail. It is expected that they will, just as all other means of power generation may in their lifetimes. When a system that contains a single solar panel fails, it is easy to understand; that solar panel begins producing at a much lower rate, and a consumer can instantly tell that their solar panel is malfunctioning. However, solar panels are commonly installed in arrays. When a single solar panel fails inside of an array, the generation of the entire array is greatly affected, and it is impossible to determine which solar panel has failed without testing each solar panel individually. This creates an extremely large workload for any engineers attempting to rectify the failed solar panel and can greatly limit power generation for days.

Implementing a sensor that can measure a solar panel's output in volts and amps, and its surrounding temperature and irradiance can greatly reduce the time it takes to pinpoint a panel that has failed and, in the best case, eliminate that time if a sensor is placed on every panel. This is what the All-In-One PV Sensor aims to be: A simple-to-install, small and cheap sensor that can attach directly between a solar panel's output and the grid that can measure a solar panel's voltage, current, temperature, and irradiance exposure, and communicate that data to a local database for analysis.

The All-In-One PV sensor will use a simple voltage divider and shunt resistor to measure the panel's output voltage and current respectively. The sensor will also optionally employ a thermocouple and/or a pyranometer, allowing the All-In-One PV Sensor to operate with or without the thermocouple and pyranometer. This will greatly reduce the cost of the average sensor, as the average irradiance and temperature of panels directly next to each other will be about the same. Therefore, a fully constructed model will feature voltage, current, temperature, and irradiance measurement, while a minimally constructed model will only feature voltage and current measurement. Both models will be completely functional and fully able to communicate this data to a local database to be stored.

This paper documents the All-In-One PV Sensor's design process. An initial overview of the project's scope is given, followed by an in-depth look into the surrounding technology that relates to our All-In-One PV Sensor and the components that will be used inside of it. The components will be greatly analyzed and brought down to a single, working design, and that design will be tested rigorously and described. Finally, this paper features the administrative details of the All-In-One PV Sensor's creation, touching on its milestones and budget. An appendix is attached at the end detailing the use of copyright materials and our references.

2. PROJECT NARRATIVE

In the Project Narrative, the background of the project is explained alongside the current objectives and requirements set forth by our customer and sponsor, the Orlando Utilities Commission (OUC). Tables listing the various specifications and constraints that limit the functionalities of our product are explained in the Project Requirements and showcased in the Initial Diagrams. These goals and guidelines help establish a sense of direction and the required physical and virtual quantities that can allow us to complete this project to scope.

2.1 PROJECT BACKGROUND

As greenhouse gas emissions continue to rise on Earth today, one of the biggest challenges is to find new ways to produce clean energy reliably and efficiently. Many companies around the world have set a goal of reaching carbon neutrality to combat global warming. The Orlando Utilities Commission (OUC) is one of many companies which has established a similar goal; OUC's goal is to reach 50% carbon neutrality by 2030, and to reach 100% carbon neutrality by 2050. Our group has taken a part in OUC's objective to achieve sustainable energy production by developing data sensing equipment to pair with OUC's existing solar panel array. We will be completing phase II of this project, emphasizing on what was not completed in phase I. Phase I completion includes functioning voltage- and temperature-sensing components, lacking current- and irradiance-sensing components.

2.2 PROJECT OBJECTIVES

The goal of our project is to develop a low-cost, all-in-one photovoltaic (PV) sensor device which will allow our customer, OUC, to gather data from their solar panel arrays. The all-in-one sensor will be able to collect voltage, current, temperature, and irradiance directly from the customer's solar panels. The data that our solution will provide the customer with includes numerous benefits. Firstly, through voltage and current values collected at each panel in an array will allow for technicians to detect a faulty panel in an easy-to-use manner. This solution would significantly reduce loss of power generation when a panel becomes faulty as this would reduce the time and money it would take for a technician to identify a faulty panel. Secondly, our solution will collect large amounts of granular data for OUC to generate accurate representations of temperature and irradiance at a solar panel array over a period, as well as energy collected over a period.

2.3 PROJECT REQUIREMENTS

Our all-in-one PV sensor will function as a series of collector nodes, or microcontrollers, mounted onto each solar panel in an array. The collector nodes will be able to collect and wirelessly transmit multiple, granular pieces of data like voltage and current, temperature, and irradiance from the onboard DC optimizers, thermocouples, and pyrometers, respectively, to a receiver node. The receiver node will be able to compile collected data into a database, as well as display collected data in real-time. It is from our solution that OUC will be able to reach 50% carbon neutrality by 2030 and achieve 100% carbon neutrality by 2050 as our all-in-one PV sensor will have a robust design that will allow for scalability to a much larger solar panel array.

2.4 INITIAL DIAGRAMS & VISUALIZED PROTOTYPES

Tables 2.1 and 2.2 showcase the specifications and some of the constraints that we will face while developing this project, respectively.

Table 2.1 Specifications

	Requirement	Specification
1	Power supply	Solar panel
2	Available input power	1500 watts
3	Sample rate	10-15 seconds
4	Specific cost	<\$20
5	Connection to Solar panels	MC4
6	Accurate Voltage Measuring	Moderate Priority
7	Accurate Radiance Measuring	Moderate Priority
8	Accurate Temperature Measuring	Within 5% of real value
9	Accurate Current Measuring	Within 5% of real value
10	Wireless Data Transfer	Effective data transfer
11	Protective packaging	Harsh weather resistant

Table 2.2 Constraints

	Requirement	Specification
1	Input voltage power supply 39V DC	High
2	Input power range 500 to 1200 W level	High
3	MC4 Standard connections	High
4	Removable device	High
5	Cost per sensor less than \$20	Moderate
6	Accommodation terminal connectors 10 AWG wire	Low
7	Connection between DC Optimizers	High
8	Designing with thermocouple and pyranometer ports	Moderate
9	Sensor Durability lifetime more than a year	Low
10	Testing point time at least a week	Moderate

The following figures, Figure 2.1, and Figure 2.2, showcase a block-diagram representation of our project's layout and scope. With this, we aim to understand how the All-In-One PV sensor will connect within itself and ultimately extend outward virtually, communicating the recorded data over a local network so that it can be stored.

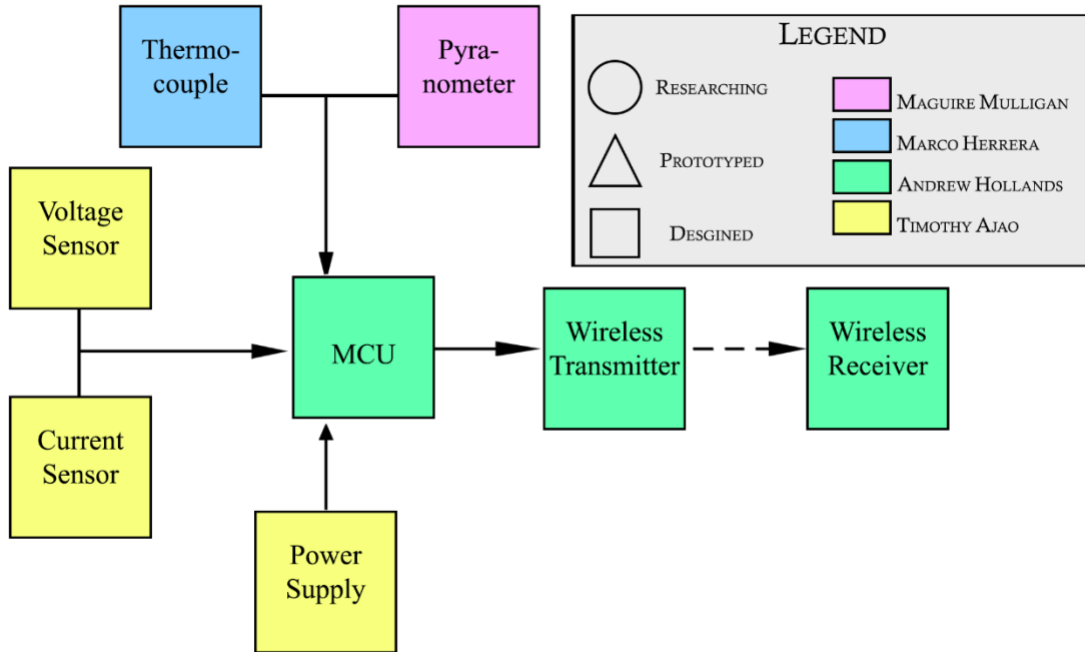


Figure. 2.1. Hardware Block Diagram by Maguire Mulligan.

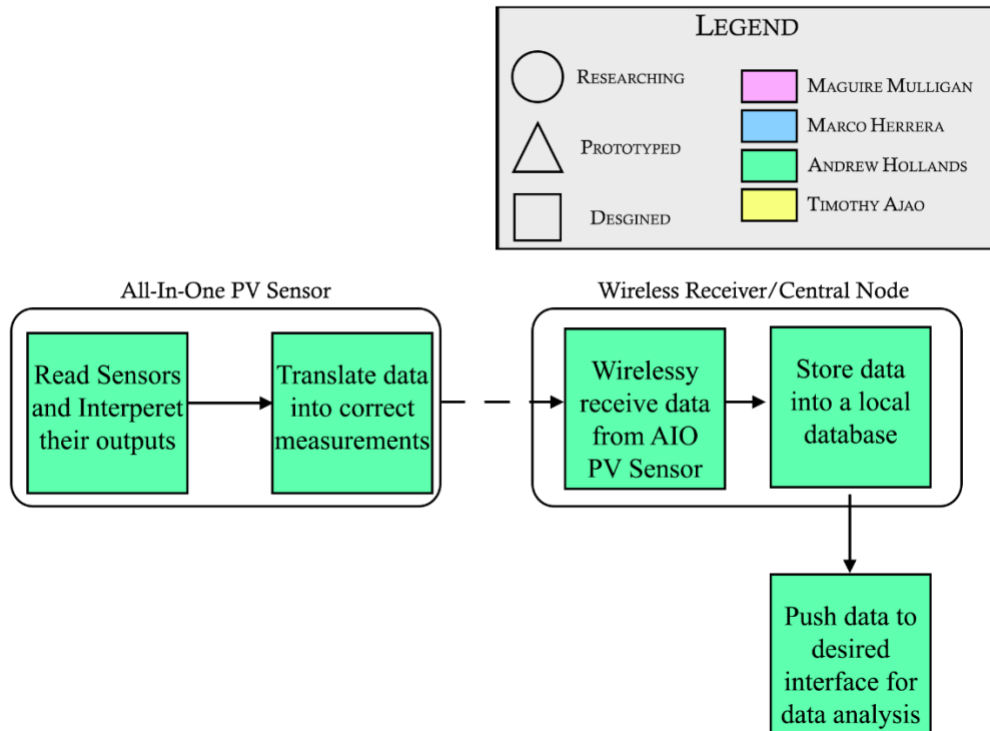


Figure 2.2: Software Block Diagram by Maguire Mulligan.

Our final diagram is the overall prototype design, not considering the inner workings of the All-In-One PV Sensor. This diagram, seen in Figure 2.3, shows how the sensor will connect on to a standard solar panel at the Pershing Research Array provided by OUC, being placed in series between the Solar Panel's output and the DC optimizer that cleans the generated power and sends it toward the grid. The All-In-One PV Sensor will be able to wirelessly communicate data to a local collector node such that the data can be stored and viewed at a local machine for data analysis.

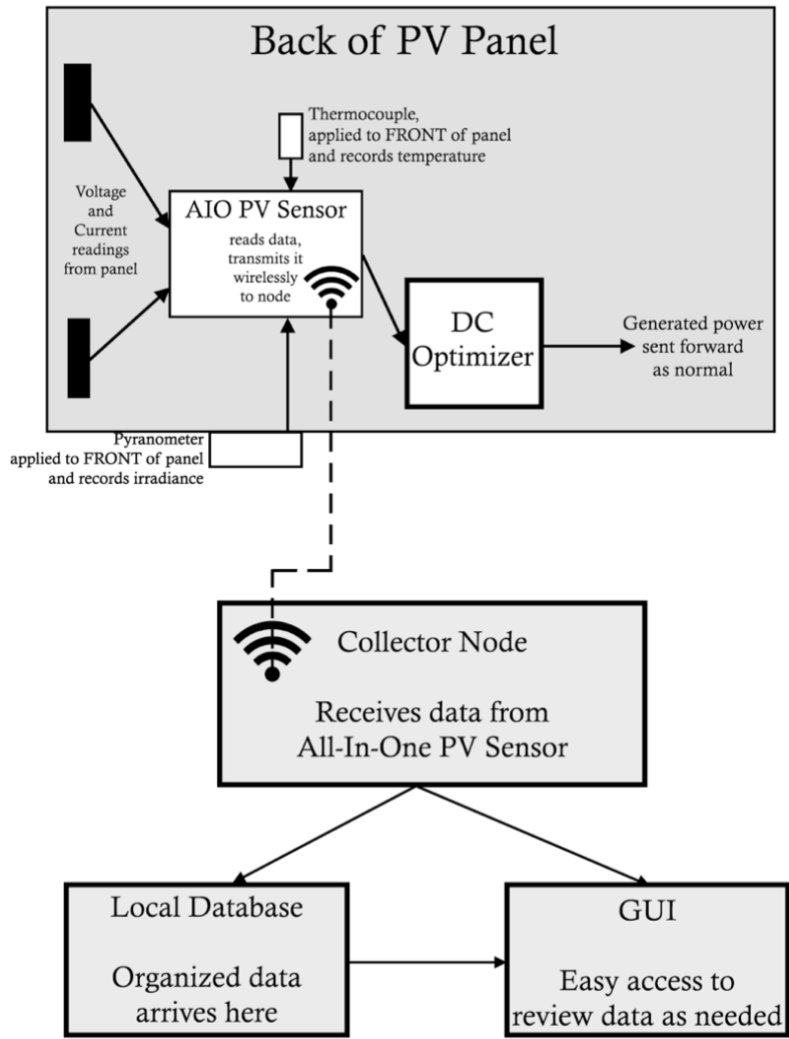


Figure 2.3. Prototype Design by Maguire Mulligan.

3. CONSTRAINTS AND STANDARDS

When it comes to make a new product specially a new technology, constraints, and standards play an important role in designing. Constraints are all special requirements that might be imposed by a customer, environment, or other factors and can affect the design limitation. Standards are all the requirements that design should follow to be considered as a standard product to work with other standard products. All Standard characterizations have been described in a formal document to define a standard product. In All-In-One PV sensor, we are committed to comply with the IEEE and organizations' standard requirements for our design.

In this project we are facing two major types of constraints: Constraints imposed by the customer/sponsor and engineering constraints which are standard requirements when designing. Because this project is directly sponsored by OUC, our customer, it is important that we prioritize customer constraints as we pursue our real design constraints to keep our funding.

3.1 CUSTOMER CONSTRAINTS

Connectors

To connect the Solar Panel to our board, OUC has instructed us to use MC4 connectors. These will connect directly to our terminal blocks such that the board can be placed directly in series with the production of the panel and the DC Optimizer that is present on-site, allowing the installation to be flexible across different types of solar panel installations.

MC4 Connector

MC4 connectors will provide our All-In-One PV Sensor with power, and they are also a type of connection that is required by the customer/sponsor (OUC). Our device should follow this requirement as another constraint. MC4 is defined as a multi-contact 4mm Pin Connector. This type of connection is easy to connect by hand but almost impossible to disconnect the same way. This is due the safety just to avoid any accidental disconnection when the system is loaded.

The newest model of MC4 PV connectors, the MC4-Evo2, was made with the highest performances to comply with the worldwide certifications and the market by giving the reliability of benefits for years expertise and the standardization for a large range of connection. The figure below shows the newest version of MC4 it is MC4-Evo2 male and female. They come with a wide range of cable cross-sections from 2.5 mm² to 10mm² for range of wire gauges of 8 AWG to 14 AWG. Therefore, the cable of 6mm² cross-section is associated with the 10 AWG that is required for the project. Figure 3.1 displays these connecting cables.

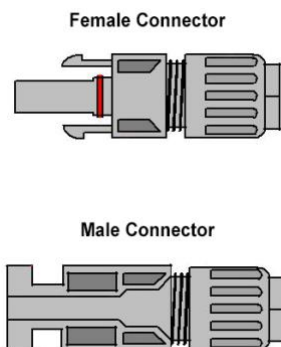


Figure 3.1. Female and Male MC4 Connectors. Reproduction permission requested from Leader Group.

Terminal Blocks

By keeping everything standard, it comes to mind to find what type of connectors that we need to make our design running smoothly. Because it is important that we must comply with the customer requirements, and we cannot change any parameters that he has requested. It is necessary for us to use the proper wires and connectors regarding the input voltage that will be across the PCB and how many connectors that will be needed. From this view, we analyze that according to the requirements of OUC and design standards, we will have two inputs coming from the solar system and in the same way two outputs that going to the DC optimizer because both input and output are carrying two wires each. A clear description of the design will be showing when we are going to test the device.

In addition, we will need to connect other components like the thermocouple and the pyranometer. Those circuits will require each an additional terminal block. For those connections, they use a single wire for their polarity unlike the MC4 cable using two for a unique pole. That means each device will use one terminal block. Therefore, our PCB will carry four terminal blocks in which there will be eight connections.

The terminal block showing below is the one that will be connected to the PCB to provide energy to the power supply. The terminal block is made to carry a range of 10 - 26 AWG that is coming from the solar panels and can go up to 300V with a maximum current of 30A. This is the TB005-762 model. This model was made with steel-zinc plated screw -rising cage clamp. It has been provided by the customer (OUC) to us. Figure 3.2 displays these terminal blocks.



Figure 3.2. 10-AWG and 16-AWG terminal blocks

3.2 ENGINEERING CONSTRAINTS

Engineering constraints are constraints that limit the creation of our device in ways that customer constraints do not. These types of constraints ensure that the All-In-One PV Sensor will consistently operate in the field all while operating as intended, following standards and codes.

The final PCB must be able to withstand a maximum of 40 V DC and 10 A DC and it must also be capable of measuring these inputs using components that are directly on the board. Along with this, it must be able to operate ‘a-la-carte’, meaning that the board should be fully functional when the temperature and irradiance sensors are not connected to the board. The All-In-One PV sensor must be able to record its measurements and transmit those measurements wirelessly to a local node database and have the values transmitted be no greater than +/- 5% of its original value. The entire design must also be capable of working from the inside of an enclosure such that it can operate in intense weather conditions without having the life or longevity of the device threatened.

Time Constraint

Time on its side plays a vital role in the development of any project. By considering other factors such as technology, resources and financial, time is a decisive challenge for the accomplishment

of the project. Managing time is one of the main aspects of our project management by coming with a good schedule and timelines regarding different steps of the project because failure and success of the design depend on it.

Set the proper schedule for the project provides to the team member a dynamic environment in which everyone knows his tasks and at what time he needs to get them done. By having a good allocation of timeframe and setting the right deadlines for different steps of the project that guarantees and secures the completion of the project for the wanted period.

To complete the project an effective timeline needs to be set otherwise there will be consequences regarding the delay of completion where the project could take longer time than expected and financial repercussion might happen as well. In other words, an ineffective project timeline could result in a non-achievement of the project and an increase in cost materials to use which could determine the failure of the design.

To come up against those situations, we need to set an effective time management where every can handle. Therefore, the project will be developed by a list of activities according to a timeframe estimation and followed all allocation resources that are available to us.

Financial Constraints

Financial is one of the most important aspects of the project. It tells the cost of the project along we are selecting the parts that we will use to make our design. As a sponsor project, we are bounded to a certain expense that means we cannot go overhead budget. For this reason, we must be very picky on the parts and components that we want to implement our design. Because we need cheap elements, it does means that we should choose materials that we cannot rely on them for standard issues such as durability, safety, and more. To obtain materials for our design, there is a couple things that need to be considered.

When designing, we want reliable parts meaning that we are looking for standard components as we are committed to building our project to meet certain standard requirements. Sometimes, according to what we need, those parts are no longer available or out of stock. In this case, we must reconsider our design and find a related part that can match. Sometimes, this new part might be more expensive than the previous one that we wanted to use. At this point, we end up to an increasing cost of materials.

Another scenario is viewing the actual situation where everything's price is going day by day. For every component of the project, we must buy more than on to be sure we purchase at least three of each item that we want to implement in our design. In case of any defecting component while testing we can have a replacement. Once again, we are doing this in order to face the financial consequences.

Environmental, Health, and Safety Constraints

Another aspect of the project that needs to be considered is safety. Safety is very important specially when it comes to machineries and power technology equipment. For our design, the safety issue can come in two categories and that need to be studied as standard and constraint requirements. There is one that is associated to the device itself and the other one is for public.

For the device, the components need to be properly enclosed to ensure the safety and the durability of the device. After designing and having all components set together, we need to have a safety enclosure to put them on and that enclosure should be built or made under certain standard conditions. Those conditions require the protection not only of device itself but also to keep any unwanted intruder to have access through it.

The second aspect of the safety is to keep everyone safe as we all know "safety comes first." It is to avoid injuries because this is electrical component that carries voltages and if they are not wired

properly that can be fatal. This is something we don't want to occur. For that, we need to choose proper wires and connectors to ensure the public safety.

3.3 OTHER RELATED STANDARDS

Pyranometer Standards & Specifications

Pyranometers come in several classes that must be considered: Classes A, B, and C which are subject to classification according to ISO 9060:2018. [3.1] These classes are summarized in Table 3.1. Because the price can be seen to be comparatively high in Classes A and B, a Class C pyranometer will most likely be selected for this project as the accuracy and response time of the pyranometer are not of high importance.

Table 3.1 Summary of ISO 9060:2018 Pyranometer Classes [3.2]

Class	A	B	C
Accuracy	High	Good	Moderate
Response Time	< 15 seconds	< 30 seconds	< 60 seconds
Smallest Detectable Change	1 W per square meter	5 W per square meter	10 W per square meter
Error	Negligible	± 1%	± 2%
Comparative Price	4x the cost of Class C	2x the cost of Class C	-

IEEE 802 Standards

The IEEE (Institute of Electrical and Electronic Engineers) 802 Standards is a group of standards which encompasses various types of area networks like private area networks, local area networks, and metropolitan area networks. This family of standards is applicable to most, if not all wireless and wired data transmission methods people everywhere are familiar with.

In our project, we will be testing our product with three types of data transmission forms: ethernet, Wi-Fi, and Bluetooth. While we are planning to test our product with two types of wireless data transmission, Wi-Fi, and Bluetooth, we ultimately plan to keep only one of the two for our final design.

The Wi-Fi certification is contained within the IEEE 802.11 standard, a part of the IEEE 802 technical standards. It provides the framework for implementing wireless LAN technology and is the world's most widely used computer networking standard. This component serves as the main component for establishing a wireless network for various devices. There are also numerous protocols contained within the 802.11 standard. The ESP32 device we will be using for our product is capable of 3 different protocols of the 802.11 standard: 802.11b, 802.11g, 802.11n. Each protocol of 802.11 is a successive advancement of the 802.11 standard, in that successive protocols support faster data transfer rates to transmit more data quicker and wider bandwidths to lessen interference from other devices. [3.3]

Bluetooth SIG Standards

The Bluetooth SIG (special interest group) standards is a set of standards or qualities a product must possess for a manufacturer to grant a Bluetooth designation to a product. Originally, Bluetooth was standardized by the IEEE as part of the 802 family of standards, specifically 802.15.1, but has since been discontinued. [3.4]

The specific Bluetooth standard we will be using in our product is Bluetooth Smart 4.x, which is a part of its parent standard, Bluetooth 4.0. Its novel characteristic versus other protocols of Bluetooth is its low-energy consumption and considerable communication ability. This has led to adoption across countless computer devices on the market today like smart phones, laptops, desktops, and of course, microcontrollers like the ESP32 we will be using for our product. [3.5]

RoHS Directive

The RoHS 1 Directive, which is a European Union regulation aimed at restricting the use of certain hazardous chemicals in electronic equipment, took effect on July 1, 2006. It is required that all member states implement it. This directive prohibits the use of ten hazardous substances in the production and use of various types of electrical and electronic equipment. It is closely linked to the WEEE Directive, which aims to reduce the amount of toxic electronic waste. [3.6]

The RoHS directive prohibits the use of ten substances: lead, mercury, chromium, polybrominated biphenyls, diphenyl ether, and more. These substances are mainly used as flame retardants in various plastics. The main component of this chemical is hexavalent chromium, which is used in various industrial processes such as chromic acid and chrome plating. The maximum permissible concentration of this chemical in non-exempt products is only 0.1 or 1000 parts per million.

The restrictions apply to the homogeneous materials used in the product, which means that they do not apply to the finished product or even to a component. For instance, a radio is made up of various components such as a case, screws, and a circuit board. A circuit board is a type of electronic component that is composed of various components such as integrated circuits, resistors, and capacitors. A switch is also made up of various components such as a case, a lever, and a contact.

A loudspeaker is also made up of various components such as paper, copper wire, and permanent magnets. If the case used for the radio was made of plastic with a concentration of 2,300 parts per million, then the entire radio would not comply with the requirements of the directive. To close the remaining non-compliant product categories, the European Commission conducted a review in May 2006. The commission also entertains requests for extensions or for the exclusion of certain substances from the scope of the directive. In 2011, a new legislation was published that supersedes the previous exemption.

In Europe, batteries are still covered by the 1991 Battery Directive. However, a new version of this regulation was recently approved and will be published in the official journal of the European Union. The new version of the directive aims to improve the environmental impact of the batteries by establishing a more ambitious program for recycling them. It also increases the number of collection sites for consumer and industrial batteries to 45% by 2016. The new version of the regulation sets limits on the amount of lead and cadmium that can be used in batteries. It also prohibits the use of certain types of lead and other toxic substances in the production and use of these products. The new version of the directive also includes several new features, such as the ability to mark the batteries with symbols that indicate their recycling status.

The categories that are covered by the directive are as follows: large household appliances, small household appliances, telecommunications equipment, and consumer equipment. These include light bulbs, medical devices, and various leisure and sports equipment. The product maker is responsible for ensuring that the products comply with the requirements of the directive. However, since the regulation applies to the entire supply chain, the data collected about the substances in

the products must be transferred to the final producer. An electronic version of the data exchange protocol known as RoHS has been developed to facilitate this process. It is free to use and can be used by both domestic and foreign producers of the products covered by the directive.

Numerous consumer electronic products, such as televisions and computer components, have been affected using restricted substances. Some of these include paints and pigments used as a stabilizer in cables and connectors. Cadmium is also commonly found in various components, such as components used in light-emitting devices and batteries. Mercury is commonly used in lighting applications, such as those used in car components and light-emitting lamps. Other metals such as chromium are also commonly used as metal finishes. The scope of the original directive was separated from that of the WEEE Directive. An open scope was also introduced in the new version of the directive.

ESD STANDARDS

Electrostatic discharge is a sudden and unexpected flow of electric current between two objects that are electrically charged. A buildup of static electricity can be caused by either tribocharging or by an electrical induction process. When two objects are brought together, the resulting electrical current can create a visible spark. However, this type of discharge can also cause damage to electronic devices. In most cases, an electric spark must have a field strength of at least 40 kV to be considered an ESD event. There are various types of discharge, such as corona discharge and brush discharge. These discharge methods can cause various harmful effects in industries such as fuel vapor and explosions. When subjected to high voltage conditions, static can cause permanent damage to certain electronic components. To prevent this issue, manufacturers often create protective areas that are free of static. They can also use simulators to test the devices. [3.7]

Static electricity is one of the main causes of ESD. It can be generated through tribocharging, which occurs when two materials are separated by their electrical charges. This can happen even when two materials are separated by several millimeters. In most cases, the breaking of contact causes tribocharging. The presence of a charged object makes an electrostatic field develop on the surface of the other object. This field then carries additional charges onto the other object. For instance, if a bag or cup has charged regions on its surface, then an electrical discharge can occur on the nearby components. Another type of discharge is caused by energetic particles that are impinging on an object.

Although a relatively small electric charge can cause an electronic component to momentarily discharge, it can also damage the device's sensitive components. This invisible form of ESD can also cause device failures. A spark can be generated when the electric field strength exceeds 4–30 kV. This can cause the air's dielectric field to become too strong, which can lead to a sudden electrical breakdown. In most cases, a spark can be produced by the electric potential between a cloud and ground, which can be hundreds of millions of volts. However, it can also be generated in air when an object is charged to as little as 380 V. During an electrical discharge, the atmospheric molecules become overstressed. They can then recombine to form ozone, which can react with organic matter and metals. If the electrical stress is too high, nitrogen oxides can form. Both ozone and nitrogen oxides are toxic to animals. They can also be used in water purification. Spark ignition is a common cause of industrial accidents. Most explosions are caused by a small electrostatic discharge. Usually, this discharge can be triggered by a fuel leak or an unexpected spark in an environment that's rich in combustible materials. [3.8]

Electronic components such as microchips and integrated circuits can be damaged by ESD. They need to be protected during their manufacture, assembly, and after use. Grounding is an important component to consider when it comes to controlling this harmful discharge. In manufacturing, the prevention of electrostatic discharge (ESD) is done through the establishment of an EPA. This is a protected area that prevents the build-up of charges on sensitive electronics.

An EPA is a set of international standards that specify the steps that need to be taken to prevent the discharge of harmful electrical charges from electronic components. Some of these include using appropriate packaging material, conducting wrist straps, and using anti-static mats and flooring materials. The presence of moisture on most surfaces prevents the formation of charged particles. In addition, ionizers are used when insulative materials are not grounded. To prevent the accidental discharge of charges, insulating materials that are prone to triboelectric charging should be kept away from sensitive devices at least 12 inches from their surfaces. On airplanes, static dischargers are used on the trailing edges of the wings.

Aside from the device itself, protection components can also be incorporated into the circuit design to prevent the discharge of charges. Most of the electronic components that are sensitive to discharge are so small that they can be handled and produced using automated equipment. This makes it important that the proper steps are taken to prevent them from getting damaged.

An effective way to prevent the discharge of charges is to use materials that are dissipative. This type of material will slowly remove static charges from the surfaces of sensitive electronic components. These materials are known to conduct electricity at a very slow rate. They can also prevent the build-up of charges from damaging the internal structure of silicon circuits.

4. RESEARCH

Before the team can create a functioning prototype and move forward with a final design, research into each part must be done. In this section, relevant technologies and existing efforts in the market will be analyzed such that the team understands the components that will surround the All-In-One PV Sensor. Following this, an extensive look into core components is done so that the team can move forward with creating the All-In-One PV Sensor.

4.1 RELEVANT TECHNOLOGIES

While we are developing our own PCB, we will also be implementing existing, popular hardware available on the market that will largely assist in organizing and transmitting our collected and filtered data. In this section, we will discuss general technologies associated with the hardware we will be implementing as well as actual chips that support wireless communication methods mentioned earlier in this document. Due to the nature of this project's existence, this sensor will be placed at the Orlando Utility Commission's Research Array and therefore it is important to understand how their arrays function. To do this, the functionalities of several out-of-scope technologies will be analyzed.

4.1.1 SOLAR ARRAYS

A solar cell panel, also known as a solar electric panel, is an assembly that consists of photo-voltaic cells. These cells convert sunlight into electricity by producing a current. A system of solar panels is also called an array. Using light energy from the Sun, solar panels convert the solar radiation into electricity. Most of the time, the cells used in these modules are thin-film or crystalline silicon. [4.1] A cross-section of a solar cell panel is pictured in Figure 4.1.

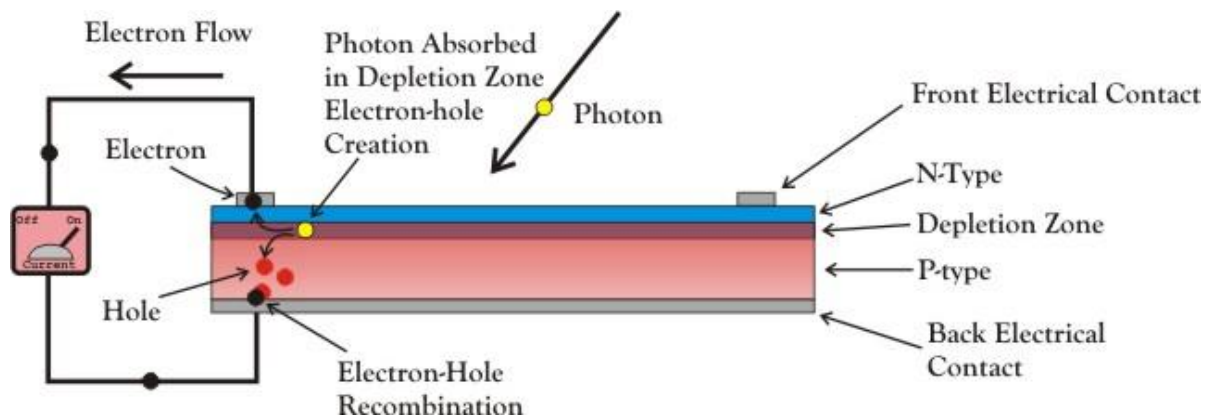


Figure 4.1: Solar Cell Cross-Section. Reproduction with the permission of Jignesh Sabhadiya.

Most solar panels are made of rigid materials, while semi-flexible ones are also available. The cells are connected in series to increase their current and voltage. Although the manufacturing process of solar panels is standardized, the actual operating conditions of the components are not always known. A solar panel's output interface is usually located on the back of the panel.

The panels are also made of metal components such as racks and troughs. They can also be connected to a standard power supply using a USB interface. Although a single solar panel can produce a limited amount of power, most installations have multiple modules that can add

additional current or voltage to the system. These components include an inverter, a battery pack, and a circuit breaker. A good solar panel installation involves carefully selecting the equipment that will help maximize its output and minimize its energy loss.

Several companies are now incorporating electronic components into the modules to enable them to perform various tasks such as monitoring and fault detection. These include MPPT and power optimizers. In 2010, electronic components were also introduced that can compensate for the effects of shading, which can reduce the electrical output of multiple strings of cells in a module.

Conducting wires are used to make connections between the modules. Each panel is typically connected in series to form strings to output a desired voltage. These components can be paralleled to provide the ideal current capability for the system. These components can be used in parallel or series connections to allow current to bypass the modules that have high resistance. They can also prevent short circuiting of other strings. [4.2]

Currently, most solar modules are produced using monocrystalline and multi-crystalline silicon cells. In 2013, the production of solar panels was dominated using crystalline silicon. Compared to other solar technologies, high-efficiency cells are more cost-effective. They are also used in space applications to provide the highest efficiency. Compound semiconductors known as MJ-cells are also being used in various solar technologies. One of these is concentrator photovoltaics. In rigid thin-film modules, the cells are produced on the same production line. The electrical connections are then made using in situ connections. The main types of cells used in this category are a-Si, a-Si+uc-Si, and a-Si tandem. They are produced using the same production line. If the substrate is an insulator, then monolithic integration can be done. The cells are then assembled into modules by bonding them to a transparent film and a polymer for bonding.

4.1.2 DC OPTIMIZERS

Our project requires lot of attention to what has been existed and why the Utility Commission needs us to come with as a new device. Despite the essential potentiality of the DC optimizer and the function that it plays in the system, OUC still requires something on the side to work with not a replacement for the DC optimizers, but something additional so he can do more analysis regarding the solar system and/or any single solar panel performance.

Because those solar arrays are set in series, any malfunctioning of any panel will affect the whole system and create a deficient performance. During a day, all areas are not covering with sun at the same intensity which can create a deficiency in one or more solar panel(s) in an array. There are several factors that can drive the system to low performance such as partially shaded conditions, multiple orientations of the sun and more. DC optimizer is a great technology that was made to encounter specially those situations. It is to optimize electricity generated by the solar arrays. When the solar panels are in contact with the sunlight, they generate DC voltage which will be converted to generate AC voltage.

DC optimizer tracks the voltage across each panel and maximize it by using a technology called MPPT (Maximum Power Point Tracker) technology before sending the right voltage to what we consider as an inverter meaning that the device that served to convert DC power of the solar panels to AC power that will be used by customers. On the other hand, our All-In-One PV sensors will in separate way by providing more data on each panel whenever it has needed. In other words, DC Optimizer can regulate the performance of the solar string up to 25% from the normal performance

of the system whereas our device can give more information to do deep analysis. Figure 4.2 displays a typical DC optimizer configuration in relation to its surroundings, and Figure 4.3 shows OUC's DC optimizer configuration placed directly on its generating panels.



Figure 4.2: Typical DC Optimizer Configuration



Figure 4.3: OUC's DC Optimizer Configuration by Maguire Mulligan.

4.1.3 INTERNET OF THINGS

The Internet of Things (IoT) is a broad term that refers to the interconnected world of physical objects that are embedded with sensors and other technologies that can exchange data with each other and with systems over the Internet. Although connected devices do not need to be on the public internet to be Internet of things, they do need to be able to be individually addressable. The concept of the Internet of Things is a broad range of technologies that enable the connectivity of various things, such as home automation and security systems. Most commonly, these include devices and appliances that are connected to one or more common ecosystems. [4.3]

The IoT is being widely used in healthcare systems. There are various concerns about the security and privacy of this technology, and various regulatory and industry initiatives have been launched to address these concerns. Many energy-consuming devices such as lights, pumps, and household appliances have already integrated Internet connectivity. This allows them to communicate with utilities and manage their energy consumption more effectively. These devices can also be controlled remotely using a central management interface.

The smart grid is a utility-side application that uses the Internet to collect and manage energy-related data. This system helps utilities improve the efficiency of their electricity distribution and production. Aside from monitoring electricity consumption, it also helps protect the environment by monitoring air quality and soil conditions. Developing the right connectivity for resource-constrained devices can help improve the efficiency of emergency services. The standardization of the Internet of Things is expected to greatly benefit wireless sensing. This is evidenced by the number of Living Labs, which are organizations that are focused on collaborating and sharing knowledge to develop new products.

Cities can also benefit from the implementation of the Internet of Things through the provision of incentives. This can help them improve the efficiency of their operations and reduce their costs. The Philippines' favorable policies and favorable conditions make it an attractive place for start-up companies and multinational companies to establish their operations. The relationship between the developers and the governments that manage the city's assets is very important to the success of the Internet of Things.

The concept of the Internet of Things is divided into three phases: Tier 1, Devices, Tier 2, and the Cloud. The devices that are connected to the Edge Gateway are typically those that use a variety of protocols. The Edge Gateway layer is a part of the data aggregation system that's used to collect and secure the data from various sensors. It provides various features such as pre-processing the data, establishing a secure connection to the cloud, and monitoring the devices. The final tier includes the cloud-based apps that are built for the Internet of Things. These apps are typically polyglot and are secure using HTTP/OAuth. [4.4]

The cloud tier of the Internet of Things system is typically composed of event-based messaging and networking systems. Some experts classify it as the platform, edge, or enterprise tier. The web of things is a part of the system that's focused on the convergence of data collected by sensors and web applications.

The goal of the Internet of Things is to control the flow of information between the various connected devices. This is done using process management techniques. The scalability of the network space is very important for the success of the Internet of Things. With the number of devices expected to grow significantly, the IETF's 6LoWPAN would be used to handle the influx of data. The processing power of the edge devices is typically limited. This limitation makes it difficult for them to process and analyze data collected by the sensors. An average illustration of IoT is shown in Figure 4.4.

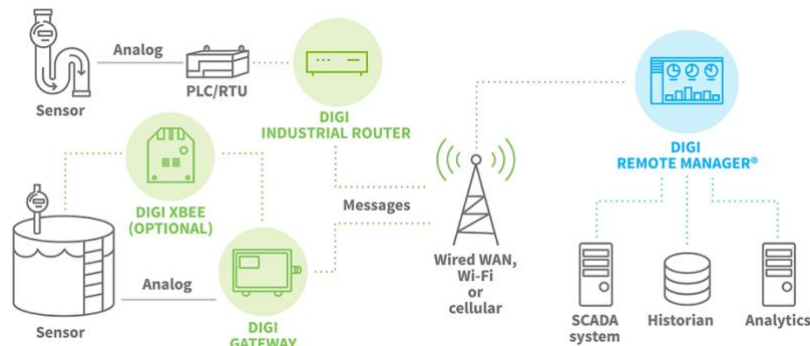


Figure 4.4: IoT Diagram. Reproduction permission requested from Digi International Inc.

4.1.4 SYSTEM ON A CHIP

System-on-a-chip, or SoC, is a prevalent technology we will be implementing in our design in both our PCB and accompanying Raspberry Pi 4 microprocessor. SoC refers to a processing unit which is composed of a single unit which at one point used to be composed of multiple units. For example, a computer 20 years ago would have a motherboard with multiple separate components soldered onto it like a CPU, memory, storage, GPU, and numerous busses to connect the components. Today, a SoC is a combination of all the previously listed components, miniaturized into something as small as a Washington quarter. [4.5]

A system on a chip is a complete electronic package that consists of various computer components. It can be used to implement various electronic functions. System on a chip usually consists of a central processing unit (CPU), graphics processing unit (GPU), and system memory. A SoC is designed to meet the requirements of incorporating multiple computer components onto a single chip. Instead of having multiple components assembled onto a circuit board, an SoC simplifies the process by creating one unit of electronic circuits. There are many types of SoCs, such as general-purpose CPUs and specialized circuits that handle various special-purpose tasks. Some of these include tasks related to image processing, video editing, and artificial intelligence.

The processor is the core of a system-on-a-chip (SoC). Unlike desktop machine CPUs, it features a wide variety of processing options. Some of these include general purpose and digital signal processor, micro-controllers, and application specific processor. Prior to 2010, most SoCs were built with a single processor, which was responsible for controlling the whole system. In 2008, most of them were built around a processor based on one of the following processor architectures: Advanced RISC Machines (ARM), MIPS (Microprocessor without Interlocked Pipelined Stages), PowerPC, or x86. The evolution of multi-processor SoCs has raised the concerns of system designers due to their dependence on super-computing. [4.6]

The bus is a major component of a SoC. Many SoCs have multiple busses, which can be used to connect various peripheral components. Some of these include the processor, memory, and hardware accelerator. The use of commercial bus protocols has been a major obstacle to the standardization of SoCs. Due to this, the use of networks on chip (NoC) has been gradually adopted.

A system-on-a-chip (SoC) is typically comprised of various control circuits, such as UART, USB, and GPS. It can also include specialized peripherals, such as FFT and turbo decoder, which are typically targeted to image processing. A hardware IP will typically provide better execution and lower power consumption than a software implementation. However, it can also increase system complexity and cost. A radio connection is provided by the addition of analog and mixed signal components. Some application domains also require specialized components such as biochips, optical computing, and millimeter wave. A generic diagram of a SoC device is included below in Figure 4.5. [4.7]

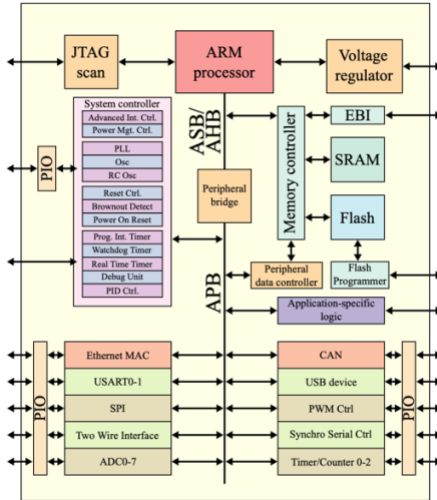


Figure 4.5: SoC Technology Diagram. [4.106]

The only objective metric that can be used to evaluate the quality of a system is its economic success. Among the various factors that go into this evaluation is its power consumption. The increasing number of tasks and clock rate can also affect the system's power consumption. It is difficult to predict the exact consumption of a system due to the complexity of its hardware. Techniques such as optimizing memory and clock traffic, gating clocks, and dynamically adjusting clock rate can help reduce the power consumption of system on chips.

Due to the complexity of a system's design, it is critical that the system's development is performed in parallel. This is done using virtual prototyping, where the software is simulated on a virtual hardware. Depending on the complexity of the system and the implementation technology chosen, a complex trade-off can be made. Some technological choices, such as FPGAs, can provide shorter time to market. [4.8] NRE cost includes the hardware and software costs, as well as the computational resources needed to complete the system's design.

4.1.5 PCB DESIGN SOFTWARE

Electronic design automation (EDA) software called EAGLE is a scriptable tool that can be used to capture and manage various design features, such as printed circuit boards (PCBs). It was acquired by software company Autodesk in 2016. [4.9]

The EAGLE schematic editor is used to create circuit diagrams. It stores the diagrams in various files with the .SCH, .BRD, and .LBR extensions. Parts can be placed on various sheets and connected through ports. It features an automatic router that automatically connects traces based on the connections in the schematic. [4.10] Although these formats are accepted by most PCB fabrication companies, many of them also accept EAGLE board files, which can be exported directly to production. This makes the software ideal for small design firms and home users. The system can be controlled using keyboard hotkeys or by entering commands at an embedded command line. It can also be combined with other scripts to create various design files.

4.1.6 TEMPERATURE SENSING

One of the main characteristics for this project is to accurately monitor the temperature of any given solar panel set up by the user to monitor its temperature over time and catalog the raw data in real time for further analysis.

A Temperature sensor is a device to measure temperature readings through electrical signals which is usually composed between two distinct types of metals or composites which generate voltage or resistance once there is a difference in temperature. In today's market a sensor designer has a wide variety of options available for temperature sensors in which there are two basic physical types to choose from Contact Temperature Sensors in which the sensor must be in physical contact with the measurable object to detect the change in temperature. The second type is Non-contact Temperature Sensor in which the object does not have to be in physical contact to measure its temperature [4.11].

On this Project will be focusing on a Contact Temperature sensor to have the ability to monitor the temperature behind any given solar cell panel in any types of configurations array. This is especially important since the main goal of this project is to be available to monitor the temperature of every single solar cell to detect any abnormalities and catalog the efficiency of different types of solar cells according to its temperature. Therefore, we will be considering only contact temperature sensors which encompass thermistors, thermocouples, RTD and diodes.

Diode as a Temperature Sensor: Diodes as a temperature transducer is a common type of application for diodes in which a moderate temperature sensing can be used for the Give an application. One of the benefits of using a diode as a temperature sensor is that linearity of the temperature coefficient Such as that it can provide negative $-2\text{mV}/^\circ\text{C}$ for the overall operating range [4.12]. The most common temperature sensor using a diode is the LM335 in which has a breakdown voltage directly proportional to the absolute temperature at $10\text{mV}/\text{K}^\circ$, low dynamic impedance of less than 1Ω , with a current operation of $400\mu\text{A}$ to 5mA [4.13]. In addition to a 25°C calibration which gives the sensor a 1°C error from its temperature sensing range of -50°C to 150°C which is highly linearized voltage over temperature output [4.13].

Thermistor: A thermistor also known as thermal resistor is a resistive load who's resistivity variates due to a change in temperature. A typical thermistor is composed of two terminals sensitive transducers composed of semiconductor-based metal oxides such as cobalt, manganese or nickel with a metallized or center connecting beat formed from a ceramic disc or bead. [4.14]. On a typical thermistor as temperature raises resistance goes down and as temperature decreases resistance increases. Thermistors offer a highly accurate resolution within a ranging from $\pm 0.05^\circ\text{C}$ to $\pm 1.5^\circ\text{C}$ and depending on the bead coting it can have a temperature range as low as -50°C to as high as 572°C [4.15]. For most applications there are two types of resistors that can be implemented Class A thermistors that offer higher measurement accuracy and Class B thermistors that offer a lower resolution but a higher temperature range.

Thermocouple: A thermocouple is a simple and basic component the consists of two junctions of two different types of metal join at one end. By having two dissimilar metals both metals heat up at different rate which causes a temperature difference between the cold junction at the base of the wire couple and the hot junction that is connection of the wire couple at the tip of the connected metals creating a thermo-electric effect inducing a voltage measured in millivolts that can be low as 10mV [4.16]. Thermocouples temperature range is one of broadest ranges of all the current temperature sensors in the market today. Thermocouples can encompass temperature as low as -200°C all the way to over 2000°C , which makes it one of the most popular temperature sensors implemented on the market [4.16]. Furthermore, there are various types of thermocouples in the market with different types of sensitivity and conductor composition which affects its temperature range as we can see in Table 4.1.

Table 4.1: Types of Thermocouples

Type	Sensitivity	Conductor Material
J	0 °C to 750 °C	Iron/Constantan
N	0 °C to 1250 °C	Nicrosil/Nisil
U	0 °C to 1450 °C	Copper/Copper Nickel
T	-200 °C to 350 °C	Copper/Constantan
E	-200 °C to 900 °C	Nickel Chromium/Constantan
K	-200 °C to 1250 °C	Nickel Chromium/Nickel Aluminum

RTD: Resistance Temperature Detector (RTD) is a high-resolution temperature sensor that is made from pure conductive metals mainly platinum, copper or nickel and the wound in form of a coil similarly to an inductor. The other form of RTD is a thin film composed of platinum paste encased in a white ceramic substrate [4.16]. RTD's are like thermistors both change their resistance with a change in temperature. But unlike thermistors the output voltage of an RTD is highly linearized which means it has a higher resolution. In the other hand while an RTD has a higher resolution then a thermistor it has a much lower Sensitivity compared to a thermistor since as temperature changes it produces a small change such as $1\Omega/\text{°C}$ [4.16]. A standard RTD has a typical resistance of 100Ω at 0°C in which the most implement type is Platinum Resistance Thermometer (PRT) and a range of -200°C to over 600°C [4.17].

Apart from the different types of contact temperature sensors there is also different wire configurations and shielding configurations that today's marketplace offers for a wide range application that offer different benefits. For instance, in some applications you want to monitor the temperature inside a corrosive environment such as in a chemistry laboratory where the lead can be exposed to corrosive chemicals, so you need a protective welded bead as seen in Figure 4.6 or shielding in your wire to prevent the distinct metals from corroding making the temperature sensor less reliable due to a change in composition.



Figure 4.6: Weld Beaded with Different Styles of Shielding Thermocouple. Reproduction permission requested from Thermosense Limited.

Beaded Wired Thermocouple: A Beaded Wired Thermocouple is composed of a welded bead composed of a metal alloyed. For these types of thermocouples is best to utilized when measuring the temperature of gases or non-oxidizing liquids that could corrode the metal alloyed. The main benefits of this type of thermocouple are the smaller profile then the average thermocouple and it can provide a high response time.

Non-Insulated Thermocouple: A non-insulated thermocouple just as the name implies is simply a thermocouple without a layer of insulation, this could have been done for various reason one of

them is costs. If a thermocouple does not need a special shielding for the wire in higher temperature implementations or if the thermocouple is not going to be exposed to the elements.

Braid/twisted Insulated Thermocouple: A Braid/twisted thermocouple is usually an insulated thermocouple that is twisted at the tip of the junction to reduce noise picked up by the wires from nearby power wires. This is commonly used in places where a thermocouple is close to a power line or if a long wire is used to connect the thermocouple. This is due to the induced electromagnetic fields pickup by a long wire that can act as an antenna picking up unwanted environmental noise. To reduce this noise, we can twist the wire in such a way that the opposing magnetic fields of the wires can cancel each other reducing the noise leaking into the system.

As presented in the design specifications one of our requirements for this project is to be available to implement a contact temperature sensor for the “All-in-One PV Sensing node” or “All-in-One Sensor Mote” with the motive of data logging the temperature behind a solar panel. One of the flexibilities that our sponsor/client from OUC gave us is the discretion of changing the temperature sensor as the design requires but prefers the use of a thermocouple. In which case for our design, we decided to follow our sponsor/client request for the use of a thermocouple in our design.

4.1.6.1 SIGNAL CONDITIONING

Signal Conditioning: Signal conditioning refers to any necessary manipulation of the voltage signal that is necessary to be available to successfully process it in the next stage of processing. In the case for a thermocouple there is a necessity for signal conditioning this is due to various factors such as environmental factors and hardware limitations. Most Signal Conditioning cases that main condition signal components include but are not limited to capacitors for low and high pass filtering, operational amplifiers to amplify small voltage of sensors if the voltage too small to detect, and differential amplifiers where the voltage ratio is an issue where you run the risk of amplifying unwanted noise. The basis of signal condition can be found in the block diagram in Figure 4.7.

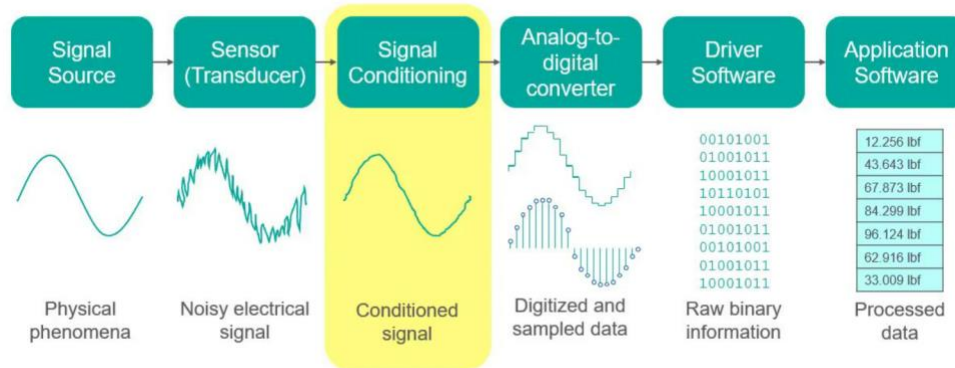


Figure 4.7: Basic Conditioning Signal Block Diagram. Reproduction permission requested from TT Electronics.

4.1.6.2 SIGNAL CONDITIONING WIRE NOISE

The main reason we look at noise to voltage ratio is due to the low voltage output in mV produced by the thermocouple and its due to this that any major noise to voltage ratio would cause a significant signal misinterpretation by the hardware that is to read the signal coming from the thermocouple. Therefore, the main resolution is limited by the noise to voltage ratio of the design.

Thermocouple Wire Noise: wire noise is considered as any signal inference cause by induce crossing magnetic fields cause by EMF from nearby sources of noise such as Alternating Current devices and power lines such as the US standard of 60 HZ AC power lines in parallel with the thermocouple wire leads, AC motors and proximity to radio transmission antennas. This noise is cause by the air capacitance created by the crossing of magnetic fields if a thermocouple wire is in parallel to such power lines or rails. Creating a capacitive coupling introducing perceptible noise in our system proportional to the neighboring power current magnitude and inversely proportional to the distance of the thermocouple wires [4.18].

Thermocouple Wire Antenna Effect: Another source of noise in the wire for a thermocouple is cause by the charging effect that cause long thermocouple wires to act as an antenna receiving environmental noise from nearby radio stations, Wi-Fi, or any type of radio wave been broadcasted.

Noise to Voltage Ratio: Noise to Voltage Ratio is the ratio between the voltage output of the thermocouple according to the spectral density W/Hz of the RMS noise voltage per square root hertz or $\frac{nV}{\sqrt{Hz}}$ [4.19].

Thermocouple Resolution/Accuracy: Resolution/accuracy regarding a thermocouple refers to the smallest temperature reading produced from the smallest voltage difference created by the thermocouple. Example of such is a Type K thermocouple HI93530N has a 0.1° resolution.

The main purpose on wanting to reduce the noise to voltage ratio is due to the low voltage output in mV produced by the thermocouple in which any major noise to voltage ratio would cause a significant signal misinterpretation by the hardware that is to read the signal coming from the thermocouple. Therefore, the main resolution is limited by the noise to voltage ratio of the design. To avoid this hurdle, we can implement a couple of tested solutions offered and recommended by the thermocouple manufactures such as implementing a twisted wire thermocouple as the name implies a twisted wire thermocouple as discussed previously is a thermocouple with twisted wire in such a way where the opposing magnetic fields of the wires can cancel each other reducing the receive noised this can be viewed in Figure 4.8.

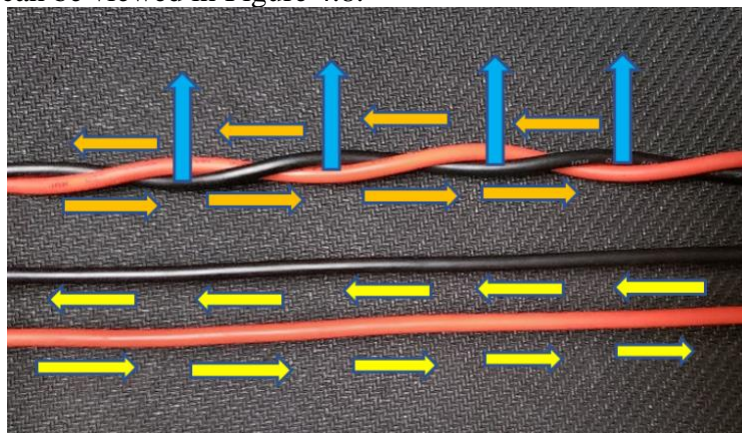


Figure 4.8: Parallel vs. Braided Wire Configuration by Marco Herrera.

As seen in Figure 4.8 twisting the wire around we can create a short of loop along the wire also known as nodes. On this nodes Electromagnetic Fields generated from the source load will rotate when passing along from node to node creating opposite magnetic fields to those generated externally in which case, they will eventually cancel each other out.

4.1.6.3 SIGNAL CONDITIONING AMPLIFICATION

Another factor that noise can affect in the conditioning of the signal is that in most cases the thermocouple voltage output has to be amplified to analyze the voltage difference and increase the resolution of our design or if the hardware requires a higher voltage, then that thermocouple can be provided to detect the voltage properly. Therefore, if a noise is introduced before the amplification circuitry the noise can be amplified leading to a high noise to voltage ratio reducing our resolution.

Operational amplifier: An operational amplifier (op-amp) is at its core voltage amplification integrated circuit or IC that can amplify a weak electrical signal usually in range of millivolts. The typical operational amplifier has a differential input where there are two input pins and one output pin [4.20]. The purpose of having two input pins is to output the voltage difference between the two input pins giving you an amplified voltage by the ratio factor of the two input pins called GAIN.

They are linear devices that have all the properties required for nearly ideal DC amplification and are therefore used extensively in signal conditioning, filtering or to perform mathematical operations such as add, subtract, integration and differentiation.

Differential amplifier: A differential amplifier behaves similarly to an operational amplifier in which the difference between the two inputting voltage pins gets amplified producing the amplified voltage in the output pin [4.21]. The main difference is that the differential amplifier also suppresses the common voltage between the two pins reducing noise in the amplified signal. This is the main implementation of a differential amplifier is mainly used to suppress noise generated by the wires of the given component that needs amplification which induces an electromagnetic induction called noise due to the potential difference of the signal source ground and circuit ground [4.22].

4.1.6.4 SIGNAL CONDITIONING COLD JUNCTION COMPENSATION

Cold Junction Compensation: Cold junction compensation is a technique used for thermocouples where the reference junction needs to appear as 0°C even if the temperature is not. This is achieved by adding a voltage or subtracting a voltage from the thermocouple's output voltage [4.89]. The implementation of this concept is typically done electronically by using a common LM355 accurate temperature sensor which is a solid-state device that behaves closely to a Zener Diode. Since a Zener Diode has reverse bias breakdown voltage which is fairly linear, therefore, the LM335 has a similar linearity on the reverse bias which causes the sensor to behave linearly according to the absolute temperature in which the sensors were calibrated by the manufacturer typically in Kelvin. An instance, if an LM335 extrapolates from 0 kelvin producing 0 volts at 273 Kelvin the breakdown voltage will be 2.73 Volts [4.89]. Due to this linearity of breakdown voltage this sensor is used to monitor the temperature at the reference leads or Cold Junction leads to subtract or add the voltage value from the Hot Junction lead or probe lead.

There are several methods for Cold Junction Compensation with different degrees of accuracy. The main five methods typically used in industry applications and labs consist of 3 types of temperature gradients below ambient temperature 0° C, above ambient temperature, and ambient temperature. The first method consists of a constantly applying 0° C to the reference junction leads by submerging the reference leads in a water and Ice mixture. The Second Method is related to the first method in which a constant temperature of 0° C will be applied to the reference junction, but this will be done by using a Peltier refrigeration device. The third method is mainly composed of hardware components where an electrical bridge method will be used to compensate the cold

junction in form of an opposite voltage that opposes the voltage produced by the LM335. The fourth method is the use of an isometric block or material in which it will be kept at room temperature, this will produce a constant ambient temperature in which a transducer such as LM335 can be placed to produce a voltage that can be subtracted or added from the voltage produced by the Hot Side or probe of the thermocouple. The 5th method is the user double oven to emulate 0 degrees Celsius, this is achieved by having two ovens at two different temperatures one at a set temperature set by the user and the second oven set twice the set temperature by user this will create an equivalent EMF resulting in a net effect of equivalent voltage simulating a thermoelectric effect of 0° C at the Cold Junction [4.89].

A commonly used method for high accurate Cold Junction Compensation and that is easily implemented is the use of an Ice bath. In this case the reference junction leads, or Cold Junction leads are placed on a container with ice water with a constant temperature of around 0°C to 0.1°C and then change regularly to main this temperature. Once the desired temperature is reached between 0°C to 0.1°C the voltage produced by the difference in temperature is now more linearly closer to the expected calibrated output of the manufacturers reference chart of voltage expected over a set temperature. Furthermore, these expected values can be theoretically calculated by the difference in temperature by the electromotive force also known as $E = \frac{W}{Q}$, while this equation is the foundation of electromotive force the equation needs to be changed to work with our system therefore, we will use:

$$E_{emf} = -S\Delta T = S(T_{HOT} - T_{COLD}) \quad [4.90]$$

Where E_{emf} is the thermocouple voltage output, T_{COLD} is the temperature of the Cold junction, T_{HOT} is the temperature of the HOT Junction where we want to know the temperature or set a temperature and S is the constant coefficient known as Seebeck for a temperature dependent material. For instance, a Type K thermocouple material coefficient is around 4.1 $\mu\text{V}/^\circ\text{C}$ for a temperature range of 0° to 1000°C [4.90].

4.1.7 DATALOGGERS

One of the main market offerings for Photovoltaic data logging is the use of dataloggers in which you can connect a great variety of analog outputting sensors. In this case once all the sensors are connected to the data logger one can access the results through a live server usually provided by the manufacturer.

Furthermore, this type of datalogger has multiple ADCs making a great choice for analog sensors. In addition to this, every single input of the datalogger offers low noise amplification. This can allow sensors that tend to have noise mixed in their output to bypass the need for filtering that it would otherwise require.

While the data logger is a great choice for monitoring a PV system and to keep track of raw data, it is not a great economic choice to do so. Furthermore, it requires the usage of additional equipment or sensors to monitor parts of the PV system in which case every single added sensor needs to be routed to the main data logger adding to the cost of installation further increasing costs. One such example of how a data logger can be used as a PV monitoring system can be found in our sponsor's OUC testing facility. On their testing array they have installed a data logger with cables going underground coming from all the sensors connected to the solar panel array installation area. As we can see in Figure 4.8 OUC Datalogger PV monitoring system not only requires all sensors to be externally connected to the datalogger it also requires the use of a bulky power supply.

4.1.7.1 CR310 & LOGGERNET

The CR310 Datalogger is a multi-purpose, compact, and low-cost measurement and control data logger that was provided to our team by our sponsor, OUC [4.23]. As said before, dataloggers are an incredibly useful technology that allow many types of sensors to congregate in a single hub to be measured and recorded. This is one of the technologies that the All-In-One PV Sensors aims to replace. If we can attach a small, cheap datalogger to the direct output of any given solar panel, the voltages and currents generated by that panel no longer need to go toward a datalogger to be measured. Along with this, the a-la-carte option of adding a pyranometer or thermocouple to the All-In-One PV Sensor eliminates the need to have a pyranometer or thermocouple running to this datalogger as well. These changes can significantly decrease the costs and workloads associated with monitoring and measuring solar panel systems. OUC's Datalogger can be seen near their Solar Testing Array where the All-In-One PV Sensors will be installed in Figure 4.9.



Figure 4.9: OUC Datalogger for Solar Testing Array by Marco Herrera.

The CR310 will primarily be used for testing as we cannot blindly assume our sensors are providing the correct data when plugged in or operating. The CR310 can be seen in Figure 4.10.



Figure 4.10: CR310 Datalogger by Maguire Mulligan.

The CR310 is an entry-level datalogger which works fine for our application. We do not intend on applying this datalogger anywhere in our system due to its bulky size, high power requirement, and an incredibly high cost. These downsides are a result of the dataloggers many functionalities: the CR310 can measure most hydrological, meteorological, environmental, and industrial sensors. The CR310 can concentrate data and make it easily available both when hard-wired to a computer for data transference or over a network when supplied on-the-go with a battery. For the team's purposes, the CR310 datalogger will be used to assist in calibrating and verifying the measurements of the pyranometer and thermocouple sensors.

The CR310 is a perfect fit for verifying the integrity of our thermocouple and pyranometers because they are both analog sensors. The CR310 has six multipurpose analog input terminals seen on the lower side of the CR310, inputs SE 1 to 6. These inputs can be single-ended, like the thermocouple, or differential, like the pyranometer, accepting an input range of -100 to +2500 mV with an internal 24 bit ADC. [4.23] These bounds are extremely generous for our sensors and ensures that the CR310 will capture all feasible outputs from the thermocouple and pyranometer. Our sensors will be connected to the green terminal blocks and screwed in to ensure that we are measuring a full and correct value. This analog data will be received by the CR310 and measured internally depending on its programming. Given this, we see that to measure the output of our sensors that we are connecting to the CR310, we must understand the layers behind the case and look at the software that is required to run the data-collection on a local desktop, LoggerNet.

LoggerNet is Campbell Scientific's main data logger support software package, supporting programming, communication, and data retrieval between data loggers like our CR310 and a PC [4.24]. This will be the bridge between the CR310's measured data and our testing. Because we do not intend on fully installing the CR310, LoggerNet can be used in its most basic form. This is done by connecting the CR310 over USB to a local computer and directly programming it via LoggerNet's CRBasic Editor or Short Cuts, depending on whether the tested sensor is natively supported.

Once the CR310 is connected to LoggerNet, a custom program can be built like many modern programming languages by incorporating public libraries and calling upon functions that are built into those libraries. Data tables must be set up so that the CR310 can store the data that it is measuring, and custom scans can be set dependent on how often the user wants their sensor to relay data. Figure 4.11 displays our CR310 configuration for testing.

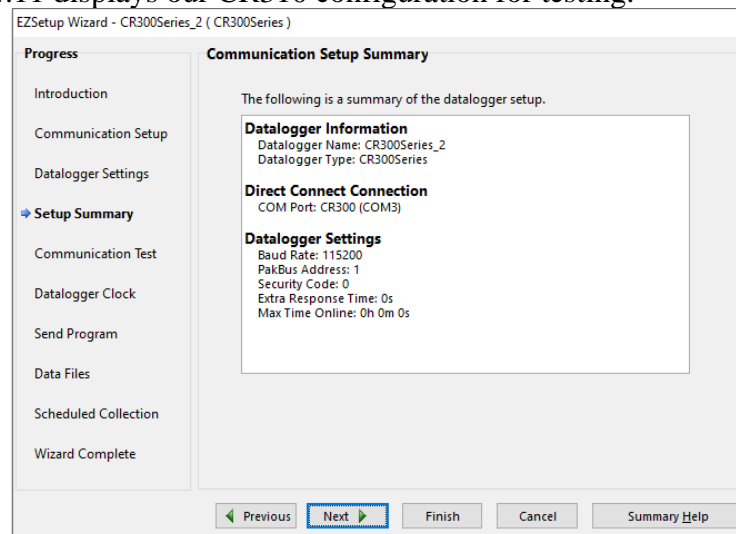


Figure 4.11: Configuration for the CR310 with LoggerNet by Maguire Mulligan.

Once the CR310 is connected and set-up for datalogging, the sensor can be connected. The code that is run on the datalogger determines what sort of data is must look for and where that data can be stored. Custom code provided by OUC allows us to measure an Apogee pyranometer and a standard Type-T Thermocouple. Figure 4.12 shows what one would expect when running the code and monitoring the real-time data collection of the CR310.

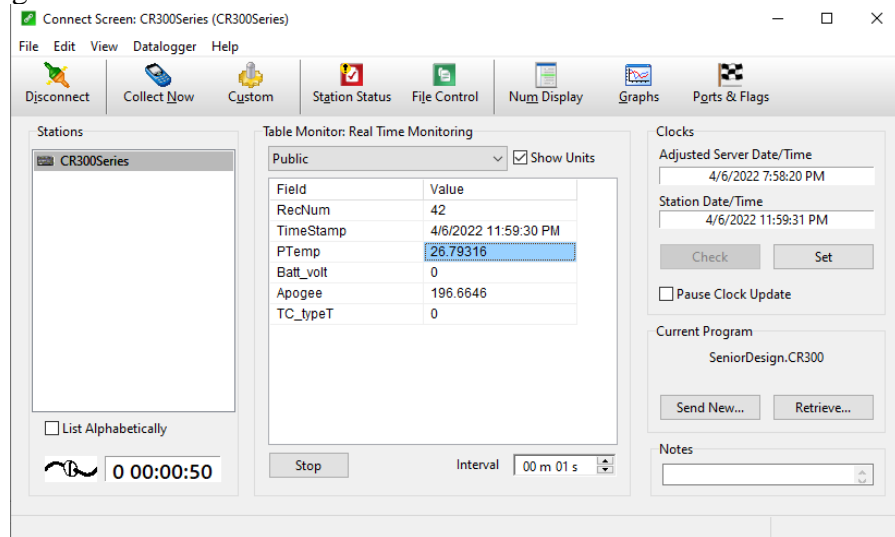


Figure 4.12: Real-Time Monitoring of the CR310 by Maguire Mulligan.

In this example, only an Apogee Pyranometer was being used to test the CR310's data collection capability. Seen in the value result for the field "Apogee" is 196.6646. This number represents the raw millivolt output of the pyranometer. The maximum output of the pyranometer is around 200 mV, and for this example, the pyranometer was pointed directly at the sun for maximum irradiance exposure. Seeing this, we can conclude that the pyranometer is working correctly and will output a correct millivolt value in accordance with its irradiance.

4.2 MARKET ANALYSIS & EXISTING EFFORTS

In this subsection, existing applications of current and voltage focused inclusive sensors will be investigated and discussed for our engineering prototype. These will provide a strong groundwork for the ideologies that will be included in our design and allow us to reflect on the work of those before us for inspiration.

4.2.1 TIDA-00640

Our team was unable to find any commercially available products that were able to sense voltage, current, temperature, and irradiance and possess the ability to transfer the data that it analyzes wirelessly to a local node or database. While that is the case, there is at least one working version of our sensor out there designed by Texas Instruments: the TIDA-00640 whose block diagram is seen in Figure 4.13. TI created this design for in-house testing purposes and does not offer this product commercially. This design featured a PCB that integrated voltage, current, and temperature sensors into a single system which was able to wirelessly communicate data to a central point through several wireless standards [4.25].

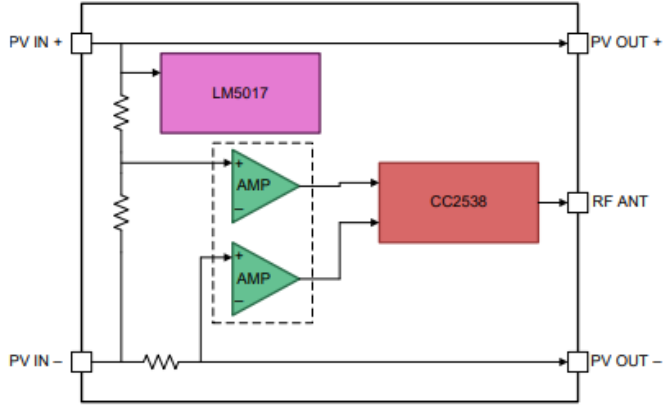


Figure 4.13: TIDA-00640 Block Diagram. Reproduction permission requested from Texas Instruments.

The scope of the TIDA-00640's design is like our project's and was the main driving point of inspiration for Phase 1 of the All-In-One PV Sensor. However, this design does not work directly with a Solar Panel but instead an MLPE, or Solar Module Level Power Electronic. While this is the case, their design would mostly work when connected directly to a Solar Panel's output via MC4 Connection Cables which was heavily incorporated by Phase 1's design.

It's important to understand how the TIDA-00640 is interconnected so that we may further understand the inner operations of it. For example, it would be best to understand how it senses voltage, current, & temperature, how the board is powered, and how the data leaves the board to a local database.

Like our design choice, the TIDA-00640 uses a simple voltage divider alongside an amplifying configuration to measure the panel voltage. Because their full-range output from the panel is around 90 V, they needed to step down the voltage to a more acceptable level to give their circuitry some room to breathe. Their voltage divider decreased the input voltage by a factor of 50.8 giving them a final voltage of around 1.77V. High value resistors were used to limit power loss in the divider and to minimize current draw from the panels. With a total drop of 510 kilohms, the voltage divider draws only 177 uA from the panel.

Concerning their current measurement, the TIDA-00640 makes use of a low-value current shunt resistor. They elected to do this to keep system complexity at a minimum and due to their sensor's location. Had they elected to be placed at the input of their MLPE module and not the output, then they would have had to account for a single module's current rather than an entire string. Their shunt resistor should be able to handle a maximum of 10 A, like the design requested by OUC. In a typical 300-W solar module, the power loss caused by the existence of a shunt resistor with a resistance value of 1 milliohm to measure current is a negligible 0.03%. The value passed to the ADC is the voltage measured across this small resistor. Due to this voltage being 0.01V even when a maximum of 10A is passing through the shunt resistor, this value is increased by a factor of 260 using an amplifying configuration to give an overhead of about 2.6V to be sent to the ADC.

The TIDA-00640's temperature sensor is a derivative of the TIDA-00649's temperature sensing functionality which is also a derivative of the internal analog temperature sensor present in the CC2538. This temperature sensor measures the system level temperature at the module level rather than at the power electronics, serving to be a part of a larger system level. This is unlike what we aim to do with our All-In-One PV Sensor. The thermocouple that we are implementing to measure

temperature will be measuring the direct temperature of the panel and not any internal temperatures of our hardware.

On the other hand, the TIDA-00640's power supply is almost identical to the intended power supply for the All-In-One PV Sensor; the TIDA-00640 is fully powered by the solar module that it is measuring. This is possible due to the selected LM5017 step-down regulator. The original output voltage that the team at TI faced was upwards to 90 V which could not power a PCB without frying their intended components. With the introduction of the LM5017, they were able to decrease any voltage in the range of 7.5 to 100 V to a more acceptable 3.3V required for their design.

Finally, it's important to understand how the TIDA-00640 transmits its data from the on-board ADC to a wireless database for data analysis. The CC2538 was mentioned in the temperature sensor section, and it continues to have its uses in wireless transmission. The CC2538 is made with an integrated IEEE 802.15.4 wireless radio supporting ZigBee PRO/2.0, ZigBee 3.0, and Contiki to transmit data for their personal reasons, TI chose to use ZigBee to send their data. While both these sensors and the All-In-One PV sensor will transmit data wirelessly, they will not be using similar transmission technologies.

4.2.2 OPENGREENENERGY

The TIDA-00640 was the closest the team could find to a mainstream product that reflected our goals and needs. However, there do exist personal research projects and hobbyist materials that also aim to monitor and evaluate connected PV systems. While these projects may not be able to accommodate the same voltage or current ranges that our All-In-One Sensor aims to, they should still be researched to review their thought processes and any observations they have made along the way.

One such project was created by a hobbyist identified as OpenGreenEnergy who created detailed instructions to create a DIY Solar Panel Monitoring system for small-scale PV systems [4.26]. While this system's specifications are lower than what OUC requires and therefore cannot be replicated to fit our requirements, understanding what OpenGreenEnergy set out to achieve and how they achieved it is ultimately more important to understand.

OpenGreenEnergy's design can measure the voltage, current, and ambient temperature of the panel, and is able to send that data wirelessly to Blynk, an app platform popular with Internet of Things users. This design measures voltages by using a voltage divider, current by using the AC723 hall effect current sensor, and ambient temperature with the DS18B20 temperature sensor. Similarly, to our tentative design, OpenGreenEnergy's concept uses the ESP32 for all calculations and wireless communications. Figure 4.14 lists all relevant components of OpenGreenEnergy's design.

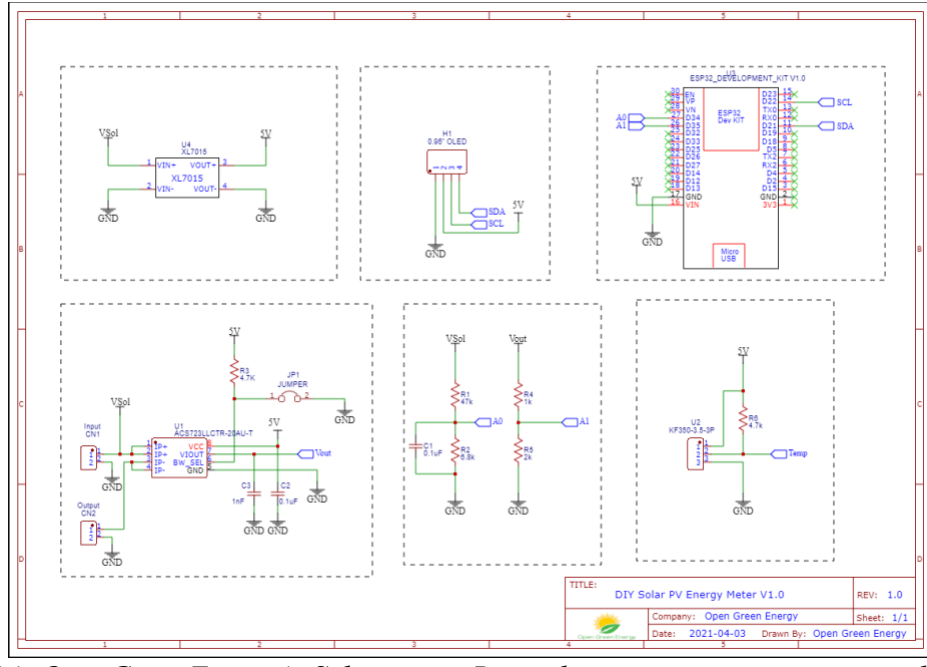


Figure 4.14: OpenGreenEnergy’s Schematics. Reproduction permission requested from Open Green Energy.

A key component of this design is the XL7015 buck converter. This is a DC-to-DC step-down module that converts a maximum voltage of 80 V down to 5V. In this design, this converted voltage will act as the supply voltage for the ESP32 and the AC723 Current Sensor. The main takeaway from this design is this component – the existence of a converter is crucial to our project to ensure that the high voltages received from the solar panel will be small enough to power our components without burning them.

4.3 COMPONENT SELECTION AND IMPLEMENTATION

In this section, the specifications of what is required for the functionality of the All-In-One PV Sensor is greatly scrutinized. We will take a deep look at the numerous sections of hardware and software involved in the creation of the All-In-One PV Sensor and understand what components will fit best in our design. Major components are selected definitively such that prototyping can begin, but many of the smaller and more volatile components may see changes based on chip availability. Decisions will be made as necessary for the health of the All-In-One PV Sensor.

4.3.1 ADC CONSIDERATIONS

The primary source of data in this project will be the voltages and currents generated by and received from the Solar Panel. The solar panel will output purely analog, nearly DC signals for our circuitry to sense and deliver wirelessly to a collector node. An Analog to Digital Converter, or ADC, can take an analog signal as an input and transform it to an easier to understand and represent signal in a digital format. In this application, an ADC can accept an analog input voltage or current and represent it as a digital number reflecting that measured value’s magnitude. This will allow our selected microcontroller to read, interpret, and transmit the necessary data.

An analogue to digital converter is an electronic device which converts continuous time-varying analog signals into discrete-time digital signals so that they can easily be read by the digital devices. They first sample the signal, then quantify it to determine the resolution of the signal, and

finally set binary values and send it to the system to read the digital signal. The ADC is essentially comprised of an analog comparator and a Digital-to-Analog Converter. Since digital devices can count in binary, bits are used to determine the resolution of the converter. The resolution of the ADC is the number of bits it uses to digitize the input samples. For an n bit ADC, the number of discrete digital levels that can be produced is 2^n . Thus, a 12-bit digitizer can resolve 212 or 4096 levels. For this project, we would require an ADC with a minimum resolution of 12-bits to obtain our values [4.27].

The data that this All-In-One PV Sensor will process will not be too large or demanding, so the ADC can be cheaper or feature lower resolutions compared to more industrial applications. A comparable All-In-One PV sensor created for in-house use by TI, the TIDA-00640, makes use of a 12-bit ADC with eight channels, so we could expect to use similar or lower resolution equivalent ADCs.

ADC Constraints

The existence of an external ADC in this project is entirely dependent on the MCU that is selected to transmit data – for example, if a Raspberry Pi model were to be selected, certain Raspberry Pi compatible ADCs would need to be considered. If a model that includes an ADC were to be selected, such as an ESP32, then an ADC would be unnecessary as it would already be present in the chip. Therefore, a large selection is required to future-proof this design.

All sensors will require an ADC, regardless of their configurations and selections of pyranometers or thermocouples as the solar panel will always send an analog voltage and current signal. Therefore, the ADC must be considerably cheap to minimize the overall cost of the All-In-One PV Sensor.

ADC Considerations – External, Surface-mounted ADC

In this section, the possibility that an MCU is selected that is not the Raspberry Pi OR a chip that includes a built-in ADC. Therefore, the considered ADCs will be surface mounted to the PCB for all other sensor elements to connect to.

MCP3428: This 16-bit, dual channel ADC has 4 differential inputs with an analog supply voltage of 2.7 to 5.5V and a singular unit price-point of \$3.11. This sensor is low noise and high accuracy and can output up to 240 samples per second when employed under its 12-bit mode. It features both one-shot conversion and continuous conversions which is suitable for both rapid data streams and considerably slower data processing speeds. [4.28]

ADC084S051CIMM/NOPB: This ADC is 8-bits with 4 inputs to accommodate for all the possible inputs in one All-In-One PV Sensor. The internal analog to digital converter is based on a successive-approximation register architecture with an internal track-and-hold circuit. It has a single unit price of \$2.94 and operates with a single power supply that can range from 2.7 V to 5.25V. However, it is limited by this – this ADC's analog input voltage must fall between 0V and its supply voltage, severely limiting this ADC's ability to function in higher voltage environments.

CC2538: The CC2538 is the ideal wireless microcontroller System-on-Chip (SoC) for high-performance ZigBee applications. The device combines a powerful ARM Cortex-M3-based MCU system with up to 32KB on chip RAM and up to 512KB on-chip flash with a robust IEEE 802.15.4 radio. This enables the device to handle complex network stacks with security, demanding applications, and over-the-air download. The CC2538 contains a power on reset (POR) module and a brown out detector (BOD) that prevent the device from operating under unsafe supply voltage conditions. It contains a 12-Bit ADC With 8 Channels and Configurable Resolution, and the current cost is \$4.464.

MCP3008: The MCP3008 is programmable to provide four pseudo-differential input pairs or eight single-ended inputs. Differential Nonlinearity (DNL) and Integral Nonlinearity (INL) are specified at ± 1 LSB. Communication with the devices is accomplished using a simple serial interface compatible with the SPI protocol. The MCP3004 A/D converters employ a conventional SAR architecture. With this architecture, a sample is acquired on an internal sample/hold capacitor for 1.5 clock cycles starting on the first rising edge of the serial clock once CS has been pulled low. The resolution is its ADC is 10-bits, and the cost of the microchip is \$4.50

CC3220x: The SoC Wireless MCU CC3220x device comes in three variants: CC3220R, CC3220S, and C3220SF. The CC3220R features 256KB of RAM, IoT networking security and device identity/keys. The CC3220S builds on the CC3220R and MCU level security such as file system encryption, user IP (MCU image) encryption, secure boot, and debug security. The CC3220SF builds on the CC3220S and integrates a user-dedicated 1MB of executable Flash, in addition to the 256KB of RAM. When a stable power is applied to the CC3220x chip for the first time or when supply voltage is restored to the proper value following a period with supply voltage less than 1.5 V, the level of each digital pad is undefined in the period starting from the release of nRESET and until DIG_DCDC powers up. This period is less than approximately 10ms. They feature a 4-Channel 12-Bit ADCs and cost \$3.696.

ADC Considerations – Raspberry Pi Extensions

In this section, the possibility that a Raspberry Pi is selected is considered. Certain models of Raspberry Pi can transmit data wirelessly and connecting an ADC to that Pi would allow the ADC to communicate directly with the wireless transmitter.

MCP3008: This ADC is low-cost, 8-channel, and 10-bit. It has a single unit price of around \$4.50 and pairs extremely well with the Raspberry Pi and its respective models. It connects directly to the Pi using an SPI serial connection and the additional channels have designated connections to all Raspberry Pi models. For example, the VDD and VREF of the MCP3008 will always connect to the Pi's 3.3V pin. [4.29]

ADS1015/ADS1115: These two ADCs are of the same branch. The ADS1015 is a 12-bit, 4-channel ADC that utilizes I2C communication to interact with the Raspberry Pi. The ADS1115, on the other hand, is an improved 1015 with a higher precision featuring 16-bits rather than 12. Because of the nature of our project, these higher bit counts are only necessary if a higher-than-expected accuracy is required from the ADC. For this reason, these parts will only be considered if that condition comes about, as they are priced much higher than the MCP3008 at \$9.95 and \$14.95, respectively. [4.29]

ADC Considerations – A review of possible chips with built-in ADCs

In this section, rather than focusing on adding an ADC to our board, we'll review the features of the ADC on any possible MCU or Wireless Transmitter that is considered for our final design.

ESP32: The ESP32 is a low-cost and low-power microcontroller that has Wi-Fi and Bluetooth capabilities. For this reason, the ESP32 is being considered to replace the Raspberry Pi for wireless transmission in addition to its market availability. Models of the ESP32 can integrate two 12-bit SAR ADCs, supporting up to 18 measurement channels which is far more than the project requires. An average ESP32 microcontroller is valued at ~\$10 and is considerably cheap when considering its additional features. [4.30]

MSP430BT5190: This MSP controller has a 12-bit ADC with Bluetooth functionality which is enough to transmit data over a range of about 20 meters. For this project, that range is acceptable, but future endeavors may seek other wireless transmission. However, this chip is expensive compared to even an external ADC, so the only thing that can be taken from this controller are its

ideals. The high-performing clock would allow us to retrieve data from the Solar Panel and translate it at much higher rates which would be ideal for rapid data collection and analysis. Table 4.2 provides a summary of these findings.

Table 4.2: Summary of considered ADCs

ADC	External/Surface Mount	Raspberry Pi Ext.	ADC in MCU
Top Choice	ADC084S051CIMM	MCP3008	ESP32
Samples per Second	200 to 500 ksps	200 ksps	200 ksps
Communication Interface	SPI	SPI	Directly to MCU
Input Channels	4 inputs	8 inputs	Up to 18 inputs
Price	\$2.94	\$4.50	\$10 for chip

For our design, we decided to use the Esp32. It met the required specifications needed for the sensor, and more importantly it uses WIFI as the communication protocol. We chose to use WIFI over Zigbee and Bluetooth to transmit our data. The CC3220x family of microcontrollers also uses WIFI, but the chips are out of stock and are hard to find to purchase from legitimate sources; this is a big and common problem when dealing with and designing real circuits that are to be implemented. The MCP3008 was also a solid option, but since it is only an ADC, we would not be able to transmit data from the chip to the node unless a secondary attachment is connected to it. So, the Esp32-Wroom-32 would be our design choice.

4.3.2 MICROCONTROLLER AND MICROPROCESSOR

We will be implementing two logic devices in our design: a microcontroller, ESP32-WROOM-32, and a microprocessor, Raspberry Pi 4 Model B+. This section will explain the details of these devices.

4.3.2.1 ESP32

The ESP32 is a low-power SoC developed by Espressif Systems which possesses both Wi-Fi and Bluetooth wireless communication capabilities. There are many variants of the ESP32 microprocessor, like the ESP32-D0WD-V3, ESP32-U4WDH, ESP32-S0WD, and many more. The variant we will be implementing in our design is the ESP32-WROOM-32, which features many functions that will help satisfy our design requirements like multi-channel analog to digital converters (ADC), digital to analog converters (DAC), multiple general-purpose input/output (GPIO) pins, serial peripheral interface (SPI), Inter-Integrated Circuit (I2C), universal asynchronous receiver-transmitter (UART), variable input power voltage, among many others. The comprehensive ESP32 block diagram is pictured in Figure 4.15. [4.31]

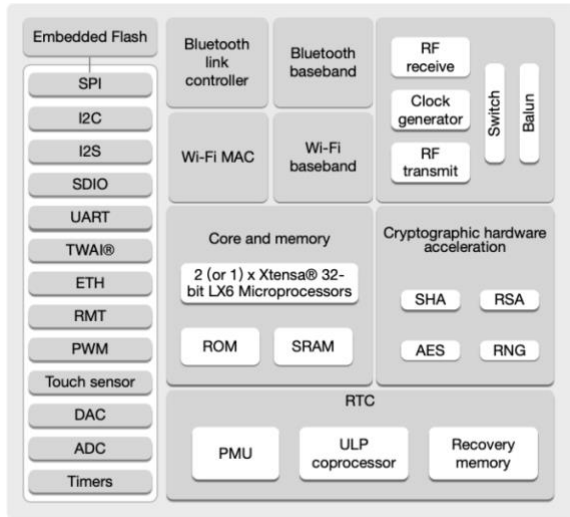


Figure 4.15: ESP32 Functional Block Diagram. Reproduction permission requested from Espressif Systems.

Figure 4.16 features the pin layout of the ESP32, which we will heavily depend on when inserting the ESP32 chip into our PCB and connecting busses from our four (4) sensor devices. [4.31]

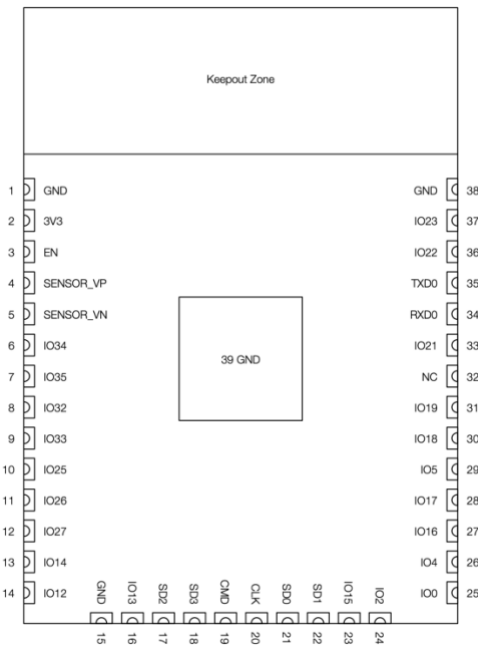


Figure 4.16: ESP32-WROOM-32 Pin Layout. Reproduction permission requested from Espressif Systems.

ESP32-D0WDQ6

At the heart of our ESP32-WROOM-32 is a ESP32-D0WDQ6. Within the Wroom is a series of connections that, such as an antenna, Crystal, capacitors, and other connections which turn the ESP32 to an easy-to-use platform. ESP32-D0WDQ6 is designed for mobile, wearable electronics, and Internet-of-Things (IoT) applications. It features all the state-of-the-art characteristics of low-power chips, including fine-grained clock gating, multiple power modes, and dynamic power scaling. For instance, in a low-power IoT sensor hub application scenario, ESP32 is woken up

periodically only when a specified condition is detected. Low-duty cycle is used to minimize the amount of energy that the chip expends. The output of the power amplifier is also adjustable, thus contributing to an optimal trade-off between communication range, data rate and power consumption.

ESP32 is a highly integrated solution for Wi-Fi-and-Bluetooth IoT applications, with around 20 external components. ESP32 integrates an antenna switch, RF balun, power amplifier, low noise receives amplifier, filters, and power management modules. As such, the entire solution occupies minimal Printed Circuit Board (PCB) area.

Integrated Crystal

The ESP32-WROOM-32 contains an in built 40 MHZ crystal. Frequency stability is very key when dealing with the output signal. To obtain a very high level of oscillator stability a Quartz Crystal is generally used as the frequency determining device to produce another type of oscillator circuit known generally as a Quartz Crystal Oscillator.

When a voltage source is applied to a small thin piece of quartz crystal, it begins to change shape producing a characteristic known as the Piezo-electric effect. This Piezo-electric Effect is the property of a crystal by which an electrical charge produces a mechanical force by changing the shape of the crystal and vice versa, a mechanical force applied to the crystal produces an electrical charge. Then, piezo-electric devices can be classed as Transducers as they convert energy of one kind into energy of another (electrical to mechanical or mechanical to electrical). This piezo-electric effect produces mechanical vibrations or oscillations which can be used to replace the standard LC tank circuit in the previous oscillators. [4.32]

The quartz crystal used in a Quartz Crystal Oscillator is a very small, thin piece or wafer of cut quartz with the two parallel surfaces metallized to make the required electrical connections. The physical size and thickness of a piece of quartz crystal is tightly controlled since it affects the final or fundamental frequency of oscillations. The fundamental frequency is generally called the crystals “characteristic frequency”. Once cut and shaped, the crystal cannot be used at any other frequency. In other words, its size and shape determine its fundamental oscillation frequency.

Crystal oscillators use the mechanical vibration of a crystal to generate the clock signal. Due to the molecular composition of the crystal matter and the angle in which the crystal is cut, this type of oscillator is very precise and stable over a wide temperature range. The most used crystal is the quartz crystal. Producing quartz crystals requires very stable temperature and pressure conditions over a few weeks. This makes crystal oscillators more expensive than RC oscillators. Due to the Crystal within the ESP32, there would be no need to attach an external integrated crystal, this helps to reduce the complexity of the circuitry, also it reduces the space used on the PCB. The crystal also makes use of decoupling capacitors to stabilize and achieve the intended oscillation frequency. Figure 4.17 shows the configuration of the integrated crystal. [4.33]

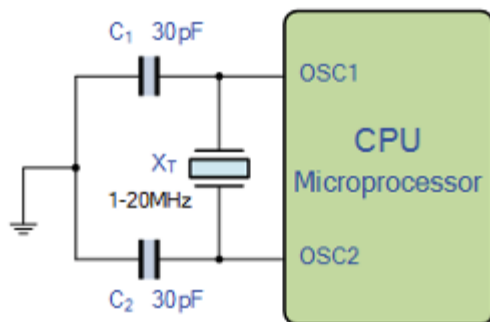


Figure 4.17: Integrated Crystal Oscillator. Reproduction permission requested Electronics Tutorial..

Capacitor

Another important part of the PBC would be the decoupling capacitor. They aren't only found close to the integrated crystal, but on other parts of the electrical components. The capacitor itself is a very important passive electronic device. The capacitor is a component which has the ability or "capacity" to store energy in the form of an electrical charge producing a potential difference (Static Voltage) across its plates, much like a small rechargeable battery.

There are many kinds of capacitors available from very small capacitor beads used in resonance circuits to large power factor correction capacitors, but they all do the same thing, they store charge. In its basic form, a capacitor consists of two or more parallel conductive (metal) plates which are not connected or touching each other but are electrically separated either by air or by some form of a good insulating material such as waxed paper, mica, ceramic, plastic, or some form of a liquid gel as used in electrolytic capacitors. The insulating layer between a capacitor's plate is commonly called the Dielectric.

Due to this insulating layer, DC current cannot flow through the capacitor as it blocks it allowing instead a voltage to be present across the plates in the form of an electrical charge. When used in a direct current or DC circuit, a capacitor charges up to its supply voltage but blocks the flow of current through it because the dielectric of a capacitor is non-conductive and basically an insulator. However, when a capacitor is connected to an alternating current or AC circuit, the flow of the current appears to pass straight through the capacitor with little or no resistance. We would take advantage of this function to create lowpass filter by placing the capacitor parallel to the input voltage of our components. This will help to filter out the AC voltage and let the DC voltage pass through, in this way, it acts as a decoupling capacitor.

In any design that involves semiconductor ICs, you'll always need decoupling capacitors. That's because the voltage supplied to the components is far from ideal. Unlike the perfect horizontal line depicted in theory, voltage readings in real-life applications tend to fluctuate even if you've got the cleanest power supply.

The decoupling functions as a reservoir and acts in two ways to stabilize the voltage. When the voltage increases above the rated value, the decoupling capacitor absorbs the excessive charges. Meanwhile, the decoupling capacitor releases the charges when the voltage drops to ensure the supply is stable. In Figure 4.18 we can see the cross section of a ceramic capacitor. This form of capacitor would be used through our project. [4.34]

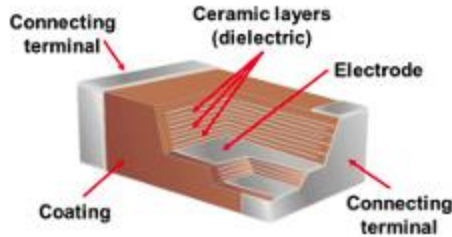


Figure 4.18: Capacitor Cross Section. Reproduction permission requested Electronics Tutorial.

4.3.2.2 RASPBERRY PI

The Raspberry Pi is a series of single-board computers made by the Raspberry Pi Foundation. It was originally developed to promote basic computer science education in developing nations. The original model was initially targeted to hobbyists and roboticists, but it has since been used in various other applications. After the release of the second model, the Raspberry Pi Foundation was renamed to Raspberry Pi Trading, and it was headed by Eben Upton.

The Raspberry Pi 4 Model B was released in June 2019. It featured a 1.5 GHz 64-bit quad core processor, 8 GB of RAM, and support for dual-monitor setups. The Pi 4 has a slightly lower price tag with 8 GB of RAM. It's also powered by a USB-C port, and it can be operated with 5 volts. The initial Raspberry Pi 4 had a design flaw that prevented third-party cables from identifying it and refusing to provide power. This issue was corrected in the 1.2 revision of the board. In 2021, the Pi 4 B variants started receiving an improved version of the Broadcom BCM2711C0, which is used for the Pi 400 and the Pi 4 B. The model we will be implementing in our design is the Raspberry Pi 4 B+ as in Figure 4.19. [4.35]

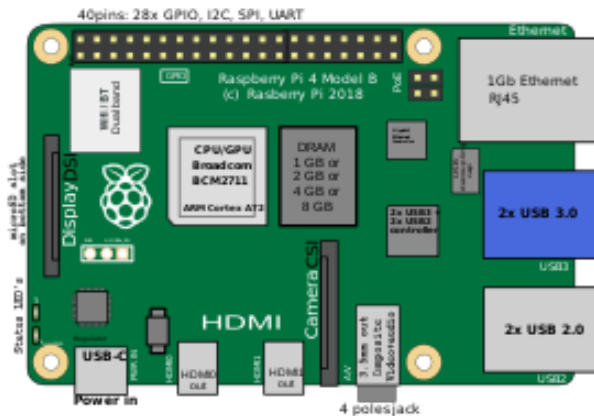


Figure 4.19: Raspberry Pi 4 B+ Diagram [4.107]

Since its inception the Pi has been a cutting-edge piece of modern technology as it contains all that a consumer computer would need to operate on a single board the size of a credit card. This means you can plug a monitor, peripherals like mouse, keyboard, and speakers, all into a single Pi. As described earlier, the Pi contains all the technology that any other SoC offers and more. [4.35] We will be using a Pi in our design as the hub where all the data from our multiple ESP32 devices will be sending data to. The Pi will compile all our data into a database so that OUC can easily access and analyze data collected by our AIO sensor.

4.3.3 CURRENT SENSOR

One of the requirements of the OUC was to incorporate a current sensor into our circuit design. This would be used to accurately measure and monitor the current flowing out of the solar panel, giving the result in 10 second intervals. This was a task that the previous group was unable to achieve with their design; in this section, we would look at different methods we can use to gain the desired result. First let us understand the tool that will be used to sense current flow in the All-In-One PV sensor

Current Sense Resistor

The current sense or shunt resistor is a resistor, typically with a low resistance value, which the load current flows into in a current sensing circuit. According to TI “The value of the resistor is usually based on achieving a desired maximum differential voltage at the highest expected current. The resistor value may also be based on the power-loss budget.” We have already been given the highest expected current and the power range of the panel, so we can determine the right shunt for the operation.

Another important consideration is the resistors tolerance since this has a direct impact on the accuracy of our measurement. A higher tolerance means it has a higher percentage of error, while a lower tolerance means the resistor has a lower percentage of error; so, we would get the lowest taking into consideration the price. There is also the resistor temperature coefficient; due to power dissipated, and environmental factors, the resistors value could be affected if the tolerance is too low. Since the sensor would be outside, and current would be flowing through the shunt, a resistor that can manage high temperature would be used. A typical shunt resistor configuration can be seen in Figure 4.20. [4.36]

The power rating is also an important factor to consider when choosing a shunt resistor. The Resistor Power Rating is sometimes called the Resistors Wattage Rating and is defined as the amount of heat that a resistive element can dissipate for an indefinite period without degrading its performance. When an electrical current passes through a resistor due to the presence of a voltage across it, electrical energy is lost by the resistor in the form of heat and the greater this current flow the hotter the resistor will get. Resistors are rated by the value of their resistance and the electrical power given in watts, (W) that they can safely dissipate based mainly upon their size. Every resistor has a maximum power rating which is determined by its physical size as generally, the greater its surface area the more power it can dissipate safely into the ambient air or into a heatsink.

We know from Ohm’s Law that when a current flows through a resistance, a voltage is dropped across it producing a product which relates to power. In other words, if a resistance is subjected to a voltage, or if it conducts a current, then it will always consume electrical power and we can superimpose these three quantities of power, voltage and current into a triangle called a Power Triangle with the power, which would be dissipated as heat in the resistor at the top, with the current consumed and the voltage across it at the bottom.

As the dissipated resistor power rating is linked to their physical size, a 1/4 (0.250) W resistor is physically smaller than a 1W resistor, and resistors that are of the same ohmic value are also available in different power or wattage ratings. Carbon resistors, for example, are commonly made in wattage ratings of 1/8 (0.125) W, 1/4 (0.250) W, 1/2 (0.5) W, 1W, and 2 Watts. So normally, the larger their physical size, the higher its wattage rating. However, it is always better to select a particular size resistor that is capable of dissipating two or more times the calculated power. When resistors with higher wattage ratings are required, wire wound resistors are generally used to dissipate the excessive heat. [4.94]

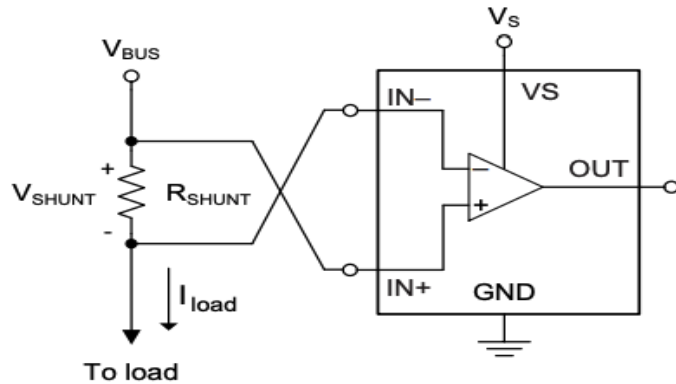


Figure 4.20. Shunt Resistor Configuration. Reproduction permission requested Texas Instruments.

Table 4.3 features the possible shunt resistor packages that we could use in the implementation of the current sensing circuitry in the All-In-One PV Sensor.

Table 4.3: Shunt Resistor Considerations

PACKAGE	TOLERANCE (%)	RESISTANCE (mΩ)	POWER RATING (W)	UNIT PRICE (\$)
805	1	10	0.5	0.53
1206	1	10	1	0.64
2512	1	10	2	0.65
1206	0.5	10	0.5	0.74
2512	0.5	10	1	1.66
2512 wide	0.5	10	2	2.16
2512	1	100	3	1.57
0805	5	100	0.25	0.68

Current sense Amplifier

Now we know what device allows the current to flow through, then what measures the current. This is where the current sense amplifier comes in play. The Current sense amplifiers, also called current shunt monitors, are specialized differential amplifiers which measure the voltage drop across a sense element; in this case it would be the shunt [4.37]. We can understand how they do this when we consider ohms law; $V=I/R$, if the resistor value is low enough, the values of the voltage would be very close to the current value. The Amplifier amplifies the voltage signal, and the ADC reads a voltage value that is like the current. They are normally easy to use and tend to be precise and less prone to noise. They can support a wide range of current, and can support common-mode voltages from -16 to +80 V.

Key parameters

When choosing the Amplifier, there are some key parameters to consider:

Common Mode Range: the DC voltage range at the input of an amplifier with respect to ground. Current sense amplifiers are typically designed to support common-mode voltages well beyond

the chip supply voltage. For example, an IC can support a common-mode voltages between -8 V to +70 V while running on a supply as low as 2.1 V.

Common mode voltage is defined as the average voltage, which is applied to the two inputs of an amplifier. In the case of an op amp, the two inputs are at practically the same potential with only a small voltage offset between them. So effectively, you can see the common mode voltage on either input.

Common mode input voltage range is also known as input voltage swing. This term describes the range of input common mode voltages that can be used for normal linear operation of the amplifier. The common mode input voltage range is always defined relative to the positive supply and the negative supply. When you exceed the common mode input range, the output becomes non-linear.

Offset Voltage: This is a differential DC error at the input of the amplifier. ICs can offer current sense amplifiers with offsets as low as $10\mu\text{V}$, enabling higher precision measurements at low currents and allowing the use of smaller value shunt resistors. Ideally this voltage would be zero, but it is always a non-zero voltage. Small offset voltages can lead to large errors, which can increase over device age and operational temperature.

The offset voltage (input offset voltage) is defined as the voltage that must be applied between the two input terminals of the op amp to obtain zero volts at the output. Ideally the output of the op amp should be at zero volts when the inputs are grounded. The input terminals are at slightly different dc potentials. V_{IO} is represented by a voltage source that is in series with either the positive or negative input terminal.

Gain: Current sense amplifiers have a variety of gain options, that have different performances over temperature and shunt resistance value. The gain of an op amp signifies how much greater in magnitude the output voltage will be than the input. For example, an op amp with a resistor, R_{IN} , of $1\text{K}\Omega$ and a resistor, R_F of $10\text{K}\Omega$, will have a gain of 10. This means that the output will be ten times greater in magnitude than the input voltage.

Temperature Stability: According to TI, “Current sense amplifiers integrate the amplifier along with all the gain-setting resistors which enables small and unified temperature drift. This allows for robust current measurements across the whole specified temperature range. The achieved temperature stability is one of the key advantages current sense amplifiers have over discrete implementations.” [4.38]

There are three main design considerations when choosing the amplifier:

High-Side Measurements [4.38]: this is a sensing technique that involves placing the sense resistor between the supply voltage and the load. This system directly monitors the current delivered by the supply, which allows for the detection of load shorts. High-side current sensing does not create ground disturbances. Ground disturbances are problematic when other circuits in a system are required to interface with the load. Placing the shunt resistor above the load, as in high-side current sensing, eliminates ground disturbances because the shunt resistor is no longer connected directly to ground. In high-side current sensing, the shunt resistor remains in the circuit and can detect a surge in current from a short to ground condition.

The main disadvantage is that because the shunt resistor is not at system ground, a differential voltage must be measured which requires the precise matching of the proper differential amplifier. A sample High-Side configuration can be seen in Figure 4.21.

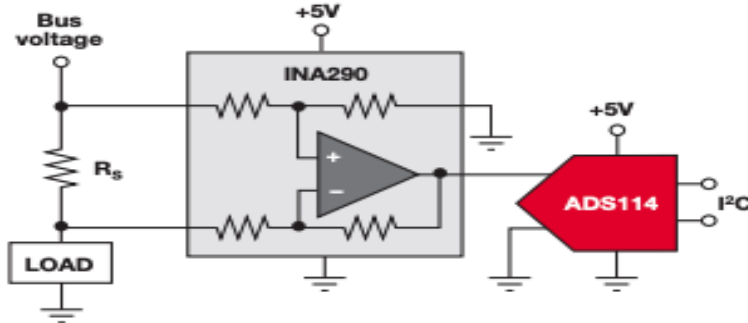


Figure 4.21: High-Side Shunt Resistance Measurement. Reproduction permission requested Texas Instruments.

Low-Side Measurements [4.38]: This is a sensing technique that involves placing the sense resistor between the Load and the ground. In this design, the common-mode voltage is near ground, which allows for the use of single-supply, rail-to-rail input/output op amps. Low-side sensing is often the least expensive and simplest method to implement because if one end of the sense resistor is at system ground, and the other end of the resistor is at the ground side of the load whose current is to be measured, then the voltage across the resistor with respect to system ground can be amplified by a simple op-amp referencing the same system ground.

The disadvantage of low-side sensing is related to its advantage, placing a resistor in the load's path to ground. This resistor placement results in the load's ground floating at a slightly higher voltage than the system ground. The most common issue with this arrangement is potential ground loop problems. Since the load is not at the same ground potential as the other loads in the system, the system can develop an audible noise, such as a hum, or even produce interference with nearby equipment, including audio and video interference. In addition, low side sensing cannot detect fault conditions such as a short or open circuit in the ground path due to connection problems or outside interference. A sample low-side configuration can be seen in Figure 4.22. [4.39]

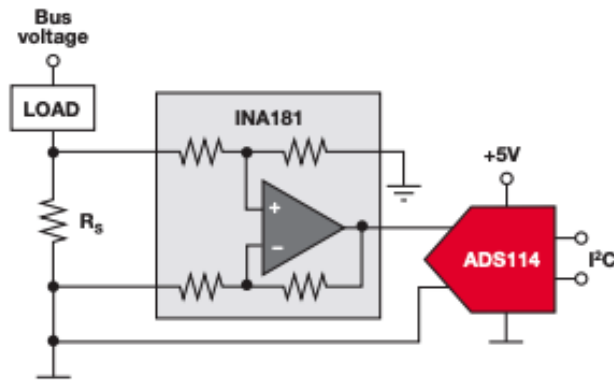


Figure 4.22: Low-Side Configuration. Reproduction permission requested Texas Instruments.

In-line Measurements [4.38]: This current sensing technique connects the current sense element in-line to the load. Here, the current being passed across the motor is measured and used in feedback and control calculations. During the slew of the PWM signal, the inputs of the amplifier are exposed to a signal that is quickly moving approximately between ground and a large input voltage. This exposure leads to large common-mode transients being injected into the amplifier; nonideal for a device attempting to pass a precise measurement for the purposes of feedback control. This can be seen in Figure 4.23:

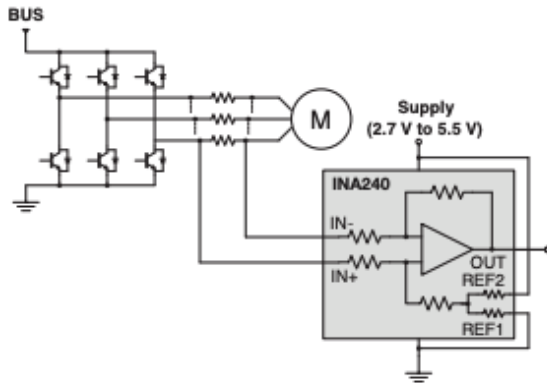


Figure 4.23: In-Line Configuration. Reproduction permission requested Texas Instruments.
The configuration for this design would be the low-side sensing technique. It is more applicable for the sensor we are designing.

Current Sense ICs

Looking into the amplifiers that we could use, there were four integrated circuit (IC) that stood out, 3 current sense amplifiers, and one Operational amplifier. The main factor of choosing the IC is the current and voltage sensing capability.

INA219[4.40]: It is a bidirectional current shunt and power monitor with an I²C- or SMBUS-compatible interface. The device monitors both shunt voltage drop and bus supply voltage, with programmable conversion times and filtering. A programmable calibration value, combined with an internal multiplier, enables direct readouts of current in amperes. The two analog inputs to the INA219, IN+ and IN-, connect to a shunt resistor in the bus of interest. The INA219 is typically powered by a separate supply from 3 to 5.5 V. The bus being sensed can vary from 0 to 26 V. There are no special considerations for power-supply sequencing (for example, a bus voltage can be present with the supply voltage off, and vice-versa). The INA219 senses the small drop across the shunt for shunt voltage and senses the voltage with respect to ground from IN- for the bus voltage.

Measuring current is often noisy, and such noise can be difficult to define. The INA219 offers several options for filtering by choosing resolution and averaging in the Configuration register. These filtering options can be set independently for either voltage or current measurement. An important aspect of the INA219 device is that it measures current or power if it is programmed based on the system. The device measures both the differential voltage applied between the IN+ and IN- input pins and the voltage at IN- pin. Figure 4.24 shows INA219 configuration.

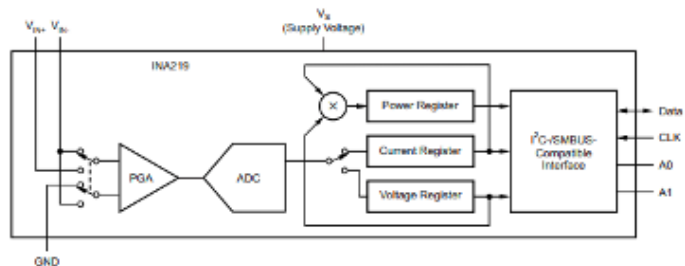


Figure 4.24: INA219 Configuration. Reproduction permission requested Texas Instruments.

INA3221[4.41]: It is a three-channel, high-side current and bus voltage monitor with an I²C- and SMBUS compatible interface. The INA3221 monitors both shunt voltage drops and bus supply voltages, in addition to having programmable conversion times and averaging modes for these signals. The INA3221 is a current-shunt and bus voltage monitor that communicates over an I²C- and SMBus-compatible interface. The INA3221 performs two measurements on up to three power supplies of interest. The voltage developed from the load current passing through a shunt resistor creates a shunt voltage that is measured between the IN+ and IN- pins. The device also internally measures the power-supply bus voltage at the IN- pin for each channel. The differential shunt voltage is measured with respect to the IN- pin, and the bus voltage is measured with respect to ground. The INA3221 is typically powered by a separate power supply that ranges from 2.7 V to 5.5 V. The monitored supply buses range from 0 V to 26 V.

The INA3221 features a software reset that reinitializes the device and register settings to default power-up values without having to cycle power to the device. Use bit 15 (RST) of the Configuration register to perform a software reset. Setting RST reinitializes all registers and settings to the default power state except for the power-valid output state. Figure 4.25 shows INA3221 configuration.

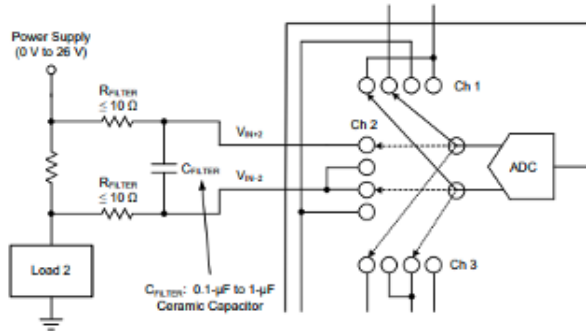


Figure 4.25: INA3221 Configuration. Reproduction permission requested Texas Instruments.

LM5056A[4.42]: It combines high-performance analog and digital technology with a PMBus complaint SMBus and interface to accurately measure the electrical operating conditions of systems connected to a backplane power bus. LM5056/LM5056A continuously supplies real-time power, voltage, current, temperature and fault data to the system management host via the SMBus interface. The LM5056/LM5056A provides intelligent monitoring of the input voltage, output voltage, input current, input power, temperature, and an auxiliary input. There exists a VDD power on reset (VDDPOR) threshold on VDD of 3.8 V. The VDDPOR threshold must be surpassed to ensure proper telemetry readings. VDD must be powered externally by a 5 V power supply with an allowable tolerance of $\pm 10\%$. The SMBus address of the LM5056/LM5056A is captured based on the states of the ADR0, ADR1, and ADR2 pins (GND, NC, VDD) during turn on and is latched into a volatile register once VDD has exceeded its POR threshold of 3.8 V.

The LM5056/LM5056A is designed to measure temperature remotely using an MMBT3904 NPN transistor. The base and collector of the MMBT3904 should be connected to the DIODE pin and the emitter to the LM5056/LM5056A AGND. Figure 4.26 shows the LM5056A Configuration.

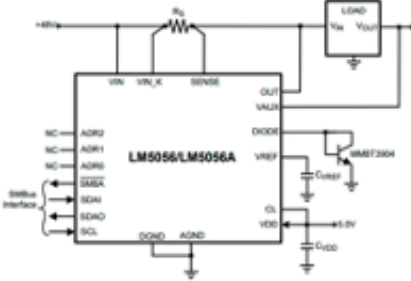


Figure 4.26: LM5056A Configuration. Reproduction permission requested Texas Instruments.

TLV342IDR [4.43] The TLV34xx devices are single and dual CMOS operational amplifiers, respectively, with low-voltage, low-power, and rail-to-rail output swing capabilities. These single-supply amplifiers are designed specifically for ultra-low-voltage (1.5 V to 5 V) operation, with a common-mode input voltage range that typically extends from -0.2 V to 0.5 V from the positive supply rail. The supply voltage must be chosen such that it is larger than the input voltage range and output voltage range. For instance, this application scales a signal of ± 0.5 V to ± 1.8 V. Setting the supply at ± 2 V is sufficient to accommodate this application. The supplies can power up in any order; however, neither supply can be of opposite polarity relative to ground at any time; otherwise, a large current can flow through the input ESD diodes. TI highly recommends adding a series resistor to the grounded input to limit current in such an occurrence. V_{sup+} must be always more positive than V_{sup-} ; otherwise, a large reverse supply current may flow. Figure 4.27 shows TLV342IDR Configuration.

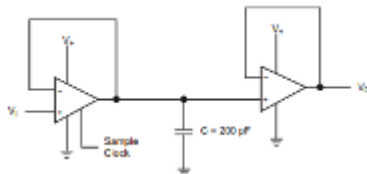


Figure 4.27: TLV342IDR Configuration. Reproduction permission requested Texas Instruments.

Current Sense Amplifier Comparison

Given the option of IC's that could possibly be used, we would now look at the specification of each device, comparing them to see which one could potentially be used as an amplifier for the All-In-One PV sensor. Table 4.4 provides a comparison of a few ICs.

Table 4.4: A comparison of Current Sense Amplifier Integrated-Chips

Current Amplifier:	INA219	INA3221	LM5056A
Common mode voltage (Min) (V):	0	0	10
Input offset (+/-) (Max) (uV):	50 100	80	300
Input offset drift (+/-) (Typ) (uV/C):	0.1	0.1	
Gain (V/V):	1 0.5 0.25 0.125	1	1 0.5
Gain error drift (+/-) (Max) (ppm/°C):	83	50	
Bandwidth (kHz):	5.5	3.5	0.5
Supply voltage (Max) (V):	5.5	5.5	80
Supply voltage (Min) (V):	3	2.7	10
Iq (Max) (mA):	1	0.35	6.8
Digital interface:	I2C SMBus	I2C SMBus	I2C PMBus SMBus
Features:	Bi-directional Programmable Gain	Alert Function Bi-directional Low-side Capable	Digital Temp Monitor
Approx. price (USD):	\$0.840 1ku	\$1.575 1ku	\$2.048 1ku

After looking at the specifications of the IC's, the probable choice for the current sensor would be the TLV342IDR. All the components have their benefit, and they can perform the operation we need. However, the TLV342IDR has an edge in necessity and price. We would need the device to sense the current from the solar panel, we would not need the other features the other IC's present. As a result, the TLV342IDR would be more efficient, also due to the features of the IC's, they become pricier, so the amplifier presents the cost-effective option. The other component that could be likely used would be the INA219, this would be due to its precision in its reading. Figure 4.28 shows a TLV342IDR current sensing configuration.

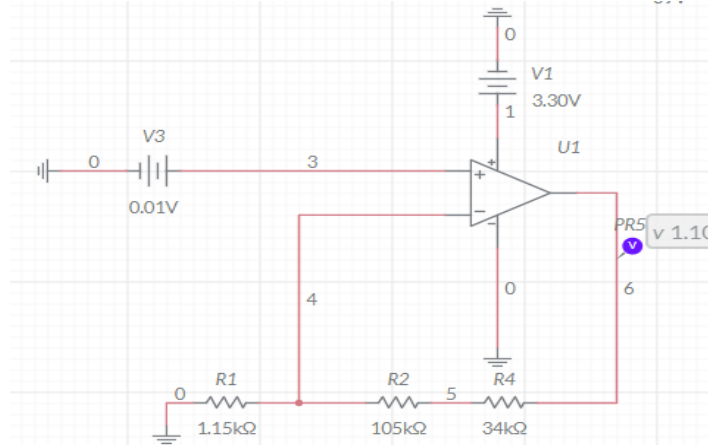


Figure 4.28: TLV342IDR Current Sensing Application in Multisim Live by Timothy Aja.

To measure the current from the solar panel, we must construct a differential amplifier circuit connected to the pins of the TLV3421DR. We aimed to achieve a result without saturation, so 1.10 - 1.22 V range was chosen to be sent to the ADC. The voltage coming through the shunt would be exceptionally low approximately 0.01 V ($10 \text{ A} \times 0.001 \Omega$), so we calculated a gain that would boost the voltage going to the ADC. We used a $1.15 \text{ k}\Omega$ and $139 \text{ k}\Omega$ precision resistor to get an overhead gain of 122; this makes the final voltage 1.22 V ($V=10 \text{ A} \times 0.001 \Omega \times 261 = 1.22 \text{ V}$).

Alternative Current Sensing Technique

After performing an exorbitant amount of research about current sensing, we noticed that there were several points of failure and factors against low side current sensing, especially due to ground disturbance which causes an increase in the offset voltage, and this would noticeable when using the TLV342 which has a 4 mV offset voltage. We decided to design another PCB that incorporates high side sensing instead, but unfortunately, the TLV342 does not have a high enough common mode voltage of about 37 V to handle the high side implementation, so a current sense amplifier would be needed.

The current sense amplifier is specifically designed to handle high common mode voltages with a low offset voltage, and they also come with a fixed gain. More details about the current sense amplifier were discussed thoroughly above.

The IC's we purchased to perform the high side current sensing is the INA290, and the INA293. The INA290 is an ultra-precise current sense amplifier that offers a common mode range of 2.7 - 120 V. This amplifier also has a low offset voltage of $12 \mu\text{V}$; this is far better compared to the TLV342. It is not only designed for DC measurement, but also for high speed applications. This Chip would work well for our application. It also operates with the 3.3 V supply. The IC we got has a fixed gain of 200. Below in Figure 4.65 we can see the error analysis when it senses current across the shunt within our given range.

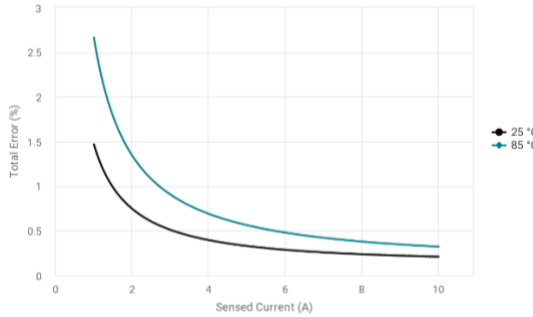


Figure 4.65: INA290 Current Sense Error Analysis

The INA293 is also an ultra-precise current sense amplifier, this one has a slightly different high common mode voltage of -4 – 110 V, extending to the negative region. It features an offset voltage of 20 μ V which is permissible in our design, compared to the higher value that the TLV342 provides. The negative common-mode voltage allows the device to operate below ground, thus accommodating precise measurement of recirculating currents in half bridge applications. [4.109] It is not only designed for DC measurement, but also for high speed applications. This Chip would work well for our application. It also operates with the 3.3 V supply. The IC we got has a fixed gain of 100. Below in figure 4.66 we can see the error analysis when it senses current across the shunt within our given range.

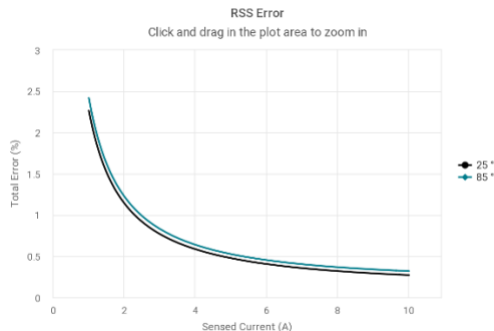


Figure 4.66: INA293 Current Sense Error Analysis

With this precautionous measure in step, we have confidence that the current sensing would work. The main downside of these alternate current sensing chips is the increase in price compared to the TLV342. The Unit price for the INA293 is \$2.966, while for the INA290 it is \$2.503. This would increase the over all cost of the sensors and may exceed the customer's cost requirement.

Hall effect sensor

The ESP32-Wroom includes a hall sensor for magnetic field-sensing applications, which is designed to feed voltage signals to the SAR ADC. It can be controlled by the ULP coprocessor, when low-power operation is required. Let us understand about hall effect sensing and how it is can be used to detect current.

Hall Effect Sensors are devices which are activated by an external magnetic field. We know that a magnetic field has two important characteristics flux density, (B) and polarity (North and South Poles).

The output signal from a Hall effect sensor is the function of magnetic field density around the device. When the magnetic flux density around the sensor exceeds a certain pre-set threshold, the sensor detects it and generates an output voltage called the Hall Voltage, V_H . Hall Effect Sensors consist basically of a thin piece of rectangular p-type semiconductor material such as gallium

arsenide (GaAs), indium antimonide (InSb) or indium arsenide (InAs) passing a continuous current through itself.

When the device is placed within a magnetic field, the magnetic flux lines exert a force on the semiconductor material which deflects the charge carriers, electrons, and holes, to either side of the semiconductor slab. This movement of charge carriers is a result of the magnetic force they experience passing through the semiconductor material.

As these electrons and holes move side wards a potential difference is produced between the two sides of the semiconductor material by the build-up of these charge carriers. Then the movement of electrons through the semiconductor material is affected by the presence of an external magnetic field which is at right angles to it and this effect is greater in a flat rectangular shaped material.

The Hall effect provides information regarding the type of magnetic pole and magnitude of the magnetic field. For example, a south pole would cause the device to produce a voltage output while a north pole would have no effect. Generally, Hall Effect sensors and switches are designed to be in the “OFF”, (open circuit condition) when there is no magnetic field present. They only turn “ON”, (closed circuit condition) when subjected to a magnetic field of sufficient strength and polarity.

The output voltage, called the Hall voltage, (V_H) of the basic Hall Element is directly proportional to the strength of the magnetic field passing through the semiconductor material ($V_H \propto H$).

This output voltage can be quite small, only a few microvolts even when subjected to strong magnetic fields so most commercially available Hall effect devices are manufactured with built-in DC amplifiers, logic switching circuits and voltage regulators to improve the sensors sensitivity, hysteresis, and output voltage. This also allows the Hall effect sensor to operate over a wider range of power supplies and magnetic field conditions. Figure 4.29 is a common depiction of hall effect sensing.

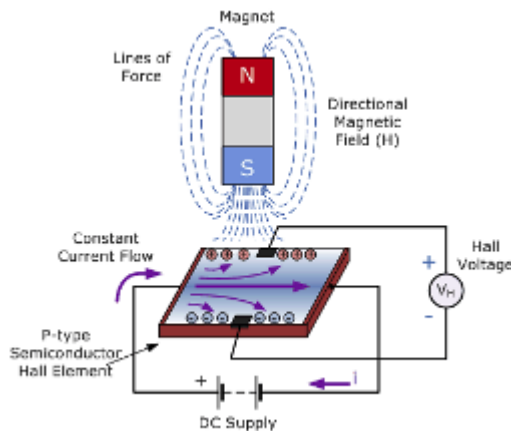


Figure 4.29: Hall Effect Sensing. Reproduction permission requested from Electronics Tutorials.

In ESP32 the Hall effect sensor is located inside ESP32 WROOM 32 chip and the sensor is a piece of wire with continuous current flowing through it. The ESP32 utilizes two 270pf capacitors attached in the chip, each on one line connection to the sensor V_n and sensor V_p pins of the IC. You can activate the hall sensor of the ESP 32 by writing a code that enables the sensor, then you can test the sensor by putting a magnet close to the IC and measure the change in voltage. We could utilize this sensing method instead of using the TLV342 for current sensing.

There are two configurations to consider when performing hall effect sensing, these are the open loop configuration, and the closed loop configuration. [4.44]

Open Loop

In the open loop configuration, the current to be measured flows through a conductor that is inside a magnetic core. In this way, the current creates a magnetic field inside the core. This field is measured by a Hall effect sensor placed in the core air gap.

The output of the Hall sensor is a voltage proportional to the core magnetic field which is also proportional to the input current. The signal produced by the Hall device is usually processed by a signal conditioning circuitry. The signal conditioning circuitry can be a simple amplification stage, or a more complicated circuit designed to eliminate the Hall device drift error.

This configuration utilizes a magnetic core to confine and guide the magnetic field produced by the current. The core offers a path of high permeability for the magnetic field and acts as a field concentrator. The magnetic field inside the core can be hundreds or thousands of times larger than that a given current can produce in free space. It also utilizes an air gap. The air gap subjects the core to the fringing flux phenomena in which some flux lines deviate from their straight path and hence, do not go through the sensor as expected. The air gap can reduce the efficacy of the core at converting the primary current into a strong magnetic field. However, if the gap length is small compared to the gap cross-sectional area, the effect of the fringing effect can be relatively small. However, the air gap allows us to modify the overall reluctance of the core. Adjusting the air gap length, we can change the core saturation level. Figure 4.30 shows effects of air gap on the magnetic field flux density (B). Smaller air gaps result in greater magnetic gain, but the saturation points that occur at the smaller air gaps limit current sensing range.

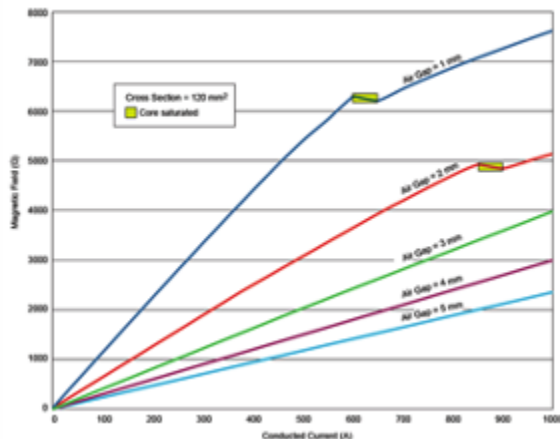


Figure 4.30: Difference in Air Gap Size. Reproduction permission requested from Allegro MicroSystems.

With an open-loop configuration, non-ideal effects, such as linearity and gain errors, can affect the measurement accuracy. For example, if the sensitivity of the sensor changes with temperature, a temperature-dependent error will appear at the output. Besides, with open-loop current sensing, the core is subject to saturation. Moreover, the offset of the Hall sensor as well as the core coercivity can contribute to errors. [4.45] Figure 4.31 shows the open loop topology for current sensing.

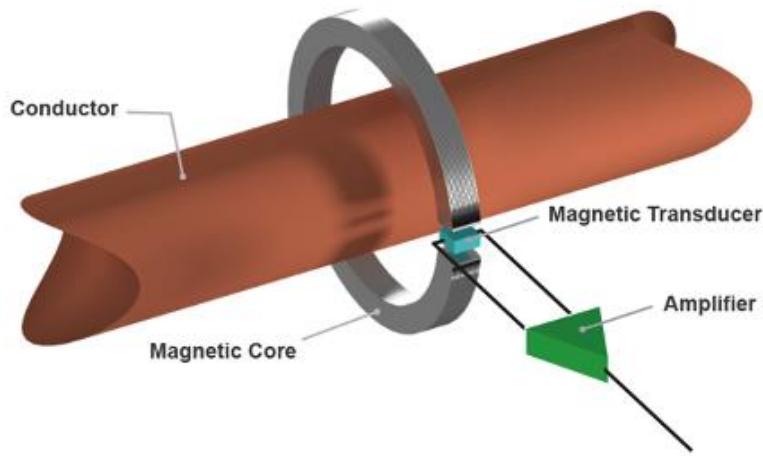


Figure 4.31: Open Loop Topology for Current Sensing. Reproduction permission requested from Allegro MicroSystems.

Closed Loop:

In closed loop configuration, there is a secondary winding that is driven by the output of the feedback path. The feedback path senses the magnetic field inside the core and adjusts the current through the secondary winding so that the total magnetic field of the core becomes equal to zero. The current to be measured flows through the primary conductor and creates a magnetic field inside the core. This field is measured by a Hall effect sensor placed in the core air gap. The output of the Hall sensor, which is a voltage proportional to the core magnetic field, is amplified and converted to a current signal that goes through the secondary winding. The system is designed in a way that the current going through the secondary winding produces a magnetic field that opposes the magnetic field of the primary current.

The negative feedback employed in closed-loop architecture allows us to reduce the non-ideal effects such as linearity and gain errors. That is why, unlike an open-loop configuration, a closed-loop architecture is not affected by drift in the sensor sensitivity. Hence, a closed-loop configuration offers a higher accuracy. A closed-loop current sensor is more robust to core saturation because the magnetic flux density inside the core is exceedingly small.

With closed-loop sensing, the secondary coil is actively driven by a high-power amplifier. The additional components employed in a closed-loop architecture led to a larger PCB area, a higher power consumption as well as a higher price.

Stability issue is another drawback of a closed-loop current sensor. With a closed-loop configuration, we need to derive the system transfer function and make sure that the system is stable. An unstable system can exhibit overshoot or ringing in response to a quick change in the input current. To make a closed-loop system stable, we usually need to limit its bandwidth. However, reducing the system bandwidth can increase its response time and make the system unable to respond to quick changes in the input. An open-loop configuration is usually expected to exhibit a faster response time. [4.45] Figure 4.32 is the closed loop topology for the current sensing.

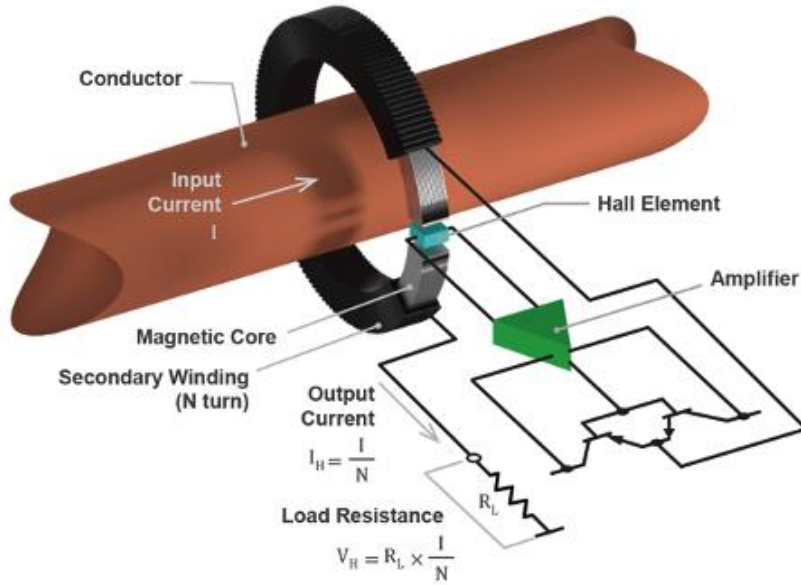


Figure 4.32: Closed Loop topology for Current Sensing. Reproduction permission requested from Allegro MicroSystems.

Performing current sensing for the All-In-One PV sensor is an integral part of the design. The topology that would be best suited for us is the closed loop configuration.

4.3.4 VOLTAGE SENSOR

A voltage divider is a passive circuit element that is used to provide different voltage levels from a common supply voltage. This is also known as a potential divider as it takes the amount potential difference between two points. This divider takes advantage of the effect that occurs when a voltage drops across components connected in series. In essence, the voltage divider turns large voltages into smaller ones. The main purpose of the design is to measure the voltage across a resistor R_2 . The value would end up being a fraction of our input voltage(V_1). This can be represented mathematically through the equation:

$$V_{out} = V_{in} \cdot \frac{R_2}{R_1 + R_2}$$

As seen in this equation, the output voltage is directly proportional to the input voltage and the ratio of R_1 and R_2 . So, by using a greater value of R_2 , we would be able to get a more accurate voltage reading. This is a simple and effective design that we would implement into our PCB to measure the voltage from the solar panel.

It is also important to consider the current going through the resistors. Making a branch between the resistors changes the configuration to parallel, but a voltage divider cannot be made when the resistors are parallel. Therefore, to null this effect, the current going through the resistors must be the same value. Since current in a series circuit is the same among resistors, the current in the resistors must be the same, and higher than the current in the branch (V_{out}). [4.46]

$$I = \frac{V_{in}}{R1 + R2}$$

Voltage Sense IC

We would need an integrated circuit that would be able to measure and handle the panel's voltage. Adding different ICs to calculate voltage and current separately could become complex, fortunately we can use one IC to perform both measurements. As already discussed, the component that would be used is the TLV342IDR. This buffer amplifier would feed the voltage to an analogue to digital converter. The main issue would be the input voltage of the solar panel, which ranges from 32-39 volts. The IC can take only between 1.5-5 volts, so to counteract this, the voltage would be stepped down to the suitable range which the IC can operate in. Figure 4.33 shows our intended TLV342IDR Voltage Sensing application.

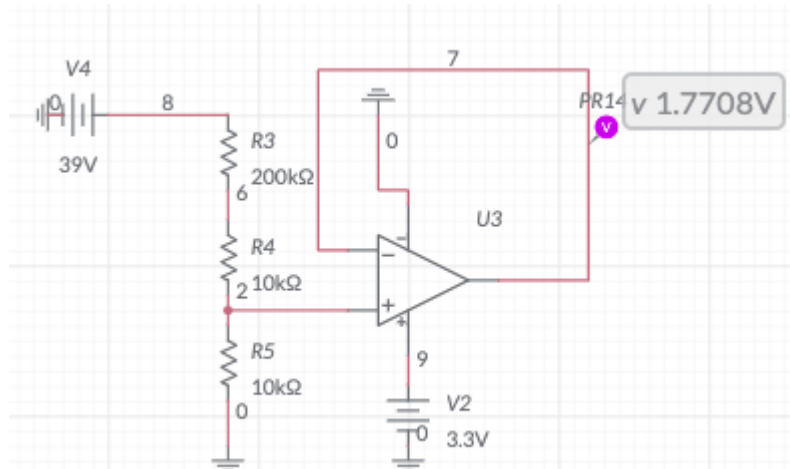


Figure 4.33: TLV342IDR Voltage Sensing Application in Multisim Live by Timothy Aja.

For our voltage sensor, we were using the direct voltage from the solar panel. The panel outputs 39 V max, but our IC can only handle between 1.5 to 5 V, and the ESP 32-WROOM-32 can handle 3.3 V max, so we had to reduce the output voltage. To solve this issue, we used a 10 kΩ and 210 kΩ resistor; this allowed a maximum voltage of 1.77 V ($39\text{ V} \times (10\text{ k}\Omega / (10\text{ k}\Omega + 210\text{ k}\Omega))$) to be read by the ADC. The unity gain buffer provided no gain, but it reduced the power consumption as power use increases if the current increase ($P = I \times V$), so the unity gain buffer minimizes current supply making it efficient for power reduction.

Circuit Design

Now that we know the parts that would be involved in current and voltage sensor, we then must incorporate these components. To design a circuit that contains these sensors, we looked for inspiration through some previously designed circuits that performs the intended function. The circuits we researched on are essentially reference designs to be used for our final product.

Reference Designs

In this section, we will discuss these reference designs in which we either considered and/or will be implementing in our design.

TIDA-00795[4.47]: The TIDA-00795 Automotive Precision eFuse reference design is a replacement to the traditional fuse, offering overcurrent protection with higher accuracy and features not found in traditional fuses. This TI Design can be used as a building block to implement a multichannel eFuse box.

To sense current, the design uses a INA300-Q1; this is a high common-mode, current-sensing comparator that is configured to detect overcurrent conditions through measuring the voltage developed across a current sensing or shunt resistor. The device can measure this differential voltage signal on common-mode voltages that can vary from 0 V up to 36 V, independent of the supply voltage. The device features an adjustable threshold range that is set using a single external limit-setting resistor. The device has a good voltage rating, but it falls short of the 39-32 voltage output of the solar panel.

To regulate the power supply, the design takes advantage of the LM9036Q. The LM9036Q ultra-low quiescent current regulator features low dropout voltage and low current in the standby mode. With less than 25- μ A ground pin current at a 0.1-mA load, the LM9036Q is ideally suited for automotive and other battery-operated systems. The LM9036Q retains all the features that are common to low dropout regulators, including a low dropout PNP pass device, short circuit protection, reverse battery protection, and thermal shutdown. The TIDA-00796 Block Diagram is seen in Figure 4.34.

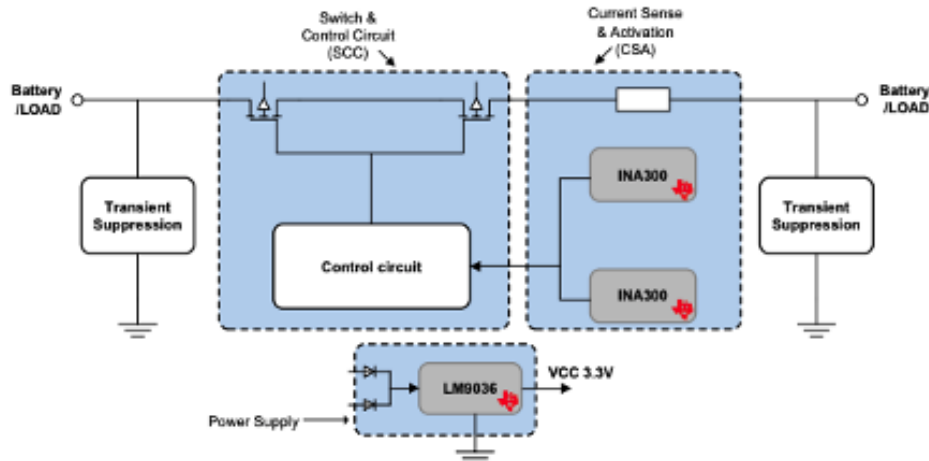


Figure 4.34: TIDA-00795 Block Diagram. Reproduction permission requested from Texas Instruments.

One of the main issues with this design is the input voltage requirement. According to the datasheet, the maximum operating voltage of the system is 28 volts, which is below the minimum voltage the solar panel outputs. Also, this design does not use an ADC. Table 4.5 summarizes the TIDA-00795's specifications.

Table 4.5 TIDA-00795 Voltage Sensing Specifications

PARAMETER	SPECIFICATIONS
Voltage Input:	DC input operating voltage –28 to 28 V
ION_TIME Output current on time:	Output load current: ≤ 30 A, 2.2 to 3.5 ms
VON_TIME Output current on time:	I LOAD ≤ 30 A, Null
VOFF_TIME Output current on time:	I LOAD = 30 A Input source off; output current less than 10 %
Design accuracy:	97.36%
Resistance:	Average measured turn on resistance of eFuse design

TIDA-00528[4.48]: This verified design can accurately measure current, voltage and power on a bus as high as 400 V using an I2C- or SMBUS-compatible interface. This design is targeted towards industrial applications where there is a need to measure system current accurately with bus voltages greater than 40 Volts such as Solar inverters, HEV/EV systems and Source generation for AC/DC electronic loads and power sources.

For the design to sense current, it takes advantage of the INA226. The INA226 is a current shunt and power monitor with an I²C™- or SMBUS-compatible interface. The device monitors both a shunt voltage drop and bus voltage. Programmable calibration value, conversion times and averaging, combined with an internal multiplier enable direct readouts of current in Amperes and power in Watts. The INA226 senses current on common-mode bus voltages that can vary from 0 V to 36 V, independent of the supply voltage.

For current amplification, the design uses a OPA333. The OPA333 series of CMOS operational amplifiers use a proprietary auto-calibration technique to simultaneously provide very low offset voltage ($10 \mu\text{V}$, max) and near-zero drift over time and temperature. These miniature, high-precision, low quiescent current amplifiers offer high-impedance inputs that have a common-mode range 100 mV beyond the rails, and rail-to-rail output that swings within 50 mV of the rails. Single or dual supplies as low as $+1.8 \text{ V}$ ($\pm 0.9 \text{ V}$) and up to $+5.5 \text{ V}$ ($\pm 2.75 \text{ V}$) can be used. These devices are optimized for low voltage, single-supply operation. The TIDA-00528's block diagram is seen in Figure 4.35.

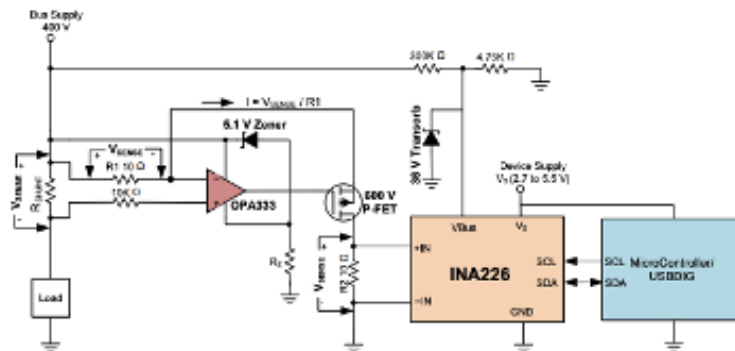


Figure 4.35: TIDA-00528 Block Diagram. Reproduction permission requested from Texas Instruments.

The OPA333 is used to mirror the sense voltage across the shunt resistor on to a precision resistor R1. OPA333 is floated up to 400 V using a 5.1 V Zener diode between its supply pins.

This design also does not use an ADC incorporated on PCB but uses an external one that would be placed on the board. Table 4.6 summarizes the TIDA-00528's specifications.

Table 4.6 TIDA-00528 Voltage Sensing Specifications

PARAMETER	SPECIFICATIONS and FEATURES
Operating Bus Voltage range:	40 V to 400 V
Operating temperature:	+25 °C
Wired Interface from Current Shunt to Application Processor:	I^2C Compatible
Accuracy at Full scale:	<1%
Form Factor:	67.8 mm x 93 mm square PCB

TIDA-01063[4.49]: The TIDA-01063 is a reference design for current sensing using a PCB Rogowski coil sensor to achieve very good linearity for wide measurement range at a very low system BOM cost. The PCB Rogowski sensor is advantageous for isolated current measurement due to its very high bandwidth of 20 MHz and fast settling time of 50 ns. The auto-zeroing, 12-nV/√Hz noise density of the INA188 makes it suitable to achieve a 12-bit system resolution for a full-scale current of 1000 A.

A three-phase AC induction motor drive system has a feedback sensor for current, speed, and rotation sensing, all integral parts for motor protection and motor drive systems. For better system accuracy and stability, sensors need to be linear and highly accurate. The design uses the INA188. The INA188 is a precision instrumentation amplifier that uses TI proprietary auto-zeroing techniques to achieve low offset voltage, near-zero offset and gain drift, excellent linearity, and exceptionally low-noise density that extends down to DC. The INA188 is optimized to provide excellent common-mode rejection of greater than 104 dB. It also uses the LP5907. The LP5907 is a linear regulator capable of supplying a 250-mA output current. Designed to meet the requirements of analog circuits, the LP5907 provides low noise, high PSRR, low quiescent current, and low line or load transient response figures. The LP5907 offers class-leading noise performance without a noise bypass capacitor and the ability to place remote output capacitors.

To supply power to the IC's it uses the LM2776. The LM2776 CMOS charge-pump voltage converter inverts a positive voltage in the range of 2.7 to 5.5 V to the corresponding negative voltage. The LM2776 uses three low-cost capacitors to provide 200 mA of output current without the cost, size, and electromagnetic interference (EMI) related to inductor-based converters. It also uses the REF2025. The REF2025 offers excellent temperature drift (8 ppm/°C, max) and initial accuracy (0.05%) on both the VREF and VBIAS outputs while operating at a quiescent current of less than 430 μA. In addition, the VREF and VBIAS outputs track each other with a precision of 6 ppm/°C (max) across a temperature range of -40°C to 85°C. All these features increase the precision of the signal chain and decrease board space while reducing the cost of the system as compared to a discrete solution. The TIDA-01063's block diagram is seen in Figure 4.36.

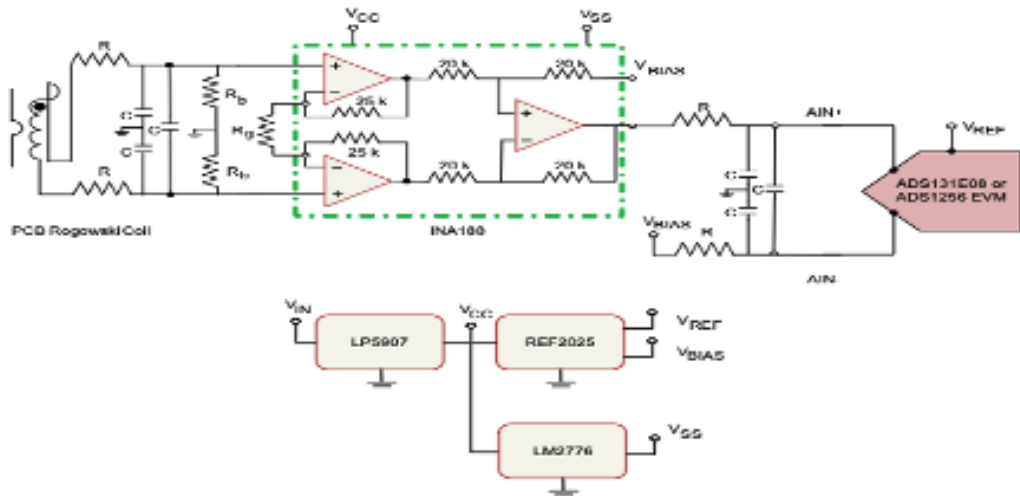


Figure 4.36: TIDA-01063 Block Diagram. Reproduction permission requested from Texas Instruments.

TIDA-00640[4.48]: The TIDA-00640 verified reference design provides an overview on how to implement a solar module level monitoring and communication sub-system. This design addresses the key need of a highly cost optimized monitoring and communication sub-system for solar Module Level Power Electronics (MLPE). This design showcases a highly integrated solution for accurate voltage, current and temperature monitoring along with ZigBee communication using CC2538 to enable Solar Module level monitoring.

To measure current, a low-value current shunt resistor was chosen as the sensor in this TI Design to keep system complexity and cost to a minimum. This design uses a low-side sense element to reduce the need for high-voltage translation typical of a high-side element. The TIDA-00640 uses the built-in ADC on the CC2538 for measurement.

For the voltage, The TIDA-00640 uses a simple voltage divider and amplifier configuration to measure the module level voltage. A low upper limit was set to give the analog circuitry plenty of overhead in the case of higher-than-expected module voltage output. The voltage sensing divider feeds a simple buffer amplifier, which shares a package with the current sensing amplifier. As in the current measurement system, a VREF of 3.3 will be used on the ADC of the CC2538. The current sense amplifier is the TLV342A that we made mention of earlier. The ADC used is the CC2538, which uses the Zigbee communication protocol. LM5017 is used to supply 3.3v to the IC's. Since the voltage coming from the solar panel will be too high for the IC's, the LM5017, since it is a buck converter, would step down the incoming voltage to the desired amount and then sends that voltage instead. Table 4.7 summarizes the specifications of the TIDA-00640

Table 4.7: TIDA-00640 Voltage Sensing Specifications

PARAMETER	SPECIFICATIONS
Voltage Input:	10- to 90-V input voltage support for modern HV modules
Sensor type:	Shunt resistor
Current measurement accuracy:	<2% calibrated and uncalibrated error full scale
Voltage measurement accuracy:	<2% calibrated and <2.5% uncalibrated error full scale
Temperature measurement:	$\pm 5^\circ\text{C}$
Wireless functionality:	1 minute of no motion detected

For the All-in-one PV sensor, we would use the TIDA-00640 as our reference design. The design contained the necessary parts needed for our sensor. We would need to modify the design because the TIDA-00640 assumes the solar panel outputs 90v. Also, the TIDA-00640 was used for a solar panel which is a perfect fit for our All-in-one PV sensor, so since the design showed promising results, it allows us to keep our minds at ease when we use the design.

For the current and voltage sensing, we would be using a component that contains two op amps, and two different configurations would be used for both

They are linear devices that have all the properties required for nearly ideal DC amplification and are therefore used extensively in signal conditioning, filtering or to perform mathematical operations such as add, subtract, integration and differentiation.

For our current sensing, we would be using the non-inverting op-amp configuration. In this configuration, the input voltage signal, (V_{IN}) is applied directly to the non-inverting (+) input terminal which means that the output gain of the amplifier becomes “Positive” in value in contrast to the “Inverting Amplifier” circuit we saw in the last tutorial whose output gain is negative in value. The result of this is that the output signal is “in-phase” with the input signal.

The voltage coming from the shunt would be a very small value, this would be what the ADC would measure, but the voltage would be too small. The op-amp would amplify the signal with a certain gain determined by the resistors, then it would send it to the ADC. Figure 4.37 is the configuration that our op amp would use for current sensing.

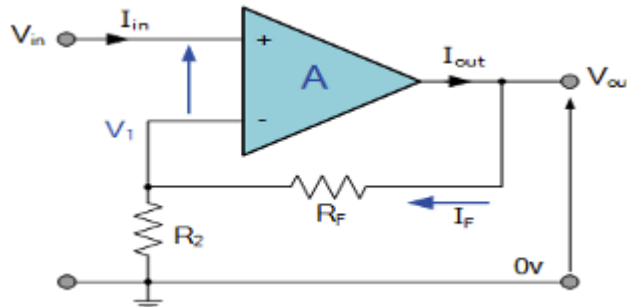


Figure 4.37: Non-Inverting Configuration. Reproduction permission requested from Electronics Tutorials.

The gain of this op-amp can be calculated as:

$$A_v = \frac{V_{out}}{V_{in}} = 1 + \frac{R_f}{R_2}$$

For voltage sensing, a voltage follower would be used. If we made the feedback resistor, R_f equal to zero, ($R_f = 0$), and resistor R_2 equal to infinity, ($R_2 = \infty$), then the resulting circuit would have a fixed gain of “1” (unity) as all the output voltage is fed back to the inverting input terminal (negative feedback). This configuration would produce a special type of the non-inverting amplifier circuit called a **Voltage Follower**, also known as a “unity gain buffer”.

As the input signal is connected directly to the non-inverting input of the amplifier the output signal is not inverted resulting in the output voltage being equal to the input voltage, thus $V_{out} = V_{in}$. This principle would be how the voltage is measured. The voltage divider would reduce the voltage coming out of the solar panel, then the unity gain buffer would send the voltage to the ADC. This Unity buffer also helps to reduce power consumption since very little current would be used. Figure 4.38 is the configuration that our op amp would use for voltage sensing.

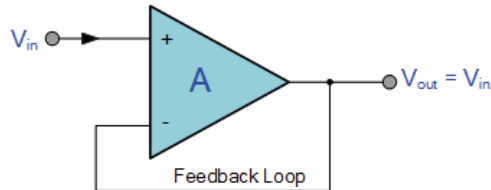


Figure 4.38: Voltage Follower Op-Amp. Reproduction permission requested from Electronics Tutorials.

The gain of this op-amp can be calculated as:

$$(A_v) = \frac{V_{out}}{V_{in}} = +1$$

4.3.5 TEMPERATURE SENSOR

One of the main components for our Sensing Node (“All in One PV Sensor”) is the successful integration of a temperature sensor as discuss in prior sections. The basic requirements in the temperature sensing side are that it must be low cost, reliable, and accurate a maximum temperature error of ± 5 °C. Furthermore, one flexible requirement that we have previously discussed is the possible integration of a Type T thermocouple as used by OUC Testing facility for easier integration with current thermocouples bought by OUC.

The use of a Type T thermocouple requirement is flexible requirement since our client OUC gave us the option to integrate another type of thermocouple instead of a Type T thermocouple. This option was given to us incase our design has certain limitation if we have a Type T thermocouple such as added costs to our design which that is the main goal. Which is to make the whole entire Sensing Node (“All in One PV Sensor”) as accurate and low cost as possible for possible mass scale implementation on a solar farm where costs could add up for every Sensing Node integrated. There are 3 critical criteria that we must take into consideration, for the selection of the contact temperature that the design will use for the entire scope of the project. The principal one is that it must have a temperature range of 15 °C to 65 °C which is the typical temperature range a solar panel in Florida could reach on a normal day [4.30]. The second criteria are that the sensor will need to be cost effective, the reason the temperature sensor must be cost effective is due to the

desire implementation of the system in which consists of implementing our design in a large-scale solar farm. The final criteria that must be met is the sensor must have a fast response time, we want the sensor to have a fast response time because it takes some time to save the data from the sensing note to the main data logger Node that we are incorporating in our system.

Table 4.8: Temperature Sensor Comparison

Temperature Sensor:	Thermistor	Thermocouple T Type	RTD
Component #:	10K Precision Epoxy Thermistor - 3950 NTC	SA1-T	TFD-ENB-4W-40
Resistance:	10kΩ	-	100Ω
Temperature Range Continuous:	-55 °C to 105 °C	-60°C to 175 °C	-70 °C to 550 °C
Response time:	15 Sec.	0.3 Sec.	1.1 Sec.
Wire Gauge:	28 AWG PVC Wire	20 AWG	-
Cost \$:	\$4.00	\$16.798	\$111.39

In Table 4.8 we catalog three different types of contact temperature sensors arrange by their typical average cost, temperature range and response time. If carefully consider all the different types of temperature sensors we can conclude that the best and most cost-effective temperature sensor for our application is a Thermocouple. Not only it provides a cost-effective solution that is lowered then the RTD it has a wide temperature range all within the temperature range of 15 °C to 65 °C that we need. In addition to the low cost and temperature range the thermocouple has one of the fastest response times at 0.3 seconds. This is one of the most crucial characteristics that we must take into consideration when selecting our temperature sensor this is due as previously stated that it takes time to data log, data from sensing nodes, therefore a fast response equilavates to faster data logging in our system.

To better understand how we can implement a thermocouple in our design first we need to understand how a thermocouple works. As previously described a thermocouple produces a small voltage usually in millivolts when there is a temperature difference between two dissimilar metals conjunct at one end cause by an external temperature difference. This effect is called Seebeck Effect which is a thermoelectric effect where an electromotive force or EMF across two points of an electrical conductor material and produces a positive voltage [4.91]. To further expand upon the Seebeck Effect, we must understand that different conductors have different charge carrier densities this means that if a temperature is applied evenly and equally to these two metals the difference in charge carrier density allows the electrons to diffuse across the junction where the two dissimilar metals are connected. By diffusing that conductor with the highest electron density loses a portion of its electrons towards the lower density conductor producing a positive voltage and therefore creating Peltier EMF in which it creates a current flow [4.91]. As seen in the Figure 4.39 the electrons move left to right according to the temperature difference of the metals this unusually means that they will have a positive voltage as heat increases.

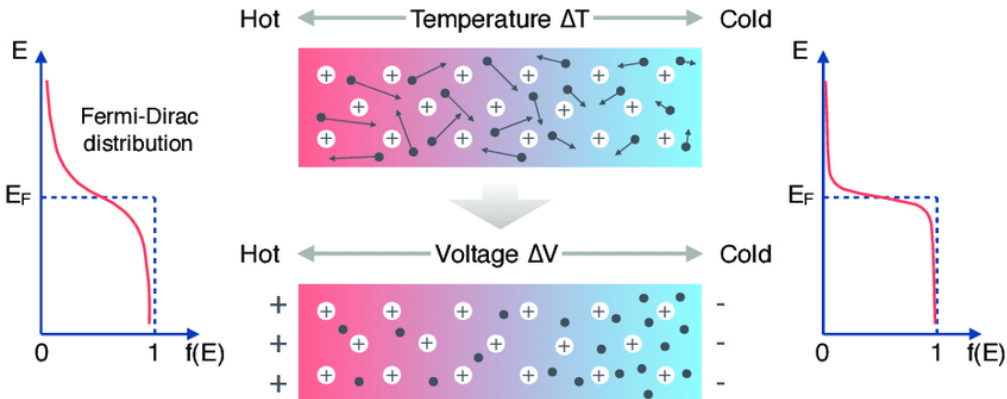


Figure 4.39: Seebeck Effect. Reproduction permission requested from ResearchGate.

Apart from the two main thermoelectric effects in the thermocouple system there is another effect that is produced by the thermocouple this effect is called Thomson effect this effect can form in between the Hot Junction and the Cold Junction of the thermocouple. This effect can occur when an electric current flows along a single conductor which temperature gradient is either absorbed or rejected depending in the direction of the current and thermal direction [4.92]. To properly analyze our selected thermocouple and how much energy it will convert in the system; we must understand the three basic equations for the Peltier effect, Thomson effect and Seebeck Effect. By using the equation below we can calculate the energy converter from the temperature difference by two dissimilar metals for Seebeck Effect.

$$E_{AB} = S_A(T_1 - T_2) - S_B(T_1 - T_2)$$

$$E_{AB} = (S_A - S_B)(T_1 - T_2) = S_{AB}(T_1 - T_2)$$

In the above equation E_{AB} is the thermoelectric EMF that produces a voltage in which the change in EMF per degree Kelvin is given by the equation below, S_A and S_B are the Seebeck coefficients of the metal with a unit of $\frac{V}{K}$, T_1 is the Hot Junction Temperature while T_2 is the Cold Junction temperature [4.92].

$$E_{AB} = \frac{dE_{AB}}{dT} \Delta T$$

As seen above E_{AB} is define as the thermoelectric power where it produces a voltage proportional to the change in temperature given by the volts per Kelvin unit $\frac{V}{K}$ which is also called the Seebeck Coefficient. [4.92]

4.3.5.1 THERMOCOUPLE TYPE

After the selection of the contact temperature sensor, there is another selection that we must make and that is the selection of a thermocouple type they are over six types of thermocouples in today's market. One key factor that we must abide in our selection for a thermocouple type is how cost-effective thermocouple is for our application, our implementing environment if the thermocouple is going to be use in an outdoor environment where is expose to the elements such as direct exposure to humidity, sunlight, and environmental pollution. Furthermore, depending on the material of the thermocouple the actual operating temperature can diverge from the overall temperature range of a thermocouple depending on the conditions the thermocouple is implemented which affects the performance of the thermocouple.

Table 4.9: Overall Temperature Range for Typical Types of Thermocouples

Type:	J	N	S	T	E	K
Component #:	FF-J-20-25	GG-N-20-25	XE-2500	FF-T-20-25	FF-E-20-25	FF-K-20-25
Conductor Type:	Solid	Solid	Braided	Solid	Solid	Solid
Temperature Range:	0°C to 200 °C	0°C to 260 °C	0°C to 1480 °C	0°C to 200 °C	0°C to 200 °C	0°C to 200 °C
Wire Gauge:	20 AWG	20 AWG	20 AWG	20 AWG	20 AWG	20 AWG

On Table 4.9 we can see the overall temperature ranges for a typical thermocouple. To maximize our temperature resolution for our All-in-One PV we decide to compare different types of thermocouples that would allow us to have a wider analytical scope to decide what thermocouple would increase the overall system temperature sensing resolution. As previously discussed, the temperature range we expect to measure in a typical solar panel is between 15 °C to 65 °C in Florida. If we carefully consider all the different types of thermocouples, we can conclude that most thermocouples can achieve our desire temperature range but that does not tell us the everything that we need to know to successfully implement a selected thermocouple type in our testing and implementation environment.

As noted previously, we will use a contact thermocouple to monitor the temperature of solar cells for this reason we need to use a thermocouple that can be potentially mounted to the back of a solar panel without using extra hardware or parts and that will damage the solar cell or modified our temperature reading when installed. Since the typical solar cell is made from glass brackets, and glue will be a poor choice as a mount option therefore we must look for some kind of high temperature tape or self-adhesive material that will not affect the performance of the temperature sensor when installed. For this reason, we decided to look for thermocouple that have an adhesive at the probes end to allow directly contact with the measure surface of the solar cell. This will allow a more precise heat conduction exchange between the solar panel and the temperature sensor giving us a better temperature reading of the actual temperature at the solar cell.

Table 4.10: Thermocouples Market Analysis

Type	Response Time	Operation Temperature Range °C	Material	Mount Option	Wire Insulation	Price
J	0.3 Sec.	0°C to 175 °C	Iron-Constantan	Self-Adhesive	PFA	\$83.99
T	0.3 Sec.	0°C to 150 °C	Copper Constantan	Self-Adhesive	PFA	\$83.99
E	0.3 Sec.	0°C to 175 °C	CHROMEGA™ -Constantan	Self-Adhesive	PFA	\$83.99
K	0.3 Sec.	0°C to 175 °C	CHROMEGA™ -ALOMEGA™	Self-Adhesive	PFA	\$83.98

As arrange on Table 4.10 we have the basic specifications of a variety of types of thermocouples. For this we decided to use the manufacturer Omega engineering Inc. for our thermocouple market

search and selection. This was majorly decided after seeing their Self-Adhesive fast response thermocouple lineup they offered. This decision to have a single manufacturer in our selection process to find a suitable type of thermocouple for our design will help us with the comparison process of the different types of thermocouples since we have more accurate specifications list. Furthermore, since is the same manufacturer rating their thermocouples, we can eliminate conflicting temperature and response ratings of the same thermocouple by other manufacturers since they could have test in a different process. We also decided to use this company because is highly rated in its precession when it comes to testing and sensor equipment furthermore this company is the default standard for OUC when it comes to buying thermocouples. As seen in Table 4.10 there are two thermocouple types missing from the previous Table this was purposely done as the reason was that Type S are not that commonly used in low-cost applications there are mainly use in medical and lab testing for its high accuracy. Adding to the same reason not many manufactures produce Type N thermocouples leaving it from our list of potential thermocouples that we can implement in our design.

To analyze better our potential options for our thermocouple we can use the Figure 4.40 and Table 4.11 to have a more accurate behavioral comparison for each thermocouple during normal operating temperatures. As seen below we have an increment in voltage according to the change in temperature produced by the Seebeck and Peltier EMF effect. The behavioral graph on Figure 4.40 includes the typical graph behavior of Type E, Type J, Type T, Type K and Type S thermocouples over range temperatures. In addition to the behavioral graph on Table 4.11 we can analyze the smallest sensitivity of a thermocouple Type such as J, T, K and Type S this will help us to find the most accurate thermocouple to implement in our project.

Table 4.11: Thermocouples Sensitivity

Type	Response Time	Overall Temperature Range/ °C	Material	Sensitivity $\mu\text{V}/^\circ\text{C}$
J	0.3 Sec.	-200°C to 900 °C	Iron-Constantan	45 $\mu\text{V}/^\circ\text{C}$ to 57 $\mu\text{V}/^\circ\text{C}$
T	0.3 Sec.	-200°C to 400 °C	Copper Constantan	15 $\mu\text{V}/^\circ\text{C}$ to 60 $\mu\text{V}/^\circ\text{C}$
E	0.3 Sec.	0°C to 850 °C	CHROMEGA™-Constantan	40 $\mu\text{V}/^\circ\text{C}$ to 55 $\mu\text{V}/^\circ\text{C}$
K	0.3 Sec.	-200°C to 1250 °C	CHROMEGA™-ALOMEGA™	40 $\mu\text{V}/^\circ\text{C}$ to 55 $\mu\text{V}/^\circ\text{C}$

As we continue to analyze the different possibilities of thermocouple types that we can use. There is a constraint the limits us from using certain types of thermocouples. On such case is the use of thermocouples made from precious metals such as platinum which is one of the most expensive thermocouples in the market. Type S thermocouples are typically implemented in Lab Testing environments where accuracy is crucial therefore disqualifying it from our design as an implementing sensor due to the costs it will procure when implanting at mass scale. Even though a platinum/Rhodium thermocouple has a wide range of temperature detection which is highly linearize voltage output over a wide range of temperature as seen in Figure 4.40. There is another factor that limits us from using this type of thermocouple and that is that Rhodium is very brittle meaning if the thermocouple is not handle with care the thermocouple will fail do the breakage in connection.

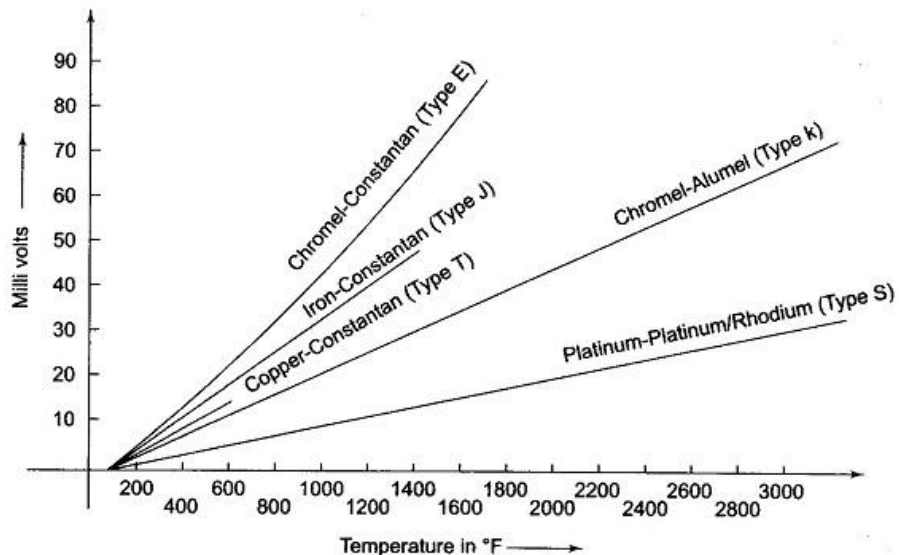


Figure 4.40: Voltage vs. Temperature Thermocouple Behavior. Reproduction permission requested from EEEGuide.com

Now that we know 4 types of thermocouples that we can implement, we can use we can move to the next requirement specification and that is the accuracy and linearity of the thermocouple of a temperature difference. The reason we want our thermocouple to be linear is that linear systems are most stable over a wider range and since the voltage rises slower the ADC can interpret smaller voltage to a digital value assign to our system accuracy adding stability to our system. In addition to linearity by knowing the smallest voltage produced per degree Celsius as seen in Table 4.11 we can quantified our systems sensitivity therefore knowing our smallest temperature we can detect. Type J is not a good choice as a thermocouple for our implementation not only does it have a shorter temperature range the increments in voltage by every degree in temperature increases rapidity from its lowest temperature potential to it maximum temperature potential. This translates to a lower sensor resolution since every temperature change will increase the voltage faster then what the ADC can measure accurately the smallest voltage per Celsius increment can be as small as $45 \mu\text{V}/^\circ\text{C}$ to $57 \mu\text{V}/^\circ\text{C}$. Another factor that restricts the use of a Type J thermocouple in our design is that weather resistance enough. As we know metals tent to corrode over time when exposed to the environment. For this reason, we cannot use the J type of thermocouple since it contains Iron for one of the leads when exposed to humidity without the proper protective coating it will corrode and even if the probe had a protective coating it will affect the sensitivity of the probe itself since know is less accurate due to different coating material.

The second thermocouple that will not work in our case is the Type E thermocouple even though it offers a good temperature range as we can see in Figure 4.40 the voltage almost increases exponentially when there is a temperature difference meaning that for every single temperature digit increase the voltage will increase higher than the temperature increment almost exponentially. This means that our system resolution will be severely impacted if we decided to use a Type E thermocouple. In addition to this the high side of the leads is made from Constantan which is a highly conductive EMF conductor which as demonstrated by Figure 4.40 it can converted emf potential to electricity more efficiently than the rest, but this is also a downside. In our application will work but with the risk of adding extra noise to our system due to the proximity to power lines coming out of the solar panels.

Therefore, the only two thermocouple that can be used appropriately in our system are Type T as provided by OUC and a Type K thermocouple. As seen in Figure 4.40 one of the best highly linearize voltage output due to temperature difference furthermore it has one of the smallest to highest Sensitivities at $15 \mu\text{V}/^\circ\text{C}$ to $60 \mu\text{V}/^\circ\text{C}$. In the other hand Type K thermocouple not only is highly linear it also does it over a wider range of temperature from the rest except for a Type S thermocouple. This is one of the reason a Type K thermocouple is one of the most commonly used thermocouple when it comes to measuring temperature on high temperature environments such as ovens. In the other hand a Type T thermocouple has a lower linearize temperature range but since is linear the rise in temperature is lower than a Type J thermocouple. Meaning it can be implemented in a similar design as a Type K thermocouple.

Table 4.12: Selected Thermocouples for Sensing Node.

Thermocouple:	Type T	Type K
Overall Temperature Range/ $^\circ\text{C}$:	-200 $^\circ\text{C}$ to 400 $^\circ\text{C}$	-200 $^\circ\text{C}$ to 1250 $^\circ\text{C}$
Operation Temperature Range $^\circ\text{C}$:	0 $^\circ\text{C}$ to 150 $^\circ\text{C}$	0 $^\circ\text{C}$ to 175 $^\circ\text{C}$
Sensitivity $\mu\text{V}/^\circ\text{C}$:	15 $\mu\text{V}/^\circ\text{C}$ to 60 $\mu\text{V}/^\circ\text{C}$	40 $\mu\text{V}/^\circ\text{C}$ to 55 $\mu\text{V}/^\circ\text{C}$
Response Time:	0.3 Sec.	0.3 Sec.
Material:	Copper Constantan	CHROMEGA™-ALOMEGA™
Price:	\$83.99	\$83.98

After carefully consideration, we opted to select a Type T and Type K thermocouple as describe in Table 4.12 due to their linearity over the operating temperature, sensitivity, and response time. After carefully analyzing all our options for thermocouples we decided to incorporate the provided Type T Thermocouple provided by OUC for our prototype design and a Type K for our design implementation. By implementing the Type T thermocouple, we successfully met out flexible requirement of implementing a Type T thermocouple. The next step we need to make is optimized our design such as that it would work with a Type K or Type T thermocouple seamlessly.

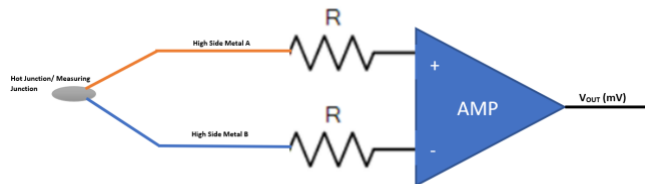


Figure 4.41. Thermocouple Basic Amplification by Marco Herrera.

The main drawback of using a thermocouple is that it produces a small amount of voltage typically in millivolts which is usually a small amount of voltage that a typical Analog to Digital (A/D) will not be available convert the signal properly. Therefore, we will need to design an amplifier circuit that can multiply the signal for the A/D to successfully convert the voltage signal as seen in Figure 4.41. The Temperature Sensor Amplification and Filtering. In addition to an amplifier circuit the design will also need to incorporate a decoupling capacitor to filter out the noise from the voltage source for the signal conditioning circuit.

4.3.5.2 THERMOCOUPLE CONDITIONING CIRCUIT

Now that we have selected the two thermocouples that we be utilizing in our design, now is time to select the proper signal conditioning circuit to allow correct communication with our selected microcontroller. In our case our microcontroller is the ESP-32 WROOM which has a 12-Bit ADC resolution with an input detection from .8mv to 3.3v. This means our signal conditioning circuit must amplify the voltage coming out from our thermocouple since the lowest voltage a thermocouple can output is 0v and there on small increments of milli volts depending on temperature. To successfully integrate our selected thermocouples with the ESP32 it is required for us to make a conditioning circuit that will create the necessary conditions for the ESP32 ADC to detect the minimum analog signal voltage of 0.8056 millivolts of the ADC for correct conversion to a digital value. One of the main components for the conditioning circuit is the addition to a cold junction compensator only necessary for a Type K thermistor. This is a downside of the use a Type K thermocouple unlike a Type T thermocouple a Type K needs cold junction compensation this is due to the potential difference in voltage between the Hot Junction which is the tip of the probe and the Cold Junction which is the base of the probe as seen in Figure 4.42 where $V_{OUT} = V_1 - V_2$.

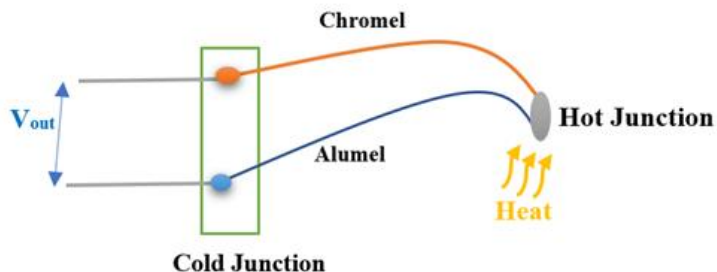


Figure 4.42: Typical Hot and Cold Junction Locations for a Type K Thermocouple Marco Herrera.

Cold junction Compensation can be accomplished by various methods one is an ice bath that reaches 0 degrees Celsius, another is adding a second temperature sensor that monitors the temperature in the cold junction to then compensate the difference later in voltage produced by the change in temperature. The main constraint for the implementation of a cold junction compensator is mainly the cost, size, and practicality of such implementation in our PCB design. Another main specification by OUC is that the sensing node or “All in One PV Sensor” needs to be available to work without having one of the two external sensors connected. Therefore, the design should accommodate a detection circuit where it can detect when the circuit is open. The addition of such open detection circuit is to ensure if the thermocouple is disconnected or not implemented the device can stop conversion and not save data that will be an outlier when the data is been analyze by Orlando Utility Commission.

The most efficient method with an acceptable percentage of error is a hardware cold junction compensator where a secondary temperature sensor is used to monitor the temperature at the reference junction or ambient temperature. To monitor the reference junction or ambient temperature there is two most popular methods to accomplish this compensation in a small profile design is the used of an isothermal block made from a high temperature conducive metal where it can easily reach room temperature where you can connect a thermistor so then we can later then subtract the difference between the Hot Junction known as the tip of the thermocouple and the Cold Junction.

As seen in Figure 4.43 to properly analyze the analog signal coming from the thermocouple, we need a conditioning circuit added to our amplifier circuit to have a voltage difference between our Cold Junction reference node to our Hot Junction tip of the thermocouple.

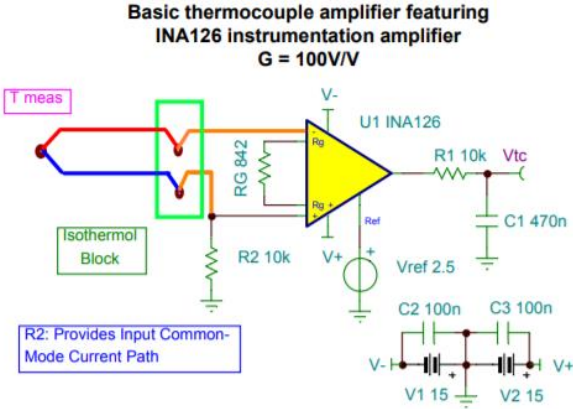


Figure 4.43: Amplifier using INA126 for Type T Thermocouple *Reproduction permission requested from Texas Instruments*.

As seen in Figure 4.44 this design features an Isothermal block to act as our part of our conditioning circuit where we will connect an 1N4148 to monitor its temperature and reference the voltage from that reference node so that in the code we can subtract the reference voltage by the output voltage of the amplified voltage giving us a more accurate voltage reading for our conversion equation. However, this design does not accommodate for open circuit detection which can make our data unstable since it will show random values for an open circuit. This can be mitigated by using bit masking where we can train a model to mask floating bits converted from the disconnected ADC. However, this does not solve the issue completely since in some cases the bits will not be masked properly leaving us strange bit conversion in data output by the Sensor Node.

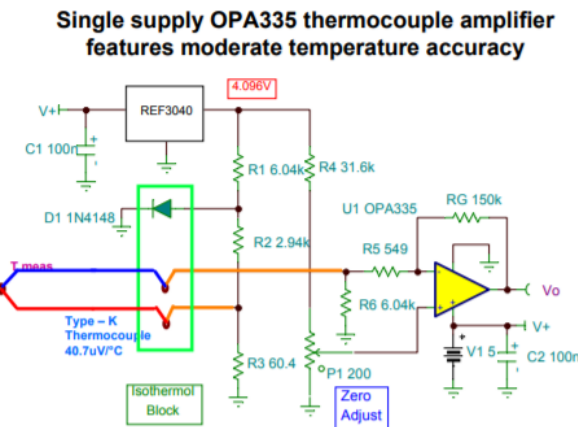


Figure 4.44: Single Supply OPA335 Type K Thermocouple *Reproduction permission requested from Texas Instruments*.

The main draw back for above reference designs is the use of an Isothermal Compensator for Cold junction compensation this means it utilizes a block of material to allow temperature reading of the cold side utilizing a diode to read this temperature then compensated by adding it or subtracting according to the set temperature function used. By using this method, we will be forced to add a piece of material to our design adding further costs.

For our purpose of finding the best possible reference design that could accommodate both Types of thermocouples for a reasonable price we found 2 possible reference designs that do not utilize an Isometric block but instead used an amplifier internal temperature. One of them is a two-stage op-amp circuit that amplifies the Type T thermocouple from its typical -10 to 77mV with an input voltage of 3.3V-5V and with a lowpass filter in the thermocouple input to filter out the interference of the thermocouple to have a more stable output as seen in Figure 4.45.

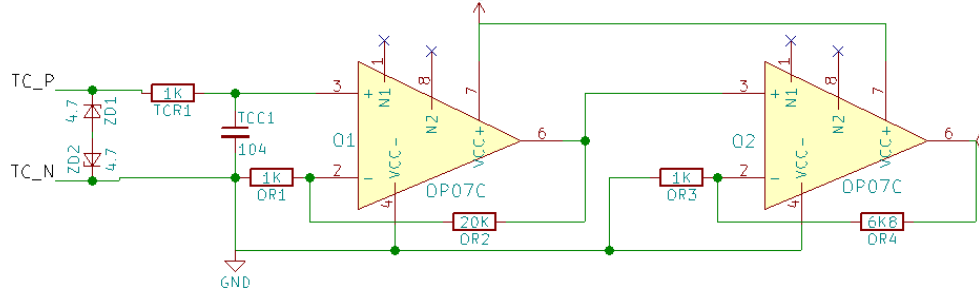


Figure 4.45: Two-Stage Amplification in EasyEDA by Marco Herrera.

The above design has both the cold junction compensation by using two 1N4148 and the input voltage range that we most use in our design since the ESP32 has a voltage range of 3.3-5V. This two-stage amplification circuit however lack the desire open detection circuit this means that if any minimal voltage passes through the amplification stage of the circuit it will amplify this noise rising our noise to voltage ratio further decreasing system resolution in our temperature sensing side.

By taking into consideration the cold junction of a thermocouple to find the rate voltage difference of our thermocouple we can implement the reference circuit above. By using 2 different op-amps we can invert the output voltage to measure the correct voltage difference that our ESP32 ADC can read as seen above in Figure 4.46.

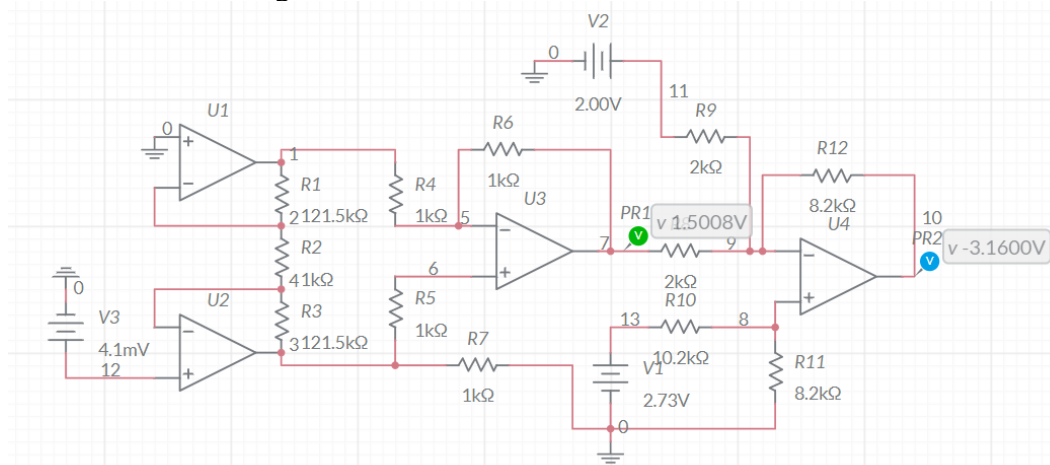


Figure 4.46: Multistage Thermocouple Amplifier in Multisim Live by Marco Herrera.

The next design on Figure was proposed as a differential amplifier setup that it would help reduce compensation of the cold junction reducing the margin of error. In addition to the cold junction compensation, it has a highly linearized output from 250mV to 5V which fall in the same range of voltage where our ESP32 ADC would work. Furthermore, the uncalibrated error is around 0.037%. The only downside on this design is the complexity and lack open circuit detection that we need

when implementing our design to stop temperature conversion when the thermocouple is not present.

As we analyze potential reference designs above, we keep encountering cold junction compensation and signal voltage amplification in our reference designs. This means that to implement our design correctly for our ADC and microcontroller to interpret the signal correctly we must first condition our signal voltage to a suitable voltage that our ADC and microcontroller can detect. For this reason we must use a conditioning circuit or also known as signal conditioning to transform our voltage signal to a suitable one for our ESP32 to detect. While the first reference design is suitable for our need in a close inspection implementing three distinct IC chip amplifier in the design it will add complexity leading to further costs and potential malfunction in one of the stages of the amplifier if we use 4 separate OP amps. On the second reference design while it only utilizes one differential amplifier due to the power rail been higher than the one, we can properly use it in design.

The three most important factors we need to understand to implement our conditioning circuit is how do we compensate for our cold junction on our thermocouple to read the appropriate voltage according to the manufacturers expected voltage according to temperature. Second how can we implement an open circuit detection system without adding cost and complexity to the system. The second one is that a thermocouple produces small amounts of voltage produced by a temperature difference between the Hot and Cold junction giving us a small but predictable mV reading. Therefore, since we have an mV output voltage, we must amplify this to around 3.3 volts which is the range for detectable voltage reading on our ESP32.

By taking the two most important factors for our design into consideration we saw a new approach for our reference design which was the use of an already existing Thermocouple amplifier industry tested and used. This proposed build thermocouple amplifiers use the combination of exiting 4 previous reference designs to both amplified, Cold junction Compensate and possibly open circuit detection as an all-in-one IC.

As seen in Table 4.13 we found two possible candidates that we could use in our design one is the MAX31856 and the MAX6675 both offer cold junction compensation, input voltage of 3.3 volts to 5 volts and compatibility with a Type K thermocouple.

Table 4.13: MAX31856 and MAX6675 Specifications

Specification	MAX31856	MAX6675
Thermocouple Type	Type K, Type T, Type J, Type S, Type R, and Type E.	Type K
Cold junction Compensation	Yes	Yes
Resolution	19-Bit, 0.078125 °C	12-Bit, 0.25 °C
Open Circuit Detection	Yes	Yes
Operating Temperature Range	-55 °C to 125 °C	-20 °C to 85 °C
Input Voltage	3V to 3.6V	3.3V to 5V
Output	Digital Value	Digital Value
Cost per unit	\$17.50	\$7.39

The first field tested conditioning circuit for a thermocouple is the MAX31856 Figure 4.47 is available to offer both cold junction compensation and verify compatibility with different types of

Thermocouples such as Type K, Type T, Type J, Type S, Type R, and Type E. Furthermore, this conditioning circuit also offers a 19-bit ADC converter that is integrated with the IC meaning that we will not have the need to utilize the on-board ADC of the ESP32. It also offers excellent 0.078125°C resolution that give us an accuracy of $\pm 2^\circ\text{C}$ over an input range of -200°C to 700°C .

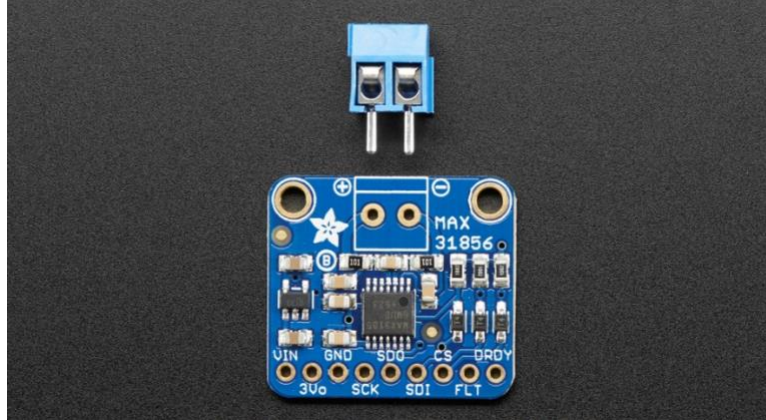


Figure 4.47: MAX31886 thermocouple amplifier and compensator

As seen in Figure 4.48 one of the most popular thermistor amplifier circuits offered in the market is the MAX6675. This chip not only offers cold junction compensation internally by using an internal diode that monitors the surrounding temperature to do a voltage difference. It also offers a simple 2 stage amplification circuit where a differential amplifier can reduce noise to voltage ratio giving us a greater accuracy of 0.25°C . In addition to this we can find that the MAX6675 with it all in one integrated chip has the simplest implementation making a great thermocouple amplifier. Furthermore, it offers a 12-bit ADC giving a digital output signal.

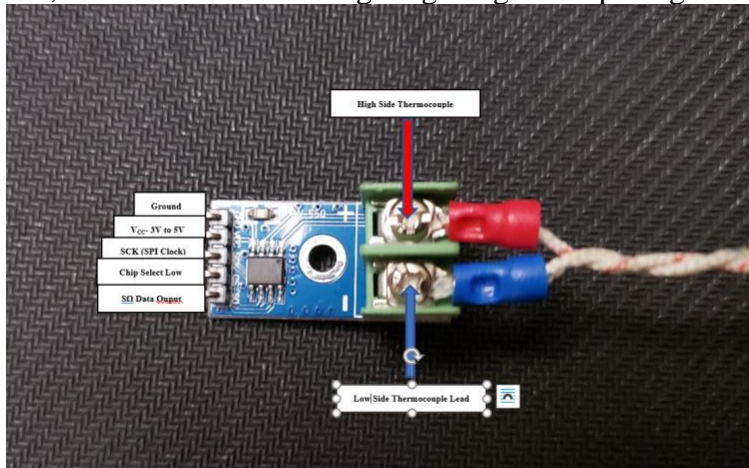


Figure 4.48: MAX6675 thermocouple amplifier and compensator.

In the other hand there is a secondary market offering to a temperature amplifier also commonly use and is the MAX31856 this amplifier offers the same characteristics as the MAX6675 with the same resolution/accuracy of 0.25°C . The only problem with this design is the addition of more components to the design making it more expensive to implement then the MAX6675. The key point of this project is to make a budget friendly PV monitoring system.

The internal composition of the MAX31856 chip as seen in Figure 4.49, we can clearly see this specialized chip has a built-in internal cold junction compensator as well a single differential amplifier for the signal amplification. For the built-in cold junction compensator instead of using

an isothermal block to monitor the temperature at the base of the thermocouple for the temperature conversion it instead uses a sensing diode. One of the benefits of using the MAX31856 is that it allows for detection of thermocouple shorts to GND or V_{CC} which is a great help when diagnosing a faulty part when implementing it in another design. Furthermore, it utilized a programmable gain amplifier that can be tune in the software to allow greater control over the amplification of the circuit this can be useful in case where you want to further amplified or fine tune a thermocouple to detect temperature on a narrow or greater range. But with all these extra features the MAX31856 comes at a cost of double that of the MAX6675 therefore to lower cost of our system we will implement the MAX6675.

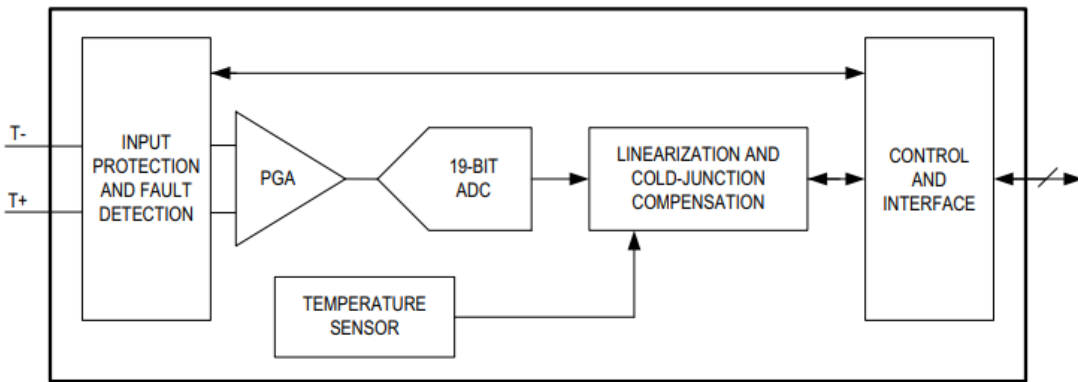


Figure 4.49: MAX31856 IC Internals. Reproduction permission requested from Maxim Integrated.

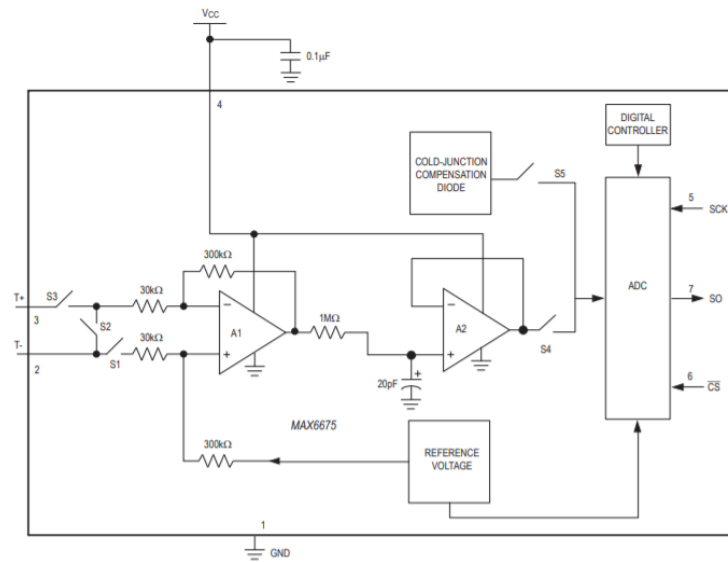


Figure 4.50: MAX6675 IC Internals. Reproduction permission requested from Maxim Integrated.

If we zoom in in the internal composition of the MAX6675ISA chip as seen in Figure 4.50, we can clearly see this specialized chip has a built-in internal cold junction compensator as well a low-noise amplifier. For the built-in cold junction compensator instead of using an isothermal block to monitor the temperature at the base of the thermocouple for the temperature conversion it instead uses a sensing diode.

This sensing diode with its internal circuitry it can sense the ambient temperature of its surroundings in this case the based or cold junction of the thermocouple insuring a more accurate temperature reading. Since we know the temperature difference from the hot junction and the cold junction of the thermocouple, we can proceed to use the linear voltage equation to convert our voltage difference between our Hot Junction temperature voltage and cold junction ambient temperature voltage to get our actual voltage output that will be send to our ADC.

As we proceed to the ADC the main function as seen in Figure 4.50 is to add the call junction dial measurement with the amplified thermocouple voltage which then converts it to a 12-bit resolution which in this case is 3.3 volts divided by 2^{12} which give us a 0.805mV ADC resolution which is within a reasonable temperature sensitivity well below 5% temperature discrepancy limit given by our client constraints.

After careful consideration between the MAX6675 better understand how the MAX6675 interacts with the ESP32 we need to understand what short of connection does the MAX6675 requires the MAX6675 utilizes a SPI connection. An SPI connection will allow to synchronize our data to the ESP32. We must be done for the design since the MAX6675 has an internal ADC outputting digital values that the ESP32 will interpret as a voltage to later converted to an actual temperature value. Therefore, is crucial for the data to be synchronize without it the digital values of the ADC will not be synchronize and the confusing the interpreter of the ESP32. Furthermore, to allow conversion an enable the output of the MAX6675 we must connect Pin 6 \overline{CS} to high and low this enables the output pin and the Serial Clock input of the MAX6675 pin 5 when \overline{CS} goes to low it enables the pins allowing the serial clock input of the MAX6675 to receive 16 cycles require to transmit 12 bits of digital values and when \overline{CS} goes to high it disables the pins.

4.3.6 IRRADIANCE SENSOR

A pyranometer is a device that can sense and measure solar irradiance. More specifically, a pyranometer measures the amount of solar energy over an area and over time on a usually flat surface. For the All-In-One PV sensor, the pyranometer will be used to understand how much light a panel is receiving. If a panel is underperforming, the pyranometer would be able to show whether the panel's exposure to light could possibly be the issue – if the pyranometer is detecting normal levels of irradiance while a panel is not, the panel could be obscured or damaged.

Pyranometers do not simply detect the amount of light that is shining on it; a pyranometer is also able to account for the angle of solar radiation by employing the use of either a diffusor or a glass dome when sensing. The pyranometer can operate based on a difference in temperatures between two surfaces, one clear and one black.

Pyranometer Technologies

There are two main pyranometer technologies: thermopile pyranometers and silicon semiconductor pyranometers. Thermopile pyranometers are based on thermopiles which convert thermal energy into electrical energy. Thermal differences are measured across the two surfaces and the radiation intensity is found to be proportional to the temperature difference that the pyranometer senses. Because of this, thermopile pyranometers are much more accurate compared to its counterpart, the silicon semiconductor pyranometer. [4.50] Silicon semiconductor pyranometers usually depend on photo-sensitive diodes which are in proportion to solar intensity. The photodiode converts this solar spectrum into a current and that current reflects the amount of irradiance that the pyranometer is measuring.

Pyranometer Constraints

For the creation of the All-In-One PV Sensor, the sensing circuit should be drawing little to no power from the generation of the solar panels. This means that the pyranometer must be self-powered or supplied with a supplementary battery or power generation source outside of the pyranometer. The pyranometer must also be able to connect to the PCB to be a part of the All-In-One PV Sensor, not a supplementary device.

Not all the created All-In-One PV Sensors will require the pyranometer; if a solar farm has multiple panels adjacent to one another, it's likely that they will all be receiving the same irradiance and the need for more than one pyranometer is unnecessary. Because of this, the cost is not as important of a factor.

Pyranometer Considerations

Because this is a research project, a Class C pyranometer will be used due to its comparatively lower cost. Additionally, certain pyranometers will not be considered due to their inability to connect directly to a PCB without intervention. There exist several commercially available pyranometers of every class, and for this project the following have been considered.

SP-110-SS Self-Powered Pyranometer: This pyranometer offered by Apogee Instruments was given to the team directly from the sponsor, OUC. The pyranometer is fully self-powered through its incorporation of a silicon-cell photodiode and features pre-tinned pigtail leads to easily connect to a PCB for datalogging. This sensor has a response time of less than one millisecond which is much higher than Class C expects from its pyranometers. This sensor was selected by the previous team for all its qualities listed thus far and will likely be re-employed for the final All-In-One PV Sensor Design. This sensor usually costs \$223 per pyranometer, \$299 from Alphaomega Electronics. [4.51][4.52]

SP-510-SS Thermopile Pyranometer: This pyranometer is also offered by Apogee Instruments but does not incorporate silicon-cell photodiodes. This thermopile has a much higher response time of around 0.5 seconds with the benefit of about half of the error compared to the SP-110-SS Pyranometer. This pyranometer also features pigtail-lead wires to easily connect to a PCB but appears to be lacking any additional functionality compared to the SP-110-SS Pyranometer offered at a cheaper price, as this sensor can cost \$333 per pyranometer. [4.51][4.52]

CS320 Digital Thermopile Pyranometer: This pyranometer offered by Campbell Scientific combines a blackbody thermopile detector with an acrylic diffuser, offering a significant improvement compared to the spectral responses of silicon-cell photodiode pyranometers with a comparable price-point. In addition to this, the pyranometer naturally offers a higher accuracy due to being thermopile. However, this pyranometer requires an input voltage of 6 to 24 V, DC to operate. Interestingly, this pyranometer returns its findings in a digital format using SDI-12 functionalities. [4.53]

The findings are summarized in Table 4.14.

Table 4.14: Summary of Considered Pyranometers

Pyranometer	SP-110-SS	SP-510-SS	CS320
Technology	Silicon-Cell	Thermopile	Thermopile
Output	Analog, ~100mV	Analog, ~400mV	Digital
Power Supply	Self-Powered	Self-Powered	6~24 V, DC
Response Time	< 1 millisecond	~ 0.5 seconds	2 second SDI response
Price	~\$230	~\$330	~\$524

For this project, it is likely that the team will continue to use the SP-110-SS Self Powered Pyranometer due to its comparatively low cost, lightweight design, and pre-tinned leads to connect itself to the PCB.

Pyranometer Implementation

If the team will move forward with the SP-110-SS Self-Powered Silicon-Cell Pyranometer, the following implementations can be considered. It is incredibly important to remember that applying any voltage into this pyranometer will damage it, as it is entirely self-powered.

The pyranometer will first be mounted on a stainless-steel mounting plate and placed on the front-side of the solar panel. This way, the pyranometer measures the direct sunlight that the solar panel is receiving. Some solar panels are equipped with a downward facing pyranometer to measure albedo, but this project does not aim to measure that irradiance. An installation guide for the SP-110-SS pyranometer notes that all Apogee pyranometer models have a standard calibration of exactly 5 W m^{-2} per mV. Multiplying the mV output by this conversion factor will allow us to find the shortwave radiation in Watts per Square meter. [4.54]

Given the above, the estimated maximum received voltage signal that the pyranometer can output from full & direct sunlight is about 200 mV. For an ADC to detect this small signal, an amplifying Op-Amp may be needed to boost the signal's strength into the Volt range rather than millivolt. Once amplified, the strengthened signal can be sent to an ADC to be analyzed and converted into a measurable value.

The following will be assumed for the proposed circuit:

- The pyranometer is outputting its maximum 200mV signal
- The ESP32 ADC is being used, which has a maximum input of 3.3V
- No noise is coming from the pyranometer
- A simple Non-Inverting Amplifier can be used to amplify the pyranometer's signal

With these assumptions in mind, the simple circuit seen in Figure 4.51 below can be implemented.

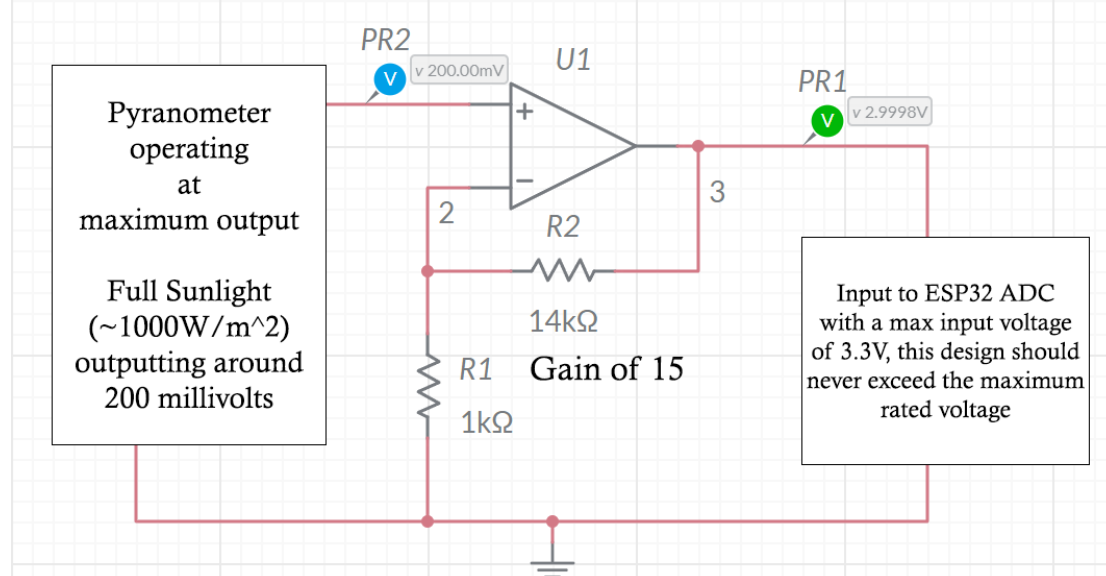


Figure 4.51: Initial Proposed Pyranometer Implementation Circuit in Multisim Live by Maguire Mulligan.

Rubin York of OUC has stated that the trends of the pyranometer's output are more important than the literal numerical output, meaning that the noise generated by the output of the pyranometer does not need to be fully eliminated, only partially.

External Research of Pyranometer Implementations

It is beneficial to research any other existing implementations of a pyranometer in similar applications for comparisons. Doing so will enable the team to implement the pyranometer in the most efficient and cost-effective matter by consulting the thought processes of other like-minded researchers who have created projects with a similar scope.

One such implementation was created by Wichtit Sirichote who aimed to implement a DC amplifier for a Pyranometer with an output of 14 uV/W/m^2 [4.55]. The analog input of a created data logger accepted $\pm 400 \text{ mV}$ with a 100uV sensitivity, so Sirichote aimed to use a DC amplifier to provide a DC gain for the output of the pyranometer to increase it from 14uV to 100uV to send toward the data logger. For this, Sirichote used the INA101, a High Accuracy Instrumentation Amplifier due to the extremely small voltages that were in use.

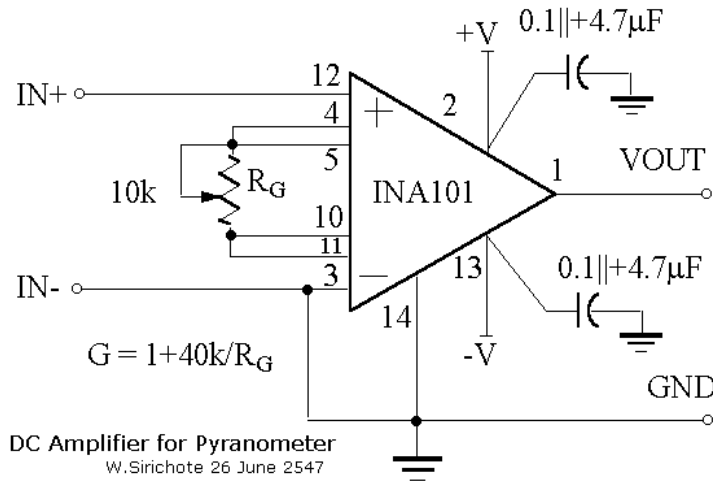


Figure 4.52. Sirichote's Implementation of the INA101 DIP Package

In Figure 4.52, Sirichote connects R_G to pins 4, 5, 10, and 11 for a DC gain adjustment and includes $4.7 \mu\text{F}$ decoupling capacitors at $+V$ and $-V$. The output V_{out} is tied to the input of their local data logging device and the inputs at $IN+$ and $IN-$ come from the pyranometer. The gain equation for the INA101 is

$$G = 1 + \frac{40,000}{R_G}$$

and given that R_G is 10,000, the gain provided by this amplifier is 5 producing a final input of 70 uV/W/m^2 to the data logger, assuming everything that Sirichote described is correct. This proves to be a good implementation for a pyranometer for connection to a data logger and could potentially be remodeled to fit our project's needs.

Referring to the INA101's datasheet [4.56], the input voltage noise that it permits is typically 0.8 uV , peak-to-peak. Using the decoupling capacitors, it's likely that this configuration with a modified gain would be a good addition to the All-In-One PV Sensor.

Pyranometer Implementation – Apogee's SP-110-SS

It is mostly assumed that this project will move forward with the Apogee SP-110-SS Self-Powered Silicon Cell pyranometer for irradiance measuring. While earlier sections had made assumptions about the pyranometer's operation, most cannot be held true in the real world. For example, there will always be noise surrounding the pyranometer's output signal. For this reason, we will have to take steps to reduce the noise output by the pyranometer and attempt to clean the signal before it reaches the on-board ADC.

This section will cover several outlooks and their considerations, mainly low-noise operational amplifiers for boosting the output signals magnitude. First, Instrumentation Amplifiers will be considered. Instrumentation Amplifiers are a type of differential amplifiers that have inner input buffer amplifiers, eliminating the need for input impedance matching which in turn makes them incredibly useful for measurement applications such as ours. Because the amplifiers that we are interested in must be low-noise and capable of operating successfully at small voltages, the prices will be high in comparison to the rest of the board's components. Most researched instrumentation amplifiers require an input voltage that falls within a range of its supply voltage and must be considered.

INA333 [4.57]: The INA333 is a lower-power precision instrumentation amplifier that offers excellent accuracy with a relatively low noise of 50 nV per square root hertz at gains over 100. This amplifier is especially interesting due to its analog input voltage; the INA333 can take a maximum of 0.3V difference from its supply voltage. In addition to this, the INA333 can provide a gain of anywhere between 1 and 1000, giving the potential output of the amplifier a large range of variety. This gain is determined by the value of only a single external resistor, making the gain highly customizable and easily accessible. A single INA333 rests at around \$6 per amplifier.

INA849 [4.58]: From a similar line of products, the INA849 is an ultra-low-noise instrumentation amplifier, offering a comparable 1 nV per square root hertz compared to the INA333's 50 nV. This amplifier has a larger range of input voltage taking up to a 0.5 V difference from its supply voltage, giving us more room to adjust. The INA849 also offers a larger range of possible gains, going up to 10000 V/V also controlled by a single external resistance with varying gain error percentages, all within 1% of its intended value.

INA126 [4.59]: The INA126 is advertised as a “great choice for … data acquisition systems” and that appears to be the case for our intended implementation. This instrumentation amplifier is low noise at 35 nV per square root hertz with an input range of 0.5 V difference from its supplying voltage. Similarly, to the previous two models discussed, this gain is controlled by a single external resistor. The INA126 is comparably cheaper than the previous parts sitting at about \$4 per amplifier circuit. At a gain of 100, the error reaches 1% meaning that any specified gain below this value will provide an acceptable output.

The findings of this section are summarized in Table 4.15.

Table 4.15: Summary of considered Pyranometer Amplifiers

Instrumentation Amplifier	INA333	INA849	INA126
Input Voltage Range*	-0.3 Vs to +0.3 Vs	-0.5 Vs to +0.5 Vs	-0.5 Vs to +0.5 Vs
Gain Range	1-1,000 V/V	1-10,000 V/V	5-10,000 V/V
Noise	50 nV/ $\sqrt{\text{Hz}}$	1 nV/ $\sqrt{\text{Hz}}$	35 nV/ $\sqrt{\text{Hz}}$
Supply Voltage Range	1.8 V to 5.5 V	8 V to 36 V	1.35 V to 18 V
Price	\$6	\$11	\$4

From these findings, the INA126 was selected as the best performing instrumentation amplifier of the 3 choices. Its low cost and high input voltage range allows us to easily implement it to the board. In addition to this, it supports a single-supply power of 3.3V which matches closely with all other components on the board thus far. If the pyranometer is to be input to the INA126 with a baseline gain of 5, the resulting circuit can be found in Figure 4.53.

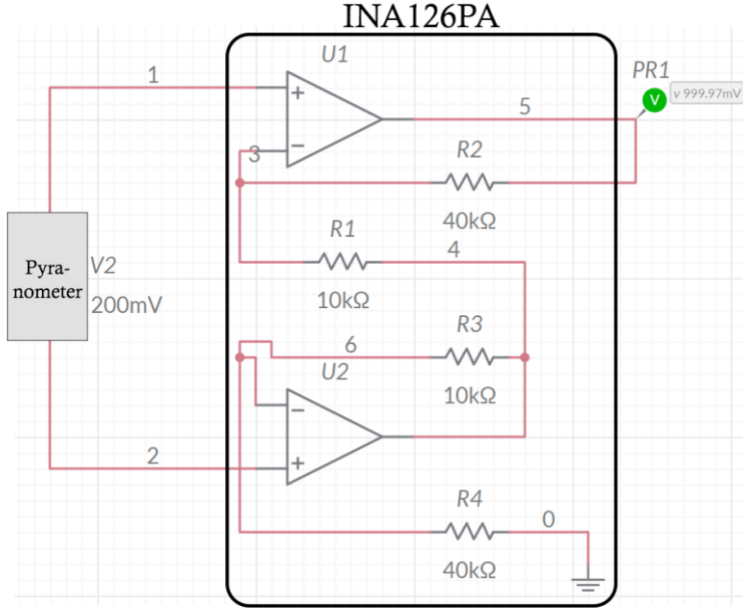


Figure 4.53: Pyranometer implementation using INA126PA

Now, at an expected maximum output of 200 mV from the SP-110-SS, we are seeing a 1V output from the Instrumentation Amplifier. With a gain of 5, this changes the pyranometer's output to 1 mV per 1 W per meter squared, allowing for a much easier conversion rate at the ESP32's ADC and increased resolution between comparable voltage values.

The INA126PA is an instrumentation amplifier and therefore has more prerequisites compared to a traditional Operational Amplifier. To measure the voltage output by the SP-110-SS, the potential difference between its positive and negative outputs must be measured. For this reason, a typical amplifier would not work as well: even on a rail-to-rail input/output Operational Amplifier, the negative input of the pyranometer would most likely fall outside the common mode voltage that can be accepted by the amplifier. For the INA126PA to behave how we want it, a few key factors must be considered.

The output of the INA126PA is compared to the output's reference, or the INA126PA's pin 5. This pin must be grounded and have a low impedance as even 8 ohms between the reference node and ground can cause a typical device to degrade to approximately 80-dB CMR [60].

The INA126PA also has an internal gain of 5. This, however, is not enough. To improve the input common-mode range, a gain resistor must be used, as the following formula limits the common-mode range:

$$V_{O2} = 1.25 V^-_{IN} - (V^+_{IN} - V^-_{IN}) (10 k\Omega/R_G)$$

Without a gain resistor, the output is limited 0.7 V from the supply rails which is nowhere near enough for our small and negative input voltages. Because of this, RG will be set to 15.8k for a gain of 10.

In the event of the INA126PA being unable to work for the All-In-One PV Sensor moving forward, then another instrumentation amplifier must be found. For this reason, further research went into selecting a back-up IC if the INA126PA must be replaced.

MAX4194[4.60]: The MAX4194 is a variable gain precision instrumentation amplifier that supports a 3.3V Single Supply operation. Along with this, it has a very generous Input Common-Mode Range, extending 200 mV below GND, which will be incredibly useful when dealing with the negative output from the pyranometer. This specific model also allows for a variable gain dependent on an external gain resistor, RG. However, the electrical characteristics detailed in the

datasheet note that the reference voltage should be half of the supplied voltage, so choosing this amplifier would mean that we must implement a voltage divider to halve the supply voltage for another pin. This should not add too much to the cost, given that the MAX4194 has a small price-point of \$3 per IC.

AD8223[4.62]: Created by Analog Devices, the AD8223 is a low power and low cost instrumentation amplifier with a variable gain of 5 to 1000. It supports 3.3V single supply operation but has a smaller common-mode input voltage range of 150 mV below GND, which may limit the output of the pyranometer depending on how far the negative output swings. This amplifier makes no specific claim on what the reference voltage must be for the input to change, so long as the reference voltage is within the supply voltage range and with very low impedance. The AD8223 base version is obsolete, but its replacement the AD8223ARZ is stocked and can still be ordered for \$3.37 per IC.

AD623[4.63]: Also, from the AD line of products comes the AD623, a rail-to-rail instrumentation amplifier that works in both single and dual supplies. The AD623 has a variable gain from 1 to 1000 V/V, supports a single power supply of 3.3V, and has an input voltage extending 150 mV below the ground on single supply. This works well for the pyranometer in the same way that the MAX4194 and AD8223 do, accommodating the negative output of the pyranometer's negative lead. The AD623 and its family of ICs stock well and sell for about \$7 per IC.

In summary, a good instrumentation amplifier will be cheap, support a single supply voltage of 3.3V, and allow an input to swing no less than 150 mV below ground such that the negative output of the pyranometer can be used effectively. Without those characteristics, the instrumentation amplifier will not serve the All-In-One PV Sensor well enough and should not be placed on the PCB.

The findings of the second round of instrumentation amplifier considerations are summarized in Table 4.16.

Table 4.16: Further Instrumentation Amplifier Considerations

Instrumentation Amplifier	MAX4194	AD8223	AD623
Input Voltage Range*	-0.2V to VCC-1.1V	-0.15V to VCC+1.5V	-0.15V to VCC+1.5V
Gain Range	1-1,000 V/V	5-1,000 V/V	1-1,000 V/V
Noise	30 nV/ $\sqrt{\text{Hz}}$	30 nV/ $\sqrt{\text{Hz}}$	35 nV/ $\sqrt{\text{Hz}}$
Supply Voltage Range	1.8 V to 5.5 V	3 V to 24 V	3 V to 12 V
Price	\$3.00	\$3.37	\$7.00

The best choice from these 3 new instrumentation amplifiers is the MAX4194 due to its large input voltage range, variable gain equation, and its low price point. Unfortunately, additional effort will have to be employed to create a reference voltage that rests at half of the supply voltage, but that small change will greatly outweigh the cons of buying a more expensive and less useful instrumentation amplifier.

4.3.7 ON-BOARD COMPONENT POWER SUPPLY

Power Supply:

An important bedrock that we had to factor in for the implementation of this project is the power supply. For the sensors on the All-In-One PV sensor to operate, they would have to be energized

by a source which produces a substantial voltage for the components to work on the PCB. A power supply provides electric power to an electric load; the electric load would be the sensors in this project. The components that we are using would require a low operating voltage, between 3.3 to 5 volts, so this factor will assist us in deciding the most efficient power supply for the sensors.

When choosing the power supply, we tried to find a low cost and effective option to perform this task. One of the first options we considered was the use of an external power supply like a battery. If we could outsource a 3.3 V battery and use it to power our system. We would have to design a contraption to hold the battery in place then wires extending to the terminals of the PV sensor to energize the components. One of the main challenges we had with this design was recharging the battery. Over time, the internal reaction occurring within the battery will slow down, causing less charge to be produced within the battery; this phenomenon will affect the performance of the sensors, causing them to underperform with a low Vcc. A solution to this issue was to use the solar panel to recharge the battery. Some of the power from the solar panel could be used to recharge the battery allowing continual use of the PV sensor. However, this could unnecessarily increase the complexity of the system, especially when we factor in the time of recharge since the solar panels produce voltage when there is access to sunlight, and the All-In-One PV sensor would be used as the solar panel is operating, so the battery cannot be recharged at night.

We had to rethink our approach to the issue; instead of using an external source, we thought using the voltage directly from the Solar panel would be a better step to take. Two issues arose from this, the first was that the voltage and current that comes out from solar panel has more characteristics of an AC signal not DC, also the voltage coming from the solar panel is the range of 32 – 39 V and the max current is 8.91 A, but the components have a significantly less max operating voltage and current. To counteract these issues, we decided to use a voltage regulator. The voltage regulator would help to adjust the voltage to a desirable amount.

Voltage regulator:

A voltage regulator is any electrical or electronic device that maintains the voltage of a power source within acceptable limits. The voltage regulator is needed to keep voltages within the prescribed range that can be tolerated by the electrical equipment using that voltage. Such a device is widely used in motor vehicles of all types to match the output voltage of the generator to the electrical load and to the charging requirements of the battery, but in our situation, it would be used to maintain the intended voltage. [4.95]

Based on the physical design, voltage regulators can be seen in integrated circuits, electromechanical devices, or solid-state automatic regulators. The most common classifications of the active voltage regulators (that use amplifying components like transistors or op-amps) are linear and switching regulators. Voltage regulators (VRs) keep the voltages from a power supply within a range that is compatible with the other electrical components. While voltage regulators are most used for DC/DC power conversion, some can perform AC/AC or AC/DC power conversion as well.

There are two main types of voltage regulators: linear and switching. Both types regulate a system's voltage, but linear regulators operate with low efficiency and switching regulators operate with high efficiency. In high efficiency switching regulators, most of the input power is transferred to the output without dissipation. [4.96]

Linear Voltage Regulator:

A linear voltage regulator utilizes an active pass device (such as a BJT or MOSFET), which is controlled by a high-gain operational amplifier. To maintain a constant output voltage, the linear regulator adjusts the pass device resistance by comparing the internal voltage reference to the

sampled output voltage, and then driving the error to zero. Linear regulators are step-down converters, so the output voltage is always below the input voltage. However, these regulators offer a few advantages: they are generally easy to design, dependable, cost-efficient, and offer low noise as well as a low output voltage ripple.

Linear regulators use a closed feedback loop to bias a pass element to maintain a constant voltage across its output terminals. In Figure 4.54, the op-amp drives the base of Q1 to ensure that the voltage at its inverting input will be equal to the voltage reference at its non-inverting input.

The op-amp in this circuit has a small load, the base current, and minimal capacitive loading. Consequently, it can respond to changes in load very quickly. Linear regulators are step-down converters, meaning that the output voltage will always be less than the input voltage. [4.97]

In fact, there is a minimum voltage difference between V_{in} and V_{out} that will allow the linear regulator to work. In datasheets, this value is called the drop-out voltage. If the $V_{out} > V_{in} - V_{DROPOUT}$, then the linear regulator can't regulate the output voltage at the desired voltage. Power is dissipated in the pass transistor. The amount of power is $P = (V_{in} - V_{out}) * I$. This power is wasted heat. This heat causes the regulator to get warm.

Linear regulators are, simple, cheap, and has a good power supply rejection ratio. Linear regulators respond quickly to changes in input voltage, producing an output voltage that is mostly free of any ripple on the input. They also respond quickly to changes in load voltage. However, a serious disadvantage of linear regulators is their low efficiency in many applications. The transistor inside the regulator, which is connected between the input and output terminals, functions like a variable series resistance; thus, high input-to-output voltage differential combined with high load current results in large amounts of power dissipation. In Figure 4.54, we can see the configuration of the regulator. [4.98]

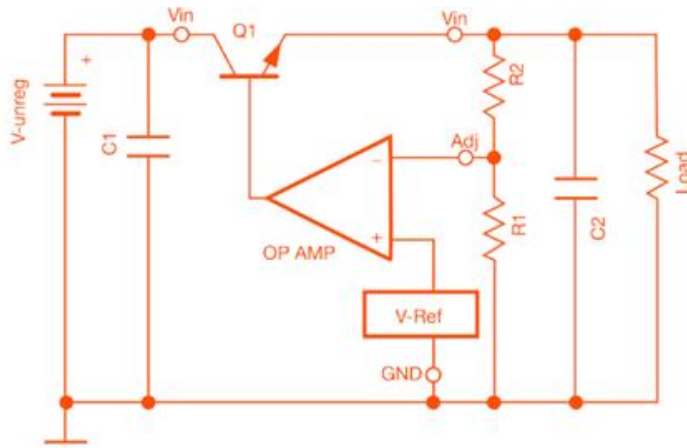


Figure 4.54: Linear Voltage Regulator Configuration. Reproduction permission requested from Digi-Key Electronics.

There are two types of linear voltage regulators, the series voltage regulator, and the shunt voltage regulator.

Series Voltage Regulator

The series voltage regulator or series pass voltage regulator uses a variable element placed in series with the load. By changing the resistance of the series element, the voltage dropped across it can be varied to ensure that the voltage across the load remains constant. The amount of current drawn is effectively used by the load; this is the main advantage of the series voltage regulator. Even when the load does not require any current, the series regulator does not draw full current. Instead

of drawing the current not required by the load to maintain the voltage, it drops the voltage difference between the input voltage and the required stabilized voltage. [4.99]

Shunt Voltage Regulators

A shunt voltage regulator works by providing a path from the supply voltage to the ground through a variable resistance. The current through the shunt regulator has diverted away from the load and flows uselessly to the ground, making this form usually less efficient than the series regulator. It is, however, simpler, sometimes consisting of just a voltage-reference diode, and is used in very low-powered circuits wherein the wasted current is too small to be of concern. This form is very common for voltage reference circuits. A shunt regulator can usually only sink (absorb) current. One of the most common examples of the shunt regulator is the simple Zener diode circuit where the Zener diode acts as the shunt element.

As such the shunt voltage regulator is an essential element within linear power supply technology. Shunt regulators are used in; low output voltage switching power supplies; current source and sink circuits; and even error amplifiers. [4.100]

Switching Voltage Regulator

A switching regulator rapidly switches a series device on and off. The switch's duty cycle sets the amount of charge transferred to the load. This is controlled by a feedback mechanism like that of a linear regulator. It is also known as a switch mode power supply. It uses semiconductor switching techniques, rather than standard linear methods to provide the required output voltage. The basic switching converter consists of a power switching stage and a control circuit.

The power switching stage performs the power conversion from the circuit's input voltage, V_{IN} to its output voltage, V_{OUT} which includes output filtering.

The major advantage of the switch mode power supply is its higher efficiency, compared to standard linear regulators, and this is achieved by internally switching a transistor (or power MOSFET) between its "On" state (saturated) and its "Off" state (cut-off), both of which produces lower power dissipation. This means that when the switching transistor is fully "On" and conducting current, the voltage drops across it is at its minimal value, and when the transistor is fully "Off" there is no current flow through it. So, the transistor acts like an ideal on/off switch.

A problem that switching regulators possess is the output ripple. Output ripple is a residual ac output voltage that is coherently related to the switching operation of the regulator. Its fundamental frequency is the same as the regulator's switching frequency. Switching transients are high-frequency oscillations that occur during switching transitions. Their amplitude, expressed as a maximum peak-to-peak voltage, is difficult to measure accurately since it is highly dependent on the test setup. Figure 4.55 shows the buck topology of a switching voltage regulator.

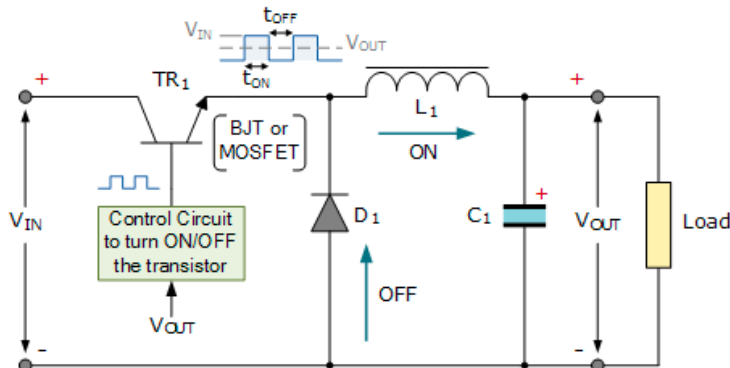


Figure 4.55: Switching Voltage Regulator Buck Configuration. Reproduction permission requested from Electronics Tutorials.

Unlike linear regulators which only offer step-down voltage regulation, a switch mode power supply can provide step-down, step-up and negation of the input voltage using one or more of the three basic switch mode circuit types, Buck, Boost and Buck-Boost.

Buck Voltage Regulator

The Buck voltage switching regulator is a type of switch mode power supply circuit that is designed to efficiently reduce DC voltage from a higher voltage to a lower one, that is it subtracts or “Bucks” the supply voltage, thereby reducing the voltage available at the output terminals without changing the polarity. In other words, the buck switching regulator is a step-down regulator circuit. The buck switching regulator is a DC-to-DC converter and one of the simplest and most popular type of switching regulator.

When used within a switch mode power supply configuration, the buck switching regulator uses a series transistor or power MOSFET (ideally an insulated gate bipolar transistor, or IGBT) as its main switching device. These switching voltage regulators offer typical input voltage capability from less than 2 V up to 100 V+, switching frequencies up to 4 MHz, and high efficiency operation up to 96%. Since we are trying to step down the voltage from the solar panel, this would likely be the design choice we would consider.

Boost Voltage Regulator

The Boost voltage switching regulator is another type of switch mode power supply circuit. It has the same types of components as the previous buck converter, but this time in different positions. The boost converter is designed to increase a DC voltage from a lower voltage to a higher one, that is it adds too or “Boosts” the supply voltage, thereby increasing the available voltage at the output terminals without changing the polarity. In other words, the boost switching regulator is a step-up regulator circuit.

Buck-Boost Voltage Regulator

The Buck-Boost switching regulator is a combination of the buck converter and the boost converter that produces an inverted (negative) output voltage which can be greater or less than the input voltage based on the duty cycle. The buck-boost converter is a variation of the boost converter circuit in which the inverting converter only delivers the energy stored by the inductor, L1, into the load. [4.101] Table 4.17 shows the difference between the linear and switch converters.

Table 4.17: Comparison of Switching and Linear Regulators

	Switching regulator	Linear regulator
Output voltage conversion system	Step-down, step-up, step-up/down, invert	Step-down only; V_{OUT} must be less than V_{IN}
Efficiency	High (negligible heat generation)	Comparatively low (high heat generation)
Output current	Large (high efficiency means high current)	Small
Noise	Large	Small
Output ripple	Present	None
Required external components	Many C_{IN} , C_{OUT} , L , (SBD)	Few C_{IN} , C_{OUT}

For our design, after researching about these types of regulators, we decided to implement the buck voltage regulator since it was more efficient for our project.

Switching regulator consideration

In order to find the perfect regulator, we decided to use WEBENCH. This platform gives various options to choose from when looking for a voltage regulator with specific parameters. It shows you the topology, cost, bill of material, and even the efficiency of the regulator.

LMR36006[4.102]: This regulator is an easy-to-use, synchronous, step-down DC/DC converter. With integrated high-side and low-side power MOSFETs, up to 0.6 A of output current is delivered over a wide input voltage range of 4.2 V to 60 V. Tolerance goes up to 66 V. The transient tolerance reduces the necessary design effort to protect against overvoltage's and meets the surge immunity requirements of IEC 61000-4-5. The LMR36006 uses peak-current-mode control to provide optimal efficiency and output voltage accuracy. Precision enable gives flexibility by enabling a direct connection to the wide input voltage or precise control over device start-up and shutdown. The IC cost \$0.74.

LMR36506[4.103]: is the industry's smallest 65 V, 0.6 A synchronous step-down DC/DC converter in 2-mm x 2-mm HotRod package. This easy-to-use converter can handle input voltage transients up to 70 V, provide excellent EMI performance and support fixed 3.3 V and other adjustable output voltages. The transient tolerance reduces the necessary design effort to protect against input overvoltage and meets the surge immunity requirements of IEC 61000-4-5. The LMR36506 uses the peak current mode control architecture with internal compensation to maintain stable operation with minimal output capacitance. The IC cost \$0.79.

LMR36015[4.104]: The LMR36015 regulator is an easy-to-use, synchronous, step-down DC/DC converter. With integrated high-side and low-side power MOSFETs, up to 1.5 A of output current is delivered over a wide input voltage range of 4.2 V to 60 V. Tolerance goes up to 66 V. The transient tolerance reduces the necessary design effort to protect against overvoltage occurrences and meets the surge immunity requirements of IEC 61000-4-5. The LMR36015 uses peak-current-mode control to provide optimal efficiency and output voltage accuracy. The IC cost \$0.84.

LMR36510[4.105]: The LMR36510 regulator is an easy-to-use, synchronous, step-down DC/DC SIMPLE SWITCHER converter. With integrated high-side and low-side power MOSFETs, output current up to 1 A is delivered over a wide input voltage range of 4.2 V to 65 V. The transient tolerance that goes up to 70 V reduces the solution size and cost to protect against overvoltage occurrences and meets the surge immunity requirements of IEC 61000-4-5. The LMR36510 uses peak-current mode control to provide optimal efficiency and output voltage accuracy. The cost of the IC is \$0.79. Table 4.18 summarizes the characteristics of all considered Switching Regulators.

Table 4.18: Comparison of Considered Switching Regulators

Converter	LMR36006B	LMR36506RF	LMR36510FA	LMR36015A
Efficiency	58.6%	65.2%	71.7%	73.8%
BOM Cost (\$)	1.68	1.59	2.36	2.58
BOM Count	11	16	12	12
BOM Area	126	204	289	247
Frequency	1Mhz	987.07 kHz	400 kHz	400 kHz

After consideration, the buck converter that we would use is the LMR36015A. Although the converter is the more expensive option, it has a higher efficiency than its other counterparts. It has a low bill of material count, and the area is optimum for our project. The LMR36015 is in a

HotRod package which enables low noise, higher efficiency, and the smallest package to die ratio. In the Figure 4.56 below, we can see the WEBENCH schematic of the regulator that outputs 3.3V.

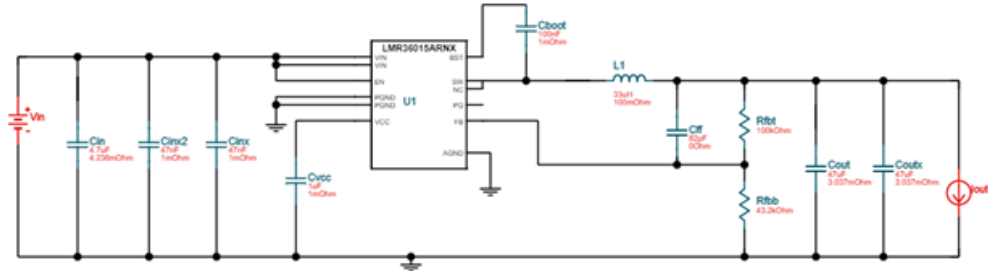


Figure 4.56: WEBENCH Schematic of LMR36015ARNXR. Reproduction permission requested from Texas Instruments.

For our All-In-One PV sensor, we would need a 3.3 V power source to activate our components. The topology shown above would output this voltage. The solar panel outputs 32 – 39 V, so the switching regulator would step down the voltage, stabilize it, then send it to the sensors which are then energized and operating. The Figure 4.57 below is the efficiency graph of the LMR36015ARNXR.

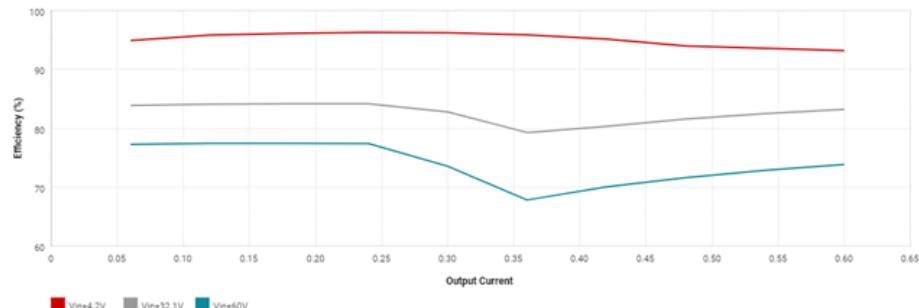


Figure 4.57: Efficiency Curve of Converter. Reproduction permission requested from Texas Instruments.

4.3.8 COMMUNICATION PROTOCOLS

A crucial component of this project is data transfer. As our device will be located on-board solar panels, variably distant from our receiver node, we must utilize wireless data transfer to communicate between our collector nodes and receiver node. There are many forms of wireless communication but there are two methods of wireless communication that are the most applicable and practical for our device. We will discuss Wi-Fi and Bluetooth wireless network protocols.

Wi-Fi

The IEEE 802.11 family of standards is commonly used for wireless networking. It allows nearby devices to receive and exchange data using radio waves. Wi-Fi is also widely used in public areas such as coffee shops, hotels, and airports to provide Internet access to mobile devices. [4.64]

The Wi-Fi Alliance is a non-profit organization that carries out interoperability testing and certification of Wi-Fi-capable devices. As of 2019, more than 3.05 billion Wi-Fi-capable devices are sold globally. Wi-Fi is a wireless networking technology that works seamlessly with the IEEE

802 protocol family. [4.65] It can connect various devices, such as mobile platforms and the Internet, through a network of access points. The various versions of the Wi-Fi standard vary in terms of radio frequency and speeds. Wi-Fi most commonly uses the 5 gigahertz and 2.4 gigahertz radio bands. [4.66] These bands are divided into multiple channels.

Wavebands of Wi-Fi are relatively high-absorption and work well for line-of-sight use. Although they can reduce range due to the presence of walls and other obstacles, they can still provide a good distance between different networks. Covering areas that are small to large can be achieved using multiple access points and walls. As of 2019, some Wi-Fi devices can reach speeds of up to 9.6 Gigabits per second. The IEEE doesn't test equipment for conformance with its standards. To address this issue, the Wi-Fi Alliance was established in 1999. Through its membership, over 800 companies have signed up to the organization. [4.66]

The Wi-Fi Alliance is responsible for enforcing the use of the Wi-Fi brand across various technologies. Some of these include 3Com, Aironet, and Harris Semiconductor. Members of the Wi-Fi Alliance are granted the right to mark their products with the Wi-Fi logo. The certification process involves testing and conformance to various standards, such as the IEEE 802.11 radio standards and the WPA and EAP2 security protocols. Although not every Wi-Fi device is certified, the lack of certification does not imply that the network technology is incompatible with other devices.

To use Wi-Fi, devices must first communicate with a common version. The version they use has various features and characteristics that can allow them to support different data rates and provide better connectivity. Since the beginning of 2018, the devices have been displaying the version of Wi-Fi that they support. These new generations, which are backward compatible with older versions, can now be connected to the device's UI. The easiest way to identify the version that's supported is by the number 4 or 5 in the list. The list of the most popular versions of Wi-Fi is as follows: 802.11a, 802.11b, 802.11g, and 802.11n. Table 4.19 below includes all versions of Wi-Fi. [4.67]

Table 4.19: Wi-Fi Generations [4.68]

Generation	IEEE Standard	Maximum Bitrate (Mbit/s)	Adopted	Radio Frequency (GHz)
Wi-Fi 6E	802.11ax	600 to 9608	2020	6
Wi-Fi 6	802.11ax	600 to 9608	2019	2.4/5
Wi-Fi 5	802.11ac	433 to 6933	2014	5
Wi-Fi 4	802.11n	72 to 600	2008	2.4/5
Wi-Fi 3	802.11g	6 to 54	2003	2.4
Wi-Fi 2	802.11a	6 to 54	1999	5
Wi-Fi 1	802.11b	1 to 11	1999	2.4
Wi-Fi 0	802.11	1 to 2	1997	2.4

Wi-Fi stations send and receive data packets individually over radio. They do it through a method known as demodulation and modulation. The differences between the different versions of the

technology are reflected in the different carriers used in each version. Like with other 802 LANs, the addresses of each Wi-Fi station are printed on the equipment's labels. These addresses are used to specify the destination and the source of the data packet. The destination address of a packet is used by the receiver to determine if the connection is relevant to the station.

Wi-Fi communication channels are typically half duplex and can be time-shared among multiple networks. When two or more devices are connected to the same channel, all the information sent by one of them is sent to the other. This method of data sharing allows the devices to use the same network interface card. Collision avoidance (CSMA/CA) is a technique that prevents networks from colliding. It sends traffic only after the channel has been sensed to be idle.

[4.69] The 802.11 standard has several radio frequencies ranges that can be used for Wi-Fi communications. These ranges are divided into various channels and are numbered from 5 MHz to 2.16 GHz. While the number of channels is limited to 5 MHz, transmitters can still occupy at least 20 MHz. In the US, 802.11b/g/n can use the 2.4 GHz band, which is considered Part 15 of the regulations. In contrast, Australia and Europe allow for the use of more channels than the 11 allowed in the US. In the US, however, devices that use the newer versions of Wi-Fi can only operate without a license. For most of the world, 802.11a/b/g/n can use the 5 GHz U-NII band, which has more channels than the 2.4 GHz band. The 5 GHz bands are absorbed better by common building materials and provide a shorter range.

As the technology evolved to support higher bandwidth, Wi-Fi protocols became more efficient in their use of available bandwidth. In addition, they can now combine multiple channels together to gain even more processing power. In addition, 802.11n can now also limit itself to 20 MHz to prevent interference in densely populated areas.

The data contained in a Wi-Fi network is organized into frames that are like Ethernet frames. The physical layer and the MAC of Wi-Fi are defined by the IEEE. These are the standards that are used by manufacturers to develop their products. The base version of the Wi-Fi standard was released in 1997. It contains numerous amendments that provide the basis for the creation of wireless network products. Aside from the IEEE 802, also known as the 802, also has specific requirements for Wi-Fi. This is because, unlike Ethernet, wireless communication media is prone to interference. Due to these requirements, the 802's Logical Link Control (LLC) uses Wi-Fi's media access control protocols to manage retries. It eliminates the need for higher levels of protocol stack.

For internetworking applications, Wi-Fi typically has a link layer that's below the Internet Protocol's layer. This means that it can provide full Internet access without overloading the network. Wi-Fi can be blocked if multiple devices are in the same area. To minimize interference, it uses Carrier-sense multiple access to prevent transmissions between devices. The number of channels in a Wi-Fi network is limited to five in the 2.4 GHz band. In addition, any two channels that are within the same band do not overlap each other. In North America, the three non-overlapping channels are the only ones that can be considered significant. However, if the two channels are more than a couple of meters apart, then the overlap is minimal. Unfortunately, many 2.4 GHz access points default to the same channel when connected to the same network. This causes congestion on certain channels and can affect the operation of other devices within the area.

Other devices such as security cameras, camcorders, and baby monitors use the 2.4 GHz band. Due to their wide variety of uses, this frequency can cause significant interference. Some 5 GHz bands can also be interfered with by radar systems. To prevent this, base stations that support these bands should implement a Dynamic Frequency Selection feature. Although unlicensed bands can be used by low-power transmitters, they can also be interfered with by unauthorized users. In most cases, these users have been issued large fines.

The IEEE 802.11 layer-2 has various characteristics. Some of these include maximum achievable throughputs that are calculated according to ideal conditions and data rates. However, this does not apply to most deployments where data is transferred between two devices that are typically connected to a wired network. The goal of this type of data rate is to provide a consistent and high-quality flow of data for an application. The main factors that contribute to this rate are the speed at which the packet is transmitted, and the energy used to transmit the signal. The distance and the power consumption of the devices are also known to affect the maximum throughput. The attached graph shows the average size of the packets, the size of the data rate, and the configuration power of the devices.

There are multiple modes of communicating through Wi-Fi as well, aside from the differing technologies in generations of Wi-Fi. Different modes of Wi-Fi involve the number of devices in which is involved in a single network. As depicted in Figure 4.58, infrastructure mode and ad hoc mode Wi-Fi are the two main modes that most Wi-Fi devices employ. [4.70]

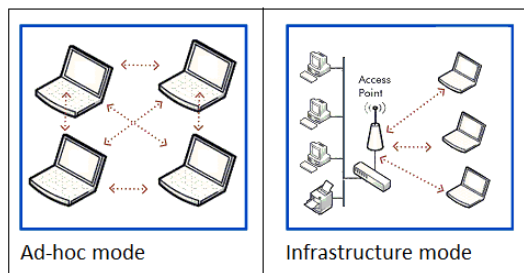


Figure 4.58. Ad-hoc mode vs. Infrastructure mode. Reproduction requested from ResearchGate.

In infrastructure mode, all communication between the network and its devices goes through a base station. This mode simplifies the protocols by allowing multiple devices to communicate with each other. Wi-Fi also allows devices to communicate without an access point. This is known as ad hoc transmission. This is also the mode that will be utilized in our devices to eliminate the need for an intermediate device. In most cases, network nodes must talk to each other to establish a connection.

In 1996, Chai Keong Toh of IBM introduced the concept of ad hoc routing using Lucent WaveLAN 802.11a wireless technology. His method was successfully implemented on IBM ThinkPads. This mode of wireless networking has become popular with various consumer electronics devices, such as the Nintendo DS and the PlayStation Portable. The Wi-Fi Alliance promotes the use of Wi-Fi for various applications. One example of this is the Wi-Fi Direct specification, which was launched in October 2010.

Bluetooth

Bluetooth is a wireless technology that is commonly found in many modern devices like smart phones and laptops. Bluetooth is a means of communicating data over short distances, usually in the range of 10 meters. Unlike Wi-Fi, Bluetooth is managed by a proprietary organization called Bluetooth Special Interest Group (SIG). [4.67]

Bluetooth can operate at frequencies ranging from 2.402 to 2.480 GHz, and it includes guard bands 2 MHz wide. [3.3] Bluetooth uses a radio technology known as frequency-hopping spread spectrum, which allows it to divide data into packets. It sends each packet to one of its 79 designated channels. Due to its 2 MHz spacing, Bluetooth Low Energy can support up to 40 channels. The only other option was the Gaussian frequency-shift keying scheme. Devices that use the GFSK algorithm can be expected to operate in the basic rate (BR) mode, where a bit rate of 1 Mbit/s is possible. They can also be operated in the enhanced data rate (EDR) mode, which provides 2 and 3 Mbits per second respectively. Each device in a piconet uses the clock provided by the master to exchange packets. The master clock has a duration of 312.5 s. [4.71] When sending single-slot packets, the master sends and receives in even slots, while the slave uses odd slots. For long-distance transmissions, the master and the slave use the same frequency, but with different slots.

A master BR/EDR device can communicate with up to seven devices in a piconet, though not all devices can reach the maximum. The devices can also switch roles, with the slave becoming the master. The master chooses which slave to address, and typically, it switches between devices in a round-robin fashion. Being a slave of multiple masters is possible in scatternets. The exact behavior is still unclear.

Bluetooth is a standard component used for low-power wireless communication. [4.72] It uses a radio network to transmit data, and it doesn't require visual line of sight to work. Range is a function that depends on the power-class of the Bluetooth device. Class 3, 2, and Class 1 are typically found in mobile devices, while Class 1 is for industrial use cases. For Class 1 and 2, the range is typically 20–30 meters, and the effective range is determined by the various factors that affect the quality of the link and the air conditions in between. Most Bluetooth applications are focused on indoor conditions, where weak signal quality and wall attenuation make the range significantly lower than the line-of-sight ranges of the devices. Sometimes, a Class 2 device can extend the data link's effective range by connecting to a Class 1 device with higher sensitivity and higher transmission power. This can be done in most cases depending on the application's requirements. Some devices can also allow up to 1 km of open field range between two similar devices. The Bluetooth core specification does not limit the range beyond 10 meters. Table 4.20 summarizes these classes. [3.4]

Table 4.20: Ranges of Bluetooth devices by class

Class	Maximum permitted power		Typical range (m)
	(mW)	(dBm)	
1	100	20	~100
1.5	10	10	~20
2	2.5	4	~10
3	1	0	~1
4	0.5	-3	~0.5

A device must be compatible with the various features of Bluetooth to use it. A Bluetooth profile is typically used to describe an aspect of wireless communication that a device can perform. The Bluetooth profile is typically placed on top of the core specification and its optional additional protocols. It can use features specific to the core specification, but only if the profile is tied to that specific version. The profiles are typically used by device manufacturers to allow their devices to work seamlessly with Bluetooth. For the Low Energy stack, a special set of profiles is required. Each profile has its own options and parameters that are used to perform its task. There are countless profiles available such as file transfer profile, cordless phone telephony, human interface device profile, personal area network profiling, LAN access profile, and many more.

Bluetooth is commonly used in various products such as mobile phones, tablets, media players, and gaming consoles. Due to the wide variety of devices that use it, its interference is prone to interference. Bluetooth is a wireless technology that enables people to transfer data between devices that are near each other. It works by allowing devices to connect to each other and perform various tasks. Through its ability to advertise various services, Bluetooth devices make it easier to use.

Bluetooth vs. Wi-Fi

Both Wi-Fi and Bluetooth are used for various and similar applications. Bluetooth is a wireless network that is commonly used for mobile devices. It is a replacement for the traditional cable connection used for various applications. Aside from smartphones, it is also commonly used for home applications such as smart energy management. While Wi-Fi is typically an access point-oriented network, Bluetooth is more prevalent in terms of applications. It can be commonly used in simple setups where two devices only need to connect using a minimal configuration. After thorough research and discussion, we opted for a Wi-Fi network to be the foundation of our devices' communication.

4.3.9 OTHER COMMUNICATION PROTOCOLS

Aside from the communication protocols that are utilized in our final design, there are additional communication protocols that were used during the prototyping stages of our product, including VNC and SSH.

VNC

[4.77] Virtual Network Computing is a desktop-sharing system that enables one computer to remotely control another. It sends the keyboard and mouse input to the other computer, and it updates the graphical-screen updates over a network. Multiple clients can connect to a server at the same time using Virtual Network Client (VNC). This technology allows users to access files stored on their work computer from their home computer. An illustration of a VNC network can be seen in Figure 4.59.

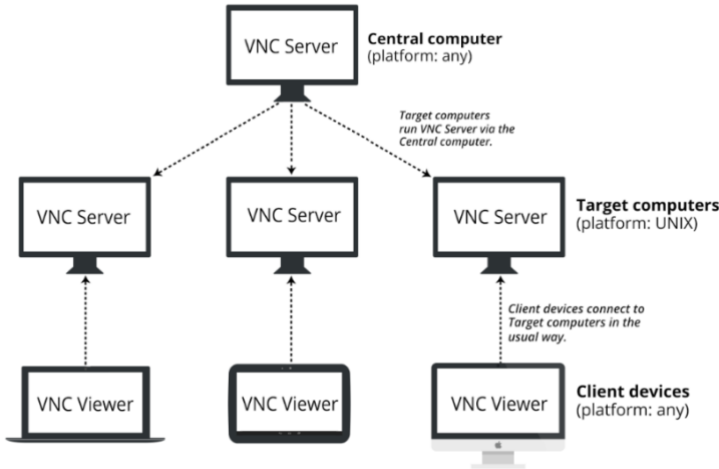


Figure 4.59: VNC Diagram. Reproduction permission requested from RealVNC.

The original source code of Virtual Network Computing is available under the GNU General Public License. There are also several variants of the system that offer their own special features, such as file transfer or optimized for Microsoft Windows. Usually, a viewer connects to a server using a standard port. However, it can also connect to the server using a browser. In listening mode, a client can connect to a server without requiring the server to configure its firewall. This feature saves the client from having to set up its own firewall. It also allows a viewer with no technical background to connect to the server.

The basic concept of the VNC protocol is that it can use a lot of bandwidth to carry out its tasks. To reduce the communication overhead, various methods have been developed. The simplest way to transfer data is to use raw encoding, which sends data in a left-to-right scanline order. This method works well if the screen changes only a small portion of the time. However, it can get very heavy if the number of pixels changes at the same time. Usually, it uses the TCP port 5900+N. Some implementations start with a basic HTTP server and provide a Java applet to allow easy connection to any Java-capable browser. Even on low bandwidth, a viewer can still connect to the Internet.

Although it can be done remotely, establishing a connection may require the proper configuration of the network address translation (NAT) and the appropriate firewall settings. You can also use a remote network connection (VPN). Xvnc is a Unix server that displays client windows. It is typically referred to as an X server when used by remote users. However, applications can still appear on the server as if they were a normal X display. Alternatively, a machine with a keyboard, mouse, and screen can be set up to run the server as a service or a daemon. It can then remove the display and its components, such as the keyboard and mouse, from the machine.

On Linux and Unix systems that support multiple X11 sessions, the system can start a new X11 session or serve an existing one. On Microsoft Windows, the current user session is used. For Mac OS X, Apple Remote Desktop for Mac OS X works seamlessly with the Xvnc client. It can also

connect to a user's current desktop if it's served with x11vnc or if it's served with TightVNC. Although RFB is a secure protocol, it doesn't encrypt passwords. A network can still break this feature by sniffing the encoded and the plain-text passwords.

For security reasons, it's recommended that the user's password be at least 8 characters. Some versions of the protocol also have an 8-character limit. In addition, some versions of the protocol support an encryption plugin that can prevent unauthorized access to the server. RealVNC supports authentication using Active Directory and NTLM accounts. However, using encryption plugins can prevent it from working seamlessly with other programs. According to the developers of TightVNC, the protocol is not secure as it sends data without encryption. To prevent this, the client should be tunneled through a secure SSH connection. There are a wide range of SSH clients available for various platforms. Some of these include UNIX, Windows, and Mac OS X. Aside from these, there are also freeware solutions that allow people to create encrypted tunnels between their devices.

SSH

The Secure Shell Protocol is a cryptographic network protocol that enables secure access to network services over an unsecured network. Its most used applications are remote login and command-line execution. It is composed of three components: the transport layer, the user authentication protocol, and the connection protocol. Unix-like operating systems is served by the Secure Shell, which was first designed in 1995. It is a replacement for the Telnet and other insecure remote Unix shell protocols. [4.78]

The initial development of the protocol was carried out in various developer groups. There are two major versions of the protocol: the first is known as SSH-1 and the second is known as SSH-2. Secure Shell is a cryptographic network protocol that enables the remote computer to authenticate its user. Basically, it works by automatically creating public-private key pairs to secure a network connection. The user then generates the public-private key pair manually. This method ensures that the authentication is performed. The public key is placed on the computer to allow the user to access the owner's private key. However, since the key is never transferred to the network, the user's authentication is never affected. To prevent unauthorized users from accessing your network, it is important to verify the public keys used by the system before accepting them as valid.

Remote users typically use the protocol to perform various tasks, such as accessing a remote machine and executing commands. It can also transfer files using the associated protocols. An SSH client is used to establish connections to an authorized server. Most modern operating systems, such as Mac, Linux, and Windows, support the use of both the standard and the advanced versions of the protocol. However, versions prior to Windows 10 do not support the use of the protocol.

For file managers that support UNIX-like operating systems, the FISH protocol can be used to provide a split-pane interface. The WinSCP client can also perform various file management tasks using PuTTY. Both the WinSCP and PuTTY are available as standalone programs that can be run directly off a USB drive. Setting up an SSH server in Windows is typically done through the Settings app. In Windows 10, an official port of OpenSSH is available. This feature allows users to connect to a cloud-based virtual machine without exposing it to the Internet.

An SSH tunnel can be used to connect to a virtual machine, which is outlined in Figure 4.60. The Internet Architecture Network (IANA) has designated various ports for this protocol, such as 22 and SCTP. These ports are commonly used by servers that support the protocol. The various versions of the protocol are used in various file transfer methods. Some of these include SCP,

which is a more efficient alternative to FTP. SFTP is a secure alternative to FTP that can be used to transfer files over a network connection.

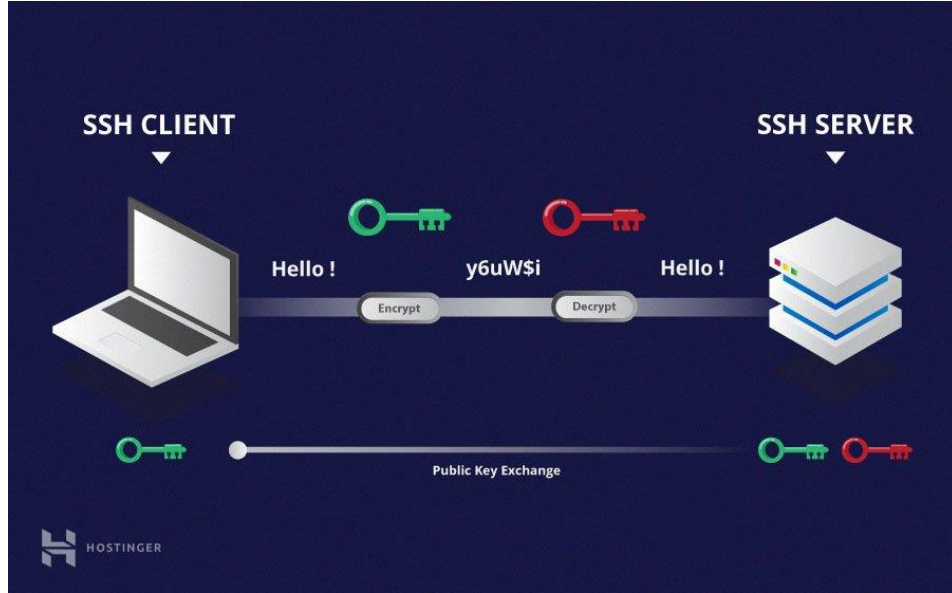


Figure 4.60: SSH Diagram. Reproduction permission requested from Hostinger.

4.3.10 PROGRAMMING LANGUAGES

In addition to modes of communication, programming languages is another crucial component of our design as we need a way to be able to interpret all the data that our hardware will be collecting. There are numerous programming languages available; however, some will be more beneficial than others to use in this application. C is a popular choice for embedded systems or any hardware-related applications, while Python is general in its applications. Each language has their benefits and downfalls, so we must make a reasonable decision in which programming language to use for our design.

After developing software in a combination of C, C++, and Python languages, we decided to use the Arduino programming language as it is a compounded language made up of the mentioned languages. Additionally, a benefit of the Arduino language is its IDE supports a wide array of libraries.

C

C is a general-purpose programming language that supports various types of programming, including structured programming and recursive programming. It has been used in many applications that were previously written in assembly language. [4.81] C is commonly used for developing operating systems and other applications for computer architectures that include embedded systems, supercomputing facilities, and programmable logic controllers. It was used during the development of the Unix operating system. During the 1980s, it gained widespread popularity. It is used by many different computer platforms and operating systems. ANSI C has been widely used since 1989. It was developed to provide a low-level programming language that is easily accessed and mapped to machine instructions. Despite its low-level capabilities, the C language was designed to encourage programming that is cross-platform. A C program that is built with minimal changes to its source code can be compiled for various platforms.

C is widely used for programming in embedded systems and operating systems. Its code can be written for portability, yet it can also be used to access and modify hardware addresses. [4.82] It can also be used to implement website programming using the Common Gateway Interface. C is often chosen over interpreted languages due to its portability, ease of use, and near-universal availability. A consequence of this is that compilers and interpreters of other programming languages are commonly used in C.

Since some libraries and other programming tools can be written in C, it can be commonly used as an intermediate language. This approach is usually used for portability or convenience. Some of the features of C are still missing, which has prompted the development of other C-based languages that can be used as intermediate languages. [4.83]

C++

[4.84] C++ is a programming language that was created by Bjarne Stroustrup. It has evolved significantly over time and now includes object-oriented constructs and functional features. C++ is a programming language that is usually built as a compiled version. Numerous vendors support it, including IBM, Microsoft, and Intel. It is designed to work seamlessly across various platforms.

C++ has been widely used in various contexts, such as web search, e-commerce, and databases. It is also commonly used in infrastructure-focused applications, such as video games. It is also widely used in performance-critical applications. In 1998, the C++ programming language was standardized as part of the International Organization for Standardization's (ISO) 14882:1998 standard. It was initially developed by Stroustrup as an extension of the C language. Before its standardization, he wanted a more flexible and efficient language that could be used by developers.

C++ is the programming language that is used by most of the major operating systems. Being able to develop an operating system in C++ makes it very fast and easy to implement. C++ is a very close cousin of the assembly language. This makes it possible to write lower-level operating system modules. Due to its low-latency, low-complexity, and high-quality, many low-latency systems implement C++ as their programming language. For instance, many high-end libraries rely on C++ as their main programming language. Due to the complexity of the math involved in learning machine learning models, many libraries have had to provide high-performance computing. C++ is typically used to provide the necessary performance.

C++ is commonly used as the main programming language for software that handle various high-end processing tasks such as image processing, computer vision, and graphic processing. Even the popular video games industry is also known to use C++ as its main programming language. Due to the high number of transactions that banks process daily, C++ is the preferred choice for banking applications. It is also used in distributed systems due to its ease of use and connection to the hardware. In cloud storage systems, C++ is often used as the programming language of choice since it is very close to the hardware and provides high-complexity and load tolerance. This is also due to its multithreading libraries.

Database software is commonly used in various applications that we use every day. Due to its proximity to the hardware, C++ is commonly used as the main programming language for embedded systems such as medical devices and smart watches. Due to the presence of lower-level languages, C++ is more advantageous than other programming languages when it comes to compilation systems.

Python

Python is a programming language that emphasizes code readability and object-oriented design. Its various constructs and object-oriented approach help developers create clear, logical code. It supports various programming paradigms, such as structured programming and object-oriented programming. It is often referred to as a "batteries included" language. Python 2.0 was released in 2000, and it included new features such as list comprehensions and Unicode support. In 2008, Python 3.0 was released, which is not backward compatible with older versions. [4.85]

Python is a multi-platform programming language that supports both object-oriented and functional programming. It also supports several other programming paradigms, including design by contract and logical programming. Python supports various programming traditions, such as Lisp. Its dynamic name resolution provides a binding between methods and variable names. The standard library has two modules: functools and itertools. Both of which are based on the same functional tools. Its core philosophy is based on aphorisms, which can be found in the document "The Zen of Python". The compact modularity of Python has made it popular to add programmable interfaces to existing apps. Unlike Perl, Python has a "there should be one" philosophy. According to Alex Martelli, a Fellow at the Python Software Foundation, Python's developers do not consider anything as "clever" as it is not considered a compliment in the culture. When time is of the essence, a Python programmer can move time-sensitive functions to extensions that are written in C or Python. [4.86]

4.3.11 OPERATING SYSTEMS

To collect data in an orderly fashion on our Raspberry Pi, we will need a lightweight, efficient operating system. There are many choices available on the open-source market, but we will be looking at two different options for our application: Linux Ubuntu and Linux CentOS.

Linux CentOS

The CentOS Linux distribution is a repository built on the Red Hat Enterprise Linux platform. Its stable, predictable, and reproducible nature make it a great choice for anyone who enjoys distributing Linux.

CentOS Linux is a free and open-source operating system that aims to be compatible with Red Hat Enterprise Linux (RHEL). It is developed by a small team of developers and is supported by a robust community. The CentOS Project is a semi-autonomous entity that draws on the Apache Foundation's structure. Its governing board is composed of various special interest groups.

Linux Ubuntu

Ubuntu is a Linux distribution that's made up of mostly open-source software. It's usually used for desktop computers and can run on various Internet-connected devices. Ubuntu is a widely used operating system for cloud computing. It has a default desktop named GNOME, and it supports various cloud computing platforms, such as OpenStack. Its long-term support is available until 2030.

The latest version of Ubuntu is called 21.10 and is supported for nine months. It is distributed by Canonical, a British company that specializes in distributing open-source software. It is owned by a group of developers known as Canonical, which generates revenue by selling premium services related to the operating system.

LAMP Software Bundle

In addition to operating systems, there are additional features that were installed onto our Raspberry Pi, including a web server, a database, and supporting programming languages. The term LAMP is an acronym for "Linux, Apache, MySQL, PHP, and Python". It's commonly used to refer to various software platforms used by web developers. The term LAMP stands for a generic software stack model. It consists of four components: Linux for the operating system, Apache HTTP Server MySQL for the database management system PHP, Python, and Perl. [4.79] This is illustrated in Figure 4.61.

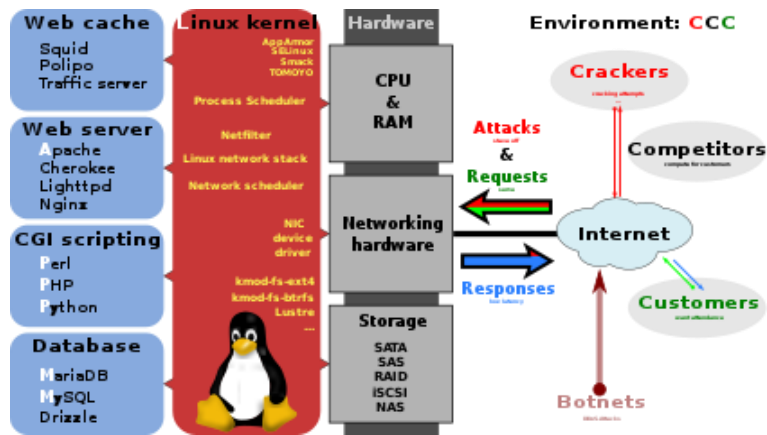


Figure 4.61: LAMP Software Bundle [4.108]

In 1998, Michael Kunze introduced the concept of LAMP in Computertechnik, a German magazine. It became a popular term among developers and media companies. The concept of LAMP became popular due to its ability to host various web frameworks, such as WordPress and Joomla. Although the LAMP model is commonly used for developing web applications, it can also be utilized for other components such as operating systems and databases. For instance, an equivalent installation of Windows on a Mac is known as MAMP. For instance, if you have a Windows-based system, an alternative called WAMP can be used instead of Apache. It can also be installed on other operating systems such as Mac OS X, SAMP, FreeBSD, and XAMPP. [4.80]

A version known as LEMP is a replacement for Apache that features the more lightweight web server Nginx. It can be combined with other open-source software packages such as SystemSnout for security testing and hardening. Another example is the software that Wikipedia and other Wikimedia Foundation projects use for their infrastructure.

The Linux operating system is a collection of open-source software packages that are assembled under the framework of the free and open-source software development community. Most of these packages provide complete LAMP setups. The role of the web server has traditionally been provided by Apache, and it has since been joined by other web servers such as Nginx. In 2013, it was estimated that Apache served over 50% of all websites on the Internet. In 2014, it was estimated that Apache served over 50% of all websites. It is an open-source software that is maintained and developed by the Apache Software Foundation. It supports a wide variety of features and is commonly used by web developers.

The role of the MySQL database management system has been provided by other components such as MariaDB and PostgreSQL. It was acquired by Sun Microsystems in 2008 and became part of the Oracle Corporation. Since its inception, the MySQL team has made its source code available under the terms of the GNU General Public License. Another database management system known as PostgreSQL is also available under the GNU General Public License. MongoDB is a NoSQL database that uses dynamic schemas and JSON-like documents.

The role of PHP, which is a server-side programming language, has also been performed by other components. It is commonly used for web development and can be interpreted by a web server. It can also be used as a command-line interface for developing standalone applications. PHP is a free software that is available under the terms of the PHP License. This means that it is not compatible with the GNU General Public License. Raku and Perl are two popular programming languages that provide advanced text processing capabilities without the limitations of modern Unix command line tools. They were also popular during the 1990s as a CGI scripting language.

4.3.12 DATA STORAGE METHOD

Once we've successfully delivered our data to our Raspberry Pi, we need to store said data in an organized database to allow for easy access and interpretation. Once our data is stored in a database, data analysis and manipulation can occur to make sense of our collected data. There are many types of databases and technologies we can implement, such as SQL and its various flavors, MongoDB, and many more. For our application, we opted for MySQL

MySQL

MySQL is a type of open-source database management system. It enables users to create, modify, and publish databases that are designed to work seamlessly with each other. SQL is a programming language that enables developers to create, modify, and extract data from a relational database. It also controls the user's access to the database. Aside from databases, MySQL also supports various other features, such as network access and backup. MySQL was originally created by MySQL AB, a Swedish company that was acquired by Sun Microsystems in 2010. After Oracle bought Sun, Widenius forked the open-source project and created MariaDB. MySQL is a component of the LAMP stack, which is an acronym for Linux, Apache, PHP, and Python. It is commonly used by web developers to create and manage database-driven applications.

There are also free and third-party administration applications that integrate with MySQL. They allow users to easily work with the database's structure and data. MySQL Workbench is an integrated environment that allows users to create graphical representations of the MySQL database's structures. It is available in three editions: the free and open-source Community Edition, as well as the Standard Edition.

MySQL also ships with many command-line tools, such as the MySQL client. These utilities are designed to perform common tasks and administrative tasks. Percona Toolkit is a utility that can be used to test the reliability of a MySQL database, fix corrupt data, and speed up servers. It is included with various Linux distributions.

4.3.13 PCB ENCLOSURE

Enclosure

Our final circuits need to be boxed safely when it is going to be installed outdoors. Talking outdoors installation, many things can happen regarding the safety and the security of the components such as harsh weather, very high temperatures, rain, severe storms, and exposure to

dust and dirt. All those conditions can impact and contribute to a short lifetime, a malfunction, and a destruction of the device. To prevent such of events, we need to use an enclosure that can protect the device under certain standard requirements conditions. To choose the appropriate enclosure for our design, we need to consider those factors: protection rating, certification approvals, size, access needs, cost, temperature environment, and corrosion resistance.

Protection Rating and Certification Approvals

To make sure about the type of enclosure to use, the enclosure protection rating is important to ensure the degree of the protection that will be provided for the inside equipment. In other terms, rating the enclosure protection means that what is the level of protection that enclosure can provide to secure the equipment from dust, dirt, liquids, and more. Usually NEMA (National Electrical Manufacturers Association) rates that type of level protection of enclosure. An electronic enclosure that is falling on NEMA 4X has a high degree of protection.

Size

The size is the dimension of the enclosure where the equipment will be installed. The size varies with the size of the component meaning that the height, the width, and the depth of that component is and by that we can choose the proper or approximate enclosure for our device. In our case the size of the PCB is approximately 3”X3” and the height of the component remaining pending until the final touch.

Access needs

The accessibility to the components inside the enclosure usually makes with a front door or a cover. That door or cover can be locked with quarter turns, latches, clamps, handles, or screws. Regarding to the type of security that we are looking for we can make the proper choice. When security does really matter, other optional accessories can be added such as padlock hasps, tamper proof screws, or key lockable hardware.

Cost

Cost is also another important aspect when choosing enclosure protection. Normally, price and quality always come to a challenge in people choices. As the quality of a product is high the cost of this product goes up and it is true for the reverse phenomenon when the quality of the product is low the of this product is low also. That means, when making our choice for the appropriate enclosure both aspects of quality and price should take into consideration base the customer requirements.

Temperature

Another crucial factor when it comes to enclosure protection is temperature. Temperature is important key for the device inside the enclosure. The ambient temperature either high or low can negatively affect the efficiency of the device when it is boxed in the environment. However, as we are living in a tropical state where the ambient temperature in Florida is most of the time high. For this reason, we need to investigate the ambient temperature and the device temperature tolerances to find the right enclosure protection. In this case compared to the size of the component a larger enclosure might encounter this issue. In addition, there are other options that we can consider compensating the heat from the ambient and the heat dissipated by the components such as using cooling fans, or heat sink devices.

Corrosion Resistance

Depending on the type of materials using for enclosure, the environment can affect enclosures and makes them very corrosive. Manufacturers for enclosures use special materials like stainless steel, aluminum, polycarbonate, and fiberglass to encounter these environment issues. A type NEMA 4X standard rated is an example of enclosure protection rating for corrosion resistance.

Figure 4.62 display two candidates for a PCB enclosure for the All-In-One PV Sensor.

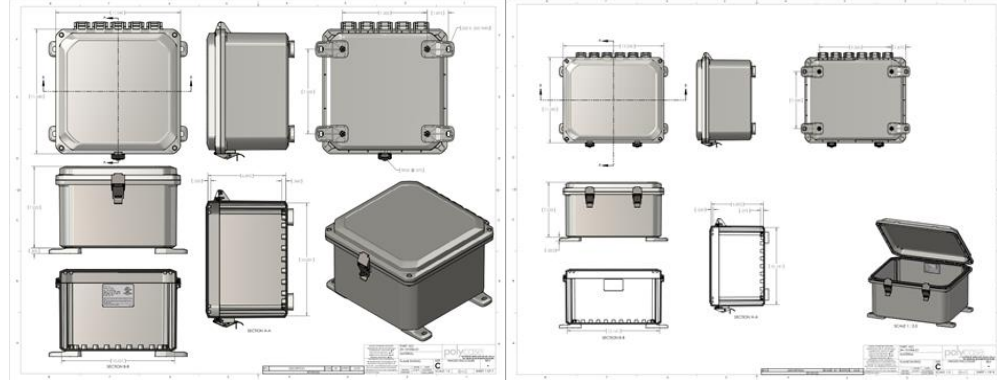


Figure 4.62: Layout of Several Prospective Enclosures

We have searched for enclosure protection for our design, and we have found a couple of options that might be an excellent choice for our components. From Polycase, we saw the ZH-101006 and the ZH-121006 Hinged NEMA enclosures. They were made with impact-resistant polycarbonate materials especially to be installed outdoors with standard requirements protection against weather, water, corrosion, dirt, and dust hazardous. These enclosures have been rated by NEMA UL and other associations for diverse levels of protection. The rated for those enclosures are IP65, IP66, IP68, NEMA 3S, 4, 4X, 12, and 13 rated. The difference between those two types of enclosures is resided in extra features so one can have and the other one does not have and cost also. Table 4.21 below summarizes the difference between the two enclosures.

Table 4.21: Comparison of ZH101006 and ZH121006 Enclosures

Enclosure	Rating	Size	Cost (\$/Unit)	Extra Features
ZH-101006	IP66 NEMA 3S, 4X, 13	11.04X11.04X7. 52in	54.41	Single Padlock
ZH-121006	IP66 NEMA 3S, 4X, 13	13.24X11.24X7. 70in	56.04	Double Padlock

Heat Sink

Things to expect in electronic circuits when they are in operation is the heat dissipation by the components. Sometimes, over the time that heat can increase, overheat the system, and create a malfunction of the device beside the environment effect. To avoid this situation, we can install a heat sink to counter that overheating to reduce that high temperature on the device and to keep it at its proper ambient temperature tolerance. Heat sink can be part of the component to absorb heat and produce a good air flow within components that have been enclosed.

A heat sink is a device that exchanges heat meaning that it transfers the heat generated by an electronic or mechanical device to a fluid medium usually it is air or liquid coolant. Therefore, this heat sink will generate the device's temperature from all its dissipated heat.

Aluminum and copper alloys are the most common materials that have been used for heat sinks. They are both excellent materials for thermal conductivity, even though they have their differences. Aluminum heat sinks are the most used for many reasons. The potent thermal conductivity is measured at 235 W/m-K. Aluminum material has been worked for pure thermal conductivities due to its low density and good corrosion resistance. On top of that it is not expensive. Copper, on the other hand, it is an excellent element for thermal conductivity, its potent is 400 W/m-K better than aluminum and can possess corrosion and antimicrobial resistance. It has been

employed in industrial works such as power plants, solar systems, and more. However, it remains expensive compared to the aluminum as seen in Table 4.22.

Table 4.22: Aluminum VS Copper Heat Sink

Material	Specific Heat [J/g* °C]	Thermal Conductivity [W/m*K]	Weight (amu)
Aluminum	0.9	235	26.98
Copper	0.385	400	63.55

Obviously, according to NEMA standardization of enclosure, our enclosure should be able to protect the components against certain degrees of temperatures because those enclosures should make with a good temperature insulation. Even though, we should not rely on that viewing the area that we live, Orlando FL is well known for its hot temperatures. At certain times in the day, the ambient temperature can vary up to 100 degrees Fahrenheit. For this reason, it is important to consider when we will have electronic circuit that can dissipate lot of energy inside a close box what type of precaution to take to prevent any inefficiency of the device.

In addition to the enclosure, we should consider all components that can disperse heat. This study can be done in two ways. First, we can look at the datasheet of each component to find out how much power they can dissipate therefore we can evaluate the total dissipation of heat that will be inside the enclosure. Another way is to have all parts set up and perform a test to measure the amount of energy dispersed out. For the first evaluation, Table 4.23 below will give us an approximate temperature tolerance of some of our components and how much heat they can dissipate.

Table 4.23: Components' temperature parameters

Components	Operating Temperature (deg C)	Maximum Ambient Temperature (Deg C)	Potential Power Dissipation (mW)
TLV342AID Op-Amp	-40 – 125	140	105
INA126PA Inst-Amp	-40 - 85		3
LM5017 DC-DC Converter	-40 - 125	150	3000
Inductors	165	165	N/A
Capacitors	165	125	N/A
Resistors	125	155	N/A

The datasheet for ESP32 gives some characteristics about the temperature of the device. The recommended operating ambient temperature range for it is -40 to + 85 degrees Celsius. The temperature of the environment that we live, Orlando, is not going over that usually it is around 40 to 45 degrees Celsius. Because it will be inside of an enclosure, we might expect an increasing

of the temperature. For that, to prevent any failure or any malfunction of the device, we need to choose an appropriate heat sink. It could be copper or aluminum heat sink depending on the parameters.

First, we need to compare both copper and aluminum heat sink to see which one can be more portable regarding the budget and more feasible to use. By looking at vendors we found the Wakefield Thermal SKV4545225-CU copper heat sink and the ESP32 Aluminum Cooling heatsink. Both have their advantages, disadvantages, and similarities.

By making comparison we see that copper heat sink SKV454525-CU is a self-adhesive, so we don't purchase any extra glue for it. The push pins are plastic just to an easy attachment and its thermal resistance is $15.90^{\circ}\text{C}/\text{W}$ with a size of 38.5X37.6X11mm. At market, it cost \$ 7.59. on the other hand, the Aluminum heat sink is also self-adhesive, relatively small for its 9mmX9mm size. It is not easy to heat, has good consumption for energy for wireless communication, and it can improve stability of the chip. For those reasons, the aluminum heat sing is a good choice for our project. The following table gives a prospective for the ESP32 heat sinks. Indeed, it is cheaper the copper heat sink.

5. SYSTEM DESIGN

To move forward with the creation and testing of the All-In-One PV Sensor, the prototype must have a completed schematic and corresponding EAGLE design. In this section, the EAGLE design for the AIO PV Sensor will be discussed. This design will eventually be used to create the PCB layout of the board as the components can be selected and their respective footprint on a board can be compared to one another and assembled on a board.

The EAGLE design will feature every component of the All-In-One PV Sensor including the pyranometer and thermocouple as their existence on the board must be accommodated whether they are connected to it.

5.1 HARDWARE DESIGN

The hardware design for the All-In-One PV sensor will fully encompass the components that will be present on the PCB attached directly to the Solar Array's outputs. Therefore, all hardware for this includes the Voltage and Current Sensors, the Thermocouple, the Pyranometer, the On-Board Power Supply, and the MCU.

5.2 TERMINAL CONNECTIONS

To measure signals, we must first connect them to the PCB. This is done via Terminal Blocks with differing gauges depending on the source of the signal. For the Panel's voltage input which will be used to measure voltage and current, a 10 Gauge AWG terminal block will be used. For the smaller order inputs from the pyranometer and thermocouple, a 16 Gauge AWG terminal block will be used instead.

The panel's input can be seen in Figure 5.1.

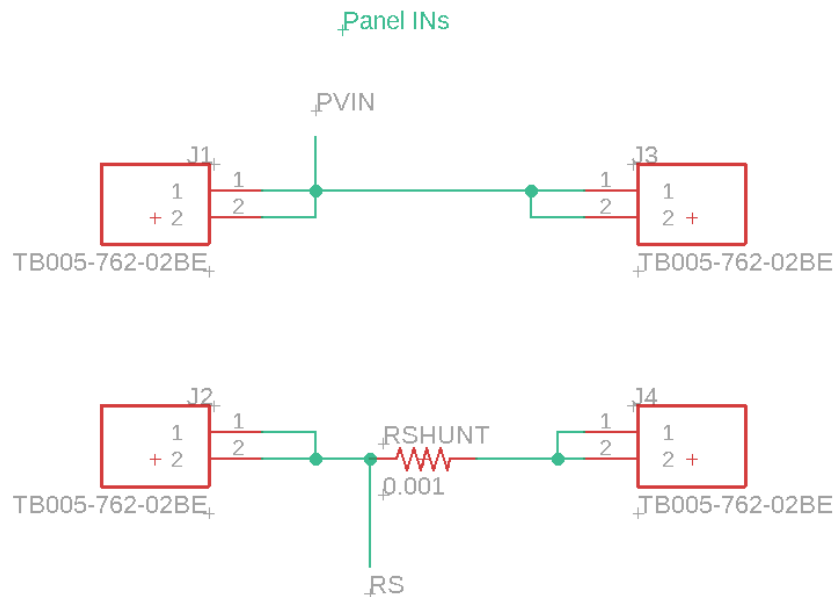


Figure 5.1. Panel IN and OUT

On the left-hand side, the voltage and current generated by the solar panel come into the PCB through TB005-762 Series Terminal Blocks, capable of holding 10 AWG wires to withstand the large output of the solar panel. Because we want our design to have minimal impact on the voltage and current generation of the panel, the inputs are passed directly through to the outputs via a new set of TB005-762 Series Terminal Blocks.

Along the way, the positive side of the solar panel's output is taken as PVIN and a value measured across a shunt resistor, RS, is taken as well. This shunt resistor serves as a current measuring component using Ohm's law to correlate the voltage drop across the small resistance to its total

current by dividing the voltage by its resistance. This decision was inspired by the TIDA-00640 which proved that, given a module can produce a maximum of 300 Watts, the panel would only lose a maximum of 0.03% power from the existence of the shunt:

$$\% \text{ power loss from shunt} = \frac{\text{Shunt power dissipation}}{\text{Maximum module power}} \times 100 = \frac{0.100 \text{ W}}{300 \text{ W}} \times 100 = 0.03\%$$

Along with the Solar Panel's voltage and current being taken into the PCB, the pyranometer and thermocouple outputs are taken in. The model used for the terminal blocks in Figure 5.2 are the 1727010 PCB terminal Blocks.

Pyranometer and Thermocouple inputs

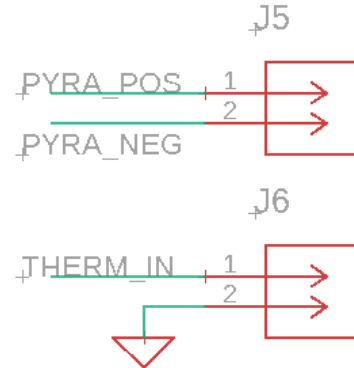


Figure 5.2. Pyranometer and Thermocouple inputs

These inputs are relatively simple as the components that are used to amplify or deliver these signals to the ADC will be placed directly on the PCB, independent of the pyranometer or thermocouple's existence in the application. Both the pyranometer and thermocouple are expected to have relatively small outputs in terms of voltage, so they must be amplified. This will be expanded upon in sections 5.5 and 5.6.

5.3 ON-BOARD POWER SUPPLY

All on-board components are powered through the VCC of the board which was decided to be 3.3V to satisfy various turn-on voltages for the different components across the PCB. This VCC is created by the LM5017 Step-Down Regulator, capable of taking 100 V and stepping it down to an acceptable 3.3 V level. This can be seen implemented in our EAGLE design in Figure 5.3.

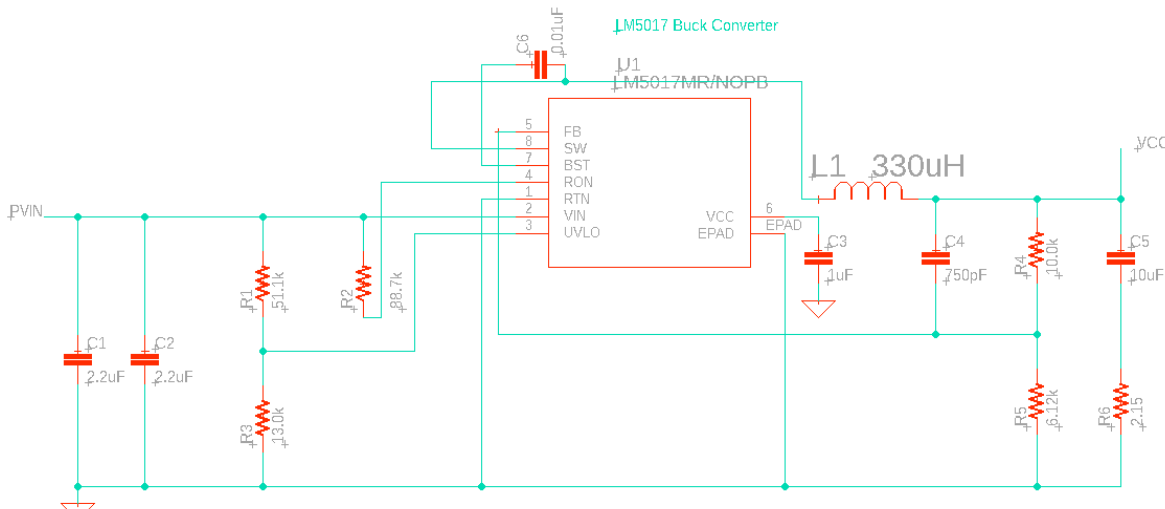


Figure 5.3. The LM5017 Step-Down Regulator

The LM5017 was selected due to its small current draw requirement and its ability to regulate relatively high voltages compared to what we expect from the Solar Panels that the All-In-One PV Sensor will be installed on. To minimize costs, the Type 2 LM5017 is selected. The respective type of the LM5017 is determined by its Ripple Configuration, and the Type 2 configuration can be seen in Figure 5.4.

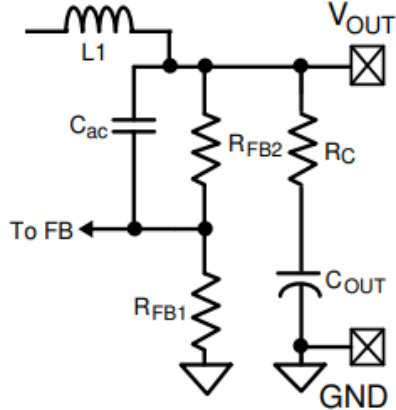


Figure 5.4: Type 2 LM5017 Ripple Configuration

This implementation can be seen on the righthand side of the LM5017's implementation in EAGLE. This selected variant has a less stable VCC, but a stable VCC will not be required as the components in our PCB do not need a constant 3.3V to operate, so long as it falls within a reasonable range.

5.4 CURRENT AND VOLTAGE SENSING

The next section of our EAGLE design lies in the current and voltage sensing circuits. The shunt resistance is used to measure a small voltage across a shunt resistor, but that must be sent to an Op-Amp to be compared to ground and sent to an ADC to prevent the loading effect. Similarly, the voltage must be sensed using the input of the solar panel and sent through an Op-Amp so that it can be converted. This configuration can be seen in Figure 5.5.

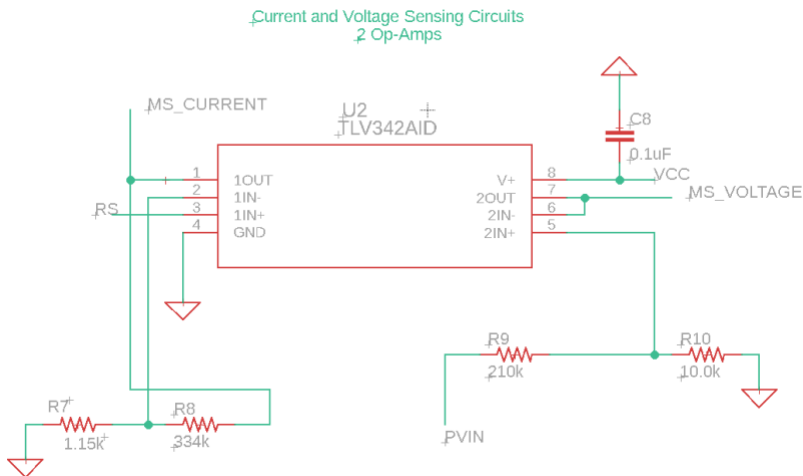


Figure 5.5: TLV342 Current and Voltage Sensing Circuitry

The selected Op-Amp for our EAGLE design was the TLV342, chosen as it was for the TIDA-00640 reference design. This Op-Amp has a low offset and is specifically designed for low voltage operation which is ideal for our implementation. The VCC is sent into this Op-Amp and is coupled to minimize noise injection and both Op-Amps in this dual module are utilized for current and voltage sensing.

The current sensing circuitry is on the left-hand side of the TLV342. The measured voltage across the shunt resistor is sent into the positive input of the Op-Amp, and the negative input is compared to ground across a 1.15k resistor and sent as a measured current, MS_CURRENT, over a 334k resistor to the ESP32's ADC to be converted. The 334k resistor serves to amplify the measured voltage so that the ADC can easily translate the received signal into tangible, digital values. The voltage that is measured across the shunt resistor is in the millivolt range, and the amplifying circuit brings it up to no greater than 3V.

A voltage divider is implemented on the right-hand side to simply measure the current. A voltage divider was chosen as the method of measuring the Panel's voltage output due to its simplicity and therefore its low cost. Because we want to measure the panel's direct output voltage, the value PVIN is sent over a voltage divider of 210k ohms and compared to ground over a 10k resistor. The total cost associated with the final 3 created PCBs can be seen in Table 5.1.

Table 5.1: Current and Voltage Sensing BOM

Component	Quantity	Cost Per Unit (\$)	Total	Notes
TLV342A	1	0.323	1	Current and voltage sensing IC
Ceramic Capacitor 0.1μf	1	0.20	1	0.1μf Decoupling Capacitor
C0805C105K 8RACAUTO	1	1.57	1	100mΩ Current sense sunt resistor
Resistor	5	0.10	1	Resistor

5.5 TEMPERATURE SENSING

As noted in Section 5.2, the expected output of the selected Thermocouple will likely be in the millivolt range. Along with this, thermocouples need reference nodes to compare their measured temperatures to maintain a higher degree of accuracy. For this reason, the MAX6675ISA is selected as the Thermocouples integration to the board, seen in Figure 5.6.



Figure 5.6. MAX6675ISA Thermocouple Amplifier

The MAX6675ISA features internal amplification and reference (cold) junctions for the thermocouple to function: It must reference the temperature that it measures to a constant

temperature, the cold junction, and those small voltages that are read from the comparison of the two junctions must be amplified so that the ADC can translate them into digital values. The MAX6675ISA takes the thermocouple's input, THERM_IN, and uses it internally to send outward to the ESP32 via THERM_SO, THERM_CS, and THERM_SCK.

The total cost associated with the final 3 created PCBs can be seen in Table 5.2.

Table 5.2: MAX6675 BOM

Component	Mfr #:	Quantity	Cost Per Unit	Total	Notes
Integrated IC Temperature Sensor	MAX6675ISA+T	3	\$15.59	\$46.77	Amp/Cold-Junction Compensation SMD Chip 8 pins
Ceramic Capacitor 0.1 μ F	C0805C105K8RACAUTO	3	\$0.20	\$0.60	Decoupling Capacitor
Total Cost:				\$47.37	Total Sensor Cost for 3 Units

5.6 INITIAL IRRADIANCE SENSING

Just as the thermocouple has an on-board amplifier for its relatively small signal, the pyranometer is making use of the MAX4194 Instrumentation Amplifier to amplify its small maximum signal of 200mV to a new maximum of 1V, allowing the on-board ADC of the ESP32 to easily read the signal output by the pyranometer. The MAX4194 EAGLE implementation can be seen in Figure 5.7.

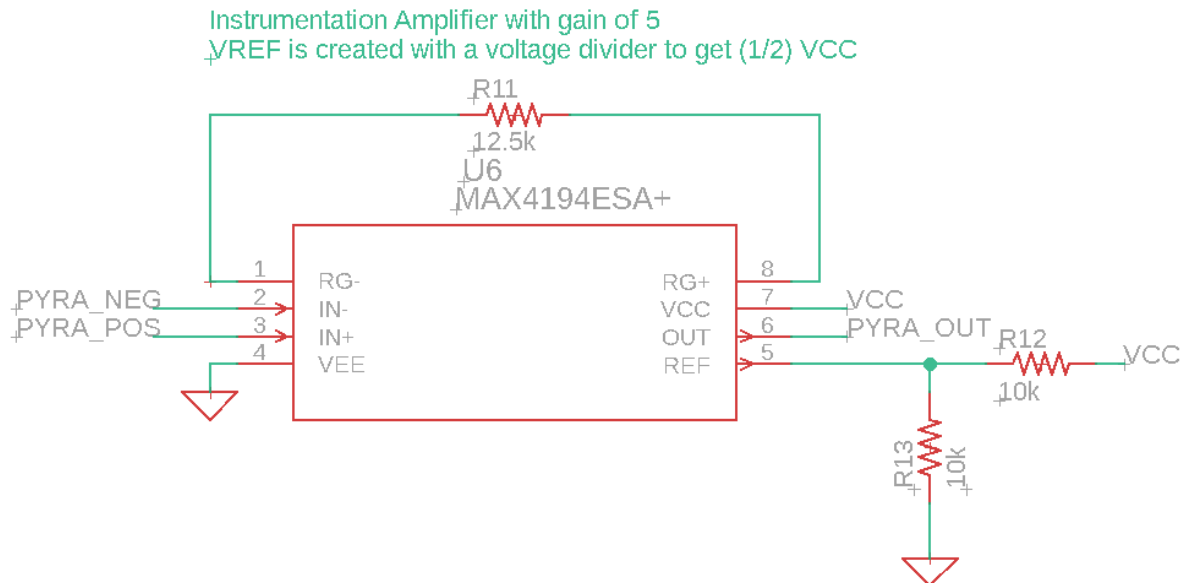


Figure 5.7. MAX4194 Pyranometer Amplifier

The MAX4194 can take the pyranometer's differential output and amplify it with a gain of 5 such that the lowest possible output is now 1 mV. This instrumentation amplifier was deemed necessary after discovering that the on-board ADC of the ESP32 had a resolution of 0.8 mV while the SP-110-SS had an output of 0.2 mV per 1W per meter squared, meaning that we would initially only be able to detect a change with every 4 W per square meter of sunlight irradiance.

The pyranometer will only be implemented on one of the three planned sensors that will be provided to OUC which is reflected in the Bill of Materials, seen in Table 5.3.

Table 5.3: Pyranometer BOM

Part	Quantity	Cost Per Unit	Total	Notes
Apogee SP-110-SS Self-Powered Pyranometer	1	\$230.00	\$230	Analog Sensor with maximum of 400 mV output, self-powered when exposed to sunlight
MAX4194	1	\$4.14	\$4.14	Instrumentation Amplifier, needed to combine the pyranometer's output.
Total Cost:		\$234.14	Total cost for OUC Implementation	

5.6.1 UPDATED IRRADIANCE SENSING

The MAX4194 was a good start, but without a dual-supply linear regulator, the IC would be subject to unmeasurable degrees of error due to its inability to operate correctly on a single supply system. For this reason, the team switched to a standalone ADC, the MCP3008. This ADC can translate a differential signal into a single analog signal using two of its input channels. The MCP3008 EAGLE implementation can be seen in Figure 5.8.

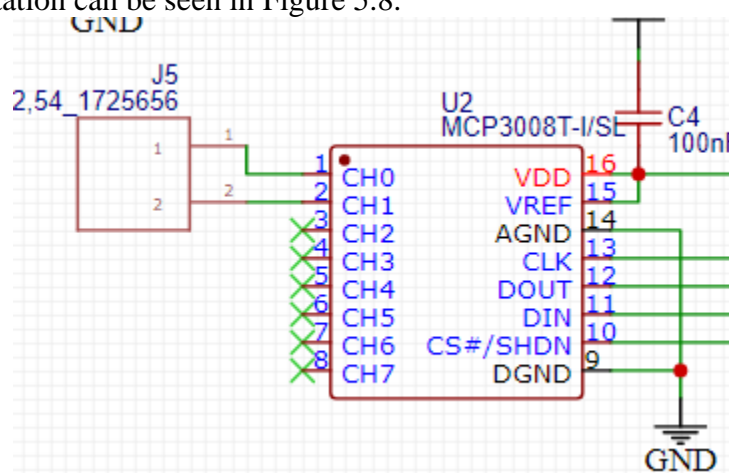


Figure 5.8. MCP3008 Standalone Pseudo-Differential ADC

The MCP3008 takes the pyranometer's differential output and translates it internally using a pseudo-differential configuration. The MCP3008 is a 10-bit ADC, so a resolution of about 15 Watts per meter squared is provided with this solution. As the pyranometer will only be implemented on a small percentage of the sensors that OUC will install on-site, this small loss in

resolution is acceptable as Rubin York stated the trend of data is more important than the raw value for irradiance.

The updated Bill of Materials for the irradiance sensing circuitry can be seen in Table 5.4.

Table 5.4: Updated Pyranometer BOM

Part	Quantity	Cost Per Unit	Total	Notes
Apogee SP-110-SS Self-Powered Pyranometer	1	\$230.00	\$230	Analog Sensor with maximum of 400 mV output, self-powered when exposed to sunlight
MCP3008	1	\$3.25	\$3.25	Pseudo-Differential Standalone ADC, needed to translate the pyranometer's output.
Total Cost:			\$233.25	Total cost for OUC Implementation

6. COMPONENT TESTING

In this section, we will test, stress test, and analyze all the necessary components for the All-In-One PV Sensor. In this preliminary testing we will test both the hardware and software elements necessary for the completion of the “All-in-One PV Sensor”. The initial testing will include tests from the Voltage, Current, Temperature, Irradiance Sensors and the ESP32 Wi-Fi Module. Follow up by the software testing where we will test the capabilities of the Raspberry Pi 4 for data logging from the data transmitted by the ESP-32s’ access point network tested in the hardware section.

6.1 HARDWARE TESTING PROTOCOL

To test our hardware in a typical testing environment we will utilize a Solderless Breadboard to perform preliminary testing of all components used in the development phase for the “All-in-One PV Sensor”. A Solderless Breadboard is a basic component that will allow us to connect, replace, and remove components without the need to solder them. In addition to this we will also use as preliminary testing a ESP32 developmental board to test our component compatibility with the ESP32 which will also help as benchmark test for possible ESP32 SMD form implementation in our design instead of a stacking method.

To properly interconnect components on a breadboard the use of 20–22 Gauge wire is recommended to prevent heavy wear and tear on the breadboard sockets that would make them less reliable due to the loss in clamping force of the sockets. Furthermore, to properly test our components implemented in our PCB design we decided to use SMD adapters as displayed in Figure 6.1. This was done to adapt our surface mount devices such as ICs to a compatible through hole form necessary for the breadboard testing environment. By soldering male header pins to the SMD adapters we can then directly connect the SMD components to the breadboard without any other modifications. This will help us test IC’s that are not sold in through hole form for testing. The second benefit of using an SMD adapter for IC’s is that it will guarantee that our tested parts will be as close in behavior as the ones implemented in the final PCB design.

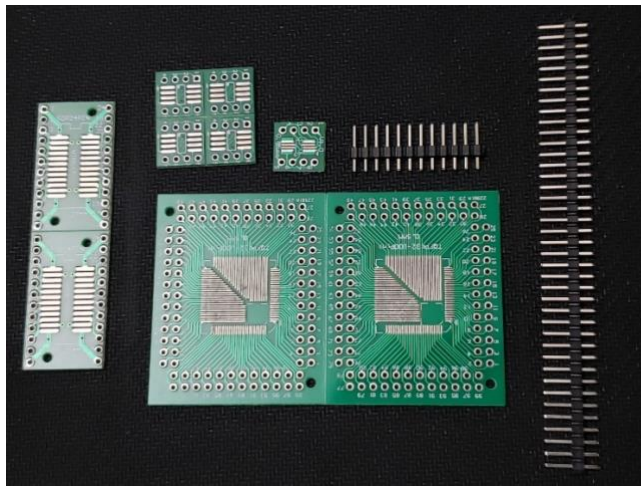


Figure 6.1: SMD Adapters by Marco Herrera
Marco Herrera

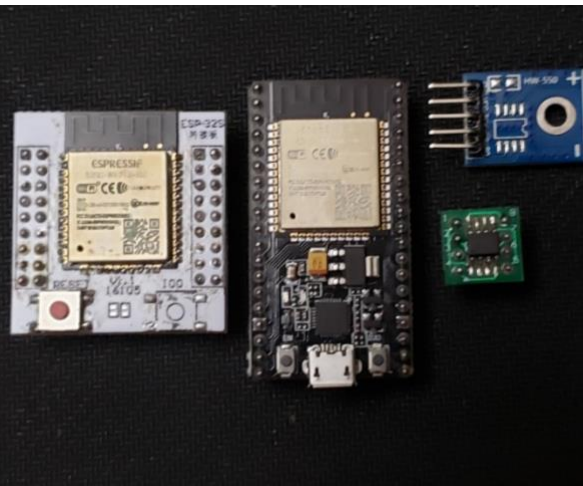


Figure 6.2: ESP-32 SMD Adapter/Dev Board by

In addition to the SMD ICs adapters we will also use a SMD ESP32 adapter as seen in Figure 6.2 to test an IC ESP32’s ability to program through the UART pins and corroborate the testing results done with the ESP32 developmental board.

6.1.1 ON-BOARD COMPONENT POWER SUPPLY TESTING

The on-board power supply is one of the most important parts of our PCB. Without it, none of the operational amplifiers will function, and the ESP32 will not be able to power on to convert any signals to digital to send any wireless signals to our local collector node. Our intended on-board voltage will be 3.3V and we aim to repurpose the LM5017 that was used for the TIDA-00640 on our board, modified slightly to output 3.3 V rather than 5 V.

Because we have not received the LM5017 converter, we cannot yet test the DC converter on a breadboard. However, the testing process can be defined as follows. In our environment, we aim to have a voltage of around 35 volts maximum coming into the board. This voltage will be processed by the LM5017 buck converter, shrinking a large voltage into a manageable 3.3V for on-board power supply. To test this, we can have a DC Power Supply hooked up to the voltage input of the LM5017 and measure any output. If the LM5017 is working correctly, then any voltage between the specified input range should give an output of 3.3V.

If the LM5017 is outputting 3.3V at varying levels of voltage, then we can consider our buck converter to be fully functional. This output VCC can then be used to further test the remaining sensing components by providing power to their respective components.

6.1.2 VOLTAGE & CURRENT SENSOR TESTING

Before designing and implementing the real circuit for the voltage and current sensing, we first must test the accuracy of the TLV342A to ensure that we can achieve the desired outcome. To verify the functionality of the op amp, the TLV342A would be tested with a DC voltage generator in conjunction with a solar array simulator and multimeter, this will prove the result that we are trying to achieve; 1.77 V max for the voltage sensing, and 1.10 – 1.22 max for the current sensing. The sensing would also be tested with the ESP32-Wroom-32; this would allow us to view the values produced by the ADC. The way we would perform these tests is by mounting The TLV342A on an SMD adapter PCB, adding necessary electronic components on the board.

6.1.2.1 Preliminary Voltage & Current Sensor Testing

The TLV342A uses SMD technology, so it must be soldered onto the PCB using header pins. The resistors we plan on using will also be placed onto the breadboard, then a DC power generator will energize the amplifier. 0.01 V will be supplied to the current sensing side of the amplifier (pin 3), since the maximum voltage across the shunt is expected to be 0.01 V. The output voltage will then be measured; after the amplification, a voltage range of 1.10 – 1.22 V should be seen. In Figure 6.3 shows the breadboard configuration for the current sensing.

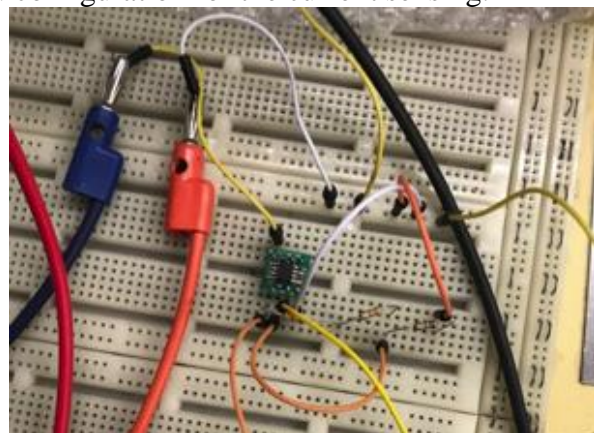


Figure 6.3: Current Sensing Breadboard Configuration by Timothy Ajao.

When we looked at the digital multimeter (DMM) value after the connection, we noticed an inconsistency in the values compared to what we were meant to get. We noticed a pattern of about a gain of 30 achieved instead of the theorized 122. We assumed it was due to the resistance of the connections. When it comes to current sensing with shunts, even the smallest resistance can change the whole result; we would realize this problem during our PCB test.

For voltage sensing, 39 V would be sent to the input of the op amp (pin 5) since the maximum voltage output from the solar panel is 39 V. The voltage moves across the voltage divider, then 1.77 V would be sent through the unity gain buffer. The output voltage would be measured by the multimeter expecting a value of 1.77 V. After this test is done, with the hope of success, we would then attach the ESP32 chip to the circuitry. The voltage and current sensing outputs would be attached to the ADC pins of the ESP32; the chip would be programmed to enable the use of the ADC ports, then the amplifier would send the results to the ESP32. The results would be transmitted wirelessly to a receiver which would display the values coming out of the sensor. Figure 6.4 shows the breadboard configuration for the voltage sensing.

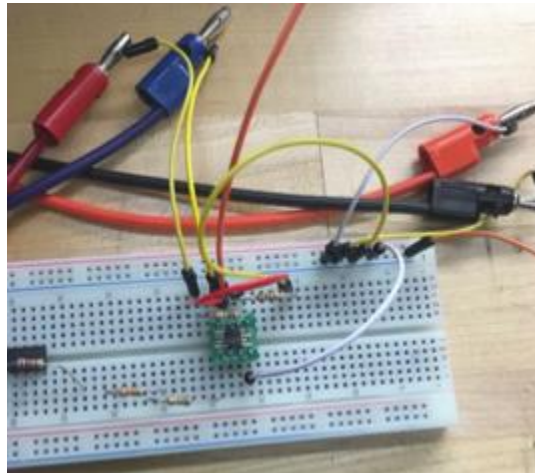


Figure 6.4: Voltage Sensing Breadboard Configuration by Timothy Ajao.

When we made the connections and varied the voltage across the voltage divider, using the DMM, we saw that the voltage at the output of the TLV342 was in line with our expectations. 39 V across the voltage divider was seen as 1.77 V at the output of the IC. With this we had confidence in utilizing this IC in our PCB design.

6.1.2.1 PROTOTYPE CURRENT SENSOR TESTING

After building a PCB with the TLV342, a $1\text{ m}\Omega$ shunt resistor, and the gain resistors. The initial plan was to use a $334\text{ k}\Omega$ gain resistor, but we noticed that anytime we measured the output voltage, it began to saturate to 3.3 V at 7 A. This would cause a serious problem as the maximum current we were preparing for was 10 A. To resolve this issue, we decided to switch out the $334\text{ k}\Omega$ resistor with a $139\text{ K}\Omega$ resistor. This decision proved to be very effective in our design.

We connected the PCB to solar array simulation to simulate our real application. We connected the load side of our system to a $1\text{ }\Omega$ power resistor with a power rating of 200 W. This would allow us to draw out the maximum current from the system without burning up the resistor. When the connection was made, we then supplied a current through the system in certain increments which would pass through the shunt, and then the gain resistor would amplify the

signal and sent it to the ESP 32. We used a DMM to find and record the input current values, and then we recorded the corresponding current value transmitted to the ESP 32. In the table below you can see the input current as well the current transmitted by the ESP 32 after conversion:

Input Current	Sensed Current
1.85	1.82
2.47	2.42
3.3	3.28
3.56	3.58
4.08	4.09
4.59	4.61
5.12	5.14
5.63	5.67
6.15	6.21
6.41	6.47
7.18	7.25
7.44	7.52
8.21	8.34

From the table above, we can see how similar the sensed current and the input current are to each other. The table shows the converted values transmitted by the ESP 32. The sensed value was converted in the code using an algorithm to produce a value close to the actual current sensed. In the Figure 6.18 below, we can see through visual representation, the accuracy of the values.

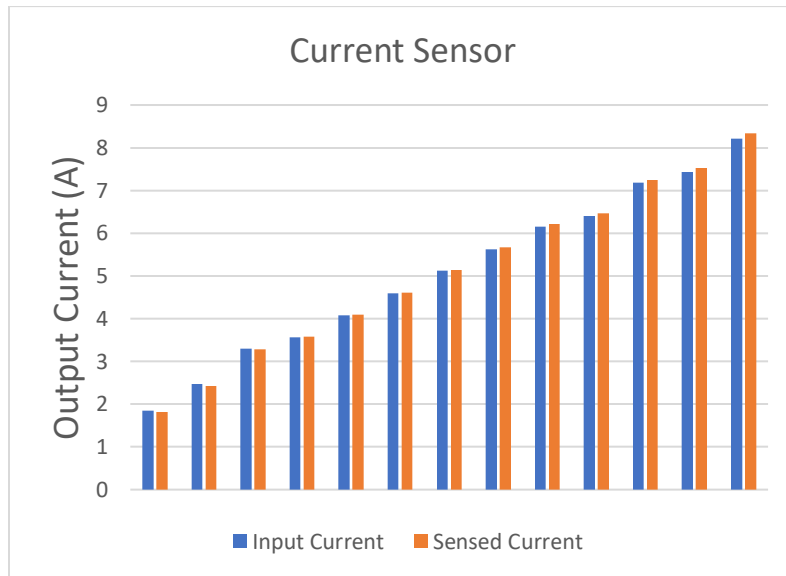


Figure 6.18: Input current Vs Sensed current

Just by looking at the graph, we can see just how close the values of the input current and the sensed current is; so, with this we were able to achieve a successful current sensing. This achieved an error of less than 5%. This same method was used with the INA current sensing IC with an even better result achieved due to their high precision.

6.1.2.2 PROTOTYPE VOLTAGE SENSING

We placed the TLV342 on our PCB, as well as the resistors involved with the voltage divider. On the load side of our design, we connected a $10\text{ K}\Omega$ axial resistor, this would ensure we maximize the voltage reading as well providing low power in the resistors. The solar array simulator was used to supply voltage to the system in certain increments, then the DMM was used to measure the input voltage, and the values were recorded. The output voltage of the TLV342 was sent to the ESP 32, and then the transmitted voltage values were also recorded. In the table below, we can see the comparison between the input voltage and the sensed voltage:

Input Voltage	Sensed voltage
4.98	4.98
9.98	9.97
14.99	14.98
19.99	19.98
24.98	24.97
29.98	29.96
34.995	34.98
39.99	39.97

We can see that the input voltage and the sensed voltage values are very similar with a less than 5% margin of error. The voltage measurement, after the raw value is converted in the code, is identical to the actual input voltage. We can see a more pictorial representation in Figure 6.19 below.

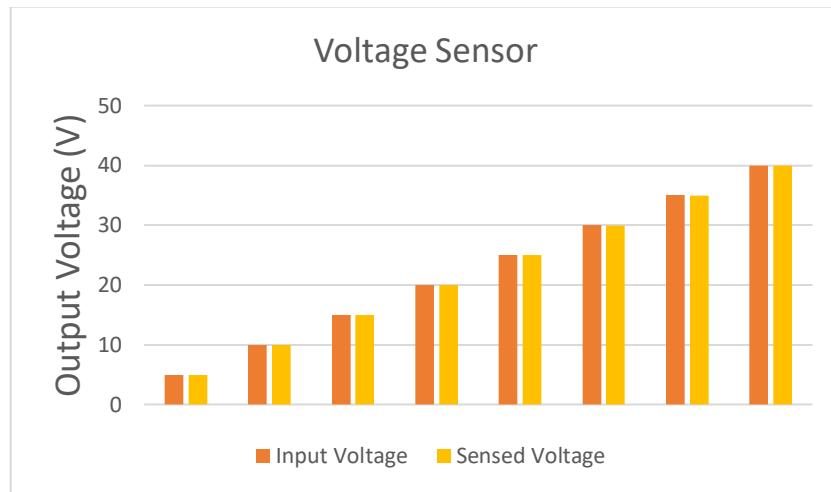


Figure 6.19: Input Voltage vs Sensed Voltage

The test was very successful, and we can say with confidence that the PCB's connected to a solar panel will produce the results that fit into the OUC specification for this project.

6.1.3 TEMPERATURE SENSOR TESTING

To appropriately test the temperature sensing abilities of the MAX6675 we will perform a variety of test such as accuracy test against current market thermocouple temperature sensor, a compatibility test to test if it would work with a Type T thermocouple and ESP32, Thermocouple Type K Linearity and lastly a single day outdoor temperature monitoring of a single solar cell.

6.1.3.1 MAX 6675 ACCURACY

To test the temperature sensing abilities of the MAX 6675 for our first preliminary testing, we used an off the shelf PCB that already has the MAX 6675 integrated chip and the capacitor already soldered to do the primary testing. The primary testing that needs to be completed before proceeding with the reference design of using the MAX 6675 is to measure the overall resolution/accuracy of the system. To accomplish this, we attach a thermocouple temperature probe from a multimeter and the MAX 6675 with the same probe lead and compare the results and graphing them on chart then do the percent difference of all the possible temperature points as seen in Figure 6.5 and Table 6.1.

Table 6.1: MAX6675 VS M400 Temperature test

Temperature Sample	M400 Type K °C	MAX6675 Type K °C
Ambient temperature	25	25
Ambient temperature	26.2	26.2
Ambient temperature	26.2	26.2
Human Temperature	35.3	35.2
Human Temperature	34.9	35
Human Temperature	34.9	35.1
Cold Water Bottle	19.7	19.7
Cold Water Bottle	19.5	19.5
Cold Water Bottle	19.3	19.4
Ice Bath	1.4	1.4
Ice Bath	1.2	1.2
Ice Bath	1.3	1.3

After comparing the results between M400 and MAX6675 on Table 6.1 we can conclude that the overall percentage error of our implemented MAX6675 with the ESP32 developmental board is 0.6117 % error accuracy. This result falls within the 5% temperature error requirement set by OUC.

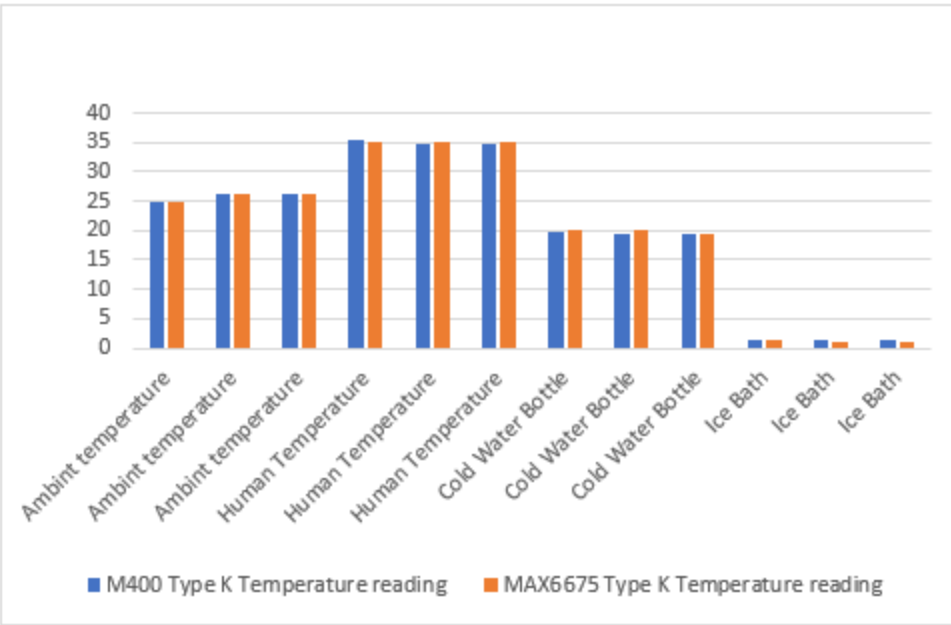


Figure 6.5: MAX6675 vs. M400 Temperature Reading by Marco Herrera.

6.1.3.2 MAX 6675 THERMOCOUPLE TYPE K LINEARITY

The Second Phase of testing is testing for the linearity of the thermocouple over a range of temperature that fall within the temperature range. To perform this test, we use a temperature control refrigeration Peltier device that can varied the temperature according to the voltage been applied to this will also work in reverse if the voltage is reverse it will heat up the refrigerated side according to the voltage applied. The voltage needs it to be applied to get a certain temperature can be found by using the following equation:

$$T_1 = \frac{(-P \times I_{tec} + I^2_{tec} \times \frac{R_p}{2} + Q_1)}{C_1 + C_p} + \frac{Q_1 + I^2_{tec} \times R_p + Q_1}{C_h + T_3}$$

As seen in Figure 6.6 the voltage response according to the change in temperature is highly linearize as the theoretical Type K thermocouple graph shown in the previous section.

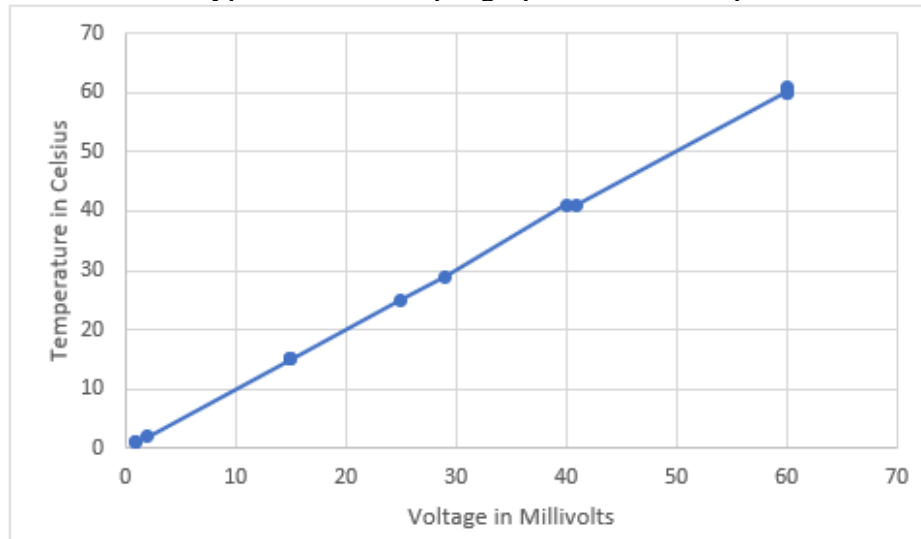


Figure 6.6: Type K Thermocouple Linearity by Marco Herrera

6.1.3.3 MAX 6675 COMPATIBILITY TEST

Passing this preliminary testing phase, we can now test the MAX6676 SMD with ESP32 developmental board but to do so we need an adapter so we can place both components in a bread board environment that will help us test the connections with the ESP32. As seen in Figure 6.7 the adapter plates can be seen we will be utilized these to solder our 8-pin chip SMD as seen in the same figure. To align properly the chip to the appropriate pin number we must align the top left bubble of the IC to the top left white circle of the PCB adapter this will tell us the proper orientation of the chip.

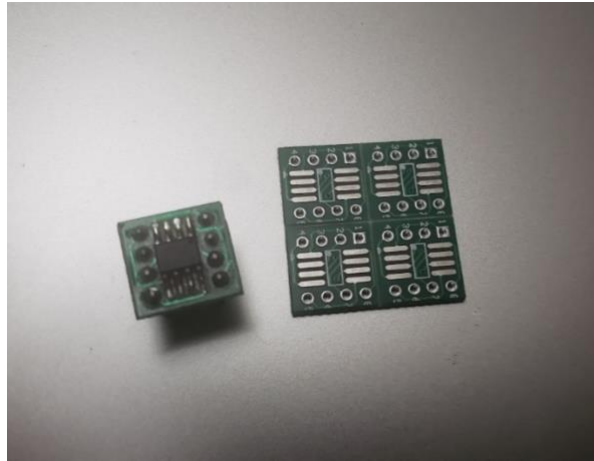


Figure 6.7: SMD to Through Hole Adapter by Marco Herrera

To test the actual functionality of the MAX6675 with ESP32 we will connect all 7 seven pins to the ESP32 developmental board. Since the MAX6675 can use both an input ranges from 3.3v all the way to 5v for our preliminary test will be using 3.3v. The first connection that we must make is to connect pin one to ground of the ESP32, pin 4 to 3.3v V_{cc} of the ESP32, followed by pin 7 to GPIO 19 of the ESP32, pin 6 to GPIO5 of the ESP32, pin 5 to GPIO 18 of the ESP32. Once these connections are made can now connect a decoupling capacitor from ground to V_{cc} this will limit voltage source noise to our system. The final connections will be to connect the high side of the thermocouple to pin 3 of the MAX6675 and the low side of the thermocouple to pin 2. After all the connection are made, we will have the first thermocouple prototype as seen in Figure 6.8 that is available to read the temperature of the thermocouple and display it using an HTLM website based on the WIFI ACESS-POINT of the ESP32 as seen in Figure 6.9 that we successfully activated using the Arduino IDE ESP32 Espressif library.

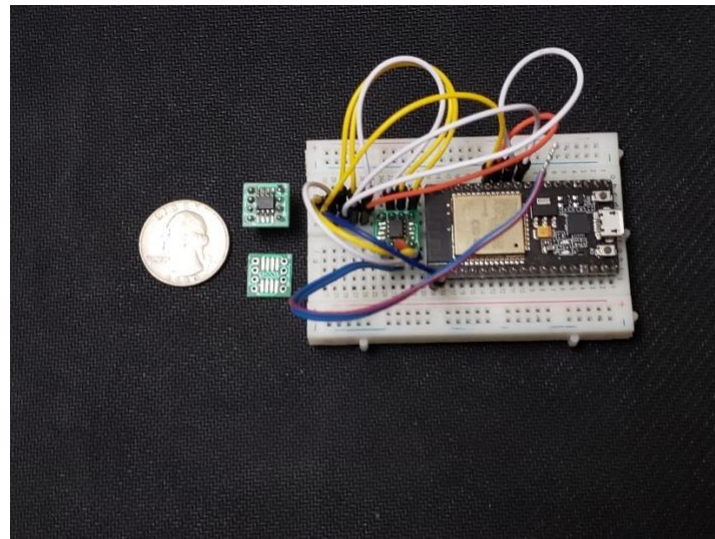
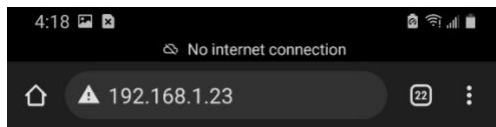


Figure 6.8: Thermocouple Type T Prototype Using ESP32 by Marco Herrera.



High Temperature Monitor

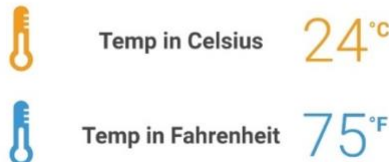


Figure 6.9: Access Point Website Temperature Output by Marco Herrera

As seen above in Figure 6.9 we see the Access Point website created using the ESP32 to display the thermocouple testing results to see if it is operating within the normal expected parameters and display the correct ambient temperature. Furthermore, as seen in Figure 6.9 we successfully tested the compatibility of a Type T thermocouple with the MAX6675 IC. Even though the specification sheet stated that only Type K thermocouple was compatible with this IC a Type T works in the same manner as a Type K with the MAX6675 IC. The reason we found that it works is that a Type T and Type K thermocouples have a similar temperature range and resolution resulting in a similar behavior with the same thermocouple amplifier. Furthermore, since the Type T thermocouple does not need Cold Junction Compensation the temperature percent error will would have due to the slight variation in resolution can be neglected.

6.1.3.4 MAX 6675 SINGLE DAY TEMPERATURE READING

In this section we setup the temperature sensor prototype with the provided self-adhesive Type T thermocouple provided by OUC and a Type K beaded thermocouple taped with heat resistant tape to a Solar cell facing the Sun at a 47° degree angle to maximize the sunlight heading the solar cell in our testing environment.

Table 6.2: Single Day Temperature reading for Type T and Type K thermocouples

Hour	Type T Temperature	Type K Temperature
8:00 AM	25	26
9:00 AM	27	27
10:00 AM	28	28
11:00 AM	38	38
12:00 PM	49	49
1:00 PM	48	48
2:00 PM	48	47
3:00 PM	39	38
4:00 PM	40	40
5:00 PM	38	38
6:00 PM	36	36
7:00 PM	30	30
8:00 PM	28	28

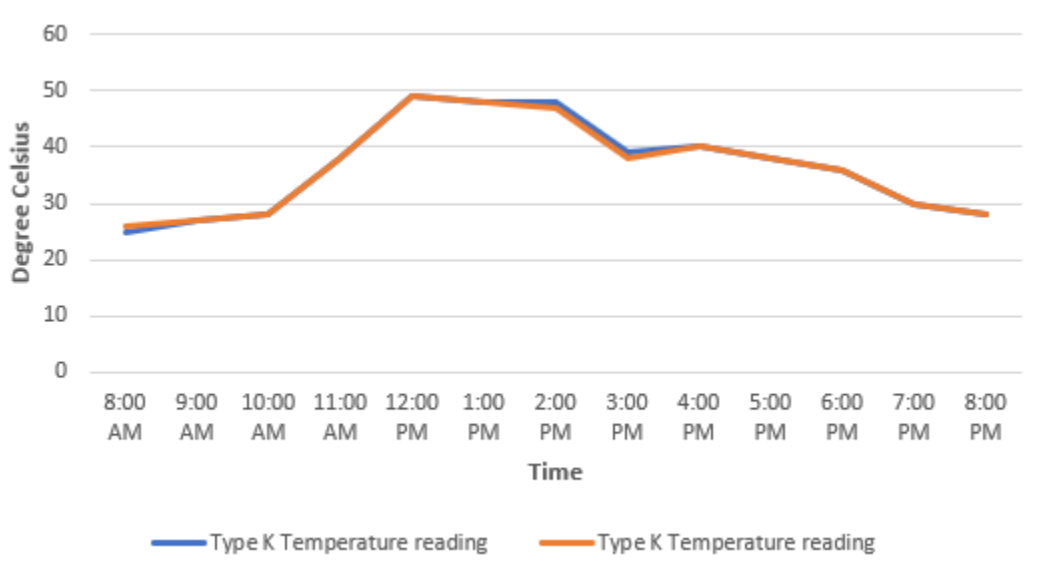


Figure 6.10: Single Day Solar Cell Temperature by Marco Herrera.

As seen Table 6.2 and Figure 6.10 the behavior of both the Type T and Type K thermocouples behave similarly in the temperature recording of a solar cell over the course of a single day. As seen in Figure 6.10 we can conclude that the temperature recording corresponds to a typical day with lowered temperatures in the morning with a high climb of temperature at the start of noon and a steady decline in temperature in the afternoon.

6.1.4 IRRADIANCE SENSOR TESTING

To ensure that the pyranometer accurately reads irradiance and transmits it correctly to the on-board ADC, the pyranometer must be adequately tested. In most cases for electrical circuits, testing whether a part functions as intended is easy; datasheets exist for specific components, oscilloscopes and function generators can serve as catalysts to measure and control a specific parts performance, and so on. It is within this regard that pyranometers are inherently different. While a datasheet exists for this pyranometer, measuring the sun's irradiance cannot be done as easily

through typical lab tools as measuring a voltage or current across a resistor, and the results are hard to verify on human intuition.

To test the functionality of the SP-110-SS pyranometer, an entirely separate pyranometer will have to be used such that the data from both pyranometers can be compared. For testing purposes, the separate pyranometer is a datalogger, a device that measures, records, and displays irradiance in a single controlled piece of equipment. This standalone device will allow us to measure irradiance with minimal noise or interference.

The datalogger that was used for testing the performance of the SP-110-SS is the Campbell Scientific CR310, provided by Rubin York of OUC. This datalogger was provided to the team alongside about 1 year of historical data from 2021 which provides us with another frame of reference for the theoretical output of the pyranometer.

Testing the pyranometer is now simple: The SP-110-SS must be connected to a device that can measure its output, that output must be converted into Watts per Square Meter, and the result will be compared to the measured result from the datalogger and the historical data from the same day and time of the previous year. For the pyranometer's output to be measured and converted, one of two things must happen. The first option involves connecting the pyranometer to a breadboard which can further connect to an oscilloscope to measure its output in millivolts, and those millivolts can be multiplied by 5 to receive the irradiance in Watts per Square Meter. The second option is testing directly on the PCB; because the connection to the ADC on the board is entirely optional for the functionality of the All-In-One PV Sensor, the pyranometer can be plugged into the board via a terminal block and fed straight to the ADC, amplified by any implemented means. The ADC will then read the output of the pyranometer and send it to the local node to be displayed.

Of these two options, the former is preferred for two main reasons. Designing the PCB without the knowledge of how the pyranometer performs with and without an amplifier is foolish. It's entirely possible that the ADC's resolution is high enough to completely measure the pyranometer's millivolt signal without any means of amplification. Not only will testing the pyranometer on the breadboard save development costs for the PCB, but it will also give the team the freedom to experiment with what the pyranometer can use before it gets to a quantifying element such as an ADC or oscilloscope.

The pyranometer will first be tested on its own. If the pyranometer cannot give accurate results based on its specifications provided by Apogee Instruments, then it cannot be expected that the pyranometer will give correct readings when passed through an Operational Amplifier. For this reason, a simple Digital Multimeter will be used in accordance with the pyranometer when exposed to direct sunlight. Table 6.3 details the SP-110-SS's relevant functionalities.

Table 6.3: The SP-110-SS's Testing Specifications [4.52]

SP-110-SS	Value
Power Supply	Self-Powered
Current Draw	0 A
Output (Sensitivity)	0.2 mV per W m ⁻²
Response Time	Less than 1 ms
Field of View	180 degrees

When tested alone, the pyranometer gives accurate results. The SP-110-SS was tested in clear-sky conditions, and the pyranometer showed to be incredibly sensitive to its exposure to light down to the angle that it was pointed toward the sun's location in the sky. When pointed flat with the earth's

surface while the sun was about 50% toward noon, the pyranometer saw an output of around 150 mV.

When pointed directly at the sun, the voltage output changed drastically to 204 mV, showing that the pyranometer is not only incredibly precise but incredibly sensitive. This must be considered in installation, as if the pyranometer is not exactly in line with the solar panel's angle toward the sky, it is likely that we will receive a different irradiance measurement than the panel is receiving.

The following table summarizes an extended test from 8 AM to 5 PM comparing the SP-110-SS Apogee Instruments Pyranometer and the CR310 Datalogger. These selected hours will have the most relevant measurements of sunlight and will be further compared to the dataset provided by OUC. There were two tests, one in direct sunlight and the other in a dependent shade. The results of these two tests are summarized below in Table X.

Table 6.4: SP-110-SS Output Vs. CR310 Recorded Value

Hour	SP-110-SS, Unshaded/Shaded	CR310, Unshaded/Shaded
8 AM	62.8 mV, 2.8 mV	64.435 mV, 2.757 mV
9 AM	108.2 mV, 9.1 mV	107.778 mV, 8.856 mV
10 AM	158.0 mV, 15.1 mV	161.820 mV, 15.091 mV
11 AM	168.5 mV, 18.9 mV	168.343 mV, 20.018 mV
12 PM	199.6 mV, 99.8 mV	199.294 mV, 100.501 mV
1 PM	199.3 mV, 121.4 mV	199.393 mV, 131.918 mV
2 PM	180.1 mV, 120.1 mV	178.366 mV, 125.422 mV
3 PM	185.9 mV, 84.8 mV	181.492 mV, 85.454 mV
4 PM	162.1 mV, 55.6 mV	165.463 mV, 55.702 mV
5 PM	112.1 mV, 9.0 mV	113.181 mV, 9.011 mV

The results of Table 6.4 can be summarized in the following graphs, Figure 6.11 and Figure 6.12.

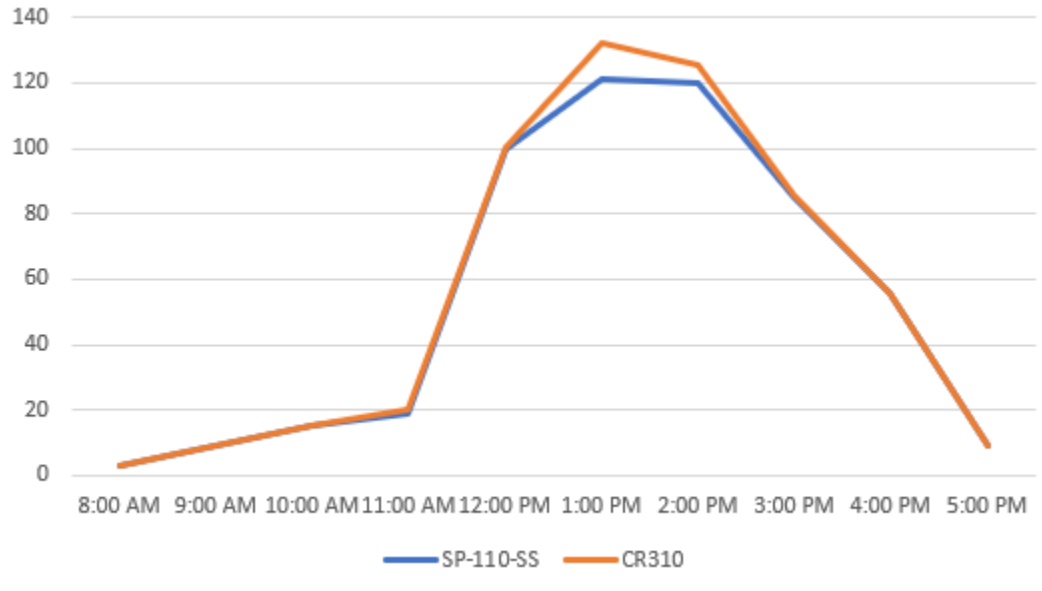


Figure 6.11: SP-110-SS Raw Output vs. CR310 Value in Excel by Maguire Mulligan.

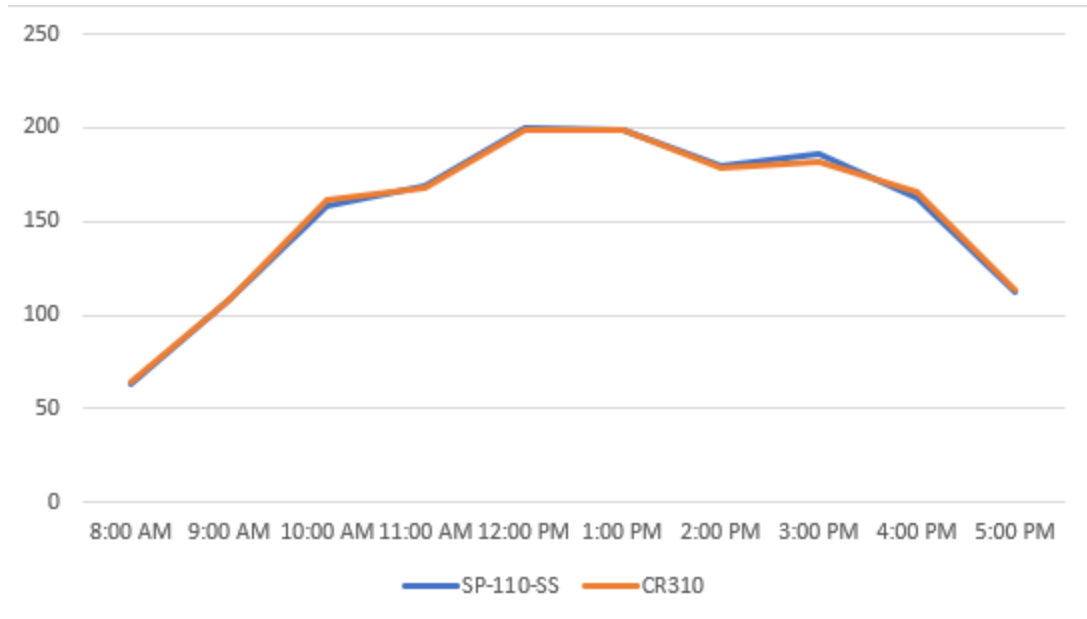


Figure 6.12: SP-110-SS Raw Output vs. CR310 Value in Excel by Maguire Mulligan.

Comparing these two datasets, the SP-110-SS raw output which was measured with a simple voltmeter and the output detected by the CR310 are almost identical, give or take a few millivolts of difference. This difference between the measured value of the voltmeter and the CR310 can be because of the time it takes to switch between measuring. The pyranometer must be directly plugged into the CR310 after being measured with the voltmeter, so by the time that the connections are made, small changes to the irradiance incident on the pyranometer can be changed by a cloud shifting its position or other similar effects.

6.1.4.1 IRRADIANCE CIRCUITRY TESTING

Now that we know the pyranometer is working as intended, we can begin testing the pyranometer as it were to be set onto a PCB. This means that the pyranometer's output will no longer be measured directly from the sensor, but after it has travelled through an instrumentation amplifier and amplified to an acceptable level for the on-board ADC to convert and record.

With the arrival of the MAX4194 three-op-amp instrumentation amplifier, breadboard testing for the SP-110-SS Pyranometer can begin. Initial tests with the MAX4194 will be done using a single-supply voltage, a reference voltage at a value of half of the supply voltage, and varying gains to determine the most accurate setting for the MAX4194. First, the gain of the amplifier will be varied and tested using a constant DC input to model the pyranometer. This will help us determine if the MAX4194 can function correctly under these conditions, and if so, what the potential errors may be.

Before we can begin breadboard testing the MAX4194, we look at the Instrumentation Amplifier's performance in LTSpice. This will allow us to see if the part is functioning as expected in a perfectly ideal scenario with no potential for human error beyond circuit connections. A DC operating point sweep will be conducted over the circuit so that input values from 0 to 0.5 V with an increment of 0.05 can be quickly tested and extracted for analysis. The MAX4194 Simulation circuit can be seen in Figure 6.13.

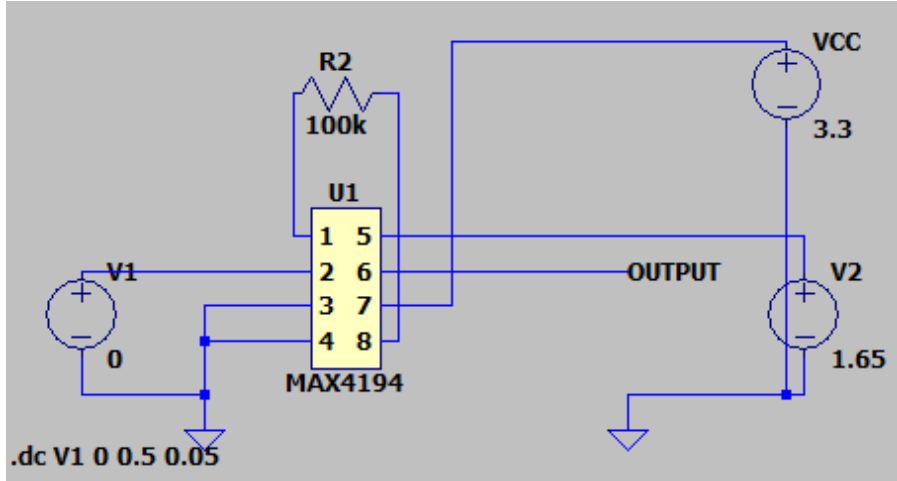


Figure 6.13: MAX4194 Simulation Circuit Layout in LTSpice by Maguire Mulligan.

Figure 6.14 features the testing results that presented us with the smallest percentage of error on the circuit's output after simulation. The theoretical expected output is found using the following formula:

$$V_{OUT} = V_{REF} + (GAIN * V_{DIFF})$$

VCC	Vref	Gain Resistor	Gain	Vin+	Vin-	Vdiff	Simulated Output	Theoretical Expected Output	Simulation Percent Error
3.3	1.65	100000	1.5	0	0	0	1.64999	1.65000	-0.001%
3.3	1.65	100000	1.5	0.05	0	0.05	1.70989	1.70750	0.140%
3.3	1.65	100000	1.5	0.1	0	0.1	1.76990	1.76500	0.277%
3.3	1.65	100000	1.5	0.15	0	0.15	1.82990	1.82250	0.406%
3.3	1.65	100000	1.5	0.2	0	0.2	1.88990	1.88000	0.527%
3.3	1.65	100000	1.5	0.25	0	0.25	1.94990	1.93750	0.640%
3.3	1.65	100000	1.5	0.3	0	0.3	2.00991	1.99500	0.747%
3.3	1.65	100000	1.5	0.35	0	0.35	2.06991	2.05250	0.848%
3.3	1.65	100000	1.5	0.4	0	0.4	2.12991	2.11000	0.944%
3.3	1.65	100000	1.5	0.45	0	0.45	2.18991	2.16750	1.034%
3.3	1.65	100000	1.5	0.5	0	0.5	2.24991	2.22500	1.120%
3.3	1.65	100000	1.5	0	0.05	-0.05	1.59013	1.59250	-0.149%
3.3	1.65	100000	1.5	0	0.1	-0.1	1.53012	1.53500	-0.318%
3.3	1.65	100000	1.5	0	0.15	-0.15	1.47012	1.47750	-0.499%
3.3	1.65	100000	1.5	0	0.2	-0.2	1.41012	1.42000	-0.696%
3.3	1.65	100000	1.5	0	0.25	-0.25	1.35011	1.36250	-0.909%
3.3	1.65	100000	1.5	0	0.3	-0.3	1.29011	1.30500	-1.141%
3.3	1.65	100000	1.5	0	0.35	-0.35	1.23011	1.24750	-1.394%
3.3	1.65	100000	1.5	0	0.4	-0.4	1.17011	1.19000	-1.672%
3.3	1.65	100000	1.5	0	0.45	-0.45	1.11011	1.13250	-1.977%
3.3	1.65	100000	1.5	0	0.5	-0.5	1.05010	1.07500	-2.316%

Figure 6.14: MAX4194 Testing with 1.5 Gain in Excel by Maguire Mulligan.

As seen in the figure above, the MAX4194 is given a supply voltage of 3.3V, a reference voltage of 1.65 V, and two different inputs, half of the test using positive and the other half using negative. The reference voltage being set to half of the supply voltage is necessary for the MAX4194 to receive its full voltage swing on the output and guarantee that we see an amplified form of the pyranometer's output. From the results, the simulation's calculated output has an error that never goes beyond 2.316% which is incredibly good for such a small input signal. Gains of 1, 1.3, 1.7, and 2 all had errors that went above the restrictions that 1.5 simulated.

Now that the different gains of the MAX4194 have been tested, we can move forward with a gain of 1.5 to minimize circuit output error. The pyranometer will be exposed to direct sunlight such that we are receiving the maximum output which will be the easiest to detect and measure. The pyranometer's outputs will lead directly into the inputs of the MAX4194, and the output of the

MAX4194 will be measured and recorded. Now that the pyranometer and MAX4194 voltage levels must be measured simultaneously, two Digital Multimeters will be used to measure the pyranometer's differential input and the MAX4194's output. The breadboard testing results can be seen in Figure 6.15

Pyra Diff	Irradiance	Circuit Output	Theoretical Circuit Output	Circuit Percent Error	Value that would have been read	Measured Irradiance	Irradiance error
0.0469	234.5	1.718	1.72035	-0.14%	0.0453	226.67	-3.34%
0.04648	232.4	1.718	1.71972	-0.10%	0.0453	226.67	-2.47%
0.02309	115.45	1.684	1.68464	-0.04%	0.0227	113.33	-1.83%
0.03982	199.1	1.702	1.70973	-0.45%	0.0347	173.33	-12.94%
0.02023	101.15	1.678	1.68035	-0.14%	0.0187	93.33	-7.73%
0.01933	96.65	1.677	1.67900	-0.12%	0.0180	90.00	-6.88%
0.02006	100.3	1.677	1.68009	-0.18%	0.0180	90.00	-10.27%
0.04026	201.3	1.706	1.71039	-0.26%	0.0373	186.67	-7.27%
0.05372	268.6	1.727	1.73058	-0.21%	0.0513	256.67	-4.44%
0.0328	164	1.696	1.69920	-0.19%	0.0307	153.33	-6.50%
0.02866	143.3	1.692	1.69299	-0.06%	0.0280	140.00	-2.30%
0.03229	161.45	1.695	1.69844	-0.20%	0.0300	150.00	-7.09%
0.06799	339.95	1.748	1.75199	-0.23%	0.0653	326.67	-3.91%
0.0641234	320.617	1.742	1.74619	-0.24%	0.0613	306.67	-4.35%
0.06155	307.75	1.738	1.74233	-0.25%	0.0587	293.33	-4.68%
0.07107	355.35	1.751	1.75661	-0.32%	0.0673	336.67	-5.26%
0.073125	365.625	1.751	1.75969	-0.49%	0.0673	336.67	-7.92%

Figure 6.15: MAX4194 Breadboard Testing in Excel by Maguire Mulligan.

When using the pyranometer as the input, the circuit's output percent error is staying relatively close to the simulated results. The pyranometer's differential input should never go far beyond 0.2V, so we should never be seeing more than 0.5% error between the expected output and the true output. However, this small percentage of error is found later in calculations. When working backwards from the output value to find the theoretical differential input as an ADC would, the following equation is used:

$$\frac{V_{OUT} - V_{REF}}{GAIN} = V_{DIFF}$$

The reference voltage and the gain will be constant, so the ADC will use the measured output value and plug it into the equation to find the differential voltage supplied by the pyranometer. Multiplying this value by 3.33 will provide the irradiance that the pyranometer is measuring. However, because the differential voltage is incredibly small compared to the output and reference voltages, the minuscule percent error from the circuit's output is seen as a much larger percentage error in the measured irradiance. For example, when 365.6 Watts per Square Meter is measured by the pyranometer, the MAX4194 would lead the ESP32's ADC to believe that 336.67 Watts per Square meter was the true measurement.

It was seen as possible that the large increase in the error between true and measured irradiance could have been due to human error, so the CR310 datalogger was used to improve accuracy. The pyranometer's output was tied directly to the MAX4194's inputs as well as the CR310 datalogger, and the output of the MAX4194 was tied as a single-end voltage to the CR310. This removed the dual-DMM testing requirement and allowed for much more data to be collected over several hours. Using this new testing environment, a datapoint was collected every 5 seconds while the pyranometer was set in the sun and the MAX4194 was constantly working to provide an output. Once several hours of testing was done, the data was summarized into graphical format. Figure 6.16 shows the measured difference between the true and theoretical MAX4194 outputs during this time, and Figure 6.17 shows the difference between the true and solved pyranometer outputs.

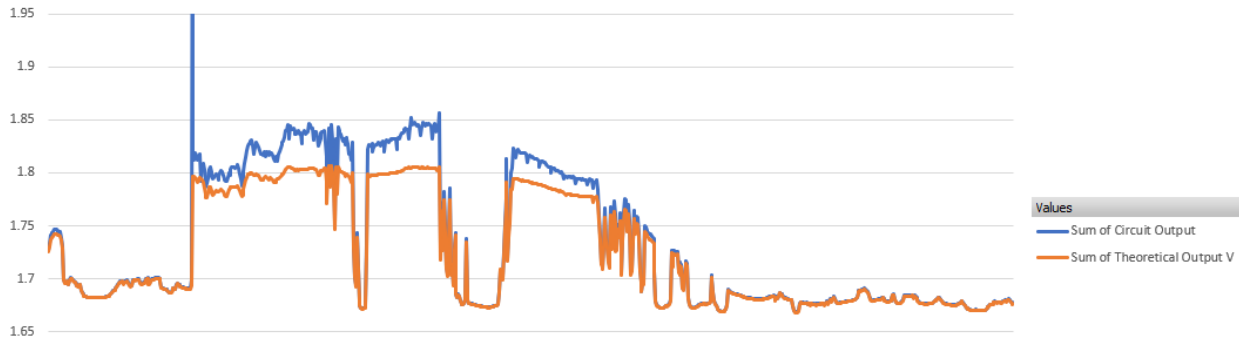


Figure 6.16: Difference between True and Theoretical MAX4194 Output in Excel by Maguire Mulligan.

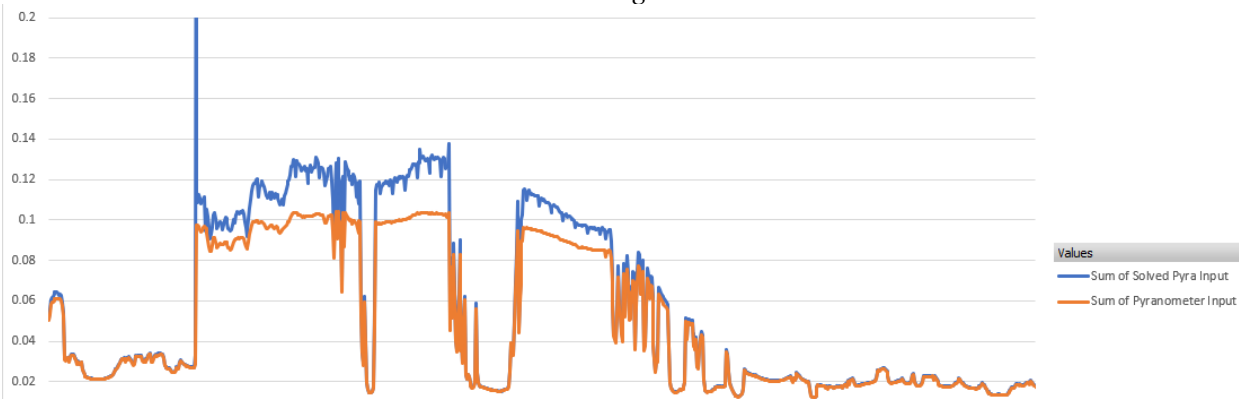


Figure 6.17: Difference between True and Solved Pyranometer Input in Excel by Maguire Mulligan.

An outlier is seen early in the data, likely an error, but otherwise the data can be treated as true and accurate. During higher moments of sunlight, the circuit output error begins to grow, and the same can be seen from the pyranometer input error. The graphs show that the error becomes much too large to be acceptable and the sheer volatility of the error's presence would create a nightmare in data acquisition. No single equation can be used to keep track of the differing values of percentage error that are seen across the MAX4194's output and the pyranometer's input across time. Further research was required to understand why the MAX4194 was not performing as the datasheet stated. An article posted by Maxim Integrated, '*Three is a Crowd for Instrumentation Amplifiers*' [4.93], explains that three-op-amp instrumentation amplifiers find limited applications in single-supply systems due to their common-mode voltages commonly being at or close to ground. To mitigate this, the common mode voltage must be above a quarter of the VCC – about 0.825 V – for the amplifier to work without a dual supply mode of operation. For this reason, before the MAX4194 can continue being tested and integrated into the PCB, we must investigate Dual-Supply Linear Regulators or methods to add a DC offset to the pyranometer's input signal such that the common mode voltage falls in the acceptable range for a three-op-amp configuration instrumentation amplifier.

6.1.4.2 IRRADIANCE CIRCUITRY CHANGES

After testing and cost analysis, the MAX4194 was no longer seen as a viable option to integrate the SP-110-SS Pyranometer into the All-In-One Photovoltaic Sensor. To utilize the MAX4194, we would need to incorporate a dual supply into the board which adds cost. This would normally

be acceptable but given that OUC has stressed that the pyranometer will not be attached to most boards, this is a large cost increase for manufacturing for very little reward. For this reason, the team decided to investigate easier methods of translating the pyranometer's analog signal. Rather than amplify the signal before sending it to the ESP32's on-board ADC, we elected to use a standalone pseudo-differential ADC for the pyranometer's input, allowing its differential & analog output to be converted to a digital signal and sent to the ESP32 over SPI. This allowed us to find a cheaper part compared to the MAX4194 and eliminated the need for a dual-supply linear regulator, allowing the board to remain simple at a low price point.

6.2 SOFTWARE TESTS

While developing our prototype, we will constantly conduct tests to ensure the reliability of our software prior to deployment. For example, we will be able to feed our software data values and ensure that data is properly delivered to our database and displayed on a GUI when necessary.

6.2.1 WIRELESS COMMUNICATION TESTS

In this section we will test the Access-Point Range using two different methods. The first test will be a directional distance range to find the maximum distance the ESP32 WI-FI signal can travel to. The Second Test we will perform is a Wi-Fi penetration range, where we will place the ESP32 prototype in our selected enclosure to find the maximum Wi-Fi range of our system when is finally placed in a weatherproof enclosure to isolated from the elements.

To ensure sound wireless communication, we have thoroughly tested the Wi-Fi communication modules on board our ESP32 devices and Raspberry Pi and can clearly see that they are communicating reliably through Wi-Fi. During our first prototyping stages, we were able to confirm that our Raspberry Pi and ESP32 devices were properly communicating by being able to send temperature data from the ESP32 to the Raspberry Pi, being supported by the ESP32's broadcasted Wi-Fi access point.

7. DEVICE FABRICATION

With the bulk of the All-In-One PV Sensor's hardware and software realized, a plan to fabricate the device is put forth. This will include the PCB that the All-In-One PV Sensor will be acting as, and the device enclosure that will keep the PCB safe from outer damage.

7.1 PCB FABRICATION

There will be 3 separate PCBs constructed for the implementation of the All-In-One PV Sensor, but they will all share the same design. Using the EAGLE configuration that was created in Section 6 and its respective subsections, the following draft design was created seen in Figure 7.1

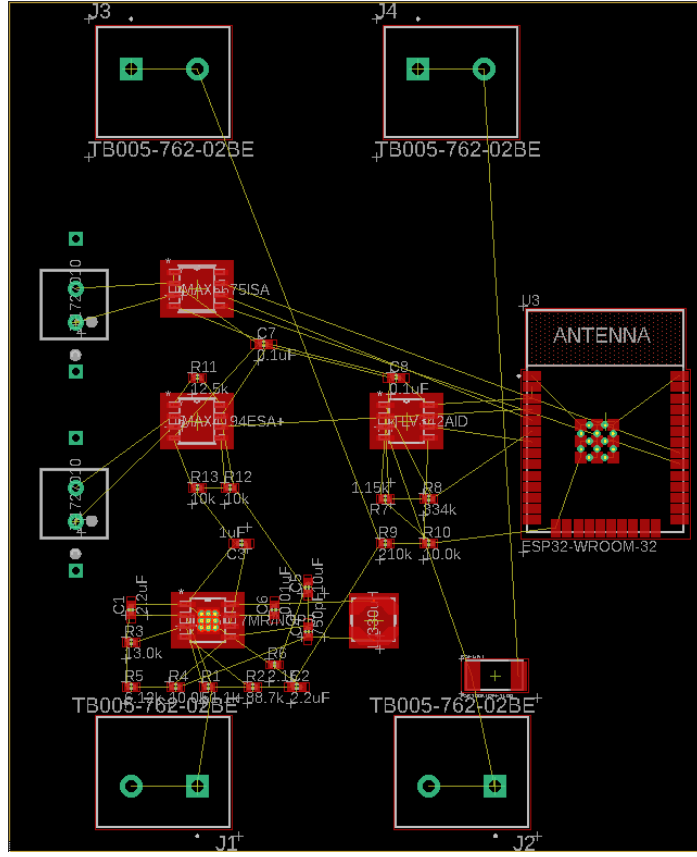


Figure 7.1: Draft of PCB Layout in EAGLE by Maguire Mulligan.

At this point in time, some parts are still being debated with the possibility of being swapped out for other parts. For that reason, the PCB will not be finalized until each part is definitively chosen as the correct part for the application. In general, the PCB will always have 4 large terminal blocks to facilitate the incoming and outgoing voltage and current that is generated by the Solar Panel. The two smaller terminal blocks, seen on the left side of Figure 7.1, house the inputs for the thermocouple and pyranometer. The existence of the sensors in the application of the All-In-One PV Sensor are fully optional, but to ensure ease of installation, the PCB will be created with the necessary terminals and amplification circuits regardless of the external sensor's implementation. This simplifies the creation of the PCBs, allowing us to make 3 identical copies rather than having a variable design.

Many of the board's inner components must be rearranged, taking the orientation, placement, and organization of the components into account before moving forward with a true printed PCB.

7.2 PCB FABRICATION REVISION

Instead of using EAGLE for our PCB fabrication we decided to use EasyEDA for PCB fabrication and production since it is a software that it would allow us to send our final PCB directly to their partner PCB manufacturing factory for ease of production from design to production reducing the time of production between our prototypes and final product. For our final product we decided to utilize 2 board versions for our final product V2.0 utilizes a smaller DC-DC converter compared to V3.0 to reduce manufacturing cost but it vastly reduces the maxing voltage the converter can take. As seen on Figure 7.2, V2.0 offers 3 ICs that measure temperature, irradiance, voltage, and low side currenting, since this design offers and IC that can measure both current and voltage is ideal for a low-cost design but is highly susceptible to noise. On the other hand, V3.0 Figure 7.3

offer the same ICs for temperature and irradiance but with a bigger DC-DC that can handle higher voltages and a separate current IC that measures current on the high side of the system making it more accurate and less susceptible to noise.

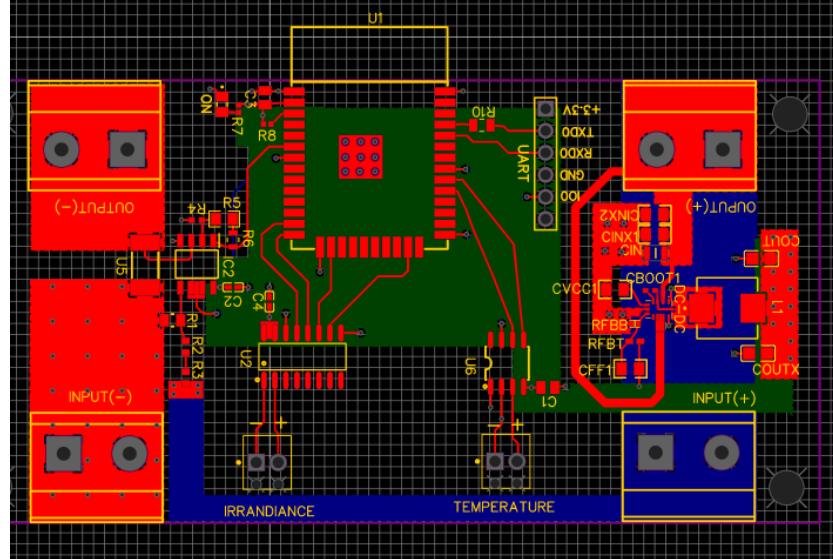


Figure 7.2: V2.0 PCB Layout in EasyEDA by Marco Herrera

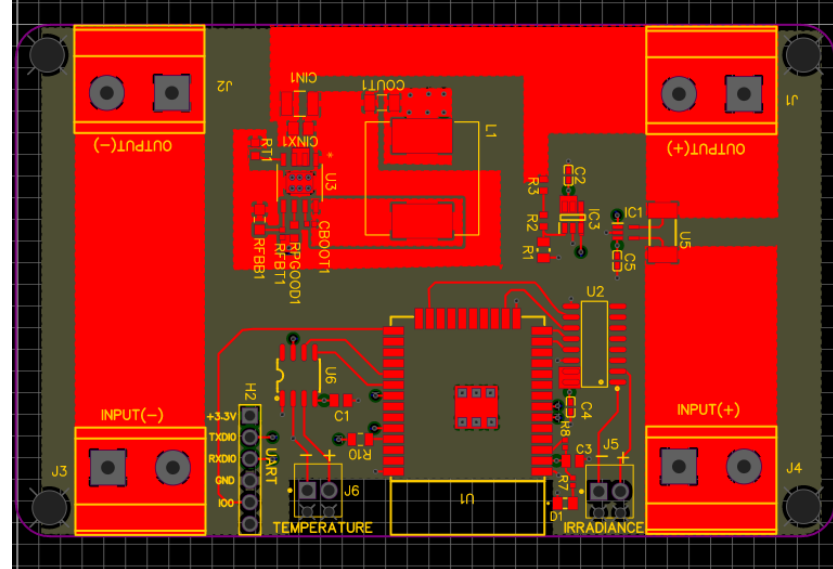


Figure 7.3.: V3.0 PCB Layout in EasyEDA by Marco Herrera

8. ADMINISTRATIVE DETAILS

The following sections below include the initial project description as well as the initial and overall project milestones need to successfully complete the “All-in-One PV Sensor”. Furthermore, there will be a budget breakdown of all parts use for the Sensing Node “All-in-One PV Sensor”.

8.1 INITIAL PROJECT DESCRIPTION & GOALS

The “All-in-One PV Sensor Phase II” consisted of fixing and redesigning some aspects of the previous design such as increasing the gauge size of the input terminals to accommodate 10-gauge wire. Designing a cheaper weather resistance waterproof casing for the sensor. Redesign the temperature sensing side of the original design since it never worked. In addition to the redesign or fixed the current sensing side of the “All-in-One PV Sensor”.

The initial phase for the “All-in-One PV Sensor Phase II” as seen in detail in Table 8.1 was to first recognize all the elements required by OUC, in addition to analyze previous attempts of the project such as Phase I. As we move on in getting familiarized with the “All-in-One PV Sensor”. We came to the realization that Phase I design had critical flaws that required us to complete it redesign the previous design as it will not work properly as it was expected. So, our initial Milestones must reflect such a decision of re-designing all of phase I design.

As seen on Table 8.1, our team designated specific target dates to stay within a set schedule and design certain aspects of the ‘All in One PV Sensor’. This was carefully selected to have a certain level of control of our workload and do not have setbacks due to lack of organization within the team.

Table 8.1: Initial Project Description & Goals

Number	Milestone	Tasked	Start Date	End Date	Status
Introduction to Project					
1	Meet the team, advisors, and customer	Group 6	1/11/2022	1/17/2022	Completed
2	Familiarize with the project	Group 6	1/17/2022	1/25/2022	Completed
3	Scout the location for implementation	Group 6	1/25/2022	1/27/2022	Completed
4	Role Assignments with tech advisor	Group 6	1/25/2022	1/28/2022	Completed
5	Part Identification and Classification	Group 6	1/27/2022	4/1/2022	Completed

8.1.1 HOUSE OF QUALITY MATRIX

Our created House of Quality matrix seen in Figure 8.1 can summarize the customer’s requirements compared to the engineering specifications that our team was given to follow. What the customer heavily prioritizes is the ability to have ‘A-la-carte’ external sensors, meaning that the pyranometer and thermocouple sensors, capable of measuring irradiance and panel temperature respectively, should not be a required component of the sensor. All sensors are expected to be able to measure a rated voltage and current and send that data wirelessly to a local collector node.

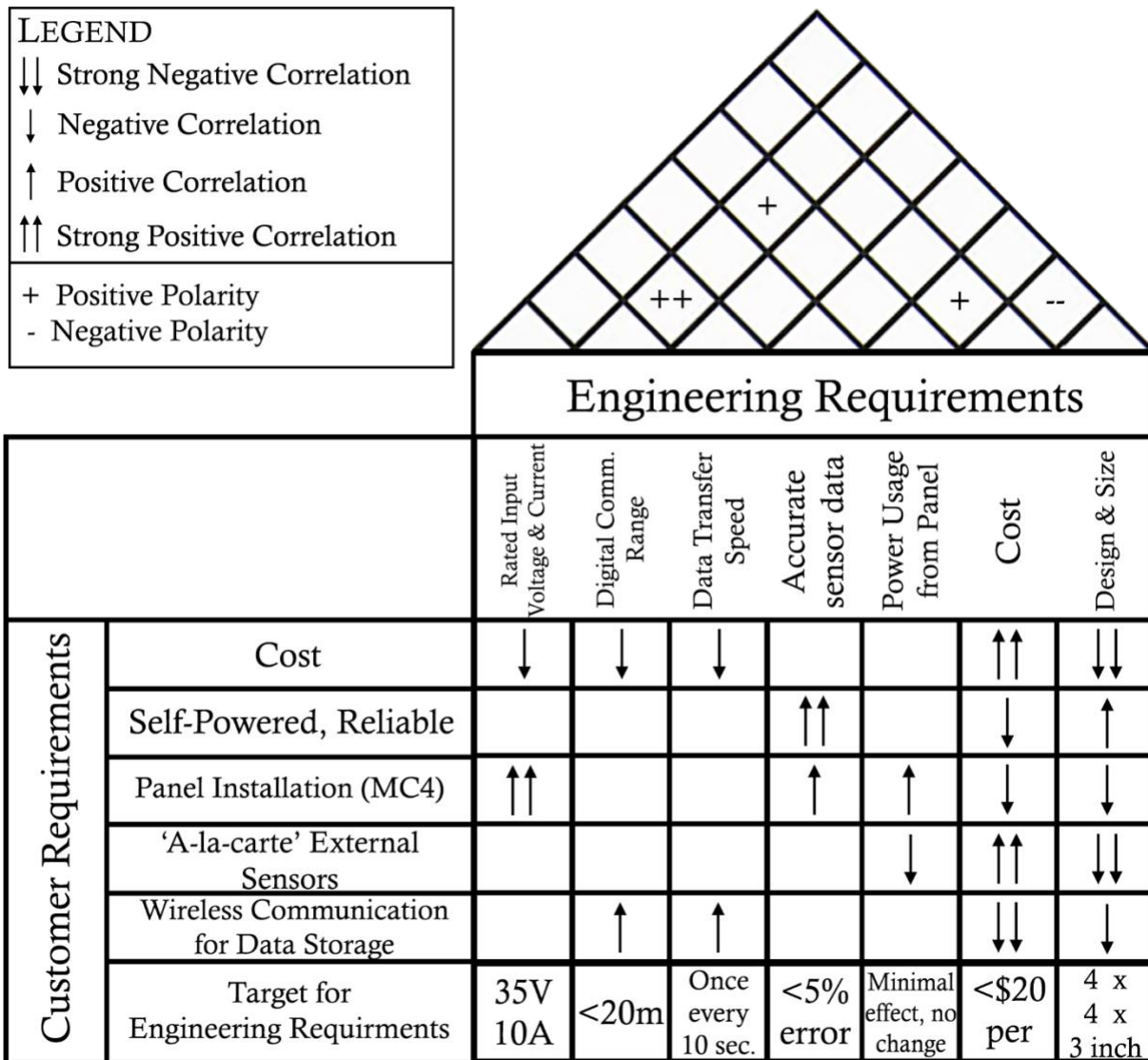


Figure 8.1: House of Quality by Maguire Mulligan.

Given that the cost is also a priority for the customer, this ‘A-la-carte’ choice allows the individual cost of a sensor to be lower than average as only one of three produced sensors for this project will make use of a pyranometer and thermocouple.

8.2 PROJECT MILESTONES

In Table 8.2, we can see the introductory part of the projects where we assign specific dates to become familiarized with the team and the project itself. We itemized the range of dates where we are task to provide documentation need to be submitted for the Senior Design advisors to provide feedback and monitor our progress. This table details our in-class deadlines along with our research and development deadlines such that we keep on a healthy pace to complete our project by the end of Summer.

The final part of Table 8.2 is the dates designated for the research and development of the ‘All in One PV Sensor’. These dates are categorized by date and individual point of research to further break down the design workload. In addition to these dates, we also included a section where we selected a range of reasonable dates for our first working prototype, prototype stress test and the first stage for PCB layout these dates also serve as progress markers targeted to the OUC sponsor for them to have a clear timeline of our design process.

Table 8.2: Senior Design I Milestones

Number	Milestone	Tasked	Start Date	End Date	Status
Project Documentation					
6	Initial Project Document	Group 6	1/24/2022	2/4/2022	Completed
7	Updated Divide and Conquer Doc.	Group 6	2/12/2022	2/18/2022	Completed
8	First Draft Senior Design I	Group 6	2/14/2022	3/25/2022	Completed
9	Second Draft Senior Design I Rev.	Group 6	3/28/2022	4/8/2022	Completed
10	Final Report	Group 6	4/11/2022	4/26/2022	Completed
Research and Development					
11	Thermocouple and Hall-Effect Sensors	Marco	1/28/2022	2/18/2022	Completed
12	Node/MCU and Communication	Andrew	1/28/2022	2/18/2022	Completed
13	Node/MCU and Pyranometer	Maguire	1/28/2022	2/18/2022	Completed
14	Power and Hall-Effect Sensor	Timothy	1/28/2022	2/18/2022	Completed
15	Power and Voltage Sensor	Timothy	1/28/2022	2/18/2022	Completed
16	Filtering Circuit and Amplification	Group 6	2/4/2022	2/18/2022	Completed
17	Board Prototyping V1&V2	Group 6	2/21/2022	3/28/2022	Completed
18	Final Prototypes Stress Tests	Group 6	3/14/2022	5/3/2022	Completed
19	PCB Layout	Group 6	3/28/2022	5/3/2022	Completed

On Table 8.3 we identified possible dates for our final paper presentation and conference paper to have a clearer picture of future dates to look out for to adjust our workload according to these dates. Furthermore, we also predict the final stage dates where our final PCB design would be built and when will be stress tested. Table 8.3 lies heavily on our forecasted progress in Senior Design 1 to meet certain criteria and goals.

Table 8.3: Senior Design II Milestones

Number	Milestone	Tasked	Start Date	End Date	Status
1	Working PCB V1 Stress Test	Group 6	4/27/2022	5/30/2022	Completed
2	Final PCB Stress Test	Group 6	5/16/2022	7/4/2022	Completed
3	All in Once PV Sensor	Group 6	5/16/2022	7/18/2022	Completed
4	Conference Paper	Group 6	5/16/2022	7/26/2022	Completed
5	Design Demonstration	Group 6	5/26/2022	7/26/2022	Completed

8.3 PROJECT BUDGET

As on both Table 8.4 and Table 8.5 some of the components for this project have an inflated price due to the distribution problems and semiconductor backlogs leading to shortage in chips. To bypass some of these limitations we be using third-party sellers for some the hardware such as the ESP32 and Raspberry Pi 4 sold in Amazon to guarantee a timely delivery. In addition, both tables' costs should not be taken as a final amount since some of our initial parts would most likely be out of stock, in back order or the part we thought it would best fit our design did not fully meet our criteria. As seen below on Table 8.4 is the previous team's main material cost which have already exceeded our overall initial budget. This is one of our client constraints which is making a low-cost PCB 'All in One PV Sensor', thus we need to monitor and decided which parts are most cost effective to us in our design without compromising quality and reliability.

Table 8.4: Initial Project Budget for Re-designing Phase I

	Component Description	Vendor	Unit Price	Quantity	Total Price
1	Raspberry Pi 4 Model B 2019 Quad Core 64 Bit WiFi Bluetooth (4GB)	Amazon	\$134.99	1	\$134.99
2	SP-110-SS: Self-Powered Pyranometer	Apogee Instruments/ Part provided by OUC	\$223.00	1	\$223.00
3	Thermocouple Probes with Lead Wire & Molded Transition	Omega/ Part Provided by OUC	\$30.42	2	\$60.84

4	Raspberry Pi Zero 2 W (Wireless / Bluetooth)	Amazon	\$49.99	3	\$149.97
5	PCB	TBD	\$30	3	\$30
6	Weatherproof Enclosure	Weatherproof cases	\$100	1	\$100
Total Estimated Cost:					\$698.80

In Table 8.5 we can see the breakdown of the major components of our new design and the cost associate with them. As seen in Table 8.5 we decided to us ESP32 instead of a raspberry pi zero since the ESP32 has an analog to digital converter already integrated making more cost effective.

Table 8.5: Phase II Budget

Part Number	Component Description	Vendor	Unit Price	Quantity	Total Price	Notes
Wireless Transmission and Data Storage						
1	Not required as per MAE for Amazon	ESP-32S Development Board 2.4GHz Wi-Fi	Amazon	\$10.99	6	\$65.94
2	Not required as per MAE for Amazon	Raspberry Pi 4 Model B 2019 Quad Core 64 Bit WiFi Bluetooth (4GB)	Amazon	\$134.99	1	\$134.99
3	Not required as per MAE for Amazon	SAMSUNG 128GB EVO Plus Class 10 Micro SDXC	Amazon	\$19.10	1	\$19.10
4	Not required as per MAE for Amazon	HDMI Micro and Mini	Amazon	\$6	2	\$12
Sensors						
5	SP-110-SS	Self-Powered Pyranometer	Apogee Instruments	\$223.00	1	\$223.00
6	700-MAX6675ISA	Thermocouple Amplifier	Mouser	\$11.34	4	\$45.36
7	SA1-T	Thermocouple Probes with Lead Wire & Molded Transition	Omega	\$30.42	1	\$30.42
8	TLV342	Current Sensor	TI	\$0.323	4	\$1.292
9	TLV342	Voltage Sensor	TI	\$0.323	4	\$1.292

Power supply for ‘All in One Sensor’							
10	TBD	MPPT Charge Controller	TBD	\$23.99	4	\$23.99	Board Power Consideration
11	926-LM5006MM/NOPB	LM5006 Series Switching Voltage Regulators	Mouser	\$4.11	10	\$41.10	Best Option Yet
12	TBD	Connectors	TBD	\$20	2	\$40	N/A
Testing Equipment							
13	Not required as per MAE for Amazon	Solderless Bread Board Kit	Amazon	\$12.49	2	\$24.98	N/A
14	TBD	PCB Development	TBD	\$300	1	\$300	N/A
15	Not required as per MAE for Amazon	uxcell Mounted Devices IC PCB Adapter Socket	Amazon	\$8.08	1	\$8.08	N/A

9. PROJECT SUMMARY & CONCLUSION

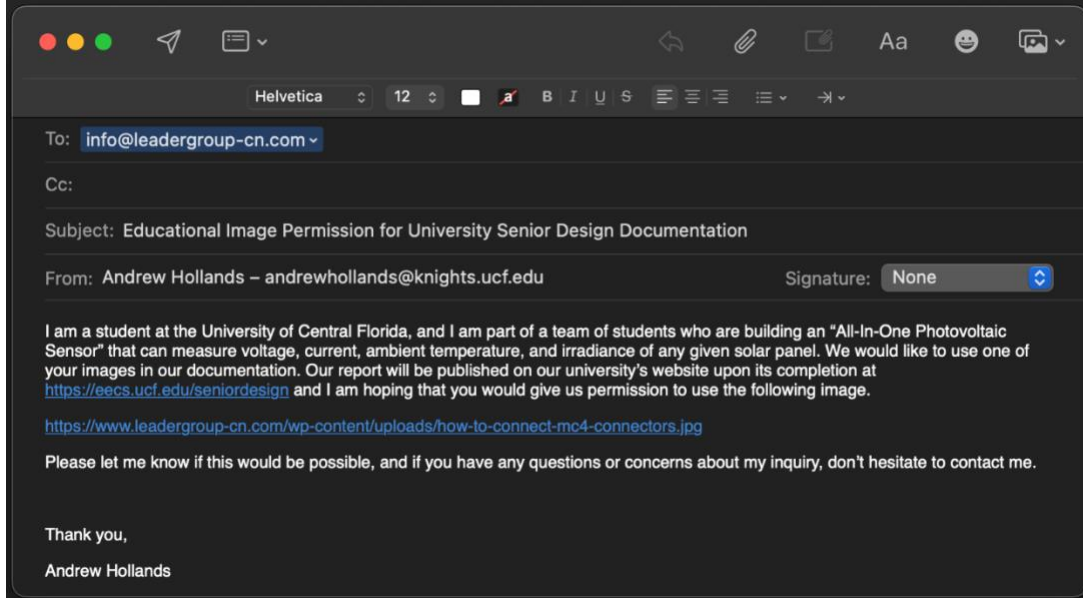
The goal of our project was to develop a low-cost, all-in-one photovoltaic (PV) sensor device which allows our customer, OUC, to gather data from their solar panel arrays. The all-in-one sensor collects voltage, current, temperature, and irradiance directly from the customer’s solar panels. The data that our solution provides the customer with includes numerous benefits. Firstly, through voltage and current values collected at each panel in an array allows for technicians to detect a faulty panel in an easy-to-use manner. This solution significantly reduces loss of power generation when a panel becomes faulty as this reduces the time and money it would take for a technician to identify a faulty panel. Secondly, our solution collects large amounts of granular data for OUC to generate accurate representations of temperature and irradiance at a solar panel array over a period, as well as energy collected over a period.

Our all-in-one PV sensor functions as a series of collector nodes, or microcontrollers, mounted onto each solar panel in an array. The collector nodes collect and wirelessly transmit multiple, granular pieces of data like voltage and current, temperature, and irradiance data from the onboard DC optimizers, thermocouples, and pyrometers, respectively, to a receiver node. The receiver node can compile collected data into a database, as well as display collected data in real-time. It is from our solution that OUC will be able to reach 50% carbon neutrality by 2030 and achieve 100% carbon neutrality by 2050 as our all-in-one PV sensor will have a robust design that will allow for scalability to a much larger solar panel array.

APPENDIX A. IMAGE/GRAFICS COPYRIGHT PERMISSIONS

For all figures reproduced from an outside source, a copyright request has been sent to the copyright holders. For figures for which permission has been granted, “reproduced with permission of [copyright holder]” appears in the respective figure captions. For figures for which a request has been sent but no response received, “permission for reproduction requested from [copyright holder]” appears in the respective figure captions.

Request for Female and Male MC4 Connectors (Figure 3.1):



Request and Permission for Solar Cell Cross-Section (Figure 3.3):

Found in Sent - UCF Mailbox

 **Andrew Hollands** 12:54 AM
Educational Image Permission for University Senior Design Docu... [Details](#)
To: Engineeringchoice.com@gmail.com

I am a student at the University of Central Florida, and I am part of a team of students who are building an "All-In-One Photovoltaic Sensor" that can measure voltage, current, ambient temperature, and irradiance of any given solar panel. We would like to use one of your images in our documentation. Our report will be published on our university's website upon its completion at <https://eecs.ucf.edu/seniordesign> and I am hoping that you would give us permission to use the following image.

<https://www.engineeringchoice.com/ezoimgfmt/10.wp.com/www.engineeringchoice.com/wp-content/uploads/2020/12/Solar-Cell.png?w=653&ssl=1&ezimgfmt=ng:webp/ngcb146>

Please let me know if this would be possible, and if you have any questions or concerns about my inquiry, don't hesitate to contact me.

Thank you,
Andrew Hollands

 **Engineering Choice** 1:01 AM
Re: Educational Image Permission for University Senior Design Do... [Details](#)
To: Andrew Hollands

Yes, of course you can.

Best Regards



Jignesh Sabhadiya
Admin & Chief editor
<https://www.engineeringchoice.com/>

[See More from Andrew Hollands](#)

Request for IoT Diagram (Figure 4.3):

To: data.privacy@digi.com

Cc:

Subject: Educational Image Permission for University Senior Design Documentation

From: Andrew Hollands – andrewhollands@knights.ucf.edu

Signature: **None**

I am a student at the University of Central Florida, and I am part of a team of students who are building an "All-In-One Photovoltaic Sensor" that can measure voltage, current, ambient temperature, and irradiance of any given solar panel. We would like to use one of your images in our documentation. Our report will be published on our university's website upon its completion at <https://eecs.ucf.edu/seniordesign> and I am hoping that you would give us permission to use the following image.

<https://www.digi.com/getattachment/Blog/post/The-4-Stages-of-IoT-Architecture/digi-emerging-architecture-business-drivers-web-SCADA-1280.png?lang=en-US>

Please let me know if this would be possible, and if you have any questions or concerns about my inquiry, don't hesitate to contact me.

Thank you,

Andrew Hollands

Request for Weld Beaded with Different Styles of Shielding Thermocouple (Figure 4.6):

To sales@thermosense.co.uk

Cc

Bcc

Educational Image Permission for Senior Design Documentation

I am a student at the University of Central Florida, I am contacting you today to ask permission to use an image from your company's website for educational purposes for Senior Design Documentation. I am currently part of a team of students trying to design and implement a cost-effective alternative device for monitoring Solar Farms. Once the paper is completed, we will need to upload to the University's website, "<https://www.ece.ucf.edu/seniordesign/>". Therefore, we ask permission to use the following image for our project:



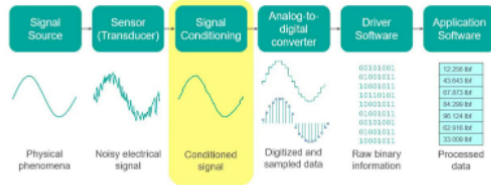
Request for Basic Conditioning Signal Block Diagram (Figure 4.7):

To S Sheffield.Admin@ttelectronics.com X
Bcc
Cc

Educational Image Permission for Senior Design Documentation

Good morning or Good afternoon,

I am a student at the University of Central Florida, I am contacting you today to ask permission to use an image from your company's website for educational purposes for Senior Design Documentation. I am currently part of a team of students trying to design and implement a cost-effective alternative device for monitoring Solar Farms. Once the paper is completed, we will need to upload to the Universities website, "<https://www.ece.ucf.edu/seniordesign/>". Therefore, we ask permission to use the following image for our project:



This image can be found [TTelectronics "Signal conditioning" Blog Post](#) by Stephen Oxley YouTube video.

Request for OpenGreenEnergy Schematic (Figure 4.10):



Maguire Mulligan <mulliganmaguire@gmail.com>
to opengreenenergy ▾

7:26 PM (0 minutes ago)



Debasish Dutta of OpenGreenEnergy,

I am a student at the University of Central Florida, and I am part of a team of students who are building an "All-In-One PV Sensor" that can measure the Voltage, Current, Ambient Temperature, and Irradiance of any given Solar Panel. We would like to use one of your images in our documentation. Our report will be published on the UCF Website upon its completion (<https://eecs.ucf.edu/seniordesign>), and I was hoping that you would give us permission to use the following picture:

https://www.opengreenenergy.com/wp-content/uploads/2021/05/Schematic_Solar-Power-Monitoring-V1.0.png

Please let me know if this is possible, and if you have any further questions or concerns about my inquiry, do not hesitate to contact me.

Thank you,
Maguire Mulligan

Request for ESP32 Functional Block Diagram (Figure 4.11):

Document Title **Version Number**

Section(s) **How do you rate our documentation? ***

Detailed Description

I am a student at the University of Central Florida, and I am part of a team of students who are building an "All-In-One Photovoltaic Sensor" that can measure voltage, current, ambient temperature, and irradiance of any given solar panel. We would like to use one of your images in our documentation. Our report will be published on our university's website upon its completion at <https://eecs.ucf.edu/seniordesign> and I am hoping that you would give us permission to use the following images:
 Figure 1: ESP32-WROOM32 Pin Layout (Top View) from [https://www.espressif.com/sites/default/files/documentation/esp32_wroom-32_datasheet_en.pdf](https://www.espressif.com/sites/default/files/documentation/esp32-wroom-32_datasheet_en.pdf)
 Figure 1: Functional Block diagram from https://www.espressif.com/sites/default/files/documentation/esp32_datasheet_en.pdf
 Please let me know if this would be possible, and if you have any questions or concerns about my inquiry, don't hesitate to contact me.

Thank you,
Andrew Hollands

Attachments

Drop file here or click to upload
 Size Limit: 5 MB. Acceptable file types: jpg, png, eps, txt, pdf, doc, docx, rar, zip, 7z, tar

Would you like to receive follow-ups from us? If so, please provide your contact information below.

Name **Email**
 Send a copy of this feedback form to my email box.

What code is in the image? * 

Request for ESP32-WROOM-32 Pin Layout (Figure 4.12):

Document Title **Version Number**

Section(s) **How do you rate our documentation? ***

Detailed Description

I am a student at the University of Central Florida, and I am part of a team of students who are building an "All-In-One Photovoltaic Sensor" that can measure voltage, current, ambient temperature, and irradiance of any given solar panel. We would like to use one of your images in our documentation. Our report will be published on our university's website upon its completion at <https://eecs.ucf.edu/seniordesign> and I am hoping that you would give us permission to use the following images:
 Figure 1: ESP32-WROOM-32 Pin Layout (Top View) from [https://www.espressif.com/sites/default/files/documentation/esp32_wroom-32_datasheet_en.pdf](https://www.espressif.com/sites/default/files/documentation/esp32-wroom-32_datasheet_en.pdf)
 Please let me know if this would be possible, and if you have any questions or concerns about my inquiry, don't hesitate to contact me.

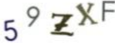
Thank you,
Andrew Hollands

Attachments

Drop file here or click to upload
 Size Limit: 5 MB. Acceptable file types: jpg, png, eps, txt, pdf, doc, docx, rar, zip, 7z, tar

Would you like to receive follow-ups from us? If so, please provide your contact information below.

Name **Email**
 Send a copy of this feedback form to my email box.

What code is in the image? * 

Request for Seebeck Effect (Figure 4.39):

To



copyright@researchgate.net

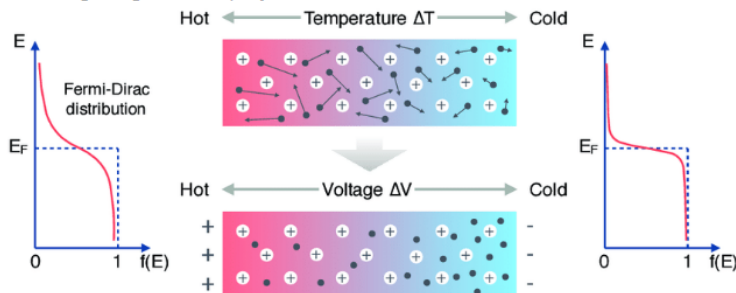


Bcc

Cc

Educational Image Permission for Senior Design Documentation.

I am a student at the University of Central Florida, I am contacting you today to ask permission to use an image from your company's website for educational purposes for Senior Design Documentation. I am currently part of a team of students trying to design and implement a cost-effective alternative device for monitoring Solar Farms. Once the paper is completed, we will need to upload to the Universities website, "<https://www.ece.ucf.edu/seniordesign/>". Therefore, we ask permission to use the following image for our project:



This image can be found at https://www.researchgate.net/figure/Illustration-of-the-Seebeck-effect-By-moving-electron-from-left-to-right-voltage_fig1_337642600

Request for Voltage vs. Temperature Thermocouple Behavior (Figure 4.40):

eeeguide.com/contact-us/

Paragraph Text

I am a student at the University of Central Florida, I am contacting you today to ask permission to use an image from your company's website for educational purposes for Senior Design Documentation. I am currently part of a team of students trying to design and implement a cost-effective alternative device for monitoring Solar Farms. Once the paper is completed, we will need to upload to the Universities website, "<https://www.ece.ucf.edu/seniordesign/>". Therefore, we ask permission to use the following image for our project (<https://www.eeeguide.com/wp-content/uploads/2017/08/Thermocouple-Circuit-1.jpg>)

Submit

Request for Typical Hot and Cold Junction Locations for a Type K Thermocouple (Figure 4.42):

electronics-tutorials.ws/contact

Message (required)

I am a student at the University of Central Florida, I am contacting you today to ask permission to use an image from your company's website for educational purposes for Senior Design Documentation. I am currently part of a team of students trying to design and implement a cost-effective alternative device for monitoring Solar Farms. Once the paper is completed, we will need to upload to the Universities website, "<https://www.ece.ucf.edu/seniordeisgn/>". Therefore, we ask permission to use the following image for our project if it is possible for educational purposes (<https://www.electronics-tutorials.ws/wp-content/uploads/2018/05/io-io9.gif>).

Submit

Request for block diagrams for MAX31856 and MAX6675 (Figure 4.49 and Figure 4.50):

maximsupport.microsoftcrmpartals.com/en-US/support/create-nontechnical%20case/

QUESTION OR ISSUE *

I am a student at the University of Central Florida, I am contacting you today to ask permission to use an image from your company's website for educational purposes for Senior Design Documation. I am currently part of a team of students trying to design and implement a cost-effective alternative device for monitoring Solar Farms. Once the paper is completed, we will need to upload to the Universities website, "<https://www.ece.ucf.edu/seniordeisgn/>". Therefore, we ask permission to use the fallowing image for our project:

<https://datasheets.maximintegrated.com/en/ds/MAX6675.pdfz> (Block diagram)
<https://datasheets.maximintegrated.com/en/ds/MAX31856.pdf> (Block diagram)

We will use the this two images for reasrch documetation purposes.

body p

Request for VNC Diagram (Figure 4.33):

First name*	Last name*
Andrew	Hollands
Email*	Company
andrewhollands@knights.ucf.edu	University of Central Florida
Subject*	
Privacy and GDPR enquiry	

Comments*

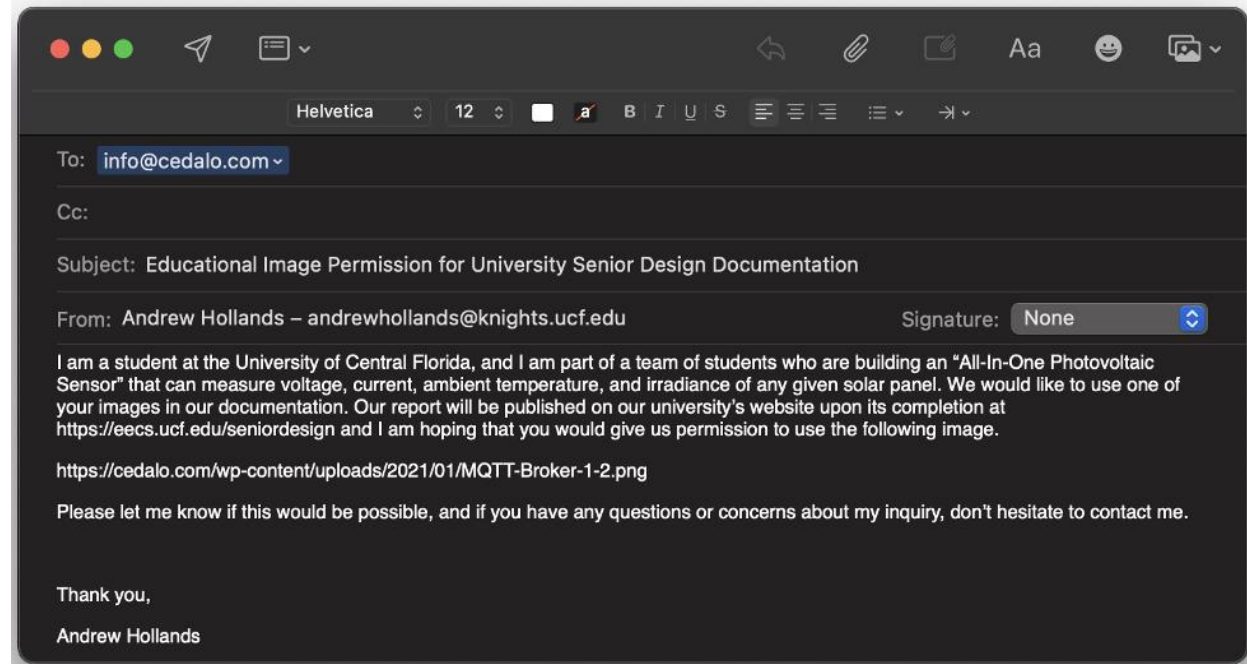
I am a student at the University of Central Florida, and I am part of a team of students who are building an "All-In-One Photovoltaic Sensor" that can measure voltage, current, ambient temperature, and irradiance of any given solar panel. We would like to use one of your images in our documentation. Our report will be published on our university's website upon its completion at <https://eecs.ucf.edu/seniordesign> and I am hoping that you would give us permission to use the following image.

https://help.realvnc.com/hc/article_attachments/4412274062609/network-share-central.png

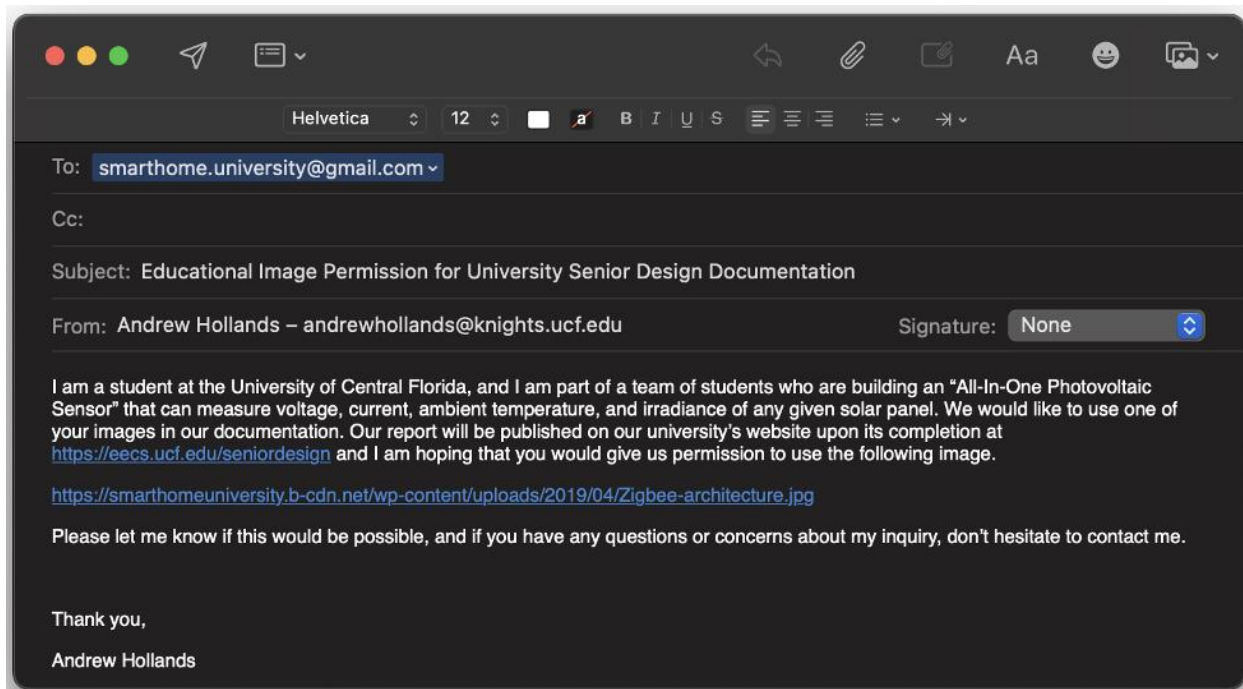
Please let me know if this would be possible, and if you have any questions or concerns about my inquiry, don't hesitate to contact me.

Thank you,
Andrew Hollands

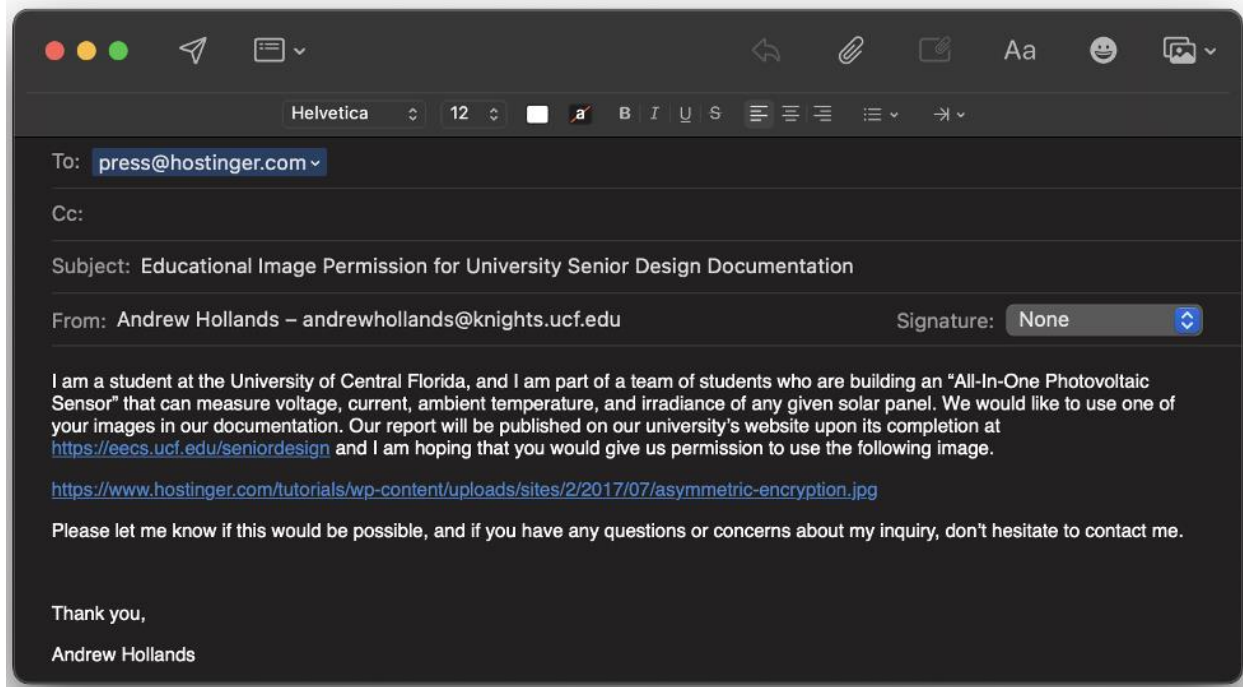
Request for MQTT Communication Diagram (Figure 4.33):



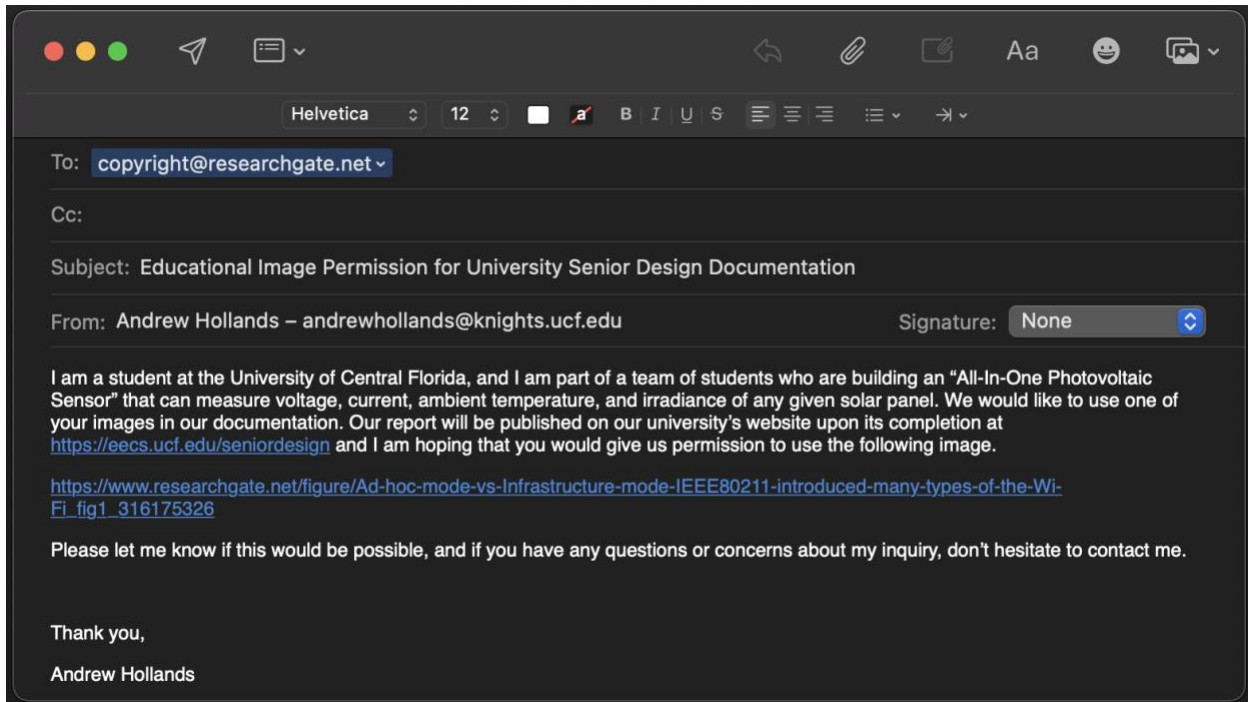
Request for ZigBee Network Diagram (Figure 4.34):



Request for SSH Diagram (Figure 4.342):



Request for Ad-hoc mode vs. Infrastructure mode (Figure 4.32):



Request for Electronics Tutorials Figures:

Email: temiajao@knights.ucf.edu

Message: Dear Electronic Tutorial representative,

I am a student at the university of central Florida, and my team and I are currently working on our senior design project in which we design a sensor device that can monitor the voltage, current, temperature, and irradiance of a solar panel. Part of our project requires us to write a report describing the approaches we take in order to perform this task. In our report, we used Images from your website, I am just writing this email to ask for your permission to use the images in our document. I have attached the images that we used, and we are hoping that you allow us to use them in our project.

Thank you for reading, and I am looking forward to your response.

.jpg 324
.jpg 328
.jpg 196
.jpg 357

Request for Texas Instrument Figures:

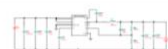
Dear TI representative,

I am a student at the university of central Florida, and my team and I are currently working on our senior design project in which we design a sensor device that can monitor the voltage, current, temperature, and irradiance of a solar panel. Part of our project requires us to write a report describing the approaches we take in order to perform this task. In our report, we used Images from your website, I am just writing this email to ask for your permission to use the images in our document. I have attached the images that we used, and we are hoping that you allow us to use them in our project.

Thank you for reading, and I am looking forward to your response.

Preferred language for your response
English

Attachments



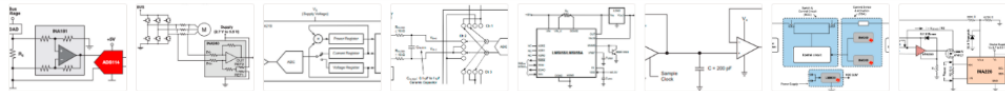
Picture11.png (22 KB)

just now



Picture12.jpg (17.5 KB)

just now

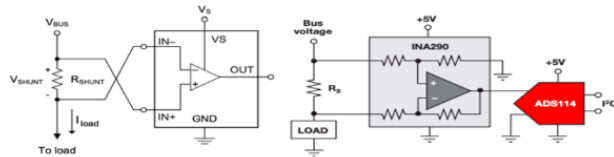


Show all 11 attachments (278 KB) Save all to OneDrive - Knights - University of Central Florida Download all

Dear TI representative,

I am a student at the university of central Florida, and my team and I are currently working on our senior design project in which we design a sensor device that can monitor the voltage, current, temperature, and irradiance of a solar panel. Part of our project requires us to write a report describing the approaches we take in order to perform this task. In our report, we used Images from your website. I am just writing this email to ask for your permission to use the images in our document. I have attached the images that we used, and we are hoping that you allow us to use them in our project.

Thank you for reading, and I am looking forward to your response.



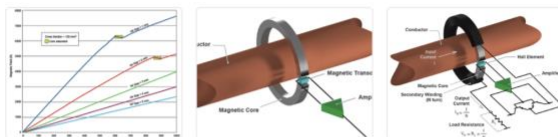
Request for AllegroFigures:



Timothy Oluwagbotemi Ajao
To: sales@megatechnologiesinc.com

⋮ ⏪ ⏴ ⏵ ⏶ ⋮

Wed 4/27/2022 5:22 PM



3 attachments (176 KB) Save all to OneDrive - Knights - University of Central Florida Download all

Dear Allegro representative,

I am a student at the university of central Florida, and my team and I are currently working on our senior design project in which we design a sensor device that can monitor the voltage, current, temperature, and irradiance of a solar panel. Part of our project requires us to write a report describing the approaches we take in order to perform this task. In our report, we used Images from your website. I am just writing this email to ask for your permission to use the images in our document. I have attached the images that we used, and we are hoping that you allow us to use them in our project.

Thank you for reading, and I am looking forward to your response.

APPENDIX B. REFERENCES

- [3.1] Hukseflux. (n.d.). *Pyranometer selection guide: how to choose the best sensor for your application*. <https://www.hukseflux.com/applications/meteorology-surface-energy-flux-measurement/pyranometer-selection-guide-how-to-choose>
- [3.2] Free Spirits Green Labs. (2021, March 19). *What are the different classes of pyranometers?* TrackSo-Solar PV Monitoring and Analytics. <https://trackso.in/knowledge-base/what-are-the-different-classes-of-pyranometers/>
- [3.3] E. Notes. (n.d.). *Wi-Fi Channels, Frequency Bands & Bandwidth » Electronics Notes.* Electronics Notes. <https://www.electronics-notes.com/articles/connectivity/wifi-ieee-802-11/channels-frequencies-bands-bandwidth.php>
- [3.4] Bluetooth® Technology Website. (n.d.). *Bluetooth Technology Website*. <https://www.bluetooth.com>
- [3.5] Qualify Your Product. (n.d.). Bluetooth® Technology Website. <https://www.bluetooth.com/develop-with-bluetooth/qualification-listing/>
- [3.6] RoHS Directive. (n.d.). European Commission. https://ec.europa.eu/environment/topics/waste-and-recycling/rohs-directive_en
- [3.7] ESD Standards. (n.d.). ESDSystems. <https://esdsystems.descoindustries.com/Standards.aspx>
- [3.8] PAC. (n.d.). *ANSI S20.20 ESD Standards*. Gotopac. <https://www.gotopac.com/art-esd-iso-standards-s20-20>
- [4.1] Solar panel history and overview. (2019, April 26). Energy Matters. <https://www.energymatters.com.au/panels-modules/>
- [4.2] This Month in Physics History. (2009, April). APS Physics. <https://www.aps.org/publications/apsnews/200904/physicshistory.cfm>
- [4.3] Gillis, A. S. (2022a, March 4). *What is the internet of things (IoT)?* IoT Agenda. <https://www.techtarget.com/iotagenda/definition/Internet-of-Things-IoT>
- [4.4] Gillis, A. S. (2022b, March 4). *What is the internet of things (IoT)?* IoT Agenda. <https://www.techtarget.com/iotagenda/definition/Internet-of-Things-IoT>
- [4.5] T.T.C. (2015, October 9). *system-on-a-chip (SoC)*. IoT Agenda. <https://www.techtarget.com/iotagenda/definition/system-on-a-chip-SoC>
- [4.6] Edwards, B. (2021, November 19). *What Is a System on a Chip (SoC)?* How-To Geek. <https://www.howtogeek.com/769198/what-is-a-system-on-a-chip-soc/>
- [4.7] PCMag. (n.d.). *Definition of SoC*. <https://www.pcmag.com/encyclopedia/term/soc>
- [4.8] Harding, S. (2019, September 11). *What Is an SoC? A Basic Definition*. Tom's Hardware. <https://www.tomshardware.com/reviews/glossary-soc-system-on-chip-definition,5890.html>
- [4.9] Acquisition of CadSoft Computer GmbH. (2009, September). Premier Farnell. <https://archive.ph/20150124191103/http://www.premierfarnell.com/media-centre/acquisition-cadsoft-computer-gmbh>
- [4.10] EAGLE Features. (n.d.). Autodesk. <https://www.autodesk.com/products/eagle/features>
- [4.11] ElectronicsTutorials. (n.d.). *Thermistors*. <https://www.electronics-tutorials.ws/io/thermistors.html>

- [4.12] Texas Instruments. (2018, March). *Diode-Based Temperature Measurement*.
<https://www.ti.com/lit/an/sboa277a/sboa277a.pdf>
- [4.13] Texas Instruments. (n.d.). *LM335*. <https://www.ti.com/product/LM335>
- [4.14] *Thermistors - An Overview*. (2016). ScienceDirect.
<https://www.sciencedirect.com/topics/engineering/thermistors#:~:text=Thermistors%20are%20made%20from%20semiconductor,as%20shown%20in%20Equation%201.10>
- [4.15] Omega Engineering. (2021, December 20). *What is a Thermistor and how does it work?*
Omega. <https://www.omega.com/en-us/resources/thermistor>
- [4.16] Electronics Tutorials. (n.d.-a). *Temperature Sensors*. https://www.electronics-tutorials.ws/io/io_3.html
- [4.17] *What is a thermocouple and how does it work?* (n.d.). Omega.
<https://www.omega.co.uk/prodinfo/thermocouples.html>
- [4.18] Ortega, A., PhD. (2019, July 2). *Effects of electrical noise on thermocouple measurements*. Electronics Cooling. <https://www.electronics-cooling.com/2002/08/effects-of-electrical-noise-on-thermocouple-measurements>
- [4.19] *Noise Voltage - An Overview*. (2017). ScienceDirect.
<https://www.sciencedirect.com/topics/engineering/noise-voltage>
- [4.20] ABLIC Inc. (n.d.). *What is an Operational Amplifier?*
<https://www.ablic.com/en/semicon/products/analog/opamp/intro/>
- [4.21] Electrical4U. (2021, March 7). *Differential Amplifiers: Gain, OP Amp & BJT Circuit*.
<https://www.electrical4u.com/differential-amplifier>
- [4.22] *What is the purpose of using a differential amplifier?* (n.d.). Toshiba.
https://toshiba.semicon-storage.com/app-en/semiconductor/knowledge/faq/linear_opamp/what-is-the-purpose-of-using-a-differential-amplifier.html
- [4.23] Campbell Scientific. (2020a, March 24). *CR310 Measurement and Control Datalogger*.
<https://www.campbellsci.com/cr310>
- [4.24] Campbell Scientific. (2020b, March 30). *LoggerNet - Datalogger Support Software*.
<https://www.campbellsci.com/loggernet>
- [4.25] Texas Instruments. (2016a). *Voltage, Current, and Temperature Monitoring for Solar Module Level Power Electronics*. <https://www.tij.co.jp/jp/lit/ug/tiducm3/tiducm3.pdf>
- [4.26] OpenGreenEnergy. (2021, May 16). *DIY Solar Panel Monitoring System*.
<https://www.opengreenenergy.com/diy-solar-panel-monitoring-system/>
- [4.27] *Analog to Digital Converter – How ADC Works and Types?* (2021, March 9).
Microcontrollers Lab. <https://microcontrollerslab.com/analog-to-digital-adc-converter-working/>
- [4.28] Mouser. (2009). *MCP3426*. <https://www.mouser.com/datasheet/2/268/22226a-81911.pdf>
- [4.29] *Raspberry Pi Analog to Digital Converters*. (2016, February 9). Adafruit Learning System. <https://learn.adafruit.com/raspberry-pi-analog-to-digital-converters/mcp3008>
- [4.30] *Analog to Digital Converter - ESP32*. (2020). Espressif.
<https://docs.espressif.com/projects/esp-idf/en/v4.2/esp32/api-reference/peripherals/adc.html>
- [4.31] Espressif. (2022). *ESP32 Series Datasheet*.
https://www.espressif.com/sites/default/files/documentation/esp32_datasheet_en.pdf
- [4.32] Storr, W. (2018, February 21). *Quartz Crystal Oscillator*. Basic Electronics Tutorials.
<https://www.electronics-tutorials.ws/oscillator/crystal.html>

- [4.33] Silicon Labs. (2021, August). *AN1335: RS9116 SoC Crystal Selection Guide*.
<https://www.silabs.com/documents/login/application-notes/an1335-rs9116w-crystal-selection-guide.pdf>
- [4.34] Storr, W. (2021, December 7). *Introduction to Capacitors, Capacitance and Charge*.
 Basic Electronics Tutorials. https://www.electronics-tutorials.ws/capacitor/cap_1.html
- [4.35] Raspberry Pi (Trading) Ltd. (2019, June). *Raspberry Pi 4 Model B Datasheet*.
<https://datasheets.raspberrypi.com/rpi4/raspberry-pi-4-datasheet.pdf>
- [4.36] Manchukonda, R. (2017). *How to Choose a Shunt Resistor*.
<https://training.ti.com/sites/default/files/docs/current-sense-amplifiers-how-to-choose-a-shunt-resistor-presentation-quiz.pdf>
- [4.37] Texas Instruments. (2014). *Simplifying Current Sensing*.
<https://www.ti.com/lit/eb/slyy154a/slyy154a.pdf?ts=1644183642564>
- [4.38] Texas Instruments. (2021). *Current Sense Amplifiers*.
<https://www.ti.com/lit/sg/slyb194e/slyb194e.pdf?ts=1644365257161>
- [4.39] EETimes. (2012, February 8). *A Current Sensing Tutorial*. <https://www.eetimes.com/a-current-sensing-tutorial-part-1-fundamentals/>
- [4.40] Texas Instruments. (2015b, December). *INA219 Datasheet*.
<https://www.ti.com/lit/ds/symlink/ina219.pdf?ts=1644610993542>
- [4.41] Texas Instruments. (2016, March). *INA3221 Datasheet*.
<https://www.ti.com/lit/ds/symlink/ina3221.pdf?ts=1644612748347>
- [4.42] Texas Instruments. (2013, April). *LM5056 Datasheet*.
<https://www.ti.com/lit/ds/symlink/lm5056a.pdf?ts=1644612750654>
- [4.43] Texas Instruments. (2016d, April). *TLV34xx Datasheet*.
<https://www.ti.com/lit/ds/symlink/tlv342a.pdf?ts=1649359874931>
- [4.44] Storr, W. (2022, January 14). *Hall Effect Sensor and How Magnets Make It Works*. Basic Electronics Tutorials. <https://www.electronics-tutorials.ws/electromagnetism/hall-effect.html>
- [4.45] *Hall Effect Current Sensing*. (2021, July 26). All About Circuits.
<https://www.allaboutcircuits.com/technical-articles/hall-effect-current-sensing-open-loop-and-closed-loop-configurations/>
- [4.46] Electronics Tutorials. (n.d.-b). *Voltage Dividers*. <https://www.electronics-tutorials.ws/dccircuits/voltage-divider.html>
- [4.47] Texas Instruments. (2015a, November). *40 V to 400 V Uni-directional Current/Voltage/Power Monitoring Reference Design*. <https://www.ti.com/lit/pdf/tidu849>
- [4.48] Texas Instruments. (2016c, April). *Automotive Precision eFuse Reference Design*.
<https://www.ti.com/lit/pdf/tidubk1>
- [4.49] Texas Instruments. (2016e, December). *Voltage, Current, and Temperature Monitoring for Solar Module Level Power Electronics*.
- [4.50] Omega. (2021, November 9). *Thermocouple Wire*. <https://www.omega.com/en-us/resources/thermocouple-wire>
- [4.51] *What is the difference between a thermopile pyranometer and a silicon photocell pyranometer?* (n.d.). Campbell Scientific. <https://www.campbellsci.com/faqs?v=2322>
- [4.52] Apogee. (2021, October). *APOGEE PYRANOMETERS*.
<https://www.apogeeinstruments.com/content/SP-100-200-spec-sheet.pdf>
- [4.53] Apogee. (2018a). *New ISO 9060:2018 Pyranometer Classifications*.
https://www.apogeeinstruments.com/content/ISO_9060_Apogee_Comparison.pdf

- [4.54] Apogee. (2018b). *SP110 Pyranometer*. https://www.alphaomega-electronics.com/en/index.php?controller=attachment&id_attachment=3075
- [4.55] Campbell Scientific. (2022). *CS320 Digital Thermopile Pyranometer*. <https://www.campbellsci.com/cs320>
- [4.56] Sirichote, W. (2004, July 11). *DC Amplifier for Pyranometer*. Kswichit. <https://www.kswichit.com/logger3/insolation.html>
- [4.57] Texas Instruments. (1998). *INA101 Datasheet*. <https://www.ti.com/product/INA101>
- [4.58] Texas Instruments. (2015c, December). *INA333 Datasheet*. <https://www.ti.com/lit/ds/symlink/ina333.pdf?ts=1633019250750>
- [4.59] Texas Instruments. (2001, March). *TLV243x Datasheet*. <https://ti.com/lit/ds/symlink/tlv2432a.pdf>
- [4.60] Texas Instruments. (2022, January). *INA126PA Datasheet*. <https://www.ti.com/lit/ds/symlink/ina126.pdf>
- [4.61] MAXIM Integrated. (2015, May). *MAX4194–MAX4197 Datasheet*. <https://datasheets.maximintegrated.com/en/ds/MAX4194-MAX4197.pdf>
- [4.62] Analog Devices. (2008). *AD8223 Datasheet*. <https://www.analog.com/media/en/technical-documentation/data-sheets/AD8223.pdf>
- [4.63] Mouser. (2020). *AD623 Datasheet*. <https://www.mouser.com/datasheet/2/609/ad623-1605360.pdf>
- [4.64] Beal, V. (2022, January 4). *Wi-Fi*. Webopedia. <https://www.webopedia.com/definitions/wifi/>
- [4.65] Wigmore, I. (2014, April 24). *Wi-Fi Alliance*. WhatIs.Com. <https://www.techtarget.com/whatis/definition/Wi-Fi-Alliance>
- [4.66] Pahlavan, K. (2020, November 19). *Evolution and Impact of Wi-Fi Technology and Applications: A Historical Perspective*. SpringerLink. https://link.springer.com/article/10.1007/s10776-020-00501-8?error=cookies_not_supported&code=4f2295fa-b1dc-4dc2-bdab-8a99a034e20d
- [4.67] *802.11 WiFi Standards Explained*. (2021, November 16). Lifewire.
- [4.68] Wi-Fi Alliance. (2018, October). *Generational Wi-Fi® User Guide*. https://www.wi-fi.org/download.php?file=/sites/default/files/private/Generational_Wi-Fi_User_Guide_20181003.pdf
- [4.69] Tjensvold, J. M. (2007, September). *Comparison of the IEEE 802.11, 802.15.1, 802.15.4 and 802.15.6 wireless standards*. <https://janmagnet.files.wordpress.com/2008/07/comparison-ieee-802-standards.pdf>
- [4.70] Shah, V. (2017, April). *Ad-Hoc vs. Infrastructure Mode*. ResearchGate. https://www.researchgate.net/figure/Ad-hoc-mode-vs-Infrastructure-mode-IEEE80211-introduced-many-types-of-the-Wi-Fi_fig1_316175326
- [4.71] Jose, R. S. (2000, February). *Bluetooth Technology*. <https://dspace.mit.edu/bitstream/handle/1721.1/9207/45483671-MIT.pdf?sequence=2&isAllowed=y>
- [4.72] Bluetooth® Technology Website. (2022). *Bluetooth Technology Website*. <https://www.bluetooth.com>
- [4.73] Lab, M. (2021, December 17). *What is MQTT and How MQTT Works?* Microcontrollers Lab. <https://microcontrollerslab.com/what-is-mqtt-and-how-it-works/>
- [4.74] Hunkeler, U. (2018). *MQTT-S – A Publish/Subscribe Protocol For Wireless Sensor Networks*. <https://sites.cs.ucsb.edu/~rich/class/cs293b-cloud/papers/mqtt-s.pdf>

- [4.75] Rana, S. (2022, February 7). *How to Connect an ESP32 WiFi Microcontroller to a Raspberry Pi Using IoT MQTT*. PREDICTABLE DESIGNS.
<https://predictabledesigns.com/how-to-connect-esp32-microcontroller-to-raspberry-pi-using-iot-mqtt/>
- [4.76] What Is Zigbee Wireless Mesh Networking? (2022). Digi.
<https://www.digi.com/solutions/by-technology/zigbee-wireless-standard>
- [4.77] Richardson, T. (1998, February). Virtual Network Computing.
<https://quintinsf.com/publications/virtual-network-computing/vnc-ieee.pdf>
- [4.78] Loshin, P., & Cobb, M. (2021, September 24). Secure Shell (SSH). SearchSecurity.
<https://www.techtarget.com/searchsecurity/definition/Secure-Shell>
- [4.79] LAMP (software bundle). (2015). DBpedia.
[https://dbpedia.org/page/LAMP_\(software_bundle\)](https://dbpedia.org/page/LAMP_(software_bundle))
- [4.80] Simic, S. (2022, January 6). What is LAMP Stack? Knowledge Base by phoenixNAP.
<https://phoenixnap.com/kb/what-is-a-lamp-stack>
- [4.81] C language. (2022, March). CPPReference. <https://en.cppreference.com/w/c/language>
- [4.82] E. (2020, September 17). Why is C the most preferred language for embedded systems? Emertxe. <https://www.emertxe.com/c-programming/why-is-c-the-most-preferred-language-for-embedded-systems/>
- [4.83] Ritchie, D. (2003). The Development of the C Language. Chistory. <http://www.bell-labs.com/usr/dmr/www/chist.html>.
- [4.84] C++ language. (2022, March). CPPReference.
<https://en.cppreference.com/w/cpp/language>
- [4.85] Sidana, U. (2021, July 15). Python vs C: Know what are the differences. Edureka.
<https://www.edureka.co/blog/python-vs-c/>
- [4.86] Welcome to Python. (2022, April 7). Python.Org. <https://www.python.org/about/>
- [4.87] MicroPython - Python for microcontrollers. (2022). MicroPython. <https://micropython.org>
- PAC. (n.d.). ANSI S20.20 ESD Standards. Gotopac. <https://www.gotopac.com/art-esd-iso-standards-s20-20>
- [4.88] About CentOS. (2022). CentOS. <https://www.centos.org/about/>
- [4.89] Elsevier. (n.d.). ScienceDirect topics. Topics - ScienceDirect | Elsevier Solutions. Retrieved April 26, 2022, from <https://www.elsevier.com/solutions/sciedirect/topics>
- [4.90] Engineering, O. (2021, November 5). Cold junction compensation for thermocouples. <https://www.omega.com/en-us/>. Retrieved April 26, 2022, from
<https://www.omega.com/en-us/resources/thermocouple-junction-principles>
- [4.91] Encyclopædia Britannica, inc. (n.d.). Seebeck effect. Encyclopædia Britannica. Retrieved April 26, 2022, from <https://www.britannica.com/science/Seebeck-effect>
- [4.92] Nepjol.info. (n.d.). Retrieved April 26, 2022, from
<https://nepjol.info/nepal/index.php/SW/article/view/5524>
- [4.93] Nepjol.info. (n.d.). Retrieved April 26, 2022, from
<https://nepjol.info/nepal/index.php/SW/article/view/5524>
- [4.94] Resistor power rating and the power of Resistors. Basic Electronics Tutorials. (2018, July 9). Retrieved April 25, 2022, from https://www.electronics-tutorials.ws/resistor/res_7.html
- [4.95] Encyclopædia Britannica, inc. (n.d.). Voltage regulator. Encyclopædia Britannica. Retrieved April 25, 2022, from <https://www.britannica.com/technology/voltage-regulator>
- [4.96] Voltage Regulator types and working principle: Article: Mps. Voltage Regulator Types and Working Principle | Article | MPS. (n.d.). Retrieved April 25, 2022, from
<https://www.monolithicpower.com/en/voltage-regulator-types>

- [4.97] Knight, D. (2016, February 13). Introduction to linear voltage regulators. Digi. Retrieved April 25, 2022, from <https://www.digikey.com/en/maker/blogs/introduction-to-linear-voltage-regulators>
- [4.98] Linear vs. switching regulators. Renesas. (n.d.). Retrieved April 25, 2022, from <https://www.renesas.com/us/en/products/power-power-management/linear-vs-switching-regulators>
- [4.99] Notes, E. (n.d.). Series voltage regulator: Series pass regulator. Electronics Notes. Retrieved April 25, 2022, from https://www.electronics-notes.com/articles/analogue_circuits/power-supply-electronics/linear-psu-series-regulator-circuit.php#:~:text=Series%20voltage%20regulator%20basics,across%20the%20load%20remains%20constant.
- [4.100] K. tk, Tarun Agarwal says: at Hi Katherine tkWe really appreciate you taking the time out to share your experience with us. Reply, says:, T. A., says:, B. D., says:, M., Says:, V. M., Tarun Agarwal says: at Thanks for your compliment For more detailed information on voltage regulators, & *, N. (2021, January 18). Types of voltage regulators : Working and their limitations. ElProCus. Retrieved April 25, 2022, from <https://www.elprocus.com/types-of-voltage-regulators-and-workingprinciple/#:~:text=There%20are%20two%20types%20of%20Linear%20voltage%20regulators%3A%20Series%20and,down%2C%20and%20Inverter%20voltage%20regulators>.
- [4.101] *Switch Mode Power Supply Basics and switching regulators*. Basic Electronics Tutorials. (2021, August 4). Retrieved April 25, 2022, from <https://www.electronics-tutorials.ws/power/switch-mode-power-supply.html>
- [4.102] LMR36006 4.2-V to 60-V, 0.6-a ultra-small ... - ti.com. (n.d.). Retrieved April 26, 2022, from <https://www.ti.com/lit/ds/symlink/lmr36006.pdf?ts=1619738911026>
- [4.103] LMR36506 3-V to 65-V, 0.6-Aultra-small ... - ti.com. (n.d.). Retrieved April 26, 2022, from <https://www.ti.com/lit/ds/symlink/lmr36506.pdf?ts=1594597317257>
- [4.104] LMR36015 4.2-V to 60-V, 1.5-a ultra-small ... - ti.com. (n.d.). Retrieved April 26, 2022, from <https://www.ti.com/lit/ds/symlink/lmr36015.pdf?ts=1593880615352>
- [4.105] LMR36510 simple switcher 4.2-V to 65-V, 1-a ... - ti. (n.d.). Retrieved April 26, 2022, from <https://www.ti.com/lit/ds/symlink/lmr36510.pdf?&ts=1589298567359>
- [4.106] Wikimedia. (n.d.). Retrieved April 26, 2022, from <https://www.wikimedia.org/>
- [4.107] Wikimedia Foundation. (2022, April 25). Raspberry Pi. Wikipedia. Retrieved April 26, 2022, from https://en.wikipedia.org/wiki/Raspberry_Pi
- [4.108] File:lamp software bundle.svg. Wikimedia Commons. (n.d.). Retrieved April 26, 2022, from https://commons.wikimedia.org/wiki/File:LAMP_software_bundle.svg
- [4.109] INA293 4-V to 110-V, 1.3-MHz, ultra-precise current sense ... - ti.com. (n.d.). Retrieved July 23, 2022, from https://www.ti.com/lit/ds/symlink/ina293.pdf?HQS=ti-null-null-manuf_df-manupromo-ds-Datasheets.com-wwe